Université de Montréal

Antigen and superantigen presentation as defined by the MHCII-accessory proteins and associated-peptides

par

Jean-Simon Fortin

Département de Microbiologie and Immunologie

Faculté de Médecine

Thèse présentée à la Faculté des études supérieures

en vue de l'obtention du grade de Philosophiae Doctor (Ph.D.)

en Immunologie

Avril 2013

Université de Montréal
Faculté des études supérieures et postdoctorales

Cette thèse intitulée:

Antigen and superantigen presentation as defined by the MHCII-accessory proteins and associated-peptides

Présentée par:
Jean-Simon Fortin

a été évaluée par un jury composé des personnes suivantes :

Nathalie Labrècque, président-rapporteur
Jacques Thibodeau, directeur de recherche
Walid Mourad, membre du jury
Joaquin Madrenas, examinateur externe
Nathalie Labrècque, représentante de la doyenne de la FESP

Résumé

Les molécules du CMH présentent une panoplie d'antigènes qui, lorsque reconnus par un lymphocyte T spécifique, indique à ce dernier de survivre ou de s'activer. Le processus menant à la liaison d'un peptide à la poche du CMH de classe II, implique trois molécules accessoires, soit la chaine invariante, DM et DO. La chaine invariante replie et dirige les molécules du CMHII jusqu'à la voie endosomale. Ensuite, DM échange CLIP, peptide découlant de la dégradation de la chaine invariante, pour d'autres ayant une meilleure affinité. Exprimé seulement chez certaines cellules présentatrices, DO compétitionne avec les molécules du CMHII pour la liaison à DM et ainsi favorise la présentation d'antigènes internalisés par des récepteurs membranaires. Ensemble, ces protéines ont un potentiel immunomodulatoire pouvant être exploité afin d'augmenter l'efficacité de vaccin peptidique.

DO requiert DM pour arriver à maturité et sortir du RE. Cette interaction, qui induit un changement de conformation dans la chaine β de DO, peut être sondée à l'aide de l'anticorps monoclonal Mags.DO5. En utilisant cet anticorps, nous avons montré que DM stabilise l'interaction entre les domaines α1 et β1 de DO et influence son repliement dans le RE. Donc, la conformation qui révèle l'épitope Mags.DO5 corrèle avec la migration de DO hors du RE. Afin d'étudier plus précisément ce changement de conformation, DO fut contraint à une ronde d'évolution dirigée. Des 41 mutants obtenus, 25% se retrouvent à l'interface DO-DM et 12% se retrouvent à la surface exposée au solvant du domain β1, région hypothétique de l'épitope Mags.DO5. De plus, la bibliothèque de mutants a été testée pour son habileté à inhiber l'activité de DM. La plupart des mutants montre

une activité inhibitrice diminuée, ce qui supporte le model où DO compétionne les molécules du CMHII en séquestrant le rôle chaperon de DM.

Les molécules du CMHII ont l'unique habileté de présenter les superantigènes, une famille de toxines virales et bactériennes qui force l'interaction CMHII-TCR de façon beaucoup moins spécifique qu'en contexte canonique. Alors que la façon dont les superantigènes bactériens s'assemblent avec le CMHII et le TCR soit bien comprise, la nature du complexe trimoléculaire découlant des superantigènes du virus de la tumeur mammaire de la souris (vSAG) reste mal définie. En l'absence d'une structure cristalline, une approche fonctionnelle a été choisie pour examiner la relation des vSAGs avec le CMHII et le TCR avec le but de dévoiler l'architecture de ce multi-complexe protéique. Je montre que le TCR lie parallèlement la chaine α du CMHII et vSAG, ce qui résulte en une interaction presque canonique. Puisque différents peptides peuvent être tolérés lors de cet ancrage, il semble que vSAG ajuste les interactions CMHII-TCR conventionnelles. En outre, mes résultats montrent que vSAG reconnait un épitope conformationnel et que cette liaison peut être abrogée par l'extension amino-terminale du peptide CLIP, laquelle s'étend en deçà de la niche. Finalement, mes résultats suggèrent que les vSAG peut réticuler plusieurs CMHII adjacents et active les cellules T via son motif TGXY.

Mots-clés: HLA-DO, HLA-DM, MMTV, superantigène, MHCII

Abstract

MHCII molecules expose a weave of antigens, which send survival or activation signals to T lymphocytes. The ongoing process of peptide binding to the MHC class II groove implicates three accessory molecules: the invariant chain, DM and DO. The invariant chain folds and directs the MHCII molecules to the endosomal pathway. Then, DM exchanges the CLIP peptide, which is a remnant of the degraded invariant chain, for peptides of better affinity. Expressed in highly specialized antigen presenting cells, DO competes with MHCII molecules for DM binding and favors the presentation of receptor-internalized antigens. Altogether, these molecules exhibit potential immunomodulatory properties that can be exploited to increase the potency of peptide vaccines.

DO requires DM for maturation and to exit the ER. Interestingly, it is possible to monitor this interaction through a conformation change on DOβ that is recognized by the Mags.DO5 monoclonal antibody. Using Mags.DO5, we showed that DM stabilizes the interactions between the DO α1 and β1 chains and that DM influences DO folding in the ER. Thus, the Mags.DO5^{+} conformation correlates with DO egress from the ER. To further evaluate this conformation change, directed evolution was applied to DO. Of the 41 unique mutants obtained, 25% were localized at the DM-DO binding interface and 12% are at the solvent-exposed β1 domain, which is thought to be the Mags.DO5 epitope. In addition, I used the library to test the ability of HLA-DO to inhibit HLA-DM and sorted for the amount of CLIP. Interestingly, most of the mutants showed a decrease inhibitory effect, supporting the notion that the intrinsic instability of DO is a required for its function. Finally, these results support the model in which DO competes against classical MHCII molecules by sequestering DM chaperone's function.

MHCII molecules are also characterized by their ability to present superantigens, a group of bacterial or viral toxins that coerces MHCII-TCR binding in a less promiscuous fashion than what is observed in a canonical setting. While the mechanism of how bacterial superantigens form trimeric complexes with TCR and MHCII is well understood, the mouse mammary tumor virus superantigens (vSAG) are poorly defined. In the absence of a crystal structure, I chose a functional approach to examine the relation between vSAG, MHCII and TCR with the goal of uncovering the overall trimolecular architecture. I showed that TCR concomitantly binds both the MHCII α chain and the vSAG and that TCR-MHCII docking is almost canonical when coerced by vSAGs. Because many peptides may be tolerated in the MHCII groove, the pressure exerted by vSAG seems to tweak conventional TCR-MHCII interactions. Furthermore, my results demonstrate that vSAG binding to MHCII molecules is conformation-dependent and abrogated by the CLIP amino-terminal residues extending outside the peptide-binding groove. In addition, they also suggest that vSAGs cross-link adjacent MHCIIs and activate T cells via a TGXY motif.

Keywords: HLA-DO, HLA-DM, MMTV, superantigen, MHCII

Table of Content

List of Tables

List of Figures

List of Abbreviations

Abs: Antibodies

Ags: Antigens

aa: amino acid

APC: Antigen presenting cell

BCR: B-cell receptor

bSAG: Bacterial superantigen

CDR: Complementary determining regions

CLX: Calnexin

CRT: Calreticulin

DC: Dendritic cell

ER: Endoplasmic reticulum

HC: Heavy chain

HLA: Human leukocyte antigen

HV4: hypervariable region 4

Ii: Invariant chain

IR: Immune response

MHC: Major histocompatibility complex

MIIC: MHCII compartments

MMTV: Mouse mammary tumor virus

PDB: Protein data base

PDI: Protein disulfide isomerase

PLC: Peptide loading complex

pMHCI: peptide-MHC class I complex

pMHCII: peptide-MHC class II complex

PRR: Pattern recognition receptor

SAG: Superantigen

TAP: Transporter associated with antigen processing

TCR: T-cell receptor

TLR: Toll-like receptor

Tpsn: Tapasin

V: Variable

vSAG: Viral superantigen

vSAG7: MMTV superantigen 7

I'm sorry, but I just don't understand anything in biology
unless I know what it looks like

Don Craig Wiley

To my parents, Suzie and Yvon

Acknowledgements

One does not succeed his Ph.D. alone. At the foremost, this achievement stems from my mentors, whom inspired, guided and taught me. To Jacques, who has never stopped believing in me, I owe everything. His unconditional love for science and constant support were always welcome and mostly, needed. With him, everything is measurable in greatness, without boundaries and led to the most exquisite experience/experiments. To Daved, whose vision is so many miles ahead, I owe a much greater understanding of my favorite proteins and of the world outside of Montréal. His friendship and hospitality shaped a relationship that I prize among all. Never will I have enough of those great arguments that pushed me outside the box. To the both of you, thank you. I cannot think of anyone for whom I have this much respect and pride.

Next I want to thank my fellow coworkers, not only because you got me in the lab with eager and enthusiasm, but also because of your help in figuring “it” out and those many crazy science talks. Yes we were doing something meaningful. My favorite tutor, Marie-Hélène “MHC” Côté, for your humbleness and down to earth attitude toward science – yes, we need to get down once in a while – you are fantastic and made me a better scientist. Laetitia, because your inestimable help and friendship led to what I believe is a brilliant article. Also, such a great thank to the many people who helped me write a better thesis, through proofreading, advices or criticism: Chris Salmon, Julie Shareck, Marianne Raymond and MCBD. More specially Julie and Marianne who were always on my back pushing me to get "IT" done and move on!

I am also much grateful to Maryse Cloutier, which was able to re-instill life in my very first project and pursued it marvelously into three phenomenal articles.

What started as a mundane colleague relation is now an esteemed friendship. Please, never stop criticizing me as this only makes me a better person.

It also goes without saying that I owe a huge thanks to my many US coworkers, which greeted me with open arms and so much knowledge to share. Olga, Chris and Lawrence, you are the stars of the Fremont lab and you never ceased to be inspirational. Bill, Vince, Megan, Kyle, Whitney and Julie you did make my stay in the Lou just what I needed it to be, something that I will always remember as my greatest journey!

Bien sûr, le soutient constant de mes parents, leur fierté et leur motivation auront été en grande partie à la base de ma réussite et je leur en suis immensément reconnaissant.

Preface

The family of proteins encoded by the major histocompatibility complex (MHC) cluster is at the core of the adaptive immune system of most chordates and first appeared in jawed fish. From a teleological standpoint, MHC provides the tools to the white blood cells to detect and build up cell-mediated immune responses (IR), leading to the elimination of invasive microbes and transformed cells. The MHC locus encodes i.a. the classical human leukocyte antigens (HLA), a group of membrane-bound receptors that bind and present small peptides to T cell receptors (TCR) and the non-classical MHC proteins, which assist peptide loading. In homeostatic state, most of the organism's HLAs are loaded with peptides derived from self-proteins and do not trigger T cell activation, a result of their thymic education. However, when novel peptides are introduced either by transformed cells or alien organisms, T cells become activated and guide the adaptive IR according to the threat.

The first description of the MHC is attributed to Jean Dausset in the fifties. His rationale came forth after observing that the antibodies (Ab) of a patient having received multiple blood transfusions could bind to other individual's leukocytes. The patient's Abs were generated post-transfusion in response to the different HLAs of the donors' leukocytes, later hypothesized to be carried on a single genetic system. Since then, the knowledge pertaining to MHC has evolved and was refined by Jan Klein who stated: "MHC is a group of genes coding for molecules that provide the framework for recognition of foreign antigens by T lymphocytes". This dogma will be carried throughout my report, while MHC will be used to define HLA molecules.

To maintain homeostasis, MHC genes play a role in generating an appropriate immune response while limiting attacks against host's cells. This intricate equilibrium has put the MHC locus under the magnifying glass of many scientists, as it is the main gene cluster associated with autoimmunity. For example, the HLA-DQ1 alleles have been linked to asthma, type 1 diabetes, multiple sclerosis and celiac disease, to name a few (Jones et al., 2006; Trowsdale, 2011). However, it is still ambiguous how these genes are involved in autoimmunity etiology. The onset of autoimmunity occurs in the presence of a precise immunogenic bound-peptide. Thus, a number of molecular events taking place prior to the peptide's association to MHC molecules influence disease outcome. Indeed, limiting the peptide exchange of an antigen presenting cell (APC), thereby biasing its peptide repertoire, was reported to prevent type 1 diabetes in susceptible NOD mice (Yi et al., 2010). Manipulating antigen loading through non-classical MHCII molecules constitutes a broad and ubiquitous approach to deflect or modulate the presentation of harmful peptides to auto-reactive T lymphocytes. Inversely, promoting the presentation of a pathogen's Ag strengthens peptide-specific IR. Before undertaking any studies assessing the therapeutic role of non-classical MHC molecules, we must first understand how they work. To this end, the first section of my work examines the structural and functional relationship between the two non-classical MHCII molecules HLA-DO and -DM.

Presentation of peptides by MHC molecules is not the only way to stimulate T cells. Certain bacteria and viruses encode superantigens (SAG), a family of proteins with the ability to provoke peptide-independent MHCII-TCR binding. As opposed to the very cohesive and specific interaction between peptide-bound MHCII and TCR, SAGs bind conserved motifs outside the peptide-binding groove leading to very strong polyclonal T cell proliferation/deletion responses. While this super-activation may cause food poisoning or toxic shock syndrome, it provides microorganisms with a way to elude the adaptive immune system. Recent work has shown that mice bearing aggressive T cell lymphoma exposed to bacterial- or viral- SAG (bSAG and vSAG) had increased survival rates or underwent complete remission, respectively (Mundiñano et al., 2010). These findings suggest that under certain conditions, SAGs can be used to treat T cell associated diseases. Unfortunately, their use in immunotherapy has remained scarce. While many bSAG's structures have been determined and picture a similar fold, mouse mammary tumor viruses (MMTV) viral SAGs' structure remains unsolved. Interestingly, the different MMTVs encode SAGs with distinct TCR variable β chain complementarities. This characteristic is appealing and could provide an arsenal of therapeutic SAGs specific to diverse T cell populations. Unfortunately, those viral SAGs (vSAG) are extremely difficult to manipulate and their mode of action remains obscure. Thus, the second part of my study makes use of vSAG7 to investigate the mechanism by which this family of SAGs succeeds in cross-linking MHCII to TCR and provides a detailed structure-function analysis.

This thesis is divided into four sections. In Chapter 1, I describe antigen presentation in depth, in terms of its regulation, the molecules implicated and the mechanism of peptide exchange in its appropriate cellular context. While I discuss both MHC class I and II, the latter is emphasized. I also describe antigenic and superantigenic presentation to T lymphocytes, focusing on the molecular requirements for TCR docking with MHC and highlighting the SAGs structure-function. In Chapter 2, I describe my work regarding the requirement of a distinct population of MHCII molecules for successful MMTV SAG stimulation. This article entitled "The mouse mammary tumor virus superantigen coerce an unconventional MHCII-TCR binding topology" has just been accepted upon revision to the Journal of Immunology. In Chapter 3, I present my findings pertaining to conformational changes of HLA-DO upon its encounter with HLA-DM, which assists HLA-DO folding and ER egress. These results were published in an article entitled "Evidence for a HLA-DM-induced structural change in HLA-DOβ" in the scientific journal Immunology. Finally, in Chapter 4, I will discuss the issues that corroborate the interplay between antigen presentation, HLA-DO and their effect on vSAG presentation and I will then propose several perspectives.

Chapter 1 : Literature review

In the forthcoming chapter, I will cover the various aspects of the conventional MHC class I and II antigen presentation, including the cellular context, the major proteins orchestrating the peptide exchange mechanism and the mechanism itself. Next, I will introduce the capability of TCR to bind MHC as well as the resulting IRs from a MHCII standpoint. Because SAGs, such as MMTV vSAG, also stimulate T cells in a MHCII-dependent fashion, I will describe the process underlying its maturation and presentation. Lastly, I will focus on the associated-peptide given its central role in the presentation. Although many have already covered the Ag presentation, my report will seek to provide a more mechanistically oriented description regarding the implicated components and pathways.

1.1. Antigen presentation: the players

Before describing the molecular events leading to the presentation of processed antigens (Ags) to T lymphocytes, it is wise to briefly overview the cellular and proteic context of the antigen presentation. Virtually all nucleated cells express MHCI molecules, which present the cell cytosolic content in the form of peptide-bound MHCI (pMHCI) complexes to $CD8_+$ T lymphocytes. Simply put, this segment of the MHC strives to clear the host transformed and virus- or intracellular bacteria-infected cells that show modified peptide repertoires. However, pMHCI-TCR contacts are not sufficient to generate cytotoxic T cells. Indeed, generation of such cells requires additional stimuli originating from CD4+ helper T cells following MHCII Ag presentation by professional APCs. Macrophages, dendritic cells (DC) and B lymphocytes are the professional APCs that present MHCII-bound peptides (pMHCII) to $CD4_+$ helper T cells. These Ags originate from exogenous proteins,

derived either from extracellular bacteria or parasites and endogenous proteins, derived either from the MHCII compartments (MIIC) or other organelles following autophagy (Neefjes et al., 2011). All professional APCs rely similarly on lysosomal degradation to generate antigenic peptides. Yet, it remains that these leukocytes possess specific characteristics, which contribute to the distinctive roles they play in the adaptive immune system. For this reason, each APC is briefly described, with an emphasis on the Ag-handling facet.

1.1.1. Macrophages

Macrophages are involved primarily in the innate immune response, as their main function is to endocytose cellular debris and pathogens (Mantovani et al., 1972). Highly versatile, macrophages have the ability to present many Ags to either $CD4^+$ or $CD8^+$ T cells (Geissmann et al., 2010). They are found in nearly every tissue and present pMHC complexes locally, especially at inflammation sites (Trombetta and Mellman, 2005). However, in response to inflammatory cytokines or pattern recognition receptors (PRR), the amount of MHCII and co-stimulatory molecules expressed at the surface of macrophages remains low. This results in antigen presentation that is generally less efficient than that seen with DCs or B cells. Nonetheless, macrophages are the first line of defense against invasive microorganisms.

1.1.2. Dendritic cells

While not as efficient as macrophages at endocytosis, DCs are by far the most devoted and skilled APCs to present Ags. Naïve DCs reside in almost every tissue, *i.a.* skin, lungs, gastro-intestinal track, where they have access to various antigenic proteins. These leucocytes undergo remarkable transformation upon

exposure to cytokines or PRR signal transduction, which lead to downstream signaling that influences the longevity of the IR (Joffre et al., 2009). Yet, what differentiates them from other APCs is their ability to migrate to lymphoid organs upon activation, following chemokine signaling. There, they encounter streams of naïve T cells seeking cognate pMHC complexes. Additionally, DCs are extremely skilled at crosspresenting Ags, which allow them to present virtually any Ag onto both MHCI and MHCII molecules (Delamarre et al., 2003). Contrary to macrophages, mature DCs express massive amounts of MHCII and co-stimulatory molecules conducive to $CD4_+$ T cell activation. DCs' roles in peripheral surveillance and centralized Ag presentation in the lymph nodes provide for the most rigorous and selective IRs.

1.1.3. B lymphocytes

Contrary to macrophages and DCs, B lymphocytes discern the Ags' tertiary structure through cell-surface clonotypic immunoreceptors, named B cell receptors (BCR) prior to endocytosis (Batista and Harwood, 2009). The specificity-mediated internalization allows B lymphocytes to almost exclusively present peptides derived from BCR-cognate ligands. However, given that follicular B cells are confined into lymphoid organs, *i.e.* lymph node and spleen, they do not readily have access to a wide spectrum of Ags like macrophages and DCs do. Therefore, Ags are supplied to follicles via afferent lymph vessels or transported *in situ* by DCs. As mentioned previously, DCs migrate to lymphoid organs upon activation to present antigenic-derived peptides to naïve T cells, but also carry undigested Ags ready to be presented to B cells (Huang et al., 2005; Platt et al., 2010). In fact, membrane-associated Ag presentation to B cells has been shown to be more important for their activation than soluble Ags (Carrasco and Batista, 2006; Depoil et al., 2008).

In summary, the clustering of proteins onto BCRs initiates strong MHCII upregulation, Ag degradation and peptide loading. Then, upon specific MHCII-TCR engagement, B lymphocytes proliferate and differentiate into extrafollicular plasmablasts or plasma cells.

Overall, the three professional APCs participate in the activation of CD4+ T cells. Despite using similar Ag uptake, which relies on endocytosis or receptor-mediated endocytosis, each professional APC has very distinct abilities. Macrophages are exceptional at endocytosis and digestion, DCs are the most specialized to generate pMHC complexes and B lymphocytes are very specific at presenting peptides derived from BCR-cognate Ags. Having introduced the cells implicated in Ag presentation, I will now introduced the MHCI and MHCII molecules in the following subsection before undertaking a more specific description of their respective peptide loading process.

1.1.4. MHC molecules

As mentioned earlier, I plan to provide a structural overview of the antigen presentation. To this end, I find interesting to begin by introducing the MHC folds and inherent characteristics, which are highly relevant given that the subsequent sections are rendered according to this information. In Figure 1.1, both class I and class II MHCs are pictured. PyMol was used to generate the crystal representation and the protein database (PBD) access code is provided in the figure legends (http://www.pymol.org; PyMOL Molecular Graphics System; DeLano Scientific, San Carlos, CA).

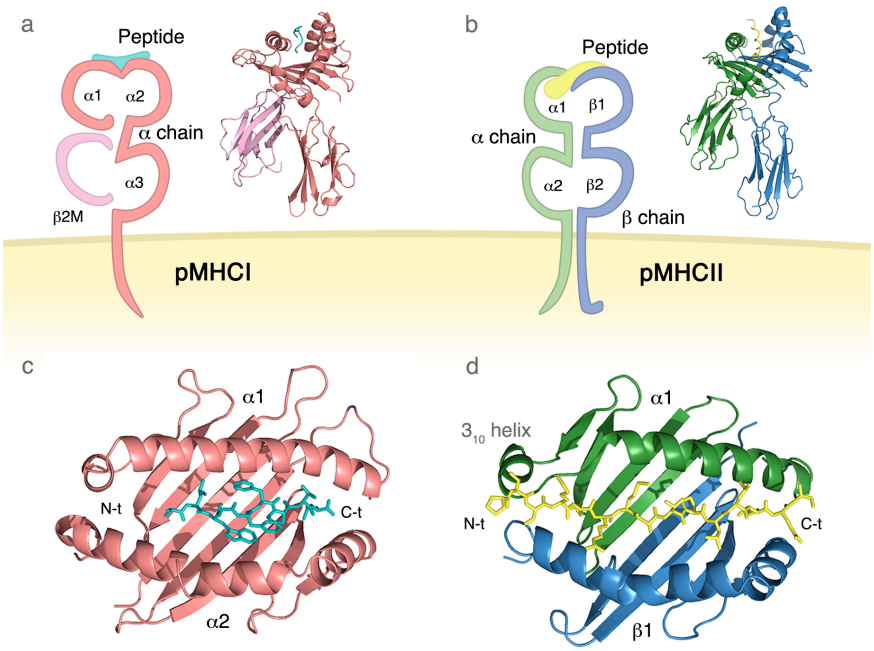

Figure 1.1. MHCI vs MHCII

Cartoon identifying the important MHC subunits and chains are given beside their crystal structure. MHCI HC is salmon, β2M is pink and MHCII α and β chain are green and blue, respectively. **(a)** Ribbon depiction of the MHCI HLA-A2 in complex with the p1049 peptide (1B0G) and **(b)** the MHCII DR3-CLIP complex (1A6A). **(c and d)** View from the top into the MHC class I and II peptide-binding groove. Notice the 3_{10} helix c onnecting the α1 domain β-sheet to the α-helix. The peptides, depicted as sticks, are cyan and yellow for MHCI and MHCII respectively.

First, MHC class I and II molecules share very much the same structure as a result of exon shuffling and gene duplication throughout evolution (Danchin et al., 2004). Both are highly polymorphic heterodimeric proteins, formed by the assembly of either the MHCI α chain (heavy chain, HC) with β2-microglobulin (β2M) or the pseudosymmetric MHCII α and β chains. They utilize a similar mechanism to bind peptides, *i.e.* a cleft composed of a β-sheet and two α-helixes forming the floor and surrounding walls, respectively. While the MHCI peptidic groove is sealed at both ends of the α-helixes junctions and only accommodates short peptides of no more than 13 amino acids (aa), MHCII's extremities remain open and unrestrictive vis-à-vis peptides length. Among their other disparities, MHCI forms its binding groove from a single α-chain, divided into α1 and α2 domains (Figure 1.1a). In contrast, MHCII niche is composed of the jointed α and β chains, linked together via the floor central anti-parallel β-strands (Figure 1.1b).

1.1.5. Non classical MHC molecules

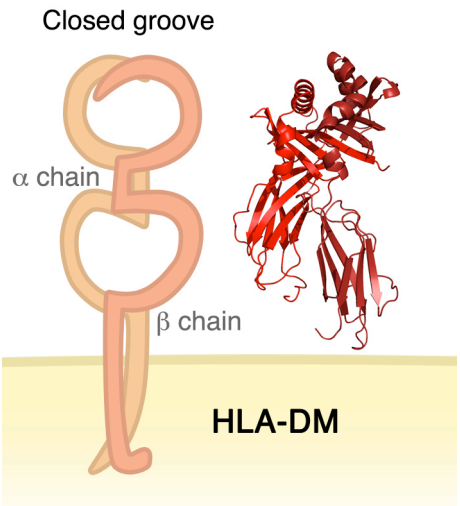

Figure 1.2. DM, non classical MHCII
Cartoon and crystal structure of DM (1HDM), highlighting the lack of a peptide-binding groove

In addition to classical MHC molecules, there is a handful of non-classical class I MHCs (or MHCI-like molecules) that share the same overall fold and may or may not bind β2M or peptides, *e.g.* T10, T22, FcRn, CD1, MR1, MICA, MICB, ULBP (Apostolopoulos et al., 2008). On the other hand, MHCII includes only two non-classical molecules, HLA-DM (DM) and HLA-DO (DO) (Busch et al., 2005). They differ from classical MHCIIs as they have little to no polymorphism and modulate the antigen loading rather than presenting antigens. While the

crystal structure of both human and mice DM were described fifteen years ago (Figure 1.2) (Fremont et al., 1998; Mosyak et al., 1998), the structure of DO has just been recently solved in pair with DM by the Stern's group (personal communication, unpublished data). DM structure revealed a stable and closed peptide-binding groove, the result of two additional disulfide bonds: one between the floor and the α-chain helix and the second between the two distal β-sheets of the β-chain. Along with DM, DO is unable to stably bind peptides, most probably a result of its inherent groove which differ from the classical MHCII. (Refer to section 1.3.5. HLA-DO)

1.1.6. Peptide-binding groove

A striking feature of MHCs is their ability to bind an incredible number of peptides and to form very stable complexes (Madden, 1995). In order to achieve such a feat, MHCs rely on a conserved hydrogen bond (HB) network and very polymorphic binding pockets. Firstly, a collection of HBs and van der Waals forces help stabilize any peptides that are able to take an extended backbone conformation. This network of interactions is formed between highly conserved MHC residues and the polar and charged atoms of the peptide main chain, independently of its side chains (Figure 1.3).

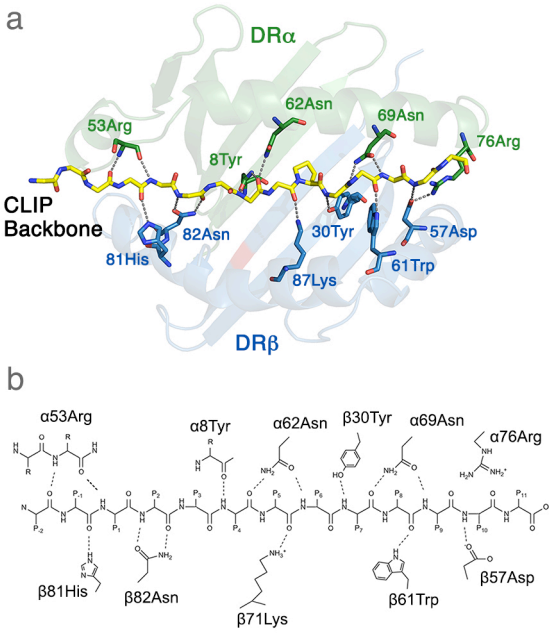

Figure 1.3. Hydrogen bond network

(a) Top view into the class II peptide-binding groove (1A6A). Conserved MHCII residues that form hydrogen bonds with the bound peptide's main chain atoms are shown as sticks. Hydrogen bonds are indicated by dotted lines. **(b)** Molecular epresentation of the panel **a**

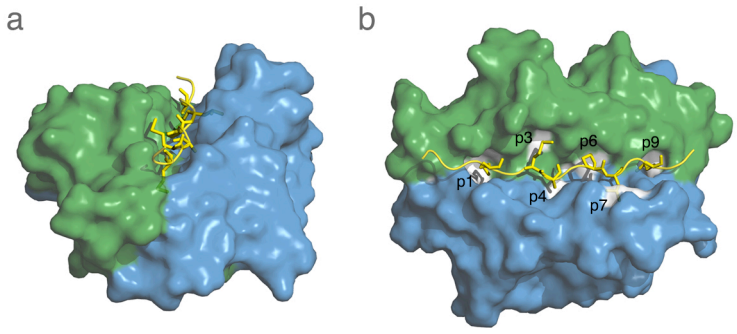

Figure 1.4. Groove and pockets

Surface rendering of a peptide-bound MHCII crystal (1A6A). The class II α and β chains are green and blue, respectively. **(a)** Lateral view of the peptide-binding cleft. **(b)** Top view (90° rotation toward the reader of **a**) of the MHCII groove, in which the pocket accommodating the associated-peptide side chains are colored in white. The peptide backbone and the residues filling the MHCII pocket are yellow.

Secondly, most of the allelic differences between MHCs are within residues protruding toward the peptide-binding groove and create pockets with different stereochemistry, the latter accommodating the specific peptide side chains (Figure 1.4). In addition to charge and hydrophobicity, the pocket dimension may differ depending on the MHC's side chains' size and thus also impose restrictions on the peptide bound by a particular MHC. Whereas this applies to both MHC classes, one has a closed groove and the other is open, causing some divergence in binding fashion.

1.1.7. Associated peptide

MHCI peptide association is mediated by highly conserved charge interactions between the HC (pocket A, B and F) and both ends of the peptide. This anchors the peptide's termini and, in certain instances, allows it to bulge out to accommodate longer chains (Figure 1.5, a vs b) (Rudolph et al., 2006; Tynan et al., 2005). On the other hand, peptide binding to MHCII is not constrained into a closed groove and lead to different peptide behaviors, as long as they extend as a polyproline conformation. First, this allows the groove to tolerate alternate peptide registers, *i.e.* allows the same peptide to use different anchor residues (Bankovich et al., 2004; Mohan et al., 2011; Stadinski et al., 2010). Second, recent work by the

Günther's group revealed that MHCIIs were able to accommodate a peptide in two orientations, a phenomenon that may have been overlooked for two decades (Günther et al., 2010). They noticed that shortening the peptide in order to prevent HB between the P_{-2} residue and the 3_{10} helix favored a flipped orientation, the latter able to form this bond (Figure 1.5, c vs d) Indeed, the authors pointed out that over half of the crystallized pMHCII stemmed from covalently associated single-chain peptide-β chains. These results may not reflect the behavior of every peptide, but could be applied to pseudo-palindromic peptides like $CLIP_{90\text{-}104}$. Further details about the CLIP peptide are given in section 1.3.3.

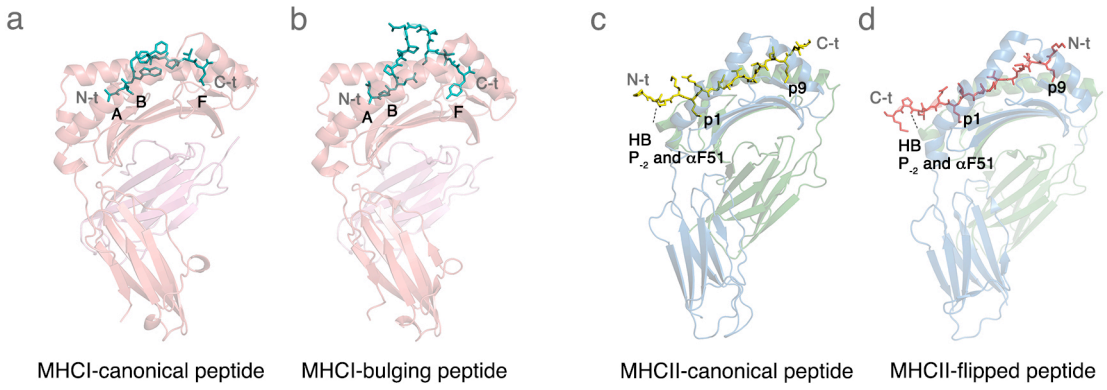

Figure 1.5. Peptide-binding into MHCs

Comparison of different canonical and alternative peptide-binding modes. Side view of the crystal structure of MHCIs associated with the p1049 peptide **(a)** and the bulging 13-mer EBV peptide **(b)** (1B0G and 1ZHL). MHCII associated with CLIP in a canonical **(c)** and flipped orientation **(d)**. HBs between the peptide P_{-2} and the α-chain Phe51 are indicated by dotted grey lines.

Third, the length of the bound peptide may vary depending on the number of peptide flanking residues (PFR) around the 9-mer core. These protruding residues have a profound effect on TCR recognition and function (Carson et al., 1997). Forth, the peptide may alternatively go through or may already have gone through different post-translational modifications (Suri et al., 2006). For example, small saccharides, nitrotyrosine, oxidized tryptophan and citrulline (an arginine

modification) have been shown to elicit distinct T cell responses when part of a given peptide. Overall, by using promiscuous and specific interactions in concert, the MHC binding cleft is able to efficiently bind the vast pool of peptides and by doing so, permits a certain freedom to the peptide's sequence, which will have distinct effects on the T cell response.

1.1.8. Peptide-MHC single-chain

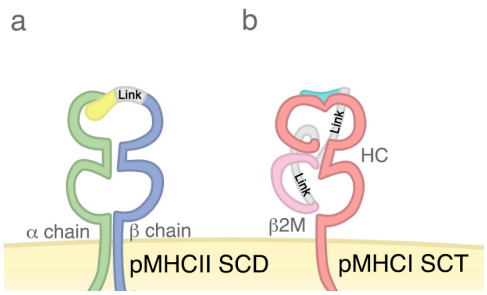

Figure 1.6. Single chain MHC

Schematic of class I and II single chains. **(a)** The peptide is covalently linked to the amino-terminal end of the MHCII β-chain as a SC dimer **(b)** The peptide is linked to the amino-terminal end of β2M, which is also linked to the HC at its carboxy-terminal end. The linkers are portrayed in light grey.

The study of antigen presentation took a huge step forward with the advent of innovative single-chain (SC) peptide-MHC constructs. Designed in the laboratory of John Kappler and Philippa Marrack in the nineties (Fremont et al., 1996; Kozono et al., 1994), this technology consists of covalently binding, with a flexible linker, the peptide and the MHCII β chain or the peptide and the β2M for class I and II, respectively. More recently, Mitasksov and colleagues even went further by designing a single chain trimer (SCT), in which the β2M is linked to both the HC and the peptide as shown in Figure 1.7b (Mitaksov et al., 2007). Not only do SCs generate an homogenous peptide-loaded MHC population, but they also provide a way to express any peptide's sequences, great tools to study peptide-specific T cell responses. With the recent discovery of peptides capable of binding the MHCII in a flipped-orientation, it was recently showed that those flipped-peptide MHCII complexes could be generated by linking the peptide to the α chain (Schlundt et al., 2012). Such SCs are key to my experimental designs, described in the next chapters.

1.2. MHC class I

Briefly mentioned earlier (1.1.4. MHC molecules), the organism is able to clear transformed or infected cells through the action of CD8+ T cells upon recognition of pMHCI. Herein, the main pathway orchestrating the generation of stable pMHCI in the endoplasmic reticulum (ER) is described in depth, emphasizing on the role of the peptide loading complex (PLC). The PLC, shown as a cartoon representation in Figure 1.7, is a multi-protein complex composed of tapasin (Tpsn), the transporter associated with antigen processing (TAP), the chaperone calreticulin (CRT) and the protein disulfide isomerase ERp57 (Garbi et al., 2005; Hughes and Cresswell, 1998). Altogether, these proteins recruit newly synthesized MHCI heterodimers and provide the necessary tools for optimal peptide binding.

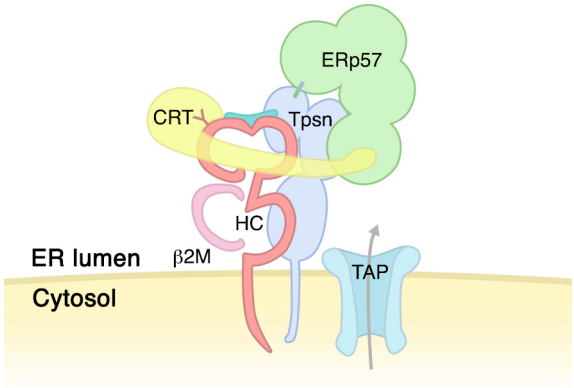

Figure 1.7. Peptide loading complex.

Multiple interactions contribute to the stability of MHCI peptide-loading complex. Central to the PLC is the Tpsn, which transmembrane domain interacts with TAP, forms disulfide bond with ERp57 and interact with the α2/3 domain of the HC. CRT binds both the HC α1 domain *N*-linked glycan and ERp57.

1.2.1 Folding and assembly within the PLC

MHCI heavy chain (HC) is a highly polymorphic glycoprotein containing two disulfide bridges, one in the α2 domain, linking the α-helix with the peptide groove platform and the other in the α3 membrane-proximal immunoglobulin-like domain (Garbi et al., 2005; Kjer-Nielsen et al., 2002). The exact mechanism allowing the

complete refolding, oxidation and recruitment to the PLC of the HC remains elusive. Early after synthesis, the lectin-binding chaperone calnexin (CNX) binds the α1 domain monoglucosylated N-linked glycan of the HC, protecting the latter from aggregation and favoring its refolding (Helenius and Aebi, 2004). The HC disulfide bridges are believed to be catalyzed by ERp57 (Antoniou et al., 2007; Lindquist et al., 2001). However, ERp57-deficient cell lines showed normal MHCI redox status (Garbi et al., 2006), suggesting that other thiol-oxidoreductases contribute to its oxidation. The Ahn's group demonstrated that protein disulfide isomerase (PDI) was also found to associate with the HC as a mixed disulfide complex and was controlling the oxidation state of the α2 disulfide bond, essential for peptide binding (Park et al., 2006). After refolding, the HC associates with the β2-microglobulin (β2M) subunit via its α3 domain, which triggers CNX replacement by its soluble homologue CRT (Cresswell et al., 2005; Garbi et al., 2005). Furthermore, this interaction stabilizes the MHCI/Tpsn interaction (Wearsch et al., 2011). Together, β2M and calreticulin maintain the HC stability and promote a peptide receptive conformation (Culina et al., 2004; Diedrich et al., 2001; Wearsch et al., 2004).

The recruitment of the MHCI HC-β2M heterodimer to the PLC is mediated by Tpsn, a multifunctional transmembrane glycoprotein (Bangia et al., 1999; Garbi et al., 2000; Grandea et al., 2000; Lehner et al., 1998; Rizvi and Raghavan, 2006). Wether Tpsn binds TAP or MHCI first is currently contested (Chambers et al., 2008; Cresswell et al., 2005). However, in both situations, the outcome is the same and is centered around Tpsn. Tpsn binds TAP through its transmembrane domain (Momburg and Tan, 2002), covalently associates with ERp57 by a stable disulfide bond (Dick et al., 2002; Peaper et al., 2005) and tethers MHCI with its amino-terminal domain (Turnquist et al., 2004). This allows ERp57's binding to CRT, further stabilizing MHCI interactions within the PLC where it ultimately binds

peptide (Figure 1.8)(Santos et al., 2007). The Cresswell's group has recently investigated the stoichiometry of the PLC, reporting that the Tpsn/MHCI ratio varies from 2:1 to 2:2 in different conditions (Panter et al., 2012). Their results highlight the fact that the PLC may dynamically adapt to variation in the peptide supply as a result of viral infection, increasing the number of MHCIs in the PLC.

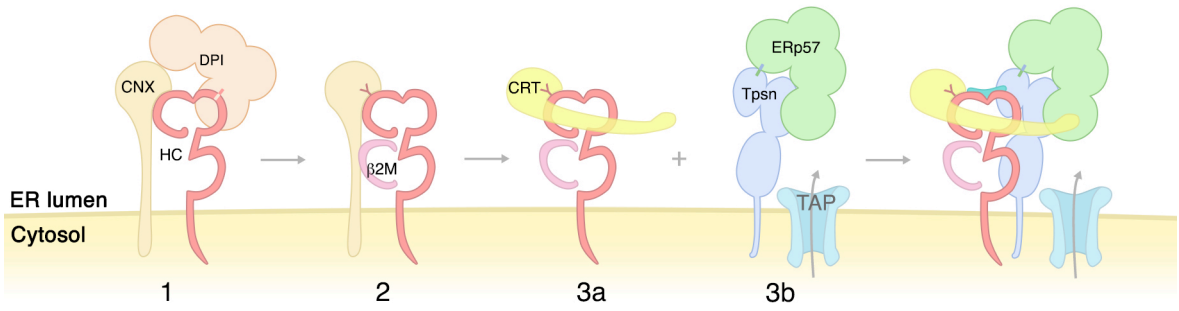

Figure 1.8: The folding and assembly of the PLC.

CNX mediates the early folding stage of the HC prior to its association with β2M **(1 and 2)**. The HC oxidation happens during this time and PDI and ERp57 facilitates this process **(1)**. Upon proper oxidation and pairing with β2M, CNX is replace by CRT **(3a)**. In parallel, newly synthesized Tpsn associates with TAP before forming a disulfide bound with ERp57 **(3b)**. Rapidly, HC/β2M/CRT subcomplexes join the Tpsn/ERp57/TAP subcomplexes forming the PLC.

1.2.2. Association/dissociation from the PLC

Having established the members and the basics underlying the assembly of the PLC, one question still remains: what triggers the association and the release of MHCI. The incorporation of MHCI within the PLC is a cooperative event between Tpsn and CRT, both linked together by ERp57 (Peaper et al., 2005). It was hypothesized that Tpsn recognizes only empty MHCI and that the conformational change occurring upon peptide binding provokes their dissociation (Hansen et al., 2005; Sadegh-Nasseri et al., 2008). On the other hand, it is unclear whether the dissociation of CRT happens before or after the cleavage of the last glucose by

glucosidase II. Given the low affinity of CRT for monoglucosylated glycan (1-2 μM) (Cresswell et al., 2005), it is more likely that the CRT dissociates prior to cleavage. Out of the PLC, pMHCI will either undergo a round of quality control by UDP-glucose glycoprotein transferase (UGT) which will re-glucosylate improperly folded MHCI or egress to the cell surface (Cresswell et al., 2005). Indeed, in absence of this second round of quality control by UGT, the quantity of MHCIs at the plasma membrane is reduced, its maturation and assembly are delayed and the peptide repertoire differs (Zhang et al., 2011).

1.2.3. Role of PDI in the PLC

The fact that two disulfide isomerases are present in the PLC raises the idea that they are implicated in the redox state of MHCI, especially since the redox status plays an important role in peptide loading (Park et al., 2006; Peaper et al., 2005). Indeed, in the absence or in the exclusive presence of suboptimal peptides, there is an increase of partially reduced MHCI (Park et al., 2006). To verify if ERp57 or PDI were implicated in the redox state of MHCI, a search for mixed disulfide was conducted. ERp57 was shown as a mixed disulfide complex with the HC, but only when not present within the PLC, hence only in the refolding process (Lindquist et al., 2001). As part of the PLC, ERp57 was not identified as a mixed disulfide with any members except for tpsn (Peaper et al., 2005). In contrast, PDI was seen in a mixed disulfide bond with one of the α2 cysteines when part of the PLC (Jensen, 2007; Park et al., 2006). Although argued, these observations allowed Ahn's group to suggest that the α2 disulfide is the target of PDI reductase activity when the MHCI are empty or loaded with suboptimal peptides (Park et al., 2006). In contrast, when the MHCI are loaded with optimal peptide, the α2 disulfide bond is protected from PDI. This seems to provide another quality control

mechanism resulting in the editing of peptide by favoring the ones with greater stability before leaving the PLC and being exported to the plasma membrane.

1.2.4. Functions of the PLC in the peptide loading of MHCI

As demonstrated by cell lines and KO mice (Garbi et al., 2000; Garbi et al., 2006; Grandea et al., 2000; Greenwood et al., 1994; Lehner et al., 1998; Stepensky et al., 2007), the loss of any PLC members decreases the efficiency of MHCI peptide loading with different magnitudes. As a consequence, pMHCI have lower stability and cell surface expression. In order to generate a strong and rapid CD8+ T cell response, every member of the PLC is required and each plays a role in facilitating optimal peptide binding by generating peptide receptive MHCIs and by increasing the availability of peptides. The translocation of self or foreign degraded proteins from the cytosol to the ER lumen is mediated by the TAP1-TAP2 complex (Cresswell et al., 2005). Since the MHCI binds only peptides of 8 to 11 residues, the action the ERAAP or ERAP1 peptidases can be required to trim longer translocated peptides prior to or concomitant to binding (York et al., 2006). It was proposed by the Ahn's group, that PDI serves as a peptide carrier and is critical for optimal peptide selection (Park et al., 2006). However, it is still ambiguous whether this is an indirect effect of the PDI peptide binding pocket protecting peptide degradation or if PDI is directly delivering peptide into the MHCI groove. Before MHCI can escape the PLC and egress to cell surface, they need to stably bind a specific peptide (Garbi et al., 2005). The Figure 1.9 illustrates the peptides' journey to the MHCI groove, the egress of pMHCI and their presentation to CD8+ T cells (Neefjes et al., 2011; Peaper and Cresswell, 2008; Wearsch and Cresswell, 2008).

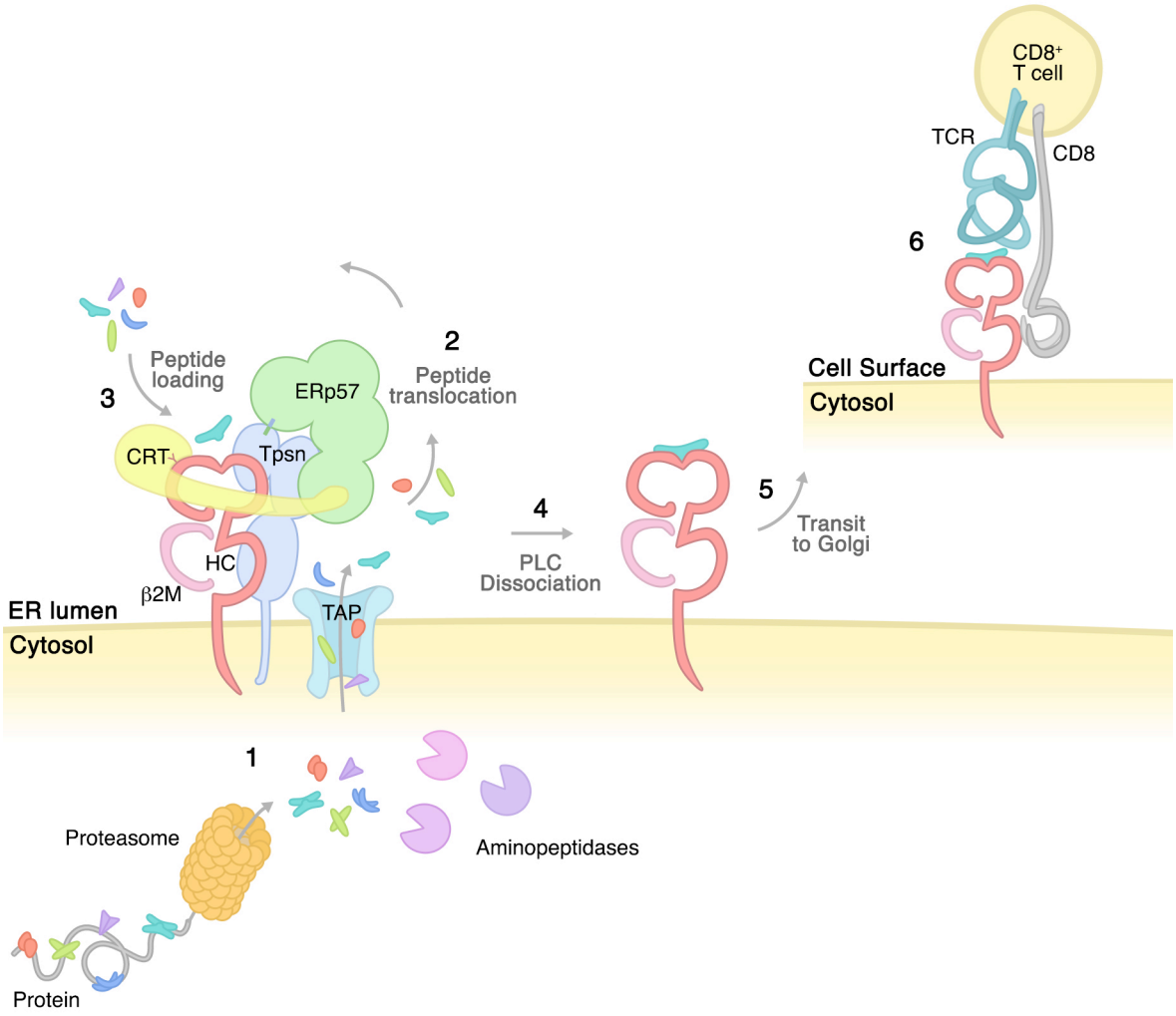

Figure 1.9: MHCI peptide loading and presentation

The presentation of pMHCI to CD8+ T cell starts by proteasomal antigen degradation and their subsequent trimming by a panel of aminopeptidases **(1)**. Those peptides are then translocated to the ER lumen **(2)** and through a tapasin-dependent manner, the loading complex facilitates the generation of highly stable pMHCIs **(3)**, leading to the release of loaded MHCIs and CRT from the PLC **(4)**. After a transit to the Golgi **(5)**, the MHCIs gain access to the plasma membrane and may present its associated-peptide to cognate $CD8^+$ T cells **(6)**.

1.2.5. ERp57-Tpsn and peptide exchange

The physical mechanism leading to efficient peptide loading is still unclear and depends on Tpsn. In addition to its supporting role, Tpsn was proposed to be a peptide exchange/editor like HLA-DM for the MHC of class II (section 1.3.4) (Hansen et al., 2005; Sadegh-Nasseri et al., 2008). Recently, the structure of Tpsn was determined by crystallography in complex with ERp57 (Dong et al., 2009) and provide the first insights as to what resembles the PLC Figure 1.10. Indeed, Dick et al. demonstrated that at steady state, all Tpsn was covalently bound to ERp57 (Dick et al., 2002). Thus, Peaper et al. suggested that the role previously described for Tpsn is a consequence of the Tpsn- ERp57 conjugate (Peaper et al., 2005). Briefly, by interacting with the HC α2 domain, Tpsn would stabilize the peptide binding groove in a peptide-receptive conformation. Given that Tpsn has a weaker affinity for pMHCIs, peptide-loading would initiate the dissociation of the MHCI from the PLC (Dong et al., 2009). The biophysical mechanism underlying this process remains hypothetical, but seems to be related to the oxidation of the α2 domain.

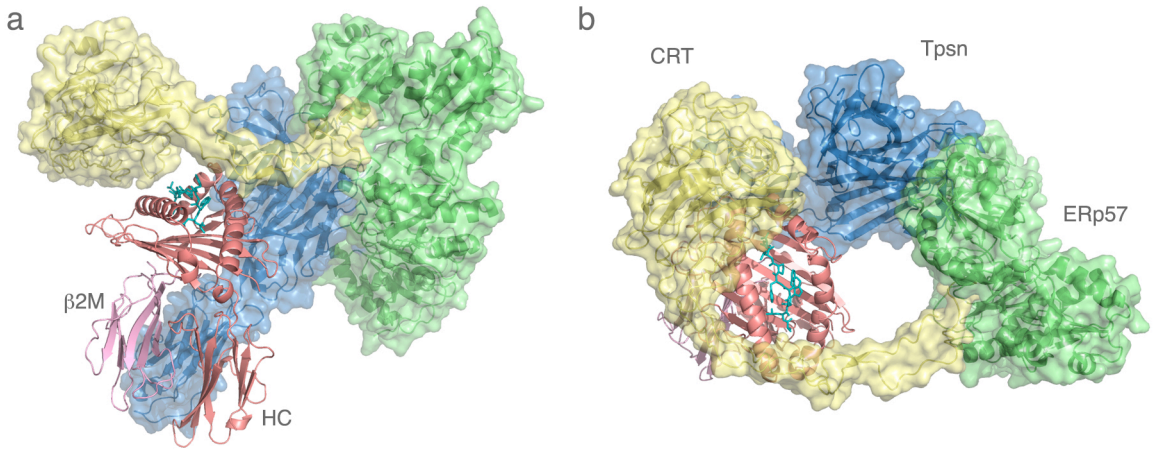

Figure 1.10: *In silico* model of the PLC

Reproduction of the PLC subcomplex model provided by Dong and colleagues (Dong et al., 2009). A side view (a) and a top view (b) of the multi-complex shows how the MHCI, Tpsn-ERp57 and CRT assemble together (1BOG, 3F8B, IJNH, respectively).

1.3. MHC class II

The molecules derived from the MHCII locus follow the same basic rule as MHCI molecules do; *i.e.* they require the work of many accessory proteins in order to present peptides to T cells. More specifically, this pathway relies on the invariant chain (Ii) and the non-classical MHCII molecule HLA-DM (DM), two chaperones leading to the expression of stable peptide-MHCII complexes (pMHCII) at the plasma membrane. Upon synthesis in the ER, Ii associates with MHCII and targets the resulting complex to the endosomal/lysosomal compartments, commonly termed MIIC, which stands for MHCII compartments (Rudensky et al., 1994). There, Ii is sequentially degraded until only the class II-associated invariant chain peptide (CLIP) portion remains in the MHCII binding groove (Cresswell and Blum, 1988). Following Ii degradation, DM facilitates the exchange of CLIP for antigenic peptides onto MHCII (Denzin and Cresswell, 1995; Sherman et al., 1995; Sloan et al., 1995). The resulting pMHCIIs then egress to the cell surface where they can ultimately meet cognate TCRs. A basic model of those events is presented in Figure 1.11. Then, the forthcoming subsections describe in further detail the steps involving the MHCII chaperones within MHCII's genesis and the various steps encompassing peptide loading.

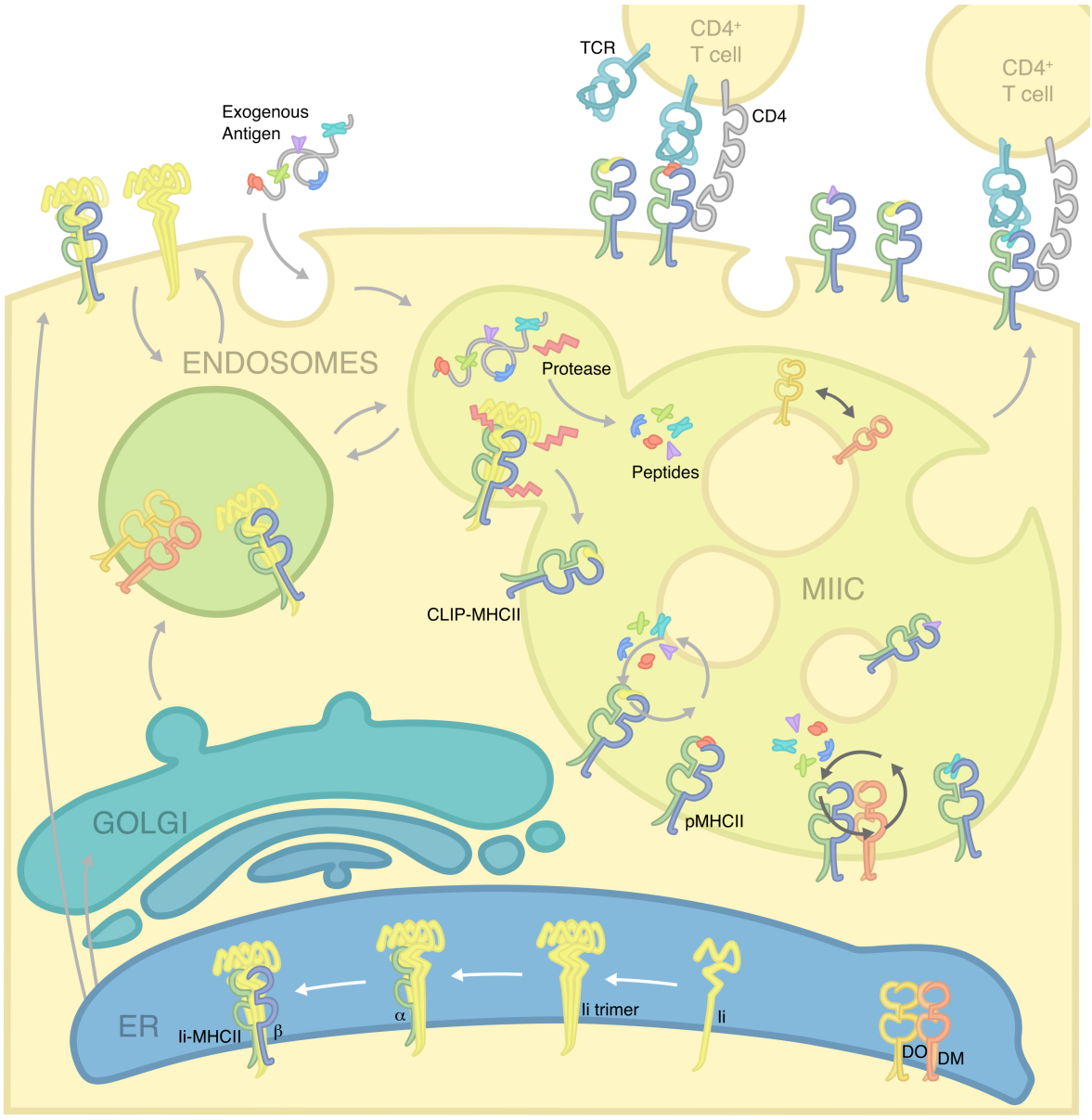

Figure 1.11: MHCII pathway

General portrait of the MHCII antigen processing and presentation. MHCII chains assemble in the ER with Ii. Ii-MHCII complexes transit through the Golgi before gaining access to the MIICs, either directly and/or via the plasma membrane. Endocytosed proteins and Ii are degraded by MIICs' resident proteases. The remaining Ii peptide CLIP is then exchanged for an antigenic peptide with the help of DM. Finally, MHCIIs egress to the plasma membrane to present their antigenic peptides to $CD4^+$ T cells.

1.3.1. MHCII isotypes

To simplify the content, I made used of MHCI and MHCII acronyms to describe the MHC molecules, omitting to introduce the MHC isotypes and their polymorphism. In human, there are three MHCII isotypes: HLA-DP, -DQ, and -DR and so far, over 870 allotypes are identified (European Bioinformatics Institute; www.ebi.ac.uk). Most of the polymorphism occurs on the β chain β1 domain and those variable residues either protrude toward the peptide-groove or the TCR binding site (1.1.6. Peptide-binding groove). Such variations of the side chains generate distinct pockets that will accommodate more fitting peptides, increase the number of peptides that can efficiently bind MHCIIs. Because of the differences between the MHCII allotypes, their relation with Ii or DM can be compromised. For example, some allotypes are refractory to DM-mediated peptide exchange and others are poor or great binding of the CLIP peptide (Busch et al., 2005).

1.3.2. Invariant chain: folding, targeting, protecting and editing

The first steps of Ag presentation begin with the generation of MHCII molecules and their association with the invariant chain (Ii). Also called CD74, Ii is a type II transmembrane glycoprotein that self-assembles into homotrimers. Ii trimerization is driven by both its transmembrane and carboxy-terminal trimerization domains (Figure 1.12) (Gedde-Dahl et al., 1997; Jasanoff et al., 1999a). In human cells, an alternative start codon and exon splicing give rise to 4 isoforms, named Iip33, -p35, -p41 and -p43, based on their molecular weight (Arunachalam et al., 1994). The shortest form of Ii is the most abundant and has two major immunological functions. Firstly, it is a MHCII chaperone that assists folding, facilitates ER egress and protects the MHCII-peptidic groove from premature peptide binding (Matza et al., 2003). Secondly, it is a receptor for cytokine and bacteria (Beswick, 2009).

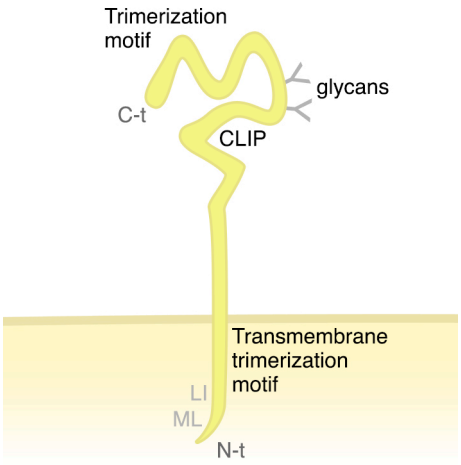

Figure 1.12. Invariant chain

Schema of Ii. Two motifs facilitate Ii trimerization and a di-leucine sorting motif directs Ii to the endosomes. The glycans at position 113 and 119 are also shown.

While my dissertation mostly revolves around Ag presentation, emphasis is set toward the participation of Ii in MHCII maturation and its influence on the nature of the forthcoming associated peptide. The invariant chain's major role is to assist the folding of MHCII and in doing so, prevents their self-aggregation. Yet, the sequence of events leading to their binding remains controversial. To date, the most appreciated dogma revolves around a nonamer $(\alpha\beta Ii)_3$ composed of three paired MHCII $\alpha\beta$ heterodimers that associate with a Ii homotrimer (Roche et al., 1991a). However, recent data suggest that Ii homotrimers would initially bind MHCII α chain, thus facilitating the subsequent pairing of β chains of the same isotype, as schematized in Figure 1.13. This revised theory originates from Koch's group, who also pushed the hypothesis that once a primary $\alpha\beta$ dimer is bound to Ii, a conformation change ensues and prevents the binding of additional MHCIIs (Koch et al., 2007). In other words, the binding of one MHCII dimer would lock the Ii scaffold into a MHCII-refractory conformation generating only $\alpha\beta Ii_3$ pentameric complexes. These results, obtained from mouse APCs, do not correlate with those obtained in human, in which nonameric complexes were formerly observed (Roche et al., 1991a). Interestingly, the human p35 Ii variant includes a RXR ER retention signal that could explain this incongruity between both species. A thorough description demonstrating Iip35 participation in nonameric complex formation is provided in the Annex I.

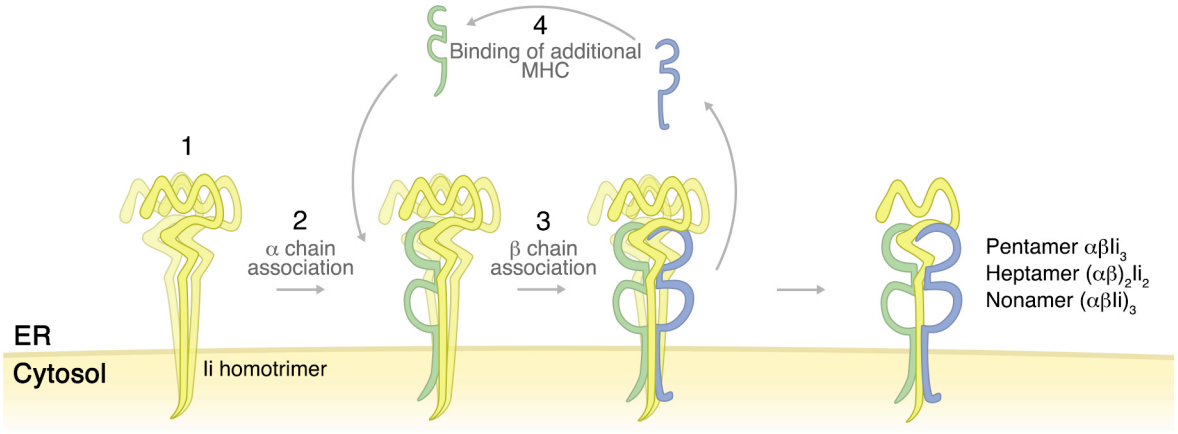

Figure 1.13: Ii association with MHCII

MHCII chains binding to the invariant chain. Ii self-assembles into a homotrimer **(1)** prior to the binding of a first MHCII α-chain **(2)**. Then, a MHCII β-chain of the same isotype associates with the αIi_3 scaffold **(3)**. Subsequent cycles of MHCII binding may happen **(4)**, forming heptameric or nonameric complexes

The p35 isoform contains a 16 aa amino-terminal extension that provokes the sequestration of Ii trimers in the ER via a RXR motif (Schutze et al., 1994). Work by a colleague has demonstrated that this di-arginine motif is masked by DRβ cytoplasmic tail upon association with Ii (Khalil et al., 2003, 2005). Consequently, in the instance of mixed Ii-trimers, *i.e.* between the p33 and p35 isoforms, Ii-MHCII complexes may be retained in the ER until sufficient β chains overcome every p35 motif. The period that Ii spends in the ER is then prolonged, providing the necessary time for the binding of subsequent MHCIIs, giving rise to nonamers (Annex 1). Indeed, it is easy to picture a situation in which MHCIIs, outnumbered by Ii (Marks et al., 1990), exit the ER as pentamers before the formation of saturated nonameric complexes, a phenomenon that may have been overlooked in mouse cells. Overall, Ii assembles into homotrimers and provides the scaffold for the efficient pairing of MHCII chains. Then, in the form of partially or fully packed $Ii_3(\alpha\beta)_{x=1-3}$ complexes, MCHII molecules gain access to the endosomal compartments.

Guided by two leucine-based motifs within Ii's cytoplasmic tail, Ii-MHCII complexes egress from the ER to the MIIC (Bakke and Dobberstein, 1990). There, the increased acidity and presence of proteases allow for Ii degradation, which occurs in a highly coordinated fashion. This process frees MHCIIs from Ii's scaffold and to leave only a small portion of Ii, the class II-associated Ii peptide (CLIP), within the peptide-binding groove (Ghosh et al., 1995). The proteolysis steps, pictured in Figure 1.14, are as follow: the Ii luminal trimerization domain is cleaved first, followed by the trimming of the CLIP extremities, releasing MHCII heterodimers from Ii's grasp and mediated targeting. A subsequent cleavage generates the cytoplasmic fragment, reported to induce NFκB (Matza et al., 2001). At this point, newly generated MHCIIs may gain access to the plasma membrane to present CLIP. Conversely, as is the case with certain MHCII alleles, CLIP-MHCII complexes of short half-life may go through a round of spontaneous peptide exchange prior to their transport to cell surface (Jensen et al., 1999). Overall, homotrimeric Ii directs MHCII from the ER to the MIICs before being sequentially degraded.

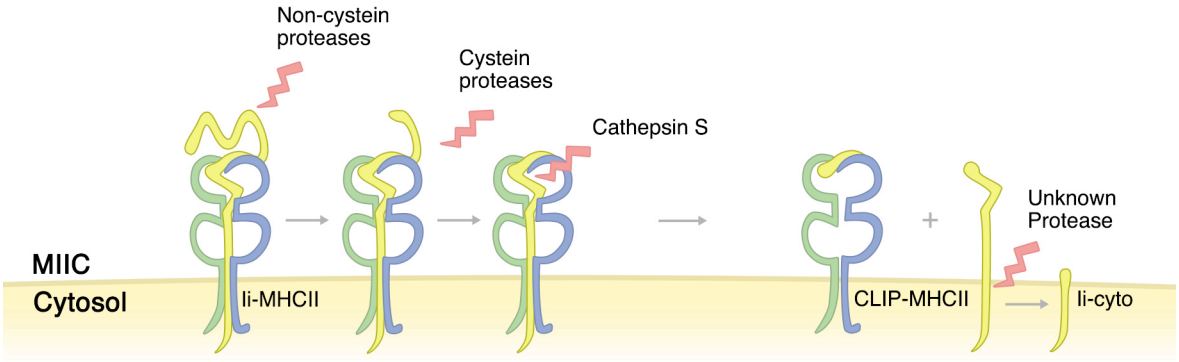

Figure 1.14: Ii degradation

Steps involved in the degradation of Ii. First, the carboxy-terminal trimerization domain is cleaved by non-cystein proteases, generating the p22 fragment. Then, cystein proteases remove the glycosylated portion to form the p10 fragment before cathepsins S cut the anchored portion, leaving the CLIP in the MHCII groove. The amino-terminal is further processed at the intramembrane generating a cytosolic fragment (Ii-cyto) with the ability to activate NFκB.

Since the eighties, Ii has mostly been viewed as the MHCII chaperone I just described. Today, such a role has been shaded by Ii versatility and its novel MHCII unrelated functions. Many studies have reported Ii expression in MHCII negative leukocytes, gastrointestinal (GI) epithelial cells and various carcinomas (Matza et al., 2003), which has led many to hypothesize new Ii roles. Chronologically, Shachar's group demonstrated that Ii cytoplasmic domain was involved in B cells' maturation by activating NFκB (Matza et al., 2001, 2002). Subsequently, Ii was found to be the macrophage migration inhibitory factor (MIF) receptor (Leng et al., 2003). Later, it was identified as *H. pylori* receptor, a bacterium that exploits Ii in order to adhere to GI cells (Beswick et al., 2005). The invariant chain does not possess domains capable of prompting signal transduction, but instead pairs up with CD44 and CXCR2, which accomplish this task (Bernhagen et al., 2007; Shi et al., 2006). A body of work is now available regarding the implication of Ii as a receptor and is addressed exhaustively in a recent review by Beswick and Reyes (Beswick, 2009).

Ii has also been shown to interact with CD70, CD1, DM and MHCIs, providing either chaperoning or targeting (Alfonso and Karlsson, 2000; Basha et al., 2012; Pierre et al., 2000; Sloma et al., 2008; Sugita and Brenner, 1995). Altogether, these data are in line with the fact that Ii does not necessarily sits inside the MHCII binding pocket. Indeed, Ii is able to bind single-chain peptide MHCIIs (Wilson et al., 1998). A body of work by the group of Hammerling, supporting this premise, has been put to second rank after the publication of the CLIP-DR3 structure.

By protecting the MHCII's groove and guiding them to the MIICs, Ii influence the pool of associated-peptides (Busch et al., 2005). In fact, the repertoire is strongly skewed in Ii KO mice, as demonstrated by mixed lymphocytes reactions (MLR) and aberrant $CD4^+$ T cell selection (Grubin et al., 1997; Tourne et al., 1995;

Viville et al., 1993; Wong and Rudensky, 1996). However, whether it is the different Ii isoforms or its ability to bind the MHCII isotypes with different affinities that is monitored, Ii's effect on the peptide repertoire varies. Moreover, upon degradation, the residual bound-CLIP peptide also participates in shaping the peptide's assortment to be presented to T lymphocytes.

1.3.3. CLIP's mission

As mentioned earlier, Ii prevents the aggregation of MHCII molecules and the binding of resident ER peptides. Following its degradation in the MIIC, this role is carried out by the associated-CLIP peptide, which, like a jack of all trades, has the ability to fit into any MHCIIs (Busch et al., 2005). To achieve such a feat, CLIP's side chains at position 1, 3, 7 and 9 are hydrophobic and not too bulky allowing torsional freedom that results in a promiscuous type of fitting (Figure 1.15). Those at positions 4 and 6 are very small and hydrophobic (Pro and Ala) thus adapted to avoid steric clash with the high polymorphism of these two pockets (Ghosh et al., 1995; Lee and McConnell, 1995).

Given CLIP's binding fashion, the half-life of CLIP-MHCIIs differs widely between MHCII alleles (Sette et al., 1995) and CLIP's protective effect can be compromised when part of short-lived complexes. In fact, there is a strong correlation between short half-life, auto-immunity and plasma membrane MHCII expression (Busch et al., 2005). Also, either very short- or long-lived complexes have debilitating effects on Ag presentation (Busch et al., 2005). Respectively, this may cause endogenous peptides to be over-represented on the cell surface, leading to auto-immunity or may prevent peptide exchange, leading to a homogenous population of CLIP-MHCIIs. Altogether, as a surrogate for peptides, CLIP helps restricting peptide exchange to DM+ MIICs, thereby ensuring a efficient editing of antigenic peptides (Rinderknecht et al., 2007, 2010).

The CLIP-MHCII structures determined so far only show the coreCLIP, *i.e.* residues 87-101, inside DR's groove and the amino-terminal residues 81-86 could not be resolved (Figure 1.15) (Ghosh et al., 1995; Günther et al., 2010). Vogt and coworker suggested that this extension, abbreviated herein as $CLIP_{81\text{-}86}$, folds back onto DRα α-helix while Neumann and Koch proposed it to interact with the DRβ Ig domain (Neumann and Koch, 2006; Vogt et al., 1995). Interestingly, binding to the β2 domain was observed only when CLIP was part of full length Ii, meaning that the polypeptide may behave differently once cleaved. Also, sequences rich in proline, as is the case for this extension, form rigid β-turns and would corroborate the former hypothesis.

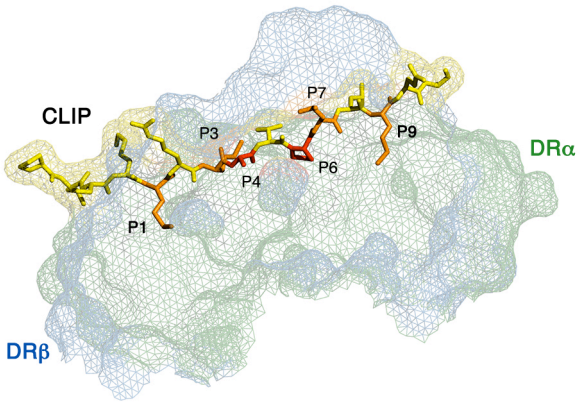

Ii CLIP 81-^{LPKPPKP}VSKMRMATPLLMQA-101

Figure 1.15. CLIP-MHCII

Slice of the CLIP-DR3 crystal's groove (1A6A). The MHCII α-chain, in green, is behind the peptide while most of the β-chain is sliced off. The CLIP side chains occupying the pockets p1, 3, 6 and 9 are shown in orange sticks. From this viewpoint, the $CLIP_{81\text{-}86}$ extension is predicted to flip into the plane, onto the α-chain.

The $CLIP_{81\text{-}87}$ portion has been reported to trigger peptide exchange via an allosteric self-release mechanism (Kropshofer et al., 1995a). Such function, mediated by the lysines (and the Pro87), seems to stem from the binding of those residues to an effector site on MHCII α-chain, disturbing the HBs of the P1 pocket (Chou et al., 2008; Kropshofer et al., 1995a, 1995b; Narayan et al., 2007; Vogt et al., 1995). This extension, later renamed helper peptide or Ii-key, has also been shown to improve the loading of antigenic peptide and was further refined by Kallinteris and colleagues to the following sequence:

LRLKLPK (Kallinteris et al., 2006; Perez et al., 2010a; Xu et al., 2012). It has also been used in phase I clinical trials against prostate cancer and may prove to be a very effective “adjuvant” (Perez et al., 2010b). Overall, the role of CLIP is twofold; i) it prevents MHCIIs from collapsing and facilitates its own release. This leads to a better editing of antigenic peptide by DM and provides an alternative to counter long-lived CLIP-MHCIIs by prompting self-release. As mentioned above (section 1.1.7), HBs are formed between the 3_{10} helix and the portion of CLIP extending further outside of the pocket 1 (Günther et al., 2010). Knowing how important these HBs are to keeping CLIP in the canonical orientation, it is possible that the CLIP/Ii key extension promotes the peptide self-release by disturbing the 3_{10} region’s HBs like DM (Stratikos et al., 2004).

1.3.4. DM functions

While the main function of DM is to improve peptide exchange (Vogt et al., 1996), thus editing a repertoire of stable pMHCII (Kropshofer et al., 1996), DM also has the important task of chaperoning empty MHCII and DO (DO: see section 1.3.5). Empty MHCIIs are very unstable complexes (Stern and Wiley, 1992) and depend on DM’s rescue in order to maintain their ability to bind peptides (Denzin et al., 1996; Kropshofer et al., 1997a) Based on these observations, one could hypothesize that DM only recognizes “peptideless” MHCII. Indeed, DM’s interaction with many stable high affinity pMHCII (e.g. DR1-HA) seems to be inexistent and thus is dependent on its occupancy state (Anders et al., 2011; Sloan et al., 1995; Vogt et al., 1996). To gain insights regarding DM’s mode of action, the Mellins group used a mutagenesis approach and identified critical residues on DR3 that disrupted its interaction with DM (Figure 1.16) (Doebele et al., 2000; Pashine et al., 2003). Two of those residues were located in a flexible loop, the 3_{10} helix (Figure 1.1d), that connects the α-helix to the platform of the MHCII cleft. Therefore, it has been suggested that this specific MHCII region undergoes conformational changes

upon peptide association/dissociation and that DM recognizes it in the absence of a bound peptide (Hansen and Fremont, 2005). A model, proposed by Stern's group suggest that DM recognize a disordered 3_{10} helical region, which does not yet form HBs with the peptide backbone (Painter et al., 2011; Stratikos et al., 2004). The interesting feature of the 3_{10} helical region nearing the p1 pocket is the presence of many highly conserved phenylalanines; three on the 3_{10} helix, three on the founding β-sheets and one on the β chain. They are reported to adopt different conformation based on the p1-filling residue (Chervonsky et al., 1998). Since it is repositioned upon DM contact, the 3_{10} helix could serve as a hinge, disturbing the HB network that tethers the peptide (Guce et al., 2012). However, it is difficult to conceive that DM can promote peptide release while interacting only with empty MHCII.

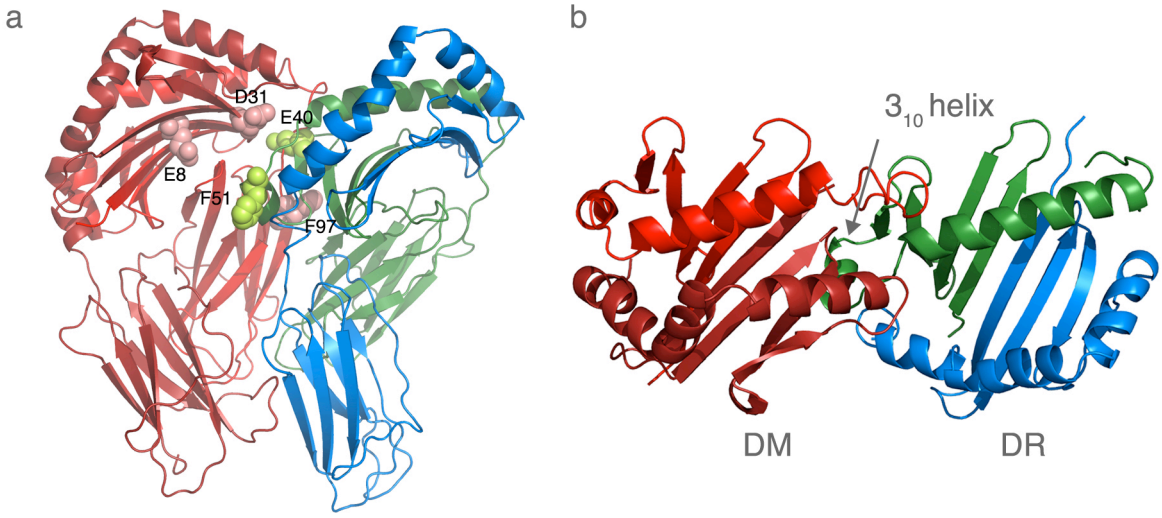

Figure 1.16: DM-DR binding interface

Model of the DM-DR (2BC4 and 16A6) binding interface based on the mutagenesis studies by Mellins' group and the ternary structure of DM-DO (Doebele et al., 2000; Guce et al., 2012; Pashine et al., 2003; Yoon et al., 2012). A side by side view (a) is given beside a top view (b). The aa implicated in DM's function are shown in light green and light red.

In order to understand how DM is able to interact with MHCII and thus promote peptide exchange, it is important to consider that the peptide binding to MHCII is a dynamic and cooperative event in which both the MHCII and the peptide fold together, the latter highly pH-sensitive (Sadegh-Nasseri and Germain, 1992; Yaneva et al., 2009). This allows a transient state between partially and completely bound peptide in function of pH. Consequently, because of the intrinsic behavior of MHCIIs, DM is able to interact with pMHCIIs that are not completely bound but still display DM binding (Schulze and Wucherpfennig, 2012). The interaction between DM and MHCII leads to the opening of the MHCII groove into a more favorable and receptive conformation for peptide binding and facilitates this cooperative refolding (Figure 1.17). Evidence suggested that the appropriate filling of the P1 pocket is the triggering event for pMHCII to adopt a DM resistant form (Chou and Sadegh-Nasseri, 2000; Narayan et al., 2007; Sadegh-Nasseri et al., 2008, 2012). However, another study based on multiple MHCII alleles and peptides has shown that interactions along the entire length of the peptide binding groove contribute to DM susceptibility (Belmares et al., 2002). This likely suggests that the P1 model may be an oversimplification that only applies to certain MHCII alleles. Indeed, promiscuous fitting at the P9 pocket has been shown to also affect DM mediated peptide exchange synergically to P1 (Stern L., personal communication). Overall, DM's functions are likely a consequence of its capacity to generate open, peptide-receptive MHCIIs. This open conformation increases the peptide exchange rate and allows MHCII to screen multiple peptides, favoring the ones inducing the conformational change required to mask DM's binding epitope and that have greater kinetic stability. However, the physical mechanism underlying DM function remains unclear partly because of the lack of a solved crystal structure MHCII-DM complex.

At the same time that DM promotes peptide exchange, it also edits the peptide repertoire (Busch et al., 2005; Kropshofer et al., 1997b; Lazarski et al., 2005; Vogt and Kropshofer, 1999). In a recent report, it was demonstrated that antigenic epitopes presented by MHCIIs in the presence of DM are more likely to engender CD4+ T cell response in the context of a virus infection (Yin et al., 2012a). Furthermore, these complexes are more refractory to DM-mediated dissociation, a correlate of their longer half-life ($t_{1/2}$), which is a distinguishing feature for T cell recognition. This study is doubly elegant, as it shows that the biophysics property of a pMHCII population does not always reflect the T cell response that it engenders, nor the immunogenicity (Lazarski et al., 2005). pMHCIIs' immunogenicity can be classified in two groups; one is refractory to DM and the other is sensitive (Kremer et al., 2012). Thus for the APC, it is essential to control the contribution of Ii, DM and DO to give rise to both types of pMHCII complexes and preserve homeostasis.

The group of Wucherpfenning just crystalized the DR-DM ternary complex, using a partially filled DR molecule (Pos et al., 2012). To succeed, they covalently linked a small peptide that occupied the DR pocket only from P4, thus allowing DR to display a DM-sensitive form and leading to strong binding between those two molecules. Also, to prevent DM from releasing the bond peptide and keep the complex stable, the peptide is trapped by a disulfide bond between the p5 residue and the α chain residue V65, which is mutated to a cysteine. Interestingly, the structure is very similar of the DO-DM complex isolated by Guce and colleagues and also implicated the 3_{10} helix to fold back into the peptide-binding groove, exchanging the αW43 P1-filling residue for αF51 (Guce et al., 2012).

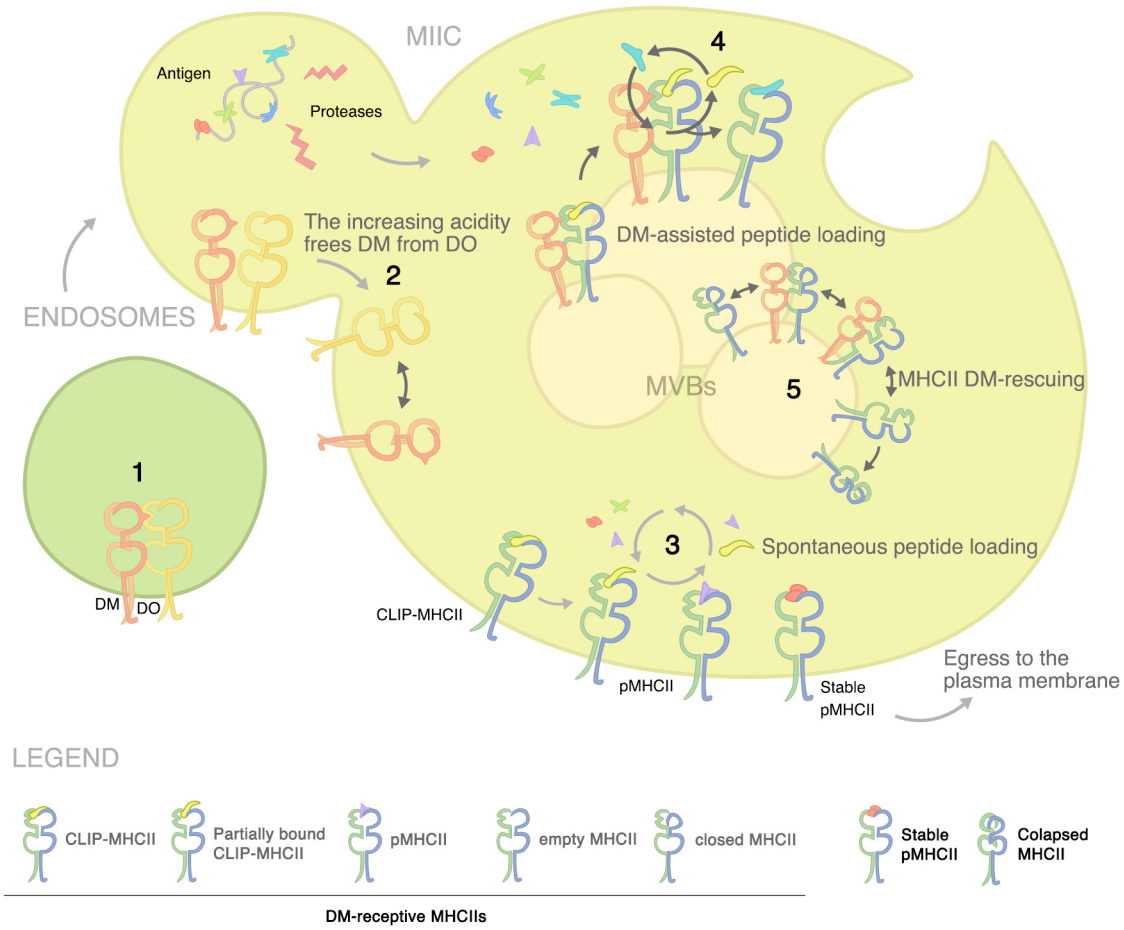

Figure 1.17: Peptide exchange

In DO^+ cells, DM-DO complexes egress from the ER to the MIICs **(1)**, in which the increased acidity provokes their dissociation **(2)**. There, spontaneous peptide release and loading occurs due to continuous peptide motion and provides a pool of MHCIIs with partially-bound peptide, susceptible to DM binding **(3)**. DM-binding site is pictured as a slot on the cartoon's MHCII α-chain. Next, DM facilitates the release of the remainder of the peptide **(4)** while the resulting DM-empty MHCII complexes can bind new peptides with very rapid kinetics. Weak MHCII binders will go through many cycles of peptide editing by DM, until strong binders induce its dissociation. These stable pMHCIIs may be displayed on the cell surface for many days depending on the APC. In parallel, DM also rescues empty-MHCII before they collapse **(5)**.

1.3.5. HLA-DO

In contrast to DM, which promotes peptide exchange, a second MHCII-like molecule hinders this effect. DO is a non polymorphic heterodimer which directly interacts with DM (Liljedahl et al., 1996). Upon synthesis in the ER, DO does not efficiently bind Ii (Karlsson et al., 1991; Liljedahl et al., 1996), like the MHCIIs, and refolds poorly. Therefore, in order to avoid rapid degradation, DO associates with DM, thereby enabling its proper folding and exit from the ER (more detail in chapter 3). Finally, in the endosomal compartments, DO prevents DM from exchanging peptide.

The manner by which DO impedes DM activity is just starting to unfold, but still remains a matter of debate. Most current theories regarding DO mechanism claim that the DO-DM complex remains associated along the endosomal pathway where DO partially or totally inhibits DM function in a pH-dependent manner (Alfonso et al., 1999; Brocke et al., 2002; Van Ham et al., 1997; Hammond et al., 1998; Jensen, 2007; Kropshofer et al., 1998, 1999; Liljedahl et al., 1998). Therefore, this model argues that DM is greatly inhibited in the early endosomal compartments, but only partially in the late, more acidic ones. A strong argument for this model was the presence of trimolecular complexes containing DO, DM and MHCII, and immunoprecipitation of DO by MHCIIs (Hammond et al., 1998). A second hypothesis is that DO is an empty MHCII and that it has higher affinity than MHCII for the DM binding site. This paradigm is supported by the concept of DM function *per se*, which binds and chaperones empty MHCIIs, and by other indirect evidences: firstly, DO shares more than 60 % homology with MHCIIs; secondly, as for DR, the same conserved glutamic acid (α40) on DO is essential for DM interaction (Deshaies et al., 2005); thirdly, in the absence of Ii, DM is able to rescue MHCII to exit the ER (Serradell et al., 1999). Based on these observations, it has been suggested that DO is a permanently empty MHCII that monopolizes DM

chaperoning capability, thereby preventing DM from associating with MHCII. Although a common misbelieve, acidification in the later stage of the endosomal pathway is not what inactivates DO or dislocate it from DM. In the MIICs, DO-DM complexes remain associated in the limiting membranes while DR-mediated peptide exchange occurs in the vesicles (Lith et al., 2001; Zwart et al., 2005). In addition, the interaction between DM and DO is very tight (personal communication - SPR experiments) and never dissociate, as it is the case with empty DR1 (Anders et al., 2011). Whether a ligand, only present in the MIICs, has the ability to bind DO and initiate a conformational change that liberates it from DM or whether those DO-bound DM molecules are doomed remains to be investigated.

Recently, in a fruitfull collaboration, the Stern and Mellins groups were able to co-crystalize DM and DO together (Guce et al., 2012). The ternary complex corresponds with initial mutagenesis studies supporting the competition model and suggesting molecular mimicry (Deshaies et al., 2005; Doebele et al., 2000). In light of their results, whether the previously observed interaction between DO and MHCIIs or DO-DM-MHCIIs are genuine remain to be confirmed, interactions that could be mediated by the transmembrane domains or other accessory proteins. In addition, knowing that empty MHCIIs tend to collapse, those trimolecular complexes may either be intrisic to their occupancy state or the tip of a yet to be discovered function of DO toward MHCIIs. On another note, van Lith and co-worker previously reported that DO could egress to the cell surface with the MHCI HC (Van Lith et al., 2003). This peculiar association is mostly observed in overexpression system and yet, no role has yet been proposed. Thus it remain possible DO escape ER-quality control once stabilized by MHCI HC in a manner similar to DM. Conversely, as mentionned previously, empty MHC molecules tend to aggregate (Arimilli et al., 1999; Ruffet et al., 2003).

1.3.6. Peptide editing by DO

The foregoing section 1.3.4 briefly introduced the impact of DM on the MHCII presentation. This will now be further developed including the role of DO, to provide a broader outlook. Until now, the role of DO on IRs is vague and it is surprising that giving all the recent structural data its function has not gotten clearer. Interestingly, the expression pattern of DO is quite unique and mostly confined to B cells, thymic epithelial cells, and certain types of primary DC, but not monocyte-derived DC, upon maturation stimuli. Many studies have suggested that DO could differentially select certain peptide epitopes, but the experimental model chosen could always be criticized and do not reveal its purpose (Alfonso et al., 2003a, 2003b; Liljedahl et al., 1998; Perraudeau et al., 2000). In a recent paper, Gu and coworkers stress the point that DO favors presentation of exogenous Ags while reducing autoimmunity (Gu et al., 2012). In this recent article, they confirmed that the concentration of CLIP-MHCIIs at the cell surface of $DO^{-/-}$ B cells is significantly lower than on *wt* cells. Thereby, peptide exchange is more extensive on MHCIIs in the absence of DO. What was really striking, however, was that $DO^{-/-}$ produced higher titers of auto-reactive-Abs, a skewed CD4+ T cell repertoire and a propensity to auto-immunity. Thus, DO edits qualitatively the different self-peptides that are presented to CD4+ T cells.

1.3.7. Ways to load peptides onto MHCIIs

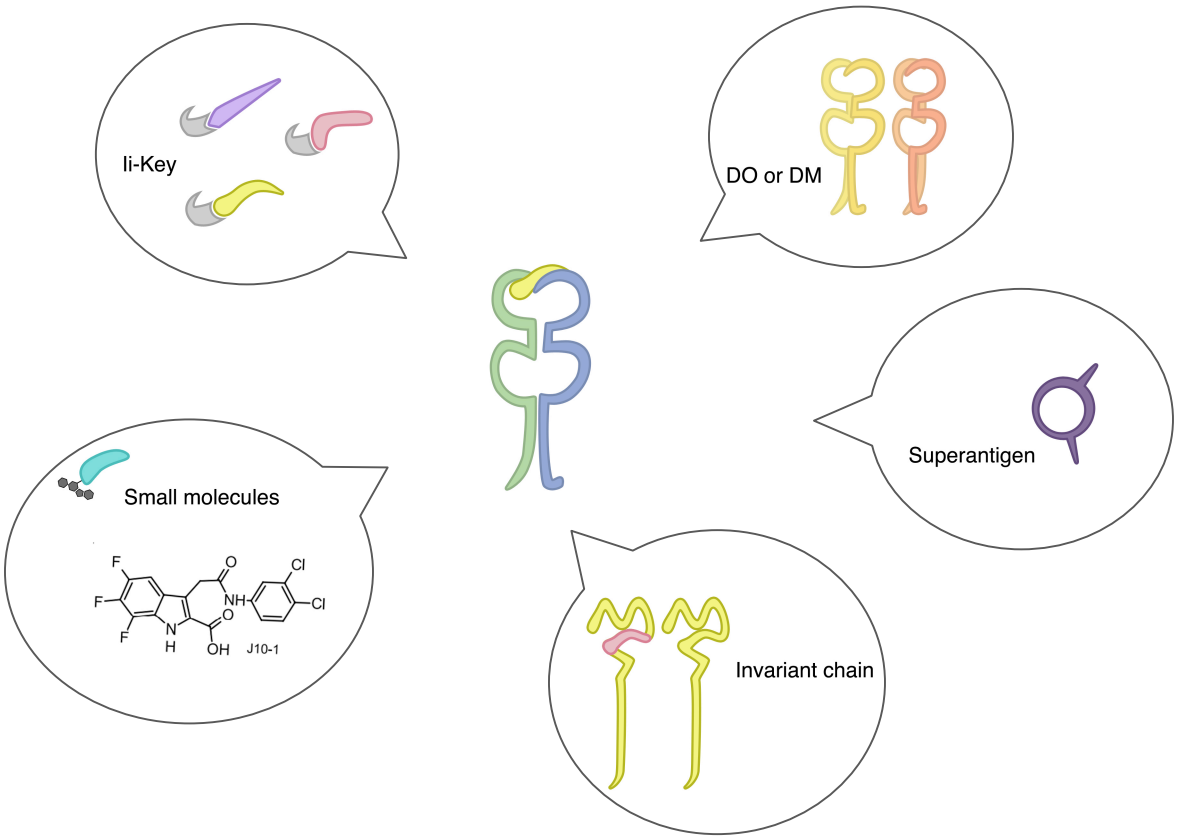

Figure 1.18: Ways to manipulate MHCII peptide loading

Manipulate the pMHCII populations with DMY (Pezeshki et al., 2011)

Increase the potency of peptide vaccines with Ii-Key (Gillogly et al., 2004; Humphreys et al., 2000; Perez et al., 2010a, 2010b; Xu et al., 2012)

Increase peptide loading with peptide bound to J10 compounds (Call et al., 2009)

Single-chain peptide-Ii-MHC construct to load peptides (Thayer et al., 2003a)

mAb-SAG hybrids as cancer vaccine or peptide carrier (Dohlsten et al., 1994; Han et al., 2011; Loh, 2006)

1.3.8. SAGs binding to MHCIIs

In addition to binding small antigenic peptides, MHCIIs are also the ligand of a family of small proteins called superantigens (See Section 1.5. Superantigens). In contrast to the former, SAGs do not interact with MHCII's peptidic groove but rather bind solvent-exposed residues located onto MHCII α-helixes. They bind relatively non-polymorphic regions and thus can be presented by numerous MHCII alleles. SAGs binding mechanism is hypothesized to rely on MHCII overall structure rather than conserved-residue interaction and supported by the affinity hierarchy of SAGs toward the different MHC isotypes (DR > DQ > DP), (Li et al., 1998a). In addition, little to no structural alterations were observed from crystallized SAGs, whether alone or as part of a complex, supporting the idea that they are dependent of the MHCII conformation (Fraser and Proft, 2008).

A decade of data on quaternary structures and *in silico* models has provided insights on strategies used by SAGs to bind MHCIIs and are depicted in Figure 1.19. So far, three major mechanisms have been identified. SAGs may bind a) MHCII α-chain, b) an epitope composed of the α-chain and the associated-peptide or c) the β-chain's HIS81 through coordination of a zinc ion (Sundberg et al., 2007). A handful of SAGs also have the ability to cross-link or oligomerize MHCIIs by using both α and β-chain binding sites. Yet, the magnitude of the oligomerization remains unknown (Bueno et al., 2007). In addition to the bSAGs' three binding modes, the SAG *Mycoplasma arthriditis*-direved mitogen (MAM) binds the MHCII orthogonally, contacting the α-chain, the peptide and the β-chain (Figure 1.19d) (Zhao et al., 2004). More details about SAGs are provided in sections 1.4.7 and 1.5, which describe how they cross-link TCR in order to activate T cells and summarize their features, respectively. First, however, a look at the TCR is called for.

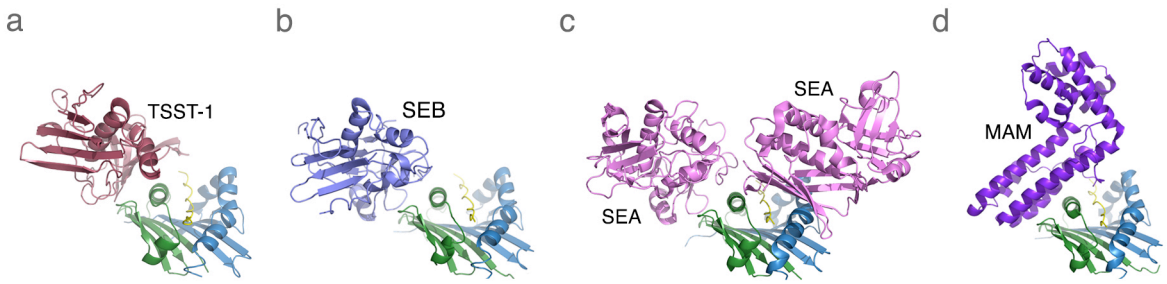

Figure 1.19: SAG binding strategies onto MHCII

Different modes by which SAGs interact with MHCIIs. **(a)** Interaction with MHCII via the α-chain and the associated-peptide (TSST-1, 2TSS). **(b)** Interaction of SAG with the α-chain (SEB, 1SEB). **(c)** Interaction of one SAG molecule with two MHCIIs; one via the β-chain using the high-affinity zinc site, the other via the α-chain (SEA, 1L05 and 1HXY (SEA was superimposed over SEH in the SEH-MHCII complex (Petersson et al., 2002))). **(d)** Binding of the SAG using the MHCII α-, β-chain and the peptide altogether (MAM, 1R5I). As usual, MHCII α- and β- chains are green and blue and the associate-peptide is yellow.

1.4. T cell receptors

Exploring the influence of associated-peptide or SAG on antigen presentation obliges a thorough structural and biophysical understanding of the T cell response. This cellular response depends on a highly sensitive and educated multi-receptor complex (Figure 1.20), composed of the T cell receptor (TCR) and CD3 chains to spot the insanely vast pMHC repertoire (Rudolph et al., 2006). Taken separately, TCRs serve the purpose of recognition while the many monomorphic CD3 components that participate in signal transduction alongside the CD4 and CD8 co-receptors. Much like MHCIIs, each TCR chain is composed of a αβ heterodimeric ectodomain anchored to the plasma membrane by a transmembrane region, followed by a small cytoplasmic tail (Davis and Bjorkman, 1988). The ectodomain is composed of variable and constant Ig-like folds analogous to Abs and are very specific pMHC ligands. TCR's ability to recognize pMHC appears to have occurred 400 millions years ago and is mediated via the TCR complementary determining regions (CDR) (Scott-Browne et al., 2011). Herein, most of the listed data reflect αβ TCRs associated with classical MHCs. These data may not govern the engagement of αβ and γδ TCR to non-classical MHC molecules, which seem to use a combination of canonical and unique

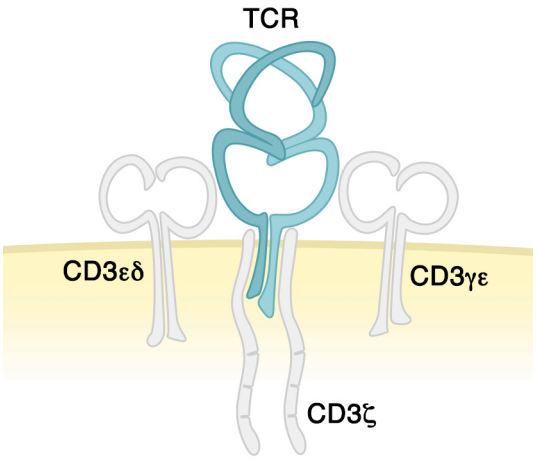

Figure 1.20. TCR-CD3 multireceptor complex

A handful of interactions allows the CD3/TCR multimeric complex to form. The transmembrane domains of the TCR and CD3 chains contain nine conserved charged residues that link the CD3 subunits in this manner: α-ε-δ, β-ε-γ and α-ζ-ζ. For simplicity, these exact contacts are not preserved in the 2D cartoon depiction.

strategies (Wucherpfennig et al., 2010).

1.4.1. TCR variability / Variable regions

In order to extend the finite genomic information into extremely diverse receptors, the immune system recombines and edits germline-encoded segments (Morris and Allen, 2012). In a process that is developmentally regulated (thymic selection), T lymphocytes generate the TCR by recombining the V(D)J segments of the locus encoding the ~80 TCRβ, and the VJ segments of the locus encoding the ~60 TCRα chains (Davis, 1990; Wilson et al., 1988). In human, the Vα region is classified into 22 subfamilies, 15 of those containing a single member. The Vβ region, for its part, is classified into 20 subfamilies and only 7 contain a single member. The Jα and Jβ regions include 46 and 13 gene segments of 16 to 25 and 15 to 17 aa, respectively. In addition, there are two Dβ regions that account for the addition of 3-4 aa to the Vβ CDR3 (Wilson et al., 1988). Since they do not go through recombination and editing, the TCR CDR1 and CDR2 loops preserve the germline-encoded information for interacting with MHCIIs (see also section 1.4.7). In contrast, the high diversity of the CDR3 loops linked to the V(D)J gene rearrangement allows for the TCR's ability to recognize the limitless pool of antigenic peptides (Bridgeman et al., 2012).

1.4.2. Complementary determining regions

Structurally, CDRs are flexible loops formed by the antiparallel β sheets junctions of the distal TCRs' Ig domains (Figure 1.21). The seemingly symmetrical TCR α and β chains, held together by a cystine bridge, draw both CDR3s at the reflection axis, *i.e.* the center of the heterodimer (Bentley et al., 1995; Garboczi et al., 1996; Garcia et al., 1996). This positions the CDR1 loops next to the TCR center and the CDR2 loops at the edge of the receptor. It is also noteworthy that

there are multiple interchain contacts between the TCR' CDRs. These interactions can occur between the two CDR3s loops or between the residues of the CDR3 and those of the CDR1 and CDR2. Reflecting those interchain contacts, different CDR rotamers exist for a given chain when paired with distinct partners (Gras et al., 2010; Pellicci et al., 2009). Thus, TCR's plasticity stems partly from the CDRs' aa variability.

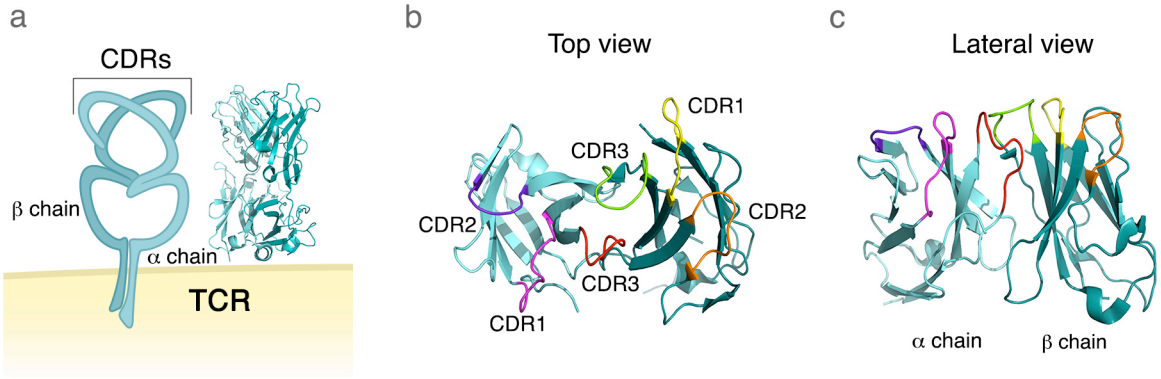

Figure 1.21: Complementary determining regions

Overview of the TCR structure and CDRs. **(a)** A cartoon depiction of the TCR is shown beside the crystal structure of the HA1.7 TCR (1FYT). TCR α and β chains are colored cyan and teal, respectively. **(b)** Top view of the TCR, as if the reader is the pMHC. The CDRs are magenta, purple and red for the alpha chain and yellow, orange and lime for the β chain. (c) A 90° angle rotation toward the slate showing the lateral face of the TCR. The CDR3s are at the center of the heterodimers while the CDR2 are distal.

1.4.3. TCR flexibility

Probably the most impressive feature of TCRs is the ability to recognize the massive quantity of peptide-associated MHC complexes with limited genetic polymorphism. It is commonly accepted that this limitation can be overruled by the TCR's structural flexibility. Interestingly, this characteristic was formerly hypothesized to be a mechanism to explained thymic selection following the determination of the first TCR-MHC structure in 1996 (Garcia, 1998). More

recently, studies have revealed that TCR V-domains may adopt alternate conformations to fit both MHC classes differentially independently of the positive or negative selection (Gascoigne, 2011; Stadinski et al., 2011; Yin et al., 2011). Other structural data have also indicated that the same TCR successfully engages distinct pMHCs and does so using exclusive strategies (Colf et al., 2007). Alternatively, there are also examples of distinct TCRs capable of binding the same pMHC in a different manner (15-16 du review 2011). Furthermore, it is reported that by differentially combining α and β chains, TCRs may vary their plasticity in order to bind a larger pool of pMHC (Stadinski et al., 2011). The following schema (Figure 1.22), inspired by Gascoigne's, offers a simplified mechanism behind this plasticity.

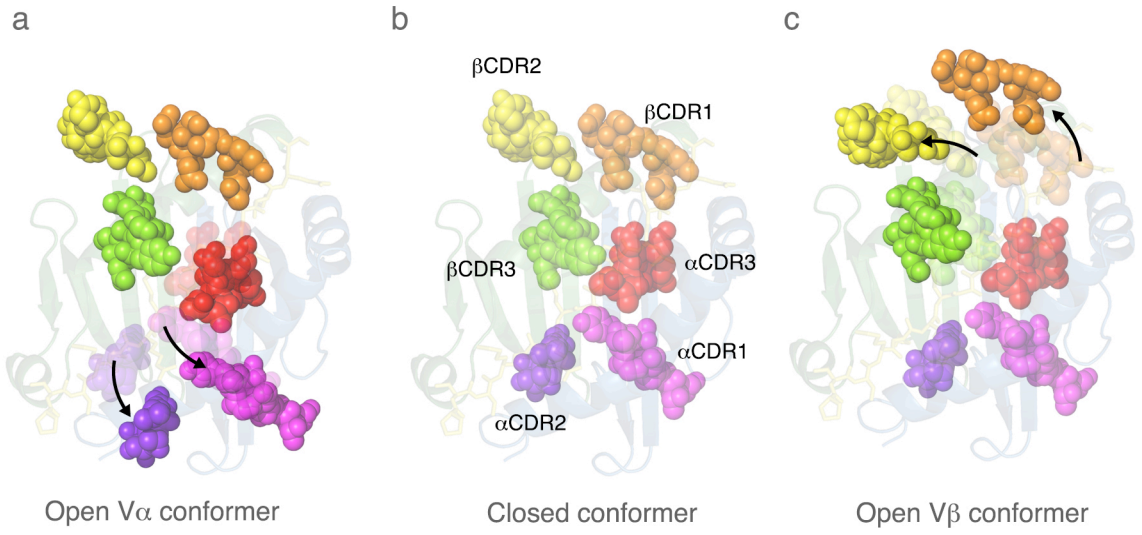

Figure 1.22: TCR flexibility

This schematic illustrates how the same TCR can give rise to three different conformers. **(a)** The closed conformer is the structure that has been most often encountered in TCRs, whether bound to ligand or free. Rotation in the J region of the V domain relocates the CDR1 and CDR2 out and away from the other chain's CDRs and is possible for both Vα and Vβ domains **(a and c)**. This rotation, in the range of 8° to 12° relative to their position in the closed conformer, results in the CDR'S distal residues to move by about 4Å. The CDRs' open conformers are superimposed on the CDRs's closed conformer, shown in paler hues.

1.4.4. Docking onto pMHC and geometry

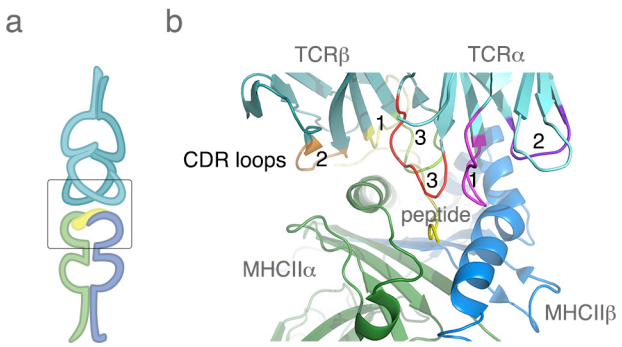

Figure 1.23. CDRs docking on MHC

Lateral view of the TCR on top of pMHCII (1FYT). The CDR loops of the Vα and Vβ domains are positioned over the amino-terminal and carboxy-terminal halves of the peptide, respectively. TCR's interaction with the peptide is mostly done by the central CDR3 loops.

Much as MHCs are capable of binding countless peptides within their peptidic groove, TCRs recognize the entire pMHC repertoire with their CDR loops. The growing TCR-pMHC structural database has provided insights on how they associate with MHC and inspired a stereotyped docking model, portrayed in Figure 1.23 (Garcia and Adams, 2005; Garcia et al., 1996; Marrack et al., 2008a; Rudolph et al., 2006). TCR's orientation over pMHC is diagonal, with a variable angle of around 45° in reference to the peptide (Figure 1.24a) (Wilson and Garcia, 1997). This angle brings the Vα and Vβ on top of the carboxy-terminal portion of the MHCII β and α chain respectively. In contrast, when docked onto MHCI, the TCRα chain is positioned over the HC's α2 domain, equivalent to the MHCII β helix (Bridgeman et al., 2012). It is generally the CDR3 loops and MHC-associated peptide that command variations in the TCRs' angle and pitch (Marrack et al., 2008a). Besides, being somatically generated, it is these loops that are fine-tuning TCR's reactivity (Rubtsova et al., 2009). More like a guideline, this general docking orientation does not apply to every resolved pMHCs, *e.g.* $MBP_{85–99}$-HLA-DR2b with the Ob.1A12 TCR, which use an unconventional topology (Figure 1.24b) (Hahn et al., 2005; Wucherpfennig et al., 2009).

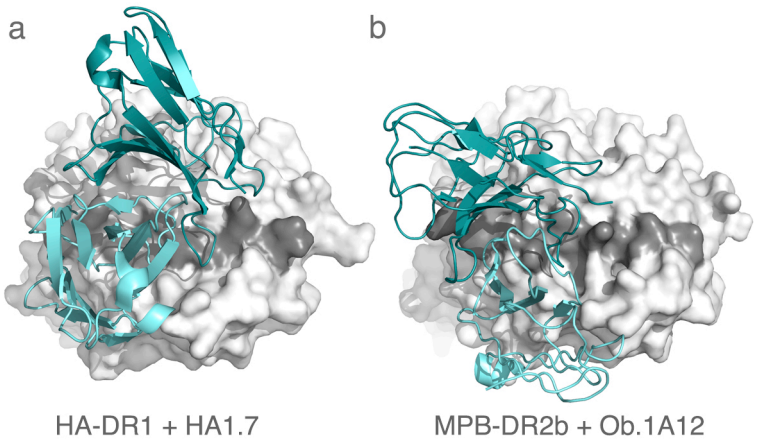

Figure 1.24. Unconventional docking

Structural comparison of TCR docked onto pMHCIIs. **(a)** Top view of the canonical human antimicrobial HA1.7–HA–DR1 complex (1FYT). MHC chains are white and the peptide is dark grey; TCR α-chain is cyan and β-chain is teal. **(b)** The human autoimmune Ob.1A12–MBP–DR2b complex (1YMM).

At first glance, this canonical orientation seems to be defined by the TCR's CDR1 and CDR2 loops that bind conserved residues on the MHC α-helixes while the CDR3 loops interact with the associated-peptide (Bridgeman et al., 2012; Cuendet et al., 2011; Wucherpfennig et al., 1993, 2010). However, as the thermodynamics of every pMHC-TCR is unique it is hard to believe in such a strict model (Miller et al., 2007) Accordingly, it has been suggested that this TCR polarity was the result of a stoichiometric pressure from the multiple surrounding co-receptors, such as CD3, CD4/CD8 (Ding et al., 1998). Given that those two viewpoints are not mutually exclusive, it is well accepted that TCRs have designated CDRs interacting exclusively with the peptide or MHC chain within the boundary of the overall quaternary structure (Wucherpfennig et al., 2010). Few exceptions have been observed that did not entirely fit this canonical rule. Among them, Wucherpfening's group have reported a pMHCII-TCR complex interacting exclusively with the peptide and CDR3s while CDR1s have also been listed as peptide binder in conjunction to the CDR3s (Hahn et al., 2005; Rudolph et al., 2006). The canonical geometry will be further developed in section 1.4.7, which will cover the evolutionary relation between pMHC and TCR. Yin and coworkers were recently able to crystalize the ternary complex between a pMHCII, TCR and CD4

(Yin et al., 2012b). This feat was possible by increasing the affinity of CD4 for the MHCII using *in vitro* directed evolution and yeast display and is shown in Figure 1.25. Having described how TCRs dock onto pMHC molecules, it is now easier to explain how this recognition is transduced into T cells activation.

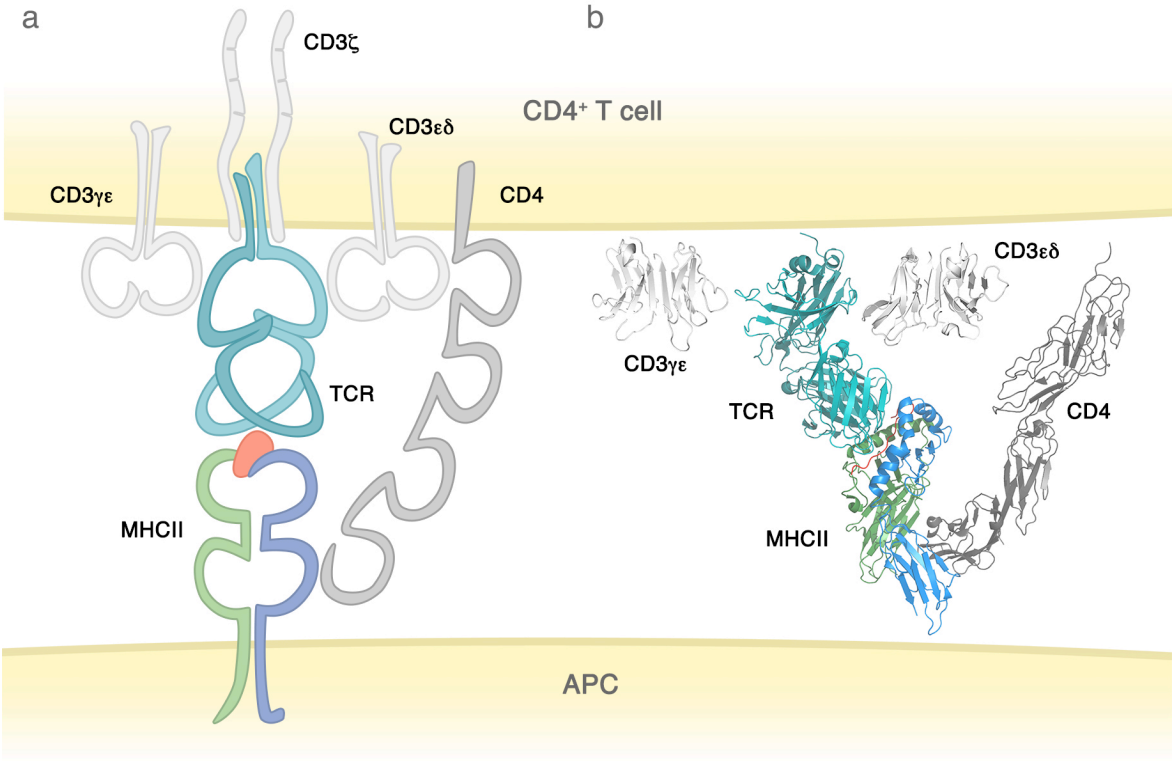

Figure 1.25: TCR-CD3-CD4 complex

Ternary complex between the CD4, MHCII and CD4. **(a)** Schematic of a docked pMHC with the TCR-CD3 multireceptor complex and CD4. **(b)** Ribbon formatted crystal structure of the MS2-3C8 TCR, MBP-DR4 and CD4 complex and the CD3 γδ and γε subunits (3T0E).

1.4.5. Biophysics of activation

The comparison of pMHC-associated TCR crystal structures portrays a frozen state that explicitly shows their plasticity. However, despite their extreme value, these structures remain far from the reality of membrane-associated receptors within the cellular laminar flow. Biophysics experiments have provided a collection of hypothesis as to how T-cells are activated and were compiled into a comprehensive table (Table 1.1) (Bridgeman et al., 2012).

Theory	Definition
Kinetic Proofreading (McKeithan, 1995)	The ability of a T-cell to discriminate between agonist and non-specific peptide–MHCs (pMHCs) based on kinetic parameters required for sequential downstream phosphorylation steps
Serial Triggering (Valitutti et al., 1995)	The ability of a small number of pMHCs to achieve a high T-cell receptor (TCR) occupancy via serial engagement of the same TCR
Germline-encoded Codon Theory (Feng et al., 2007)	The theory that germline-encoded codons permit specific TCR variable-domain recognition of certain MHC molecules
Induced Fit Model (Boniface et al., 1999; Savage et al., 1999)	A thermodynamic mechanism by which TCRs 'scan' the pMHC to 'search' for complementarity – this structural reordering may be transmitted along the entire length of the TCR, inducing a conformational change that may trigger TCR signaling
Conformational Change Model (Gil et al., 2002; van der Merwe and Dushek, 2011)	A model to explain TCR activation based on the premise that ligand engagement by the TCR induces a conformational change in the TCR/CD3 complex that permits linkage to T-cell signalling
Permissive Geometry Model (Minguet and Schamel, 2008)	A refinement of the conformational change model, based on the premise that dimeric/multimeric pMHC binding promotes rotation of the ab TCR subunits with respect to each other – this rotation induces a scissor-like movement of the CD3 chains, permitting their phosphorylation
Aggregation Models (Van der Merwe and Dushek, 2011)	Models of T-cell activation based on the premise that pMHC engagement induces aggregation of co-receptor in the vicinity of TCRs (co-receptor heterodimerization) and/or aggregation of TCR complexes (pseudodimer aggregation)
Kinetic Segregation Model (Davis and Van der Merwe, 1996)	A model that explains the progression of TCR signaling based on size exclusion of phosphatases from the vicinity of activated TCRs

Table 1.1: T cell activation theories

Before taking a side as to which T cell activation theory is the best, facts pertaining to the binding biophysics should be introduced. First, there is a hierarchy of TCR binding affinities toward their respective cognate ligands; pMHCI cognate TCRs bind with more affinity (K_D = 32 μM) than pMHCII cognate TCRs (K_D = 92 μM). Second, it is also suggested that the affinity of TCRs is generally weaker for self or degenerated-self pMHCs compared to foreign peptides, which explain partly why tolerance ensues preferentially to an immune response (Bridgeman et al., 2012; Cole et al., 2007). However, it is now clear that the T cell mediated response is not a direct correlate of the binding affinity and should account for other parameters, *i.e.* half-life, on- and off- rates. By comparing self and foreign Ags, a striking relationship between the origin of the associated peptide and these biophysical parameters becomes apparent: TCR binds i) self-pMHC with weaker affinities, faster off-rates and slower on-rates and ii) foreign-pMHC with higher affinities, slower off-rates and faster on-rates (Bridgeman et al., 2012). These dynamics allow for multiple binding and serial triggering of events that may arise with as little as 10 pMHCs (Manz et al., 2011; Purbhoo et al., 2004).

Structural and biophysical studies hint at an active rather than static model. Moreover, transposing these data to a cellular and multireceptor context in respect to the recent *studies relative to CD3 and pMHC-induced signal transduction suggest that TCRs are anisotropic mechanosensor, i.e. direction matters* (Adams et al., 2011; Husson et al., 2011; Kim et al., 2009; Li et al., 2010; Wang and Reinherz, 2011). For example, using a very elegant approach, Kim and colleagues demonstrated that MHC-coupled beads could only activate T cells after a tangential force was applied using optical tweezers (Kim et al., 2009). This model fits very well the laminar flux within which APCs and T cells come across and is schematized in Figure 1.26.

Overall, one can picture a pMHC-TCR docking scenario that stems from the TCR's plasticity, allowing TCRs to distinguish and "mold" ligands in fast, serial events. Yet, this recognition happens as a whole, *i.e.* TCRs do not discriminate the associated-peptide from its ligand. As cells are not bouncing into each other but are rather crossing paths, the accumulation of pMHC-TCR punctual bindings induces a lateral force that is detected by the CD3 multi-complex. As mentioned earlier, the kinetics of this interaction is influenced by many parameters. This way, self and foreign pMHCs engender a distinct "pressure" against the TCR-CD3 complex, which results in either T cells' survival or activation.

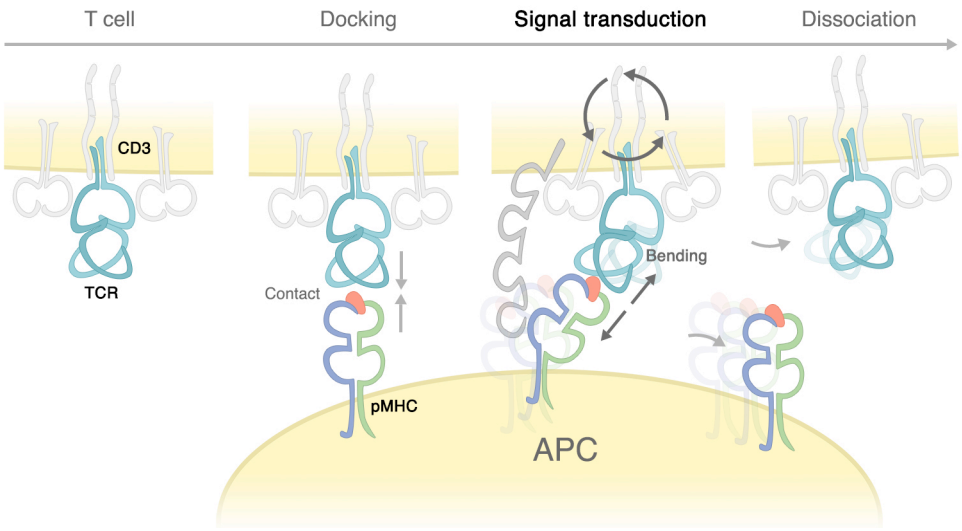

Figure 1.26: Anisotropism model

Initial ligation of the TCR by pMHC (docking) constitutes a detachable mechanosensor that, as a result of continued T cell scanning, transmits an external torque (bending) into initial signaling (circling arrows) via the rigid components of the TCR complex prior to dissociation.

1.4.6. Downstream TCR signaling and T cell activation

MHC-TCR engagement is only the first step to what will lead to an intricate signaling cascade. Thorough descriptions of the TCR signal transduction and T cell activation has been recently reviewed and thus, I will abridge them and offer only the essential background material (Morris and Allen, 2012; Smith-Garvin et al., 2009). At the immunological synapse, the MHCs interact with the TCR multireceptor complex and the CD4 or CD8 co-receptors. This engagement is transduced by conformational changes within CD3 and leads to its phosphorylation, either directly or with the help of the Lck kinase, the latter associated to CD4/8. The synapse promotes TCR signaling and the recruitment of the transmembrane adapter protein LAT and generates a local stoichiometry favoring a phosphorylation cascade, which ultimately activates phospholipase C-γ1 (PLC-γ1). Then, PLC-γ1 hydrolyses PIP_2 to form inositol triphosphate (IP_3) and diacylglycerol (DAG). IP_3 then induces Ca^{2+} flux-mediated signaling, leading to NF-AT activation, while DAG recruits Ras and PCK-θ at the plasma membrane.

On one side, the Ras pathway leads to the phosphorylation of Erk, which activating the transcription factor Elk1, and to the expression of the activator protein-1 (AP-1) (Genot and Cantrell, 2000). On the other side, PCK-θ regulates the transcription factor NF-κB by triggering the phosphorylation, ubiquitination and degradation of IκB, which prevents NF-κB from gaining access to the nucleus (Vallabhapurapu and Karin, 2009). Altogether, these transcription factors act synergically to control the fate of the T cell. For example, NF-AT co-expression with AP-1 leads to IL-2 production and activation, while NF-AT alone leads to anergy. Figure 1.27 schematizes the signaling pathways participating in T cell activation.

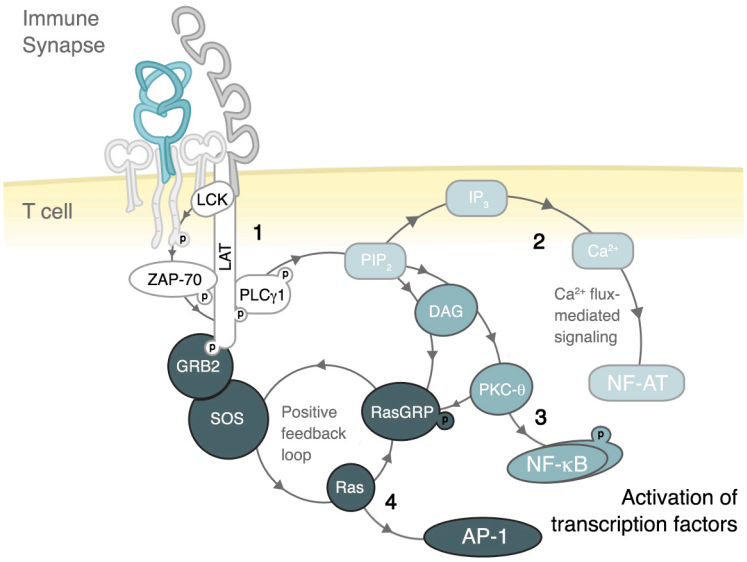

Figure 1.27: TCR signaling pathway

(1) The white boxes represent the major members of the proximal signaling complex: Lck, LAT, ZAP-70 and PLC-γ1 that initiate the signaling cascade and the hydrolysis of PIP_2. (2) Binding of IP_3 to its receptor triggers a Ca^{2+} flux from the ER and cell membranes and activates NF-AT. DAG recruits PKC-θ and RasGRP to the plasma membrane, which prompts NF-κB's activation (3) and to the positive feedback loop responsible for Ras activation (4), respectively.

It is noteworthy that at the immunological synapse, cosignaling is crucial for T cell activation and depends on the concomitant binding of CD28 and CTLA-4 to CD80/86 (Smith-Garvin et al., 2009). Once the signaling cascade is in motion, multiple outcomes are possible depending on the MHC class of the APC that the naïve T cell encounters. From this meeting stems a pronounced clonal expansion generating numerous T cells with a wide range of effector functions such as cytotoxity and cytokine production (Jabbari and Harty, 2006; Kallies, 2008; O'Shea and Paul, 2010). According to the cytokines' profile, these T cells will differentiate into many subtypes as part of the adaptive arm of the immune system.

1.4.7. MHC-TCR co-evolution

Aside from the structure-function, one of the most interesting question regarding TCRs is whether or not they co-evolved with MHC molecules (Marrack et al., 2008a, 2008b). This is even more relevant given that, although a conserved TCR docking mode has been put forth, no ubiquitous determinants were found to

define it. While the TCRβ CDR2 loop has often been linked to interact in a pairwise manner with MHCs, this does not stand as a general rule. Many crystals have confirmed that CDRβ residues Y46, Y48 and E54 engage with a variety of pMHC ligands (Feng et al., 2007; Garcia et al., 2009; Sim et al., 1996; Stadinski et al., 2011). Indeed, these residues have been shown to interact with the highly conserved MHCII α-chain residues K39, Q57 and Q61, providing crucial support to the pairwise co-evolution model (Burrows 2010, Rudolph 2006).

Despite this peculiar MHC class restriction attributed to the CDR1 and CDR2 loops of the V domains, the docking mechanism remains unclear. A handful of groups with results supporting the co-evolution dogma have also identified aa of the TCR Vβ8 and Vα4 that confer intrinsic ability to bind certain MHC alleles, even in the absence of a bound-peptide or with reactivity against both MHC classes (Dai et al., 2008; Marrack et al., 2008a, 2008b; Yin et al., 2011). Accordingly, these results also pointed out that the CDR2 loops are partly responsible for this recognition. In the same vein, a very recent report from Scott-Browne and colleagues suggest that the features controlling the TCR specificity for MHC stemmed from a common ancestor over 400 million years ago and was conserved throughout evolution (Scott-Browne et al., 2011). Elegantly, they generated many chimeric TCRs with sequences of highly divergent species and showed that these TCRs have yet retained their ability to bind MHCs. This report is in line with the Nobel Laureate Neils Jerne's premise, which hypothesizes the evolutionary selection of the TCR variable regions toward MHCs (Jerne, 1971).

A recent report by Stadinski et al. stresses the fact that TCR specificity for pMHC ligands is not driven by germline-encoded pairwise interactions. Notably, they described a single TCR Vβ using alternate strategies to bind pMHC when paired with different Vα (Stadinski et al., 2011). The authors argue that since CDR1 and CDR2 loops have the flexibility to bind their ligands in many ways, this could

not fit a pairwise co-evolution model. Accordingly, the Mariuzza group just demonstrated that the CDR3 loops can markedly alter those evolutionarily selected contacts (Deng et al., 2012). Besides, reports from the Singer group have provided very interesting results showing that deletion of either CD4/8 or thymic selection allowed TCRs to recognize Ags in an Abs-like fashion, independently of MHC ligands (Van Laethem et al., 2007; Tikhonova et al., 2012). Additionally, Baker and colleagues have put forth the hypothesis that TCR's binding is mostly orchestrated by the associated peptide and less so by conserved MHC motifs (Gagnon et al., 2005).

Altogether, TCR bias toward MHC may well be a combination of conserved evolutionary feature, thymic selection and co-receptors pressure (Collins and Riddle, 2008; Garcia, 2012; Garcia et al., 2009; Marrack et al., 2008a). While it is outside the scope of my thesis to answer this question, it remains that TCR engagement with MHC is a very central factor to consider in evaluating how SAGs are able to manipulate this mechanism for their own purpose. Based on the co-evolution premise and CDR2β's key role, the McCormick's group recently proposed that this loop is the critical determinant for bSAGs' function (Nur-ur Rahman et al., 2011). As many pathogens mimic or exploit conserved motifs/interactions to elude the immune system, SAG binding to a TCR region described to be evolutionarily linked to MHC recognition adds to this viewpoint pros' list.

1.4.8. TCR relationship with SAGs

In order to activate T cells, SAGs elicit a biochemically distinct MHC-TCR engagement and signaling (O'Rourke et al., 1990; Sundberg et al., 2007). As a general rule, SAGs bind a cognate TCR Vβ domain (Figure 1.28a-c), which prompts a massive proliferation and deletion of T cell expressing SAG-specific Vβ elements, creating holes in the repertoire (Biasi et al., 1994; Penninger et al., 1995; Wahl et al., 1993). This "repertoire hole" is what led to their identification in the mouse almost forty years ago (Festenstein, 1973).

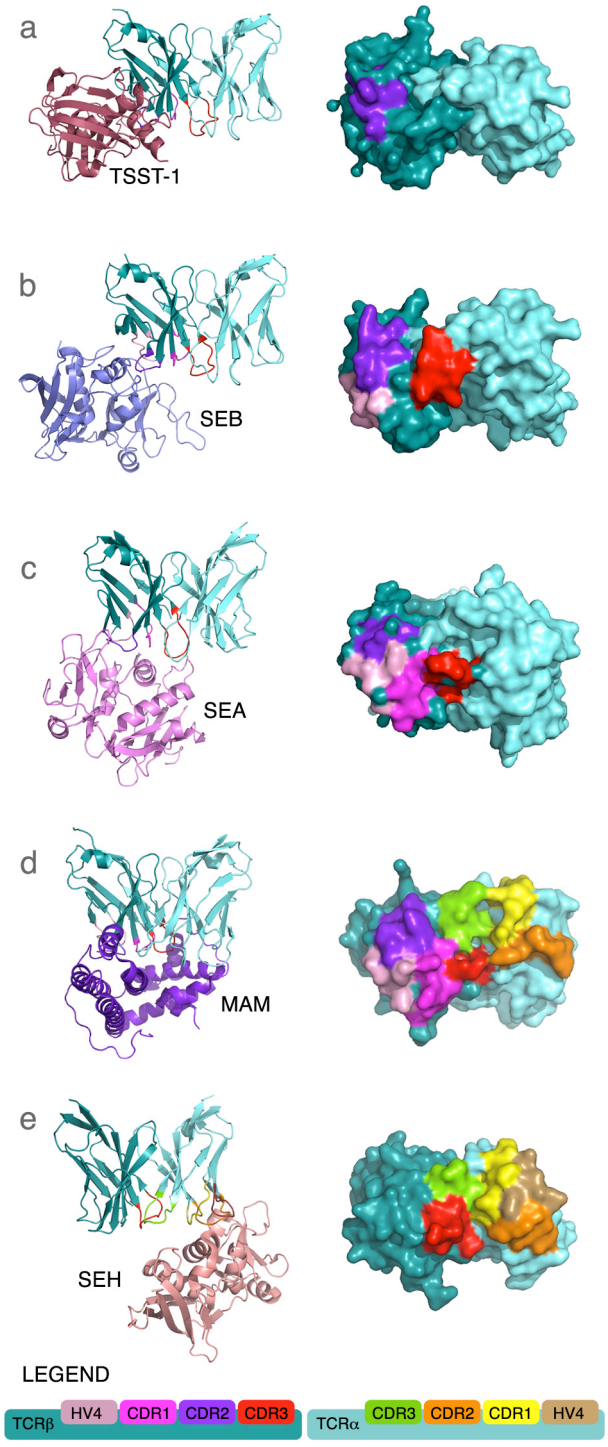

Figure 1.28: SAG docking onto TCR

SAG-TCR interaction is shown beside the CDR-binding imprints. **(a)** Interaction between TSST-1 and the TCR CDR2β and FR3β regions (2IJ0). **(b)** Interaction between SEB and the TCR CDR2β, FR3β and HV4β regions (1SBB). **(c)** Modelization of the interaction of SEA with the TCR CDR1β, CDR2β, CDR3β and HV4β regions (1L05 and 1KTK (SpeC was used as a reference for SEA superimposition)). **(d)** Binding of the SAG MAM use most of the distal TCR interface, including the Vα (2ICW). (**e**) Interaction of

SEH with the TCR Vα and CDR3β (2XNA).

The first effect of SAG presentation is a strong polyclonal T cell expansion (Acha-Orbea et al., 1993a). However, in addition to Vβ, specific Vα repertoire skewing is also described (Aude-Garcia et al., 2000; Smith et al., 1992a; Vacchio et al., 1992). Interestingly, recent data pertaining to *Staphylococcus* enterotoxin H (SEH) and MAM have demonstrated that SAG-mediated TCR engagement can also stem from Vα binding (Figure 1.28d and e) (Saline et al., 2010; Wang et al., 2007). However, this does not explain how Vβ-specific SAGs could also give rise to Vα skewing, which is the result of direct TCR-MHCII interaction. Altogether, SAGs bind TCRs differently, either recognizing the overall conformation, for least specific SAGs, or forming very specific HBs between SAG and the CDRs' aa lateral chains (Sundberg et al., 2007). As a consequence, this limits/broadens the number of Vβ a given SAG can bind and thus affects its potency.

The fate of SAG-activated T cells differs from that of T cells activated by conventional Ags and bypasses conventional Ag processing and presentation. Whereas conventional Ag could activate a small 0,0001% of the naïve T cell, up to 20% of the those cells could be activated by a given SAGs (Ford and Burger, 1983; Fraser and Proft, 2008). SAGs ability to activate that many T cells is explained by their ability to predominantly bind non-variable region of the TCR (Acha-Orbea and MacDonald, 1995). The greater potency of the response initiated by SAGs leads to both proliferation and cytokine release and ultimately results in activation-induced cell death, while those T cells that survive become unresponsive or anergic (White et al., 1989). Interestingly, SAG presentation activates both CD4+ and CD8+ T cells although CD4 is reported to enhance T cell response by increasing the overall avidity of the interaction (Thibodeau and Sékaly, 1995). Given the MHCII interface used for SAGs binding, CD4 should proficiently interact with the MHCII β2 domain although the possibility remains that this instead occurs on an adjacent SAG-free

MHCII. CD4-deficient cell lines or mAb blockage of CD4 also result in T cell activation by SAGs, suggesting that the downstream activation cascade also functions without contribution from CD4 (Bueno et al., 2007). Given CD4/8's role in localizing Lck to the proximal TCR signaling complex and the role of Lck in initiating the canonical signaling, the phosphorylation of CD3 must be induced directly by TCR ligation. This may occurs when a high degree of cross-linking is attained at the immunological synapse (Stanners et al., 1995). Alternatively, it was proposed that SAGs could bypass this pathway by binding additional ligands or co-receptors. The Madrenas group proposed a Lck-independent pathway that relies on the induction of PLC-β by the heterotrimeric G protein family member Gα11 (Bueno et al., 2006). Figure 1.29 depicts this alternative pathway.

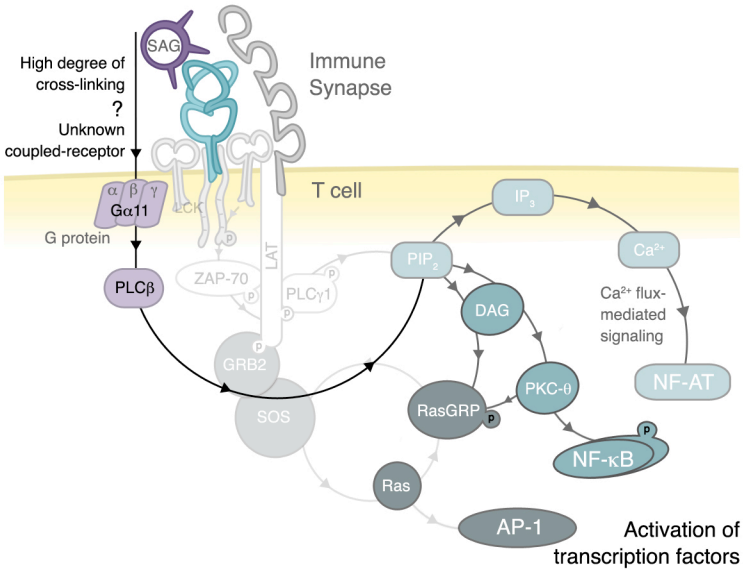

Figure 1.29: Alternative TCR signaling pathway
SAG-mediated T cell activation via Gα11-dependent PLCβ activation. The question mark highlights uncertainty over whether it is triggered by a high degree of cross-linking at the proximal TCR signaling complex or by an unidentified G protein coupled receptor.

In addition to SAG-MHCII binding to the TCR multireceptor complex, costimulation and late downstream events are important for the T cell fate. As opposed to canonical Ag presentation, which relies on CD28/CTLA-4 costimulation, that mediated by SAG is less dependent on this mechanism, but costimulation can intensify the response (Vella et al., 1997). Interestingly, the effect of these

costimulatory molecules can vary and go from T cell response attenuation to dependency, depending on the system used (Fikri et al., 2002; Krummel et al., 1996). Clearly, Ags and SAGs have distinct ways to activate T cells and much remains to be deciphered. Whether unidentified receptors are implicated in this response remains to be verified but seems likely given the participation of G proteins in signaling and the ability of a handful of bSAGs to stimulate T cells independently of MHCII ligands (Avery et al., 1994; Bueno et al., 2006). It is noteworthy that the ability of distinct SAGs in activating either TCR signaling pathway may differ.

Recently, Arad and colleagues suggested that SEB could bind to the costimulatory molecule CD28, which is constitutively expressed on naïve T cells and binds B7 ligands on APCs (Arad et al., 2011). The CD28 binding site on SEB, which is relatively conserved among bSAGs of this family, is located on the opposite side of those of the TCR and MHCII, and fits in a model including CD28 (Figure 1.30). The downstream signaling cascade stemming from CD28 engagement remains to be elucidated. It will also be of interest to evaluate how CD28 impacts the presentation of other SAGs.

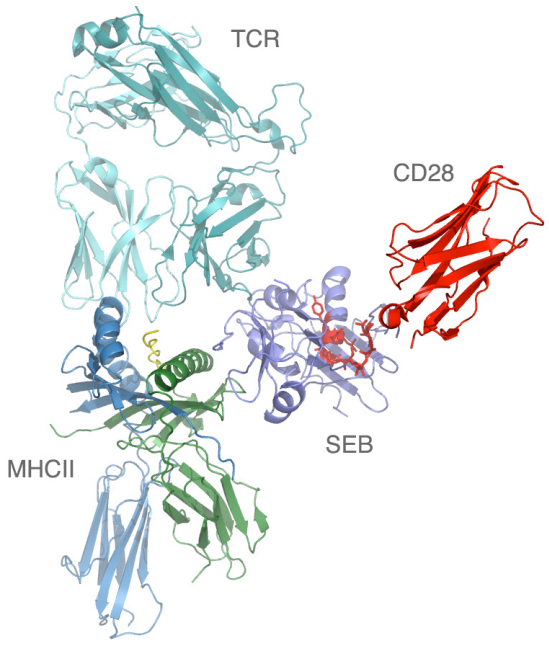

Figure 1.30: SEB binds CD28

SEB-mediated MHCII-TCR engagement complex showing the possibility of CD28 binding. The region 150-161 of SEB is colored red and corresponds to the CD28 binding interface. The model is based on the SEB-MHCII and SEB-TCR co-crystals (1SEB and 1SBB). To easily portray the possibility of such multimeric complexes, CD28 structure was added and oriented as if bound to the T cell membrane.

1.5. Superantigens

I have begun this chapter by presenting SAGs in relation to MHCII and TCR, yet neglecting to present them properly. Now, I describe the diversity and potent immunostimulatory role of these mitogens and offer a structural overview of the topology underlying TCR-MHCII engagement. SAGs are a group of toxins, commonly known for their implication in food poisoning and toxic shock. They are small 15 to 30 kDa byproducts of different pathogenic microorganisms, such as bacteria, viruses and protozoa (Thibodeau and Sékaly, 1995). For most of their existence, SAGs have been described as molecules with the ability to polyclonally activate T cell bearing specific TCR Vβ elements. This dogma, however, has been challenged in the recent years and now includes specific Vα elements of the TCR. SAGs possess structural features allowing to concomitantly bind the MHCII and the TCR outside of the usual Ag-binding site (Figure 1.31). The most characterized bacterial SAGs (bSAGs) and viral SAGs (vSAGs) are those of *Staphylococcus aureus* and *Streptococcus pyogenes*, and those encoded by the MMTVs, respectively. Paradoxically, whereas bSAGs have very well characterized structure/function but a poorly defined role, vSAGs have a well-defined role but structural knowledge is lacking.

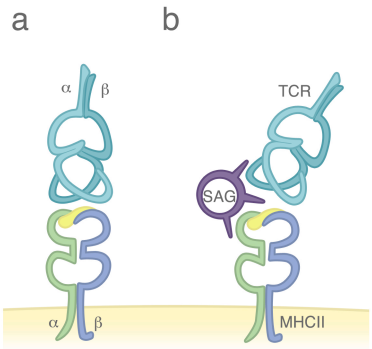

Figure 1.31. Ag vs SAG
Comparison of conventional Ag MHCII-TCR topology (a) vs an example of the one coerced by SAG (b)

The contribution of SAGs in the bacterial life cycle is vague. An immunosuppressant role has been put forth, whereby bSAGs allows the bacteria to colonize their host, thus providing the bacteria with an evolutionary advantage. Alternatively, the SAG-mediated inflammation may stimulate bacterial growth

(Marrack et al., 1993; Stow et al., 2010). That many distinct SAGs are known to bind the different MHCII allotypes and the TCR V elements suggests that their diversity has been compelled by a need to stimulate as many T cells as possible and that they are crucial for the bacteria (Fraser and Proft, 2008). Yet, 20 years after their identification, the roles of *S. aureus* and *S. pyogenes* toxins remain hypothetical, but all the same, come with their share of side effects for the host. Indeed, they are associated with the onset of Kawasaki disease, atopic dermatis and chronic rhinosinusitis (Xu and McCormick, 2012). Moreover, in mouse models, bSAGs were shown to increase the severity of a model of multiple sclerosis (EAE) and rheumatoid arthritis (Torres and Johnson, 1998).

On the other hand, vSAGs' role in the MMTV cycle is well understood. By using SAGs to recruit T cell help, MMTV exploits the immune response in order to instigate the infection in long-lived memory B cells and plasma cells (Acha-Orbea et al., 2007). Also, by causing a vSAG-specific Vβ T cell deletion, the occupying virus prevents subsequent infection from other MMTV bearing vSAGs with the same Vβ specificity (Golovkina et al., 1992). Figure 1.32 portrays the role of vSAG in MMTV's infection cycle. Notably, recent findings by the Golovkina group show that MMTV transmission requires additional stimuli from the commensal microbiota (Kane et al., 2011). MMTV infection often leads to breast cancer, although its etiology seems independent of the encoded vSAG (Acha-Orbea and MacDonald, 1995). Interestingly, MMTV-like sequences were found in human breast carcinomas and encoded functional vSAGs (Wang et al., 2004). It was also reported that MMTV can infect human cells and thus arose the hypothesis that, like in mouse, this virus was a tumorigenic factor (Indik et al., 2005). However, a recent epidemiology report that reviewed 85 original studies pertaining to this field concluded that no significant relationship exists between human breast cancer and the presence of MMTV-like sequences (Joshi and Buehring, 2012).

Marginal knowledge about SAGs encoded by other viruses, such as those of HERV-K18, is available and remains controversial (Azar and Thibodeau, 2002; Sutkowski et al., 2001; Woodland, 2002). However I will not discuss these SAGs in this work.

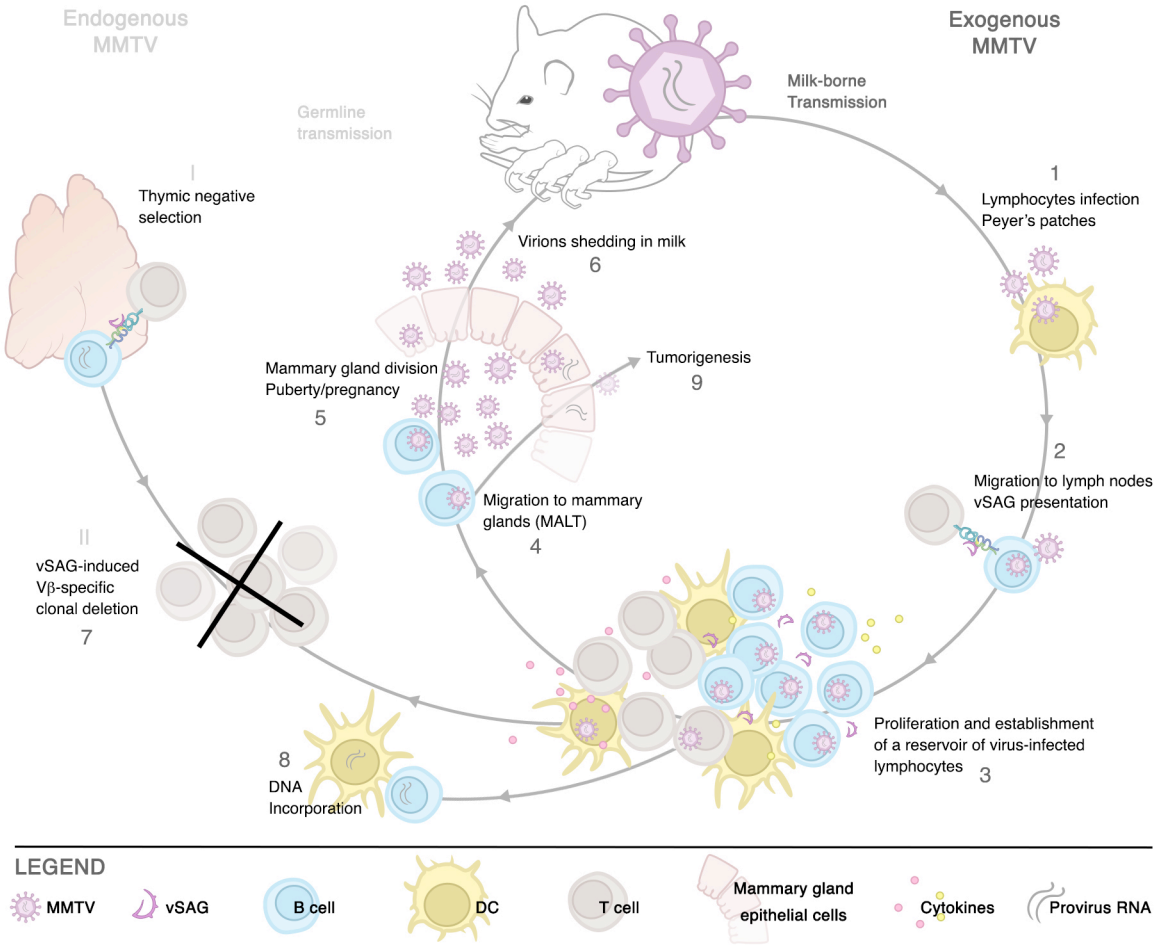

Figure 1.32: Transmission and infection cycle of MMTV

The exogenous MMTV transmission is milk-borne; virions contained in ingested milk first infect DCs (1) then spread to B and T cells in the Peyer's patches and ultimately, with the help of its vSAG (2), to other lymph nodes and lymphoid organs. A rapid T cell proliferation follows, providing help to B cells and recruiting additional lymphocytes (3), leading to a pool of infected cells. These cells gain access to mammary glands (4), a mucosal-associated lymphoid tissue (MALT), in which the virus replicates (5) and is later shed via the milk (6). Because of the vSAG, a slow and almost complete deletion of cognate Vβ T cells follows the infection (7). As a result of the virus' multiple integration in lymphocytes (8) and mammary gland epithelial cells, tumorigenesis may arise to varying degrees (9). Germline transmitted, endogenous MMTVs cause thymic negative selection of vSAG-cognate T cells (I) leading to deletion (II). Most of endogenous viruses are unable to produce infectious particles.

1.5.1. Bacterial superantigens

More than 30 bSAGs are expressed by *S. aureus* and *S. pyogenes*. They are classified into five distinct evolutionarily groups and, according to their sequence, are hypothesized to share the same tertiary structure. However, as presented above, they bind MHCII and TCR using different strategies. Table 1.2 highlights the major characteristics of the subgroups whereas Figure 1.33 shows *in sillico* models of SAG-MHCII-TCR ternary complexes.

	Toxins	Strain	MHCII binding mechanism
Group I	TSST-1	*S. aureus*	Binds MHCII α chain through a low affinity N-terminal domain that is peptide-dependent (Kim et al., 1994)
Group II	SEB, SEC, SpeA	*S. aureus,* *S. pyogenes*	Bind MHCII α chain through a low affinity binding domain, independently of the associated-peptide (Jardetzky et al., 1994)
Group III	SEA, SED, SEH	*S. aureus*	Bind MHCII like group II and group IV and can cross-link MHCIIs (Mehindate et al., 1995; Petersson et al., 2002)
Group IV	SpeC, SpeG, SpeK	*S. pyogenes*	Binds MHCII β chain H81 through coordination with a Zinc ion (Li et al., 2001)
Group V	SEI, SEK, SpeI	***S. aureus,*** *S. pyogenes*	Bind MHCII similarly to group IV, but posses an additional loop important for TCR interaction (Günther et al., 2007)

Table 1.2: Overview of bSAGs classification

Because Streptococcus enterotoxins often resemble those of *Staphylococcus*, I will concentrate my effort in describing the latter regarding the ability of groups I, II and III to bridge MHCII to the TCR, which covers the three existing binding strategies and will briefly highlight the main features of the groups IV and V.

Sole member of the group I, TSST-1 concomitantly binds to the MHCII α chain and C-terminal end of the associated-peptide (Kim et al., 1994). Consequently, its presentation is highly dependent on the bound-peptide sequence and is completely null in situation where the C-terminus protrudes outside the groove (Hogan et al., 2001; Wen et al., 1997a). Moreover, TSST-1 Vβ specificity is very strict and linked to an aa insertion in the CDR2β loop (Moza et al., 2007). Finally, TSST-1 engagement is devoid of MHCII-TCR contacts (Figure 1.33a).

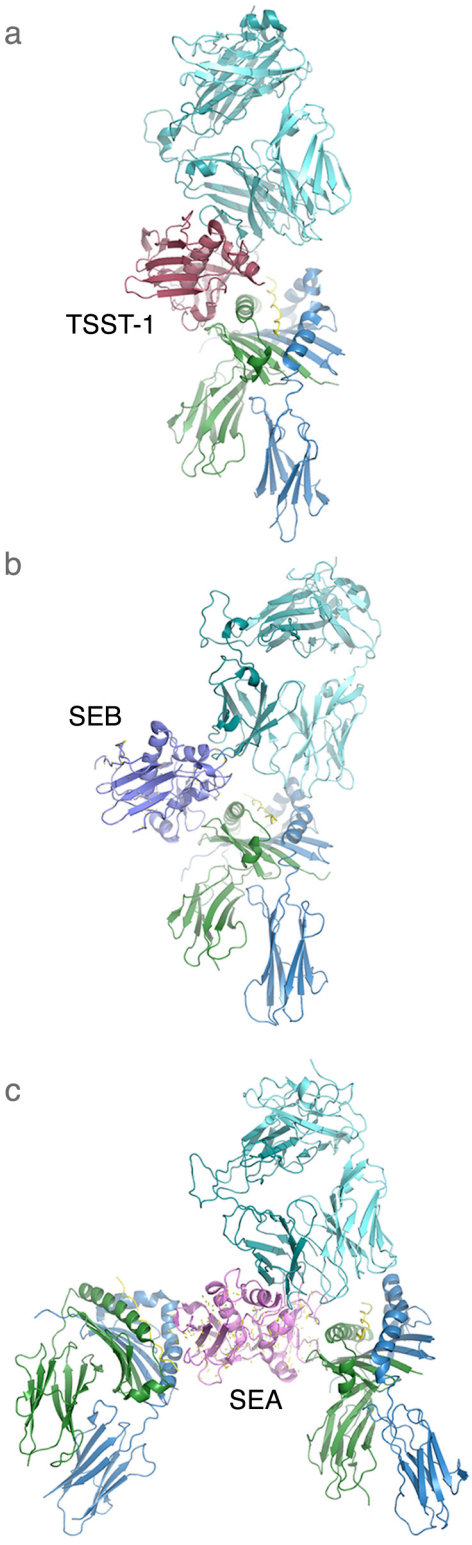

Figure 1.33: SAG-mediated T cell activation complexes

Different strategies used by SAGs of groups I, II and III to bridge MHCII and TCR together. **(a)** Model of the TSST-1-mediated T cell activation complex based on the TSST-MHCII and TSST-TCR co-crystals (2TSS and 2IJ0). **(b)** Model of SEB-mediated T cell activation complex based on the SEB-MHCII and SEB-TCR co-crystals (1SEB and 1SBB). **(c)** Model of the SEA-mediated T cell activation complex based on the SEA-MHCII and SpeC-TCR co-crystals (1L05 and 1KTK (SpeC was used as a reference for SEA superimposition)).

More promiscuous than TSST-1, the group II member SEB binds a broader range of Vβs and its successful presentation depends on extra Vα-MHCII β chain interactions (Figure 1.33b) (Sundberg et al., 2007). This SAG binds both the MHCII and TCR in a conformation-sensitive fashion, interacting with the main chain of these molecules (Fields et al., 1996; Li et al., 1998b).

Members of group III, which includes SEA, have the notable ability to cross-link MHCIIs (Figure 1.33c). Remarkably, they bind MHCIIs in two ways, using distinct binding sites (Thibodeau et al., 1997). The first is similar to that used by group II SAGs and the second, which relies on a Zn ion and the MHCII βHIS81, also characterizes the group IV SAGs. Little structural information is currently available on how group III SAGs engage TCRs. However, given the respective Vβ and Vα skewing stemming from SEA and SEH presentation and lack of competition for the TCR between those SAGs, it is conceivable that the member of this group differentially bridge TCRs and would benefit to be reclassified accordingly (Petersson et al., 2003; Saline et al., 2010). Finally, group V behave similarly but also posses a loop extension crucial for T cell activation, by contacting the apical loop of the TCRβ FR4 region (Brouillard et al., 2007; Günther et al., 2007).

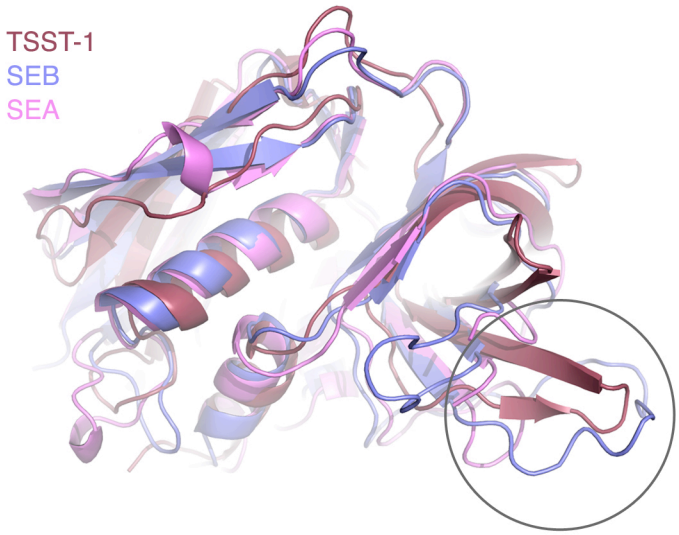

Figure 1.34: Overlay of bSAGs
A superimposition of groups I, II and III SAGs indicate very similar tertiary structure. Most changes are located in the connecting loops and the area delimited by a circle. Absent from SEA, ordered on SEB and highly ordered (β-sheets) on TSST-1, this region interacts with the TCR, MHCII α chain or associated-peptide, respectively.

In addition to the SAGs classified into the five classic groups is the MAM SAG, which possesses a unique fold and binding strategy (Figure 1.35). In the case of MAM SAG, MHCII-TCR engagement stems from its concomitant association with the membrane distal interface of the receptors and prevents any contact between the two (Wang et al., 2007). MAM has also been reported to form zinc-dependent homodimers, which would allow MHCII cross-linking (Zhao et al., 2004).

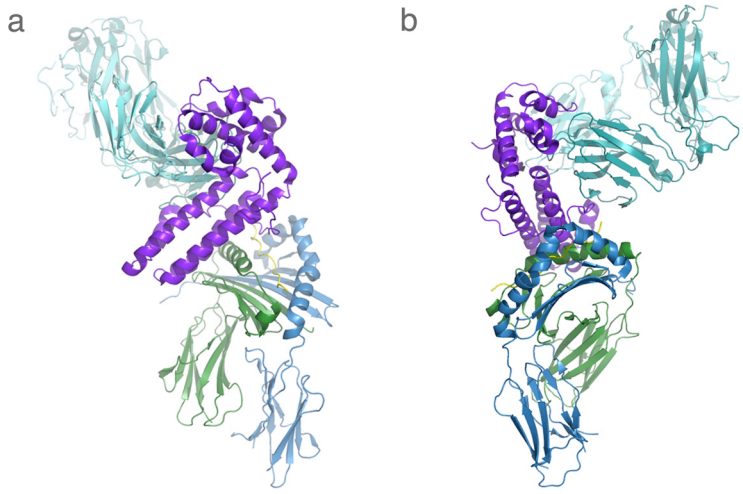

Figure 1.35: MAM-mediated T cell activation complex
Ribbon depiction of the ternary complex between MHCII, MAM and TCR (2ICW). MAM-mediated bridging reveals a near-perpendicular topology between the MHCII and TCR. (b) 90° CCW rotation of (a), highlighting the perpendicular binding.

Altogether, the many bSAGs have evolved to activate T cells using different architecture, using many tweaks that allow them to modulate their potency and thus their impact on the immune response (Sundberg et al., 2002).

1.5.2. Viral superantigens

Faceless for almost 20 years, the superantigens of MMTV (vSAGs) were initially described as the minor lymphocyte stimulating (Mls) antigen by Festenstein (Festenstein, 1973). They were documented as MHC unrelated genes that led to strong mixed leukocyte reactions in mice strains with identical MHC (Acha-Orbea and Palmer, 1991). The name “superantigen” was offered by Kappler and Marrack in an effort to explain the function of these potent stimulatory factors*, unrelated to bSAGs, that could bind MHCIIs and stimulate T cells in a Vβ-specific manner (Marrack and Kappler, 1990). As a consequence of Mls antigens, responsive T cells are deleted, creating holes in the T cell repertoire (Acha-Orbea et al., 1993b). It is only in the early nineties that three groups concurrently linked the deletion of specific T cell Vβ subsets to a gene within the mouse genomic *mtv* sequence (Acha-Orbea et al., 1991; Choi et al., 1991; Woodland et al., 1991). The next years were very prolific and shed light on the nature of these type II transmembrane glycoproteins (Figure 1.36) encoded by the MMTV long terminal repeat ORF (Acha-Orbea and MacDonald, 1995). Grouped in seven families, there are over 50 described vSAGs that are encoded either by the endogenous *mtv* loci or exogenous viruses (Acha-Orbea et al., 2007). They share about 85% overall aa homology and have a hallmark variable 21 to 38 C-terminal stretch that correlates well with their Vβ specificity (Acha-orbea, 1995; Acha-Orbea and Palmer, 1991).

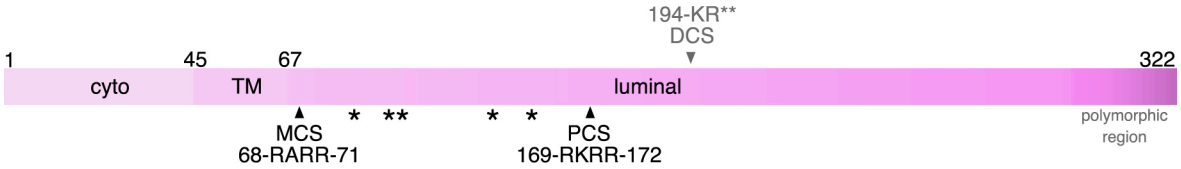

Figure 1.36: Schematic of vSAG polypeptide

General features of the type II vSAG polypeptides: up to five N-linked glycosylation sites, the membrane cleavage site (MCS), the proximal cleavage site (PCS) and the optional distal cleavage site (DCS), which is only present on certain vSAGs.

** note that I did not use the word protein here as, at the time, the possibility was that Mls could also be lipidic*

As I mentioned earlier, the structure-function of vSAG is ill defined. The first major finding pertaining to vSAG was its TCR binding interface. Pullen and colleagues noticed residues of the solvent-exposed lateral face of the TCR Vβ (red and pink in Figure 1.37) that impaired vSAG stimulation but not conventional Ag presentation (Pullen et al., 1990). Interestingly, most of the vSAG-inactivating Vβ mutations tested did not affect bSAGs presentation, which suggest that vSAGs and bSAGs have non-overlapping binding site. Moreover, introduction/deletion of N-linked carbohydrates can prevent/restore presentation of vSAG, respectively.

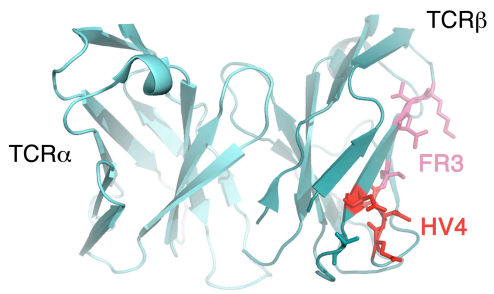

Figure 1.37: TCR-vSAG binding interface
vSAG7 critical residues for T cell activation include the Vβ8.2a V17, T18, N22,, T24 D51, E70, N71, which are part of the FR3 and HV4. In contrast to bSAGs, vSAG7 do not bind the CDRs. The TCR is shown as if the MHC was below.

A further article by Pullen and coworkers revealed a TCR Vβ residue (T24) that affected both the presentation of OVA peptide and vSAG (Pullen et al., 1991a). This result suggests that this mutation disrupted an essential TCR-MHCII contact. Of note, this threonine is part of the CDR1, region implicated in canonical MHC/peptide (Figure 1.23) binding and the fact that it affects both OVA and vSAG presentation will be further discussed in the forthcoming chapters. Overall, vSAGs bind the TCR Vβ at the lateral, solvent-exposed β-pleated sheet.

While the TCR binding site was being defined, Winslow et al. succeeded in isolating vSAGs and identified B cells as expressing this 45 kDa glycoprotein, only present on the cell surface as a 18.5 kDa processed fragment (Winslow et al., 1992). Processing at the PCS (Figure 1.38) is indeed essential to unlock vSAG stimulatory function, even though the two resulting fragments may remain non-

covalently associated after cleavage (Krummenacher and Diggelmann, 1993; Park et al., 1995; Winslow et al., 1994a). I will refer those two fragments as the N-vSAG and C-vSAG throughout this work.

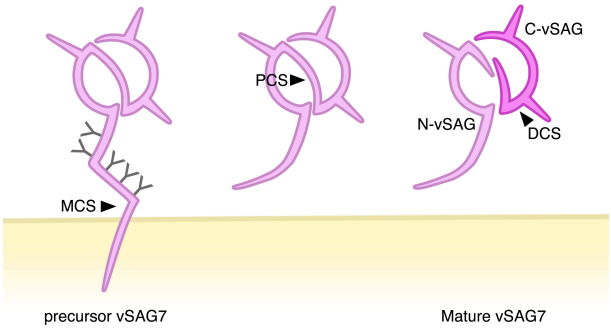

Figure 1.38: vSAG maturation
First, up to 5 N-linked glycan are co-transnationally added to the immature vSAG polypeptide. The maturing vSAG then transit to the Golgi where it is cleaved at the MSC and PCS, generating the N-vSAG and C-vSAG (also 18kDa or mature vSAG) moieties. Some vSAG family members contain an additional cleavage site, which renders C-vSAG inactive if processed. Processing at the PCS is essential for vSAG ability to activate T cells.

1.5.3. vSAG presentation

The association of vSAG with MHCIIs is probably the most enigmatic aspect underlying the ability of these SAGs to mediate the T cell signaling complex. Indeed, the vanishingly small quantity of vSAG produced, even upon super expression, remains a major obstacle in characterizing and defining the biophysics of vSAG (Krummenacher and Diggelmann, 1993). Earlier studies described N-vSAG to interact with the MHCII β chain at the βHis81-dependant SEA binding interface (Figure 1.19) and suggested a second biding site elsewhere (Mottershead et al., 1995; Torres et al., 1993). The second site, used by C-vSAG, overlaps the one of SEA on the MHCII α chain (Figure 1.19) (Delcourt et al., 1997a). Interestingly, it was also proposed that vSAG binds the MHCII groove similarly to Ii (Hsu et al., 2001). The three proposed binding modes are depicted in Figure 1.39. C-vSAG binding to the MHCII α chain leads to TCR engagement and T cell

stimulation (Grigg et al., 1998a; Winslow et al., 1994b). The C-vSAG moiety also have the ability to be intercellularly transferred from MHCII$^-$ cells to MHCII$^+$ APCs, in what is called the paracrine transfer (Delcourt et al., 1997a).

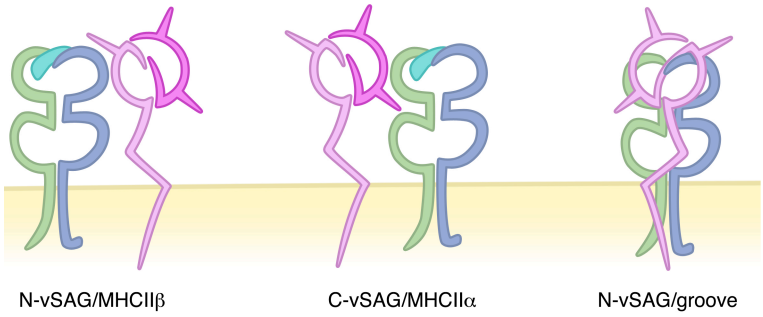

Figure 1.39: Proposed vSAG-MHCII binding modes
N-vSAG binds to the MHCII β chain and C-vSAG bind to the α chain. Conversely, N-vSAG may bind to the MHCII groove like Ii before being processed.

An interesting feature of vSAGs, is their ability to bind both human and mouse MHCIIs (Labrecque et al., 1993a). The different alleles have distinct vSAG presentation capability and follows a hierarchy in which I-E > I-A >>> I-A^q and DR > DQ > DP and where I-E and DR are the best presenters (Kappler et al., 1988; MacDonald et al., 1989; Subramanyam et al., 1993). As I mentioned previously (1.3.8. SAGs binding to MHCIIs), this phenomenon seems to indicate that C-vSAGs associate with MHCIIs in a conformational manner.

The question as to whether immature vSAGs associate synergically to MHCII upon synthesis is being challenged. Reports have argues that both can bind in the ERs (Hsu et al., 2001) and other observed MHCII-vSAG interaction only at the cell surface between mature MHCII and C-vSAG (Grigg et al., 1998a). In the second model, vSAGs traffic independently of MHCIIs and finally associate at the cell surface with mature, SDS-resistant pMHCII complexes. Also, given the dependency of human HeLa cells to only present vSAG after being transfected with Ii and DM (or CIITA), interaction between vSAG and MHCIIs depends on the bound-peptide and occurs at the cell surface (Azar et al., 2005b).

1.5.4. The associated-peptide influence

I mentioned earlier that the group I SAG directly binds the associated-peptide and therefore, its presentation is directly affected by nature of the latter. In the case of TSST-1, it is the peptide C-terminus end that impacts its binding and thus, many inherent pMHCIIs do not allow presentation (Wen et al., 1996). In their study, Wen and colleagues conducted a thorough saturation mutagenesis of a peptide, evaluating each residue in their ability to present TSST-1. Interestingly, whereas most substitution did not affect the ability of the pMHCIIs to promote TSST-1 presentation, C-terminal PFRs sterically blocked its binding and hampered presentation (Wen et al., 1997b).

In the case of vSAGs, the nature of the associated-peptide correlates with the ability of pMHCII to present vSAG. However, the part of the peptide (N- or C-terminus) or whether it is a direct binding or indirect effect, reflected on the MHCII comformation, remains to be elucidated and is more thoroughly discussed in the next chapters.

1.5.5. Interplay between MHCII maturation and SAG

Given the apparent correlation between the associated-peptide and SAGs presentation, one must ask if non-classical MHCIIs can influence their presentation by differentially altering the MHCII peptide repertoire. Indeed, It was previously shown that DM-deficient human cells could not present TSST-1 or vSAGs (Azar et al., 2005b; Lavoie et al., 1997). Similarly, presentation of these SAGs by cells from H2-DM-deficient mice was inefficient (Golovkina et al., 2001; Hogan et al., 2001; Tourne et al., 1997). As mentioned above, DM edits the peptide repertoire by exchanging CLIP for a variety of peptides with better kinetic stability (Schulze and Wucherpfennig, 2012). Thus, in the absence of DM, MHCIIs display a different peptide repertoire in which associated-CLIP peptides are overrepresented. Given the ability of DO to inhibit

DM, it is possible that similarly to DM-deficient cells/mice, DO affect SAG presentation. Accordingly, a recent report by a colleague just acknowledged a role for DO in SAGs presentation (Pezeshki et al., unpublished data). His data indicate that both SEA and TSST-1 are favorably presented following DO over-expression in contrast to SEB and vSAG7, which were both unaffected. Based on these results, it is tempting to link this effect to the increased abundance of CLIP-MHCII complexes. However, while DM-deficient cells failed to present TSST-1, its inhibition by DO did not lead to a presentation defect, as it should have been expected if its presentation was tied to the CLIP peptide. Therefore, intricacies resulting from the MHCIIs maturation are perhaps reflected in SAG presentation more that by the nature of the bound-peptide. Overall, DO effect on the tested bSAGs can sometime be counterintuitive, much like it is with conventional Ag presentation (1.3.6. Peptide editing). What is therefore very interesting is the possibility that there is a co-evolutionary relation between an “invariant pMHCII complex” that ensure efficient SAG presentation given their inherent expression (Rudensky et al., 1991).

1.6. Problematic, Hypothesis and Objectives

Even though the mouse mammary tumor virus superantigens were the first ones identified, they remain poorly defined. Indeed, vSAGs are produced in vanishingly small quantities, which rendered structure/function studies quite a challenge. Stemming from the work of Azar *et* al., which reported that vSAG presentation was restored upon Ii and DM expression in defective human cell lines, I aimed to further characterize the contribution of the MHCII-bound peptide in vSAG presentation (Azar et al., 2005). Also, I aspired to unveil the architecture of the T cell signaling complex mediated by vSAGs, which I hypothesized unlike any of those mediated by bSAGs.

Interestingly, while both Ii and DM impact vSAG presentation, DO does not (Pezeshki, 2012). One would think that overexpressing DO would inhibit DM and reduce its peptide exchange activity, and thus would lead to ineffective vSAG presentation. However, the function of DO is quite remarkable in that it is following the Schrödinger's paradox. Indeed, depending of the experimental system used to witness its effect, the observed results are often antipodal. Thus, to better understand DO, we directed our efforts in figuring out its biophysics. Starting from the idea that DO was an inherently unstable molecule, we conducted experiments to monitor its conformation upon DM binding, event leading to its stabilization. Furthermore, a point mutation, engineered by a previous laboratory member, induces a similar conformation change that unfetters DO from DM and allow DO egress to the plasma membrane, independently of DM (Deshaies et al., 2005). Knowing that a single aa substitution had such an effect on DO, I undertook to screen a library of randomly mutated DO to reveal other aa that could further stabilize this molecule.

vSAGs were proposed to bind MHCIIs like Ii (Hsu et al., 2001). However, given the utmost importance of a peptide-filled MHCII “state” for vSAG presentation, this proposal fell short at explaining how vSAG could bind the peptide groove concomitantly to a peptide. Interestingly, co-expressing two SCDs, one consisting of vSAG bound to MHCIIβ and the other consisting of Ii bound to MHCIIα, led to structurally-sound CLIP-MHCIIs, indicating that Ii and vSAG do not have overlapping binding site. Of note, It was recently proposed that Ii trimers could only bind a single MHCII heterodimer and that this interaction would lock the Ii scaffold, preventing binding of additional MHCIIs (Koch et al., 2011). This report contradicts seminal work in which nonameric complexes were observed (Roche et al., 1991b). Also, the fact that the two SCDs properly assembled suggested that high order complexes arose. Thus, we used the Ii-SCD to indubitably prove the existence of nonameric Ii-MHCII complex.

The articles presented in the forthcoming chapters recount these experiments.

Chapter 2 : Functional analysis of the MMTV superantigen

Experimental design: JSF, NHS and JT

Performed experiments: JSF[70%], LG[25%] YS[3%] and DYD[2%]

Writing: JSF[90%] and JT[10%]

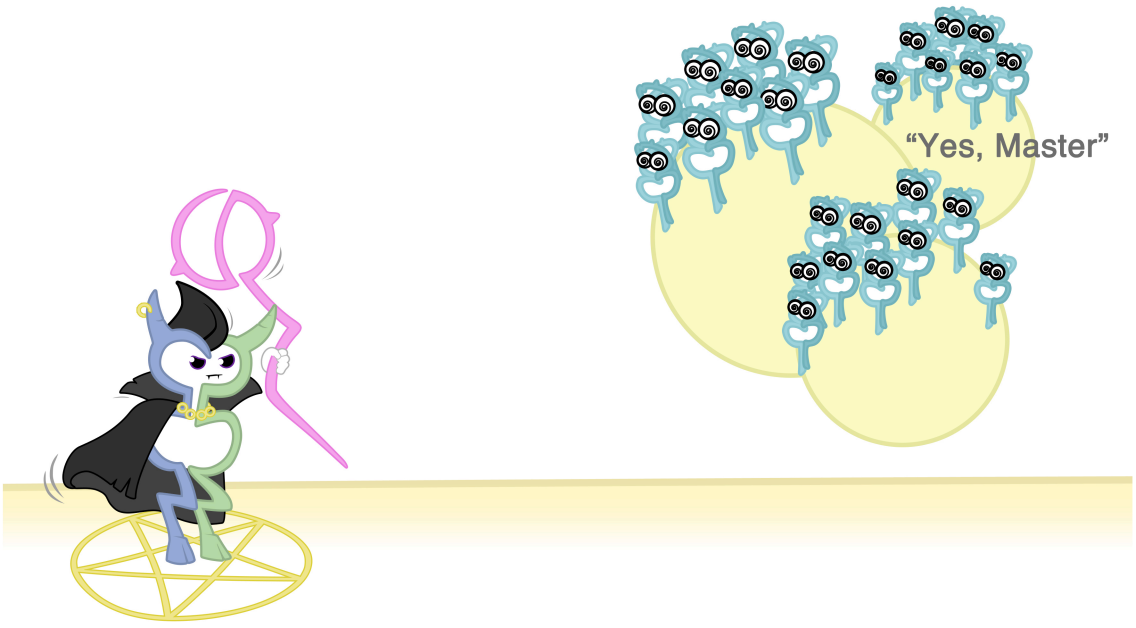

With this staff of power, I will rule them all!

- MHCII teaming up with a superantigen to control T cells

Unconventional Topology between the TCR and MHC Class II Molecule is Coerced by MMTV Superantigens

Jean-Simon Fortin,*§[1] Laetitia Genève,*[1] Naglaa H. Shoukry,¶ Georges A. Azar, *[2] Younes Souheil,¶ Bader Yassine-Diab,¶ Rafick Pierre Sékaly, ‡ Daved H. Fremont§ and Jacques Thibodeau*†

* Laboratoire d'Immunologie Moléculaire, Département de Microbiologie & Immunologie, Université de Montréal. Montréal, QC, Canada.

§Department of Pathology & Immunology, Washington University School of Medicine, St. Louis, MO, United States

¶Département de Médecine, Université de Montréal and Centre de Recherche du Centre Hospitalier de l'Université de Montréal (CRCHUM), Montréal, Québec, Canada.

‡Division of Infectious Diseases, Vaccine and Gene Therapy Institute - Florida (VGTI-FL), Port Saint Lucie, FL, United States

† **Corresponding author**: Jacques Thibodeau,
Laboratoire d'Immunologie Moléculaire, Département de Microbiologie & Immunologie, Université de Montréal, CP 6128, Succursale Centre-Ville, Montréal, QC, Canada, H3C 3J7
Tel : (514) 343-6279; Fax: (514) 343-5701;

Running title: Structure-function analysis of the MMTV superantigen

ABSTRACT

Mouse mammary tumor virus (MMTV) superantigens (vSAG) are notorious for defying structural characterization and a consensus has yet to be reached regarding their ability to bridge the TCR to MHCII molecule. In this study, we determined the topology of the T cell signaling complex mediated by vSAG by examining the respective relation of vSAG7 with the MHCII chains, MHCII-associated peptide and TCR. We used various covalently linked peptide-MHCII complexes to demonstrate that vSAG presentation is tolerant to variation in the protruding side chains of the peptide, but sensitive to a protruding N-terminal extension. An original approach in which vSAG was covalently linked to either MHCII chain confirmed that maturing vSAG binds the MHCII β chain outside the peptide binding groove. Also, whereas mature vSAG binds to the MHCII α chain in a conformation-sensitive manner, immature vSAG binds the β chain. Because both vSAG moieties remain non-covalently associated after processing, our results suggest that vSAG crosslinks MHCII molecules. Comparing different T cell hybridomas, we identified key residues on the MHCII α chain that are differentially recognized by the CDR3β when engaged by vSAG. Finally, we describe a highly conserved TGXY motif responsible for vSAG-mediated T cell activation. Our results reveal a novel SAG-MHCII-TCR architecture in which vSAGs coerce a near-canonical docking between MHCII and TCR that allows eschewing of traditional CDR3 binding with the associated-peptide in favor of MHCII α chain binding. Our findings highlight the plasticity of the TCR complementary determining regions.

Keywords: Mouse mammary tumor virus/superantigens/antigen presentation/MHC class II/T-cell receptor.

INTRODUCTION

Superantigens (SAGs) are bacterial or viral proteins that have the ability to stimulate up to 20% of the total T cell population, bypassing conventional MHC class II (MHCII) antigen processing and presentation (1). SAG-activated T cells undergo a strong proliferation phase that is followed by either anergy or deletion (2). In contrast to canonical MHCII-TCR docking, which relies on the intimate binding of the complementary determining regions (CDRs) to the MHCII α-helixes and associated-peptide, TCR bridging to MHCII by SAGs relies on distinct strategies (3). On the one side, they commonly bind to the TCR CDR2, framework region 3 (FR3) and hypervariable region (HV4) that are within a specific variable (V) family (4). On the other side, they either bind i) the MHCII α chain, ii) a binding interface composed of the MHCII α chain and associated-peptide, iii) the MHCII βHis81 residue through coordination of a zinc ion or iv) the entire MHCII membrane-distal surface spanning the α, β chain and the associated-peptide (4, 5). Moreover, a handful of SAGs have the ability to crosslink or oligomerize MHCII molecules by using both the MHCII α and β chain binding sites (6). SAGs of viral origin have yet to provide a clear picture in terms of their ability to compel such interactions.

The best-characterized viral SAGs (vSAG) are those encoded by the mouse mammary tumor viruses (MMTVs). Contrary to other SAGs, vSAGs are produced by the host cell machinery and must undergo post-translational modifications in order to stimulate T cells (7). First, a precursor polypeptide forming a type II transmembrane protein of 37 kDa is modified by the addition of up to five N-linked glycans (8). Then, the 45 kDa glycoprotein transits to the Golgi where it is cleaved at two specific R-X-X-R dibasic motifs, resulting in the N-vSAG and C-vSAG (also called 18 kDa) moieties. After processing, both N- and C-terminal domains remain non-covalently associated and detached from the membrane (9). This maturation allows cells to shed vSAGs, even if devoid of MHCIIs, a feature called paracrine transfer (10). Finally, by binding both MHCII

and TCR, the C-vSAG domain is responsible for cognate T cell stimulation (11, 12). Within this fragment is the most polymorphic region of the MMTV SAGs, the C-terminal 21 to 38 residues responsible for Vβ specificity (13). Extensive TCR mutagenesis has revealed that the TCR-binding site of C-vSAG includes the TCR Vβ FR3 and HV4 (14–18). Interaction with MHCIIs, in contrast, is puzzling and has been reasoned from competition experiments in which vSAG and the staphylococcal enterotoxin A (SEA) compete for binding on both the α and β chains (10, 19).

The molecular basis for successful T cell stimulation by vSAG7 is an interesting conundrum. Our group and others have described vSAG presentation to be influenced by the peptide repertoire (12, 20, 21). However it is unknown whether this characteristic is linked to vSAG binding to MHCII or TCR recognition of the vSAG-bound MHCII complex. Conflicting evidence of vSAG binding to the MHCII α, β chains or peptide-binding groove exists in the literature and none provides a consensual model on how they successfully generate the T cell signaling complex (10, 19, 22, 23). In the present study, we aimed to determine the topology of the vSAG-MHCII-TCR complex by examining the respective relationship of vSAG7 with the MHCII chains, associated-peptide and TCR. To this end, we used a panel of covalently linked peptide-MHCII molecules, point mutants and MHCII-vSAG single chain (SC) constructs. Altogether, our results define a novel MHCII-SAG-TCR architecture.

MATERIAL AND METHODS

Plasmids and mutagenesis

The vSAG7 sequence was codon optimized using GeneOptimizer™ (Invotrogen). pBUD-DRα, and -DRβ have been described elsewhere (24). Lumenal portions of DRα (aa 1-191) and DRβ (aa 1-199) were linked to the lumenal part of vSAG7 (aa 667-322) or Ii (a 72-297) by the PCR overlap extension method (25). The chains were joined by a small glycine-serine linker (G_3-S-G_3) introduced in DR chains, Ii and vSAG7 by complementary overlapping primers. DRα mutants, peptide-linked DRβ (26), HASCT, SCDΔCt and HASCTΔCt were generated by the PCR overlap extension method using the Phusion polymerase (NEB). The resulting cDNAs were cloned into pCDNA3 vector (Invitrogen).

Antibodies and reagents

The following antibodies were used: VS7 (mouse monoclonal antibody (mAb) IgG1 to the C-terminal end of MMTV7 SAG) (27), L-243 (mouse IgG2a mAb) and ISCR3 (mouse mAb IgG2b) bind a specific DRα conformational epitope (28), XD5 (mouse IgG1 mAb to a linear epitope in the β1 domain of all class II molecules) (29), BU45 (mouse IgG1 mAb to the C-terminal portion of human Ii) (30) and CerCLIP.1 (mouse IgG1 mAb to the N-terminal portion of CLIP) (31). The anti-DRα (rabbit anti-serum against the DRα chain) and anti-DRβ (rabbit anti-serum against the DRβ*0101 chain purified from SDS-PAGE; R.P. Sékaly, unpublished). The anti-SEA mAb was a kind gift of Dr W. Mourad (University of Montreal) (32). SEA was purchased from Sigma Aldrich (St-Louis, MO).

Cell lines and transfections

Human epithelial HEK 293T, HeLa DM.5 and HeLa CIITA cells (21), and murine DAP cells were culture in DMEM (Wisent) with 5% fetal bovine serum (FBS; Wisent) while Kmls.13.11 and Kmls 12.6 T cell hybridomas (33) were cultured in DMEM with 10% FBS. CTLL-2 (ATCC TIB-214; American Type Culture

Collection) and HA1.7 TCR+ Jurkat cell line, CH7C17 (34), were cultured in RPMI (Wisent) with 10% FBS and 4 μM of β-mercaptoethanol. HeLa and DAP cells were transfected with the fusion proteins using lipofectamine LTX reagent (Invitrogen) according to the manufacturer's instructions. The cells were selected for resistance against geneticin (500 μg/mL; Wisent) and sorted by flow cytometry, using a FACSVantage SE (BD). HEK 293T cells were transfected using the calcium phosphate method as described previously (35) using 8 μg of plasmid DNA. Cells were harvested and analyzed 48 h post-transfection.

Flow cytometry

Cells were incubated in PBS with the primary Ab for 30 min on ice. Cells were washed twice with PBS and incubated a further 30 min with the Alexa fluor-488-coupled goat anti-mouse IgG Ab (Invitrogen) for 30 min on ice. After two more washes, cells were analyzed by flow cytometry using a FACScalibur (BD biosciences). Alternatively, cells were incubated for 1 h with SEA (1μg/ml) on ice and washed twice with PBS prior to the addition of Abs. Intracellular stainings were performed as mentioned on fixed, permeabilized cells (4% paraformaldehyde, 0.05% saponin).

T cell stimulation assays

vSAG7-expressing APCs were co-cultured at a 1:1 ratio with $5x10^4$ T cell hybridomas for 18h at 37°C. IL-2 production was determined by the ability of the co-culture supernatant to sustain the proliferation of the IL-2-dependent T cell line CTLL-2 and measured by [^{3}H]thymidine incorporation (47). For indirect presentation, APC (donors) were co-cultured with BJAB cells (acceptors) and responder T cell hybridomas at a ratio of 1:1:1.

Immunoblot

Stable or transfected cells were lysed for 30 min on ice at a density of $2x10^7$ cells per mL in 1% (v/v) Triton X-100 in lysis buffer (20 mM Tris-HCl, 150 mM NaCl)

and Complete Protease Inhibitor (Roche). Heated (65°C) or boiled total protein extracts were then separated by SDS-PAGE (10 %) under reducing conditions, unless mentioned otherwise. Samples were transferred to Hybond-ECL nitrocellulose membrane (Amersham Biosciences). Membranes were blocked for 1 h with 5% (w/v) dry milk in TBS-T (TBS with 0.1% (v/v) Tween® 20). The following steps were also performed in TBS-T with 5% dry milk. Primary antibody to DRα, DRβ and vSAG7 were incubated for 1 h at room temperature. Membranes were washed three times for 10 min and incubated for 1 h with HRP-conjugated secondary antibodies (BIO/CAN Scientific) followed by three more 10-min washes. Bands were visualized by the BM Chemiluminescence Blotting Substrate (Roche). For endo H sensitivity, 500U of endoglycosidase H (NEB) were added to the protein extract and incubated for 1h at 37°C. Samples were analyzed on SDS-PAGE as above.

RESULTS

The MHCII associated-peptide influences vSAG7 presentation

It was previously shown that DM-deficient human cells could not present the toxic shock syndrome toxin-1 (TSST-1) or vSAGs (21, 36). Similarly, presentation of these SAGs by cells from H2-DM-deficient mice was inefficient (37–39). DM edits the peptide repertoire by exchanging CLIP for a variety of peptides with better kinetic stability (40). Thus, we wondered whether the accumulation of CLIP-MHCII complexes observed in DM negative cells was responsible for the lack of vSAG7 presentation. We used the well-characterized DM-negative T2-DR3 cell line (41). In these cells, over 90% of the DR molecules are loaded with CLIP, a phenotype that is lost upon transfection of DM (42). As shown in Figure 1A, whereas T2-DR3 cells failed to present vSAG7, T2-DR3-DM^+ cells led to strong T cell proliferation, similar to that observed with DM-proficient BJAB and COX B cell lines. Of note, in this experiment, vSAG was provided by co-culturing APCs with the class II-negative DAP-vSAG7+ cell line (10). These results suggest that CLIP-DR3 complexes do not support vSAG7 presentation.

We next aimed to determine how the CLIP peptide could affect vSAG7 presentation. Considering the MHCII associated-peptide, vSAG presentation can be influenced by: i) the peptide's flanking residues (PFR) extending outside the groove, ii) the peptide's protruding side chains or iii) a peptide-induced MHCII conformational change. To discriminate between these possibilities, we generated cell lines displaying distinct homogenous pMHCII populations by transfecting DRα with various peptide-DRβ fusion proteins (43). The mouse DAP cells were chosen as model APCs as they are easily transfected and allow vSAG7-specific T cell stimulation upon co-transfection of MHCIIs and vSAG (44). Once stable peptide-DR1 DAP cell lines were obtained, we transiently transfected vSAG7 and monitored proliferation of mouse vSAG7-responsive T

cell hybridomas (45). We used two different hybridomas bearing Vβ6 regions cognate for vSAG7. Because vSAG7 expression is low, we co-expressed a reporter GFP to monitor transfection efficiencies and plotted MFI in bar graphs below or beside histograms of all cell lines.

Firstly, we tested whether the PFRs of CLIP were affecting vSAG stimulation. We hypothesized that the hallmark N-terminal extension of CLIP would affect vSAG7 presentation based on analyses of CLIP peptides found in T2-DR3 cells, which all bear 4 to 6 PFRs (46, 47). We generated cell lines expressing MHCIIs charged with either longCLIP$_{81\text{-}101}$ or coreCLIP$_{87\text{-}101}$ peptides, herein named lCLIP and cCLIP, respectively (Fig. 1B). To ensure that the quaternary structure of the different complexes was not disturbed by the peptide, we used two different mAbs: L243, which binds a conformational epitope on DRα chain and XD5.117, which binds a linear epitope on DRβ chain (29, 48). Figure 1C shows for each cell line the MHCII cell-surface expression and the MFI of the reporter GFP (lower panels). Both cell lines expressed similar amount of MHCIIs and were similarly receptive to DNA upon the subsequent transient transfection of vSAG7 and GFP.

After vSAG7 transfection, cells were incubated with the Vβ6^{+} T cell hybridomas Kmls 13.11 or 12.6. As shown in Figure 1D, vSAG7 presentation by lCLIP-DR was inefficient compared to cCLIP-DR, the latter giving rise to strong T cell response. Interestingly, we also observed a decrease in L243 mAb reactivity with the lCLIP-DR1 transfectant (Fig. 1C), better portrayed by the graph in Figure 1E showing normalized MFI for L243 over XD5. The reduced L243 reactivity for lCLIP-MHCII complexes can either stem from an MHCII conformation alteration or steric hindrance between the CLIP$_{81\text{-}86}$ extension and L243. This result suggests that vSAG7 presentation is sensitive to variations in pMHCII that are also sensed by the mAb L243. However, it is hard to pinpoint whether it is one of these effects, or a combination of both, that account for the reduction in

stimulatory capacity of vSAG7. On the one hand, it was reported that the L243-like 14-4-4S mAb, specific for mouse MHCII, competes against vSAG7 on I-E^d (49). Likewise, the *Staphylococcus* enterotoxin B (SEB), which binds to the MHCII α chain and competes with L243, is also affected by lLCIP (50, 51). On the other hand, superimposition of the crystal structures of DR1 bound to either $CLIP_{86\text{-}101}$ or $CLIP_{90\text{-}101}$ showed conformational alteration in the loop connecting the third and forth strands of the MHCII β-sheet platform that includes lysine α39 (52). Mutation of K39 abolishes L243 and SEB binding but does not affect vSAG presentation (53). Therefore, although there is a known conformational change between CLIP-MHCII variants, it is unlikely to affect vSAG7 presentation. Together these results suggest that the reduced vSAG7 stimulation observed when presented by lCLIP-DR1 is due to steric hindrance of vSAG7 by terminal PFRs of CLIP. Also, the above-described data corroborate the notion that vSAG7 binds to the MHCII α chain (10).

Secondly, we sought to evaluate the contribution of TCR-contacting peptide residues by comparing the capacity of peptides with distinct protruding side chains to present vSAG7. To this end, we employed a covalently linked hemagglutinin $HA_{(307\text{-}319)}$ peptide (HADR1). We selected this peptide over CLIP given the availability of the HA peptide-DR1-HA1.7 TCR structure and the responsive modified Jurkat cell line expressing the HA1.7 TCR (thereafter simply referred to Jurkat) (34, 54). Our rationale was to be able to distinguish both the conventional and vSAG presentation in the same setting, using different T cells. In addition, to minimize adverse effects linked to the bound-peptide's primary sequence, we performed the same assays using another peptide supporting vSAG presentation, the tetanus toxin peptide ($TT_{829\text{-}842}$). Like the HA-DR1, TT-DR1 has great kinetic stability and also fills the P1 pocket with a tyrosine, thus providing a system to test the exclusive contribution of peptide protruding side chains (Fig. 1B) (55, 56). The TCR contacting side chains of these two peptides were interchanged, resulting in the backbone (b) HA_b and TT_b variants, and

involved a charge reversal at P-1 (K-Q), a change of a small residue (V) to a bulkier one (I) at P2, and finally a change from a negatively charged residue to a highly hydrophobic one (K-F) at P8. If any of the peptide protruding side chains were implicated in specific vSAG7 contacts, one should expect to see differential stimulation between these peptides, independently of the T cell Vβ specificity. The stably transfected HAβ and TTβ constructs (Fig. 1F, H) were then tested for their capacity to stimulate T cells (Fig. 1G, I). Every variant successfully presented vSAG7, suggesting that a peptide's protruding side chains are not critical for vSAG7-mediated response (Fig. 1G, I). Conversely, presentation of HA_b failed to stimulate Jurkat T cells (Fig. 1J) as specific TCR contact residues have been modified (54). All covalently-linked peptides (except ICLIP) supported strong vSAG7 presentation, ruling out a role for the peptide's C-terminal linker and thus, PFR at this end. Altogether, these results suggest a model in which vSAG7 presentation is tolerant to the nature of the peptide's protruding side chains, but sensitive to peptides bearing an N-terminal extension.

N-vSAG7 has an overlapping binding site with SEA on the DRβ chain

The above-described data support the notion that C-vSAG7 binds to the MHCII α chain. However, it has been proposed that the vSAG7 polypeptide has two binding site on MHCII, one of which shares the same interface as SEA on the β chain or binds the peptide-binding groove (19, 22, 23). Maturing vSAGs are composed of two domains that remain non-covalently associated upon processing. C-vSAG participates in MHCII-TCR bridging but the role of N-vSAG is less clear. To gain insight on the role of the latter, we designed two single chain polypeptides in which the luminal domain of either DR chain is linked to that of vSAG7. These straightforward single chain dimers (SCDs) were inspired by a similar SC between MHCII and Ii (57). Such SCDs were made possible because HLA-DR and vSAG7 are type I and type II proteins, respectively, allowing fusion of the C-terminus of DR chains to the N-terminus of vSAG7. The

resulting DRα and β-based fusion molecules were named αSCD and βSCD, respectively and are depicted in Figure 2A. For brevity, when a SCD is mentioned in an experimental setting, it is always co-transfected with its matching complementary wild type DR chain partner, *e.g.* DRα+βSCD is referred to βSCD.

First, we characterized the interaction between the SCDs and their complementary MHCII chain partner. For these experiments, we used HEK 293T cells given their high transfection efficiency. As shown in Figure 2B, the αSCD apparently failed to associate with DRβ upon transfection, as judged by the lack of L243 surface staining and unusual degradation pattern (Supplemental Fig. 1). In contrast, the βSCD properly associated into heterodimers with DRα, trafficked to the plasma membrane and was recognized by a panel of conformational mAbs (Fig. 2B). Using the anti-C-vSAG7 mAb VS7, we also observed MHCII-bound vSAGs at the cell surface (Fig 2B, right panel). Altogether, these results indicate that only the βSCD can generate ordered complexes and allow vSAG surface expression.

Next, to confirm that vSAG7 behaved like the *wt* vSAG when part of the βSCD, we verified whether it still competed the binding of SEA. We transfected HEK 293T cells with either *wt* DR or βSCD and performed SEA binding assays monitored by flow cytometry. Figure 2C shows the DR (left panel) and SEA (right panel) staining profiles, which reveal weak SEA binding to cells expressing βSCD. Once normalized for MHCII surface expression, we noted a two-fold MFI reduction for βSCD compared to the *wt* or βIi-SCD controls (Fig. 2D). These results indicated that the vSAG moiety on DRβ prevented SEA binding. However, as SEA has a minor low affinity binding site on the MHCII α chain, the possibility remained that the observed competition was due to the presence of vSAG7 on DRα (58, 59). To test this, we performed the same experiment using a DRα

mutant that is unable to bind SEA (DRαK39A) (58). As shown in Fig. 2E, competition is observed whether βSCD is associated with *wt* MHCII α chain or K39A mutant. Moreover, truncating C-vSAG from βSCD, generating the βSCDΔCt, resulted in a similar reduction of SEA binding, confirming that N-vSAG7 and SEA have an overlapping binding interface (Fig. 2F). The high SEA concentration and affinity for βHis81 are factors likely to favor displacement of some of the vSAG7 molecules and could explain why competition was not total. Likewise, processing of the vSAG7 moiety is observed and could favor its dissociation from the β chain (Supplemental Fig. 1). These data confirmed that N-vSAG has an overlapping binding site with SEA on the MHCII β chain.

vSAG7 does not bind the MHCII peptide groove

Our results described so far define the binding site of C-vSAG7 and N-vSAG to the MHCII α and β chain, respectively. Thus, it was difficult to envision a model where vSAG7 interacted with both DR chains at once. The Huber group proposed that a segment of MMTV vSAGs (called the MIIPBM, MHCII peptide binding motif) interacts with the MHCII peptide-binding groove upon synthesis in the ER (23). The CIIPBM motif is part of N-vSAG and could bridge both vSAG segments through the MHCII cleft. To verify whether vSAG7 occupies the MHCII groove, we designed a new construct, HA-single chain trimer (HASCT), in which the HA peptide was appended to the βSCD N-terminus (Fig. 2A). Based on the Hsu et al. premise, our rationale was that N-vSAG7 would prevent HA binding to the groove. Figure 3A shows the surface DR expression for both βSCD and HASCT in comparison to *wt* DR and HADR. Interestingly, DR surface staining was increased in both transfectants expressing the linked-HA peptide. These data corroborate well with the MHCIIs increased stability when optimal peptide occupies the groove (26). Soluble versions of DRβ and HAβ (sβ and sHAβ) chains were used as controls and ruled out transmembrane (TM) domain-mediated bias between the TM-devoid βSCD and controls. L243 MFI ratios of sβ

and βSCD against sHAβ and HASCT, respectively, showed a 4-fold increase in expression when HA was fused to DRβ (Fig. 3B). That the tethered HA peptide increased expression of DR is incompatible with a model in which vSAG would occupy the binding groove.

To confirm that the HA peptide was lodged inside the groove and not displaced by the immature vSAG7 polypeptide, we tested the complex for SDS sensitivity. Indeed, HA-DR1 complexes resist SDS-denaturation and migrate as compact peptide-loaded heterodimers under non-boiled conditions (60). Cell lysates obtained from the transfectants presented in Figure 3A as well as a βIi-SCD control were analyzed by SDS-PAGE. XD5 mAb was used to probe the resulting immunoblots. As expected, in absence of HLA-DM, neither Ii- nor vSAG7- SCDs formed compact complexes with DRα (Fig. 3C, lane 4 and 6). In contrast, when HA was linked to either DRβ or βSCD (lane 2 and 8), compact, SDS-resistant heterodimers were observed, confirming that the HA-peptide was present in the groove.

To unequivocally prove that vSAG7 did not bind to the MHCII cleft, we tested whether the HASCT could induce both Jurkat and vSAG-specific T cell responses. To this end, we moved from the HEK 293T to HeLa cells, the former being unable to present vSAG (21). Of note, although the molecular basis of this defect remains obscure, HeLa cells are unable to present vSAGs unless transfected with CIITA or treated with IFN-γ (21). This provided a useful system to evaluate the presentation of HA independently of vSAG in absence of CIITA and of both HA and vSAG7 in the presence of CIITA. We transiently transfected our various β chains into either HeLa or HeLa CIITA+ cells and assessed the response of Jurkat or Kmls 13.11 cells. As expected, vSAG7 presentation only occurred in the presence of CIITA, whether from the SCD and SCT (Fig. 3E). Surprisingly, HeLa cells transfected with HASCT failed to stimulate Jurkat cells in contrast to the control sHAβ (Fig. 3D). The lack of HA presentation can be

attributed to either an MHCII conformation flaw or to the vSAG moiety of the HASCT hampering proper TCR docking. We argue for the latter alternative because the tested mAbs did not distinguished the HASCT from the sHAβ control (Fig. 3A) and in the presence of CIITA, HA presentation was restored (Fig. 3D). However, that Jurkat failed to respond to the HASCT in CIITA-negative cells was puzzling. This is not due to degradation of the SCT-HA peptide and its subsequent association to endogenously expressed MHCIIs as the DRβ*0102 allele in the homozygous HeLa CIITA+ cells does not present $HA_{307-318}$ to Jurkat T cells (61) and therefore must arise from the HA-DR1 moiety of the SCT. One explanation is that in presence of a pool of MHCIIs, C-vSAG is transferred from the processed SCT onto the endogenous pMHCIIs (supporting vSAG presentation), thus revealing HA to the HA1.7 TCR bearing Jurkat T cells. The implications of this finding are discussed below.

vSAG7 presentation relies on MHCIIα-TCR interactions

To better pinpoint the C-vSAG7 binding site on DRα and investigate the TCR binding topology, we generated an array of mutants of the α-helix lining the peptide groove. Most mutants were modeled from DQ2 and IA^q, which present vSAG poorly and span aa63 to 68, the interface associated with SEB binding (13). Figure 4A shows the point-mutants on the HA-DR1 cartoon depiction (Protein data base (PDB): 1FYT) as well as DRα residues implicated in L243 mAb binding (28, 54). Flow cytometry analysis of the resulting stable DR expression in DAP cells is given in Figure 4B assessed by L243 and XD5 staining. As above, stable cell lines were transiently co-transfected with vSAG7 and the reporter GFP. Then, cells were co-cultured with Kmls 13.11 and Kmls 12.6 T cells and IL-2 production was measured. In an effort to minimize the effect of the cells' intrinsic associated-peptides, we co-expressed each DRα variant with the HADRβ chain. In addition, this allowed us to monitor the stimulation of HA-specific Jurkat cells, which could be impeded by the α chain mutations (Fig 4D). As predicted from the HA-DR1-HA1.7 TCR co-crystal (54), only mutation of

TCR contact residues α64, 65 and 67 abrogated presentation of HA to Jurkat cells.

Noteworthy, the reactivity of L243 was strongly decreased towards DR mutants α63 and α67 (Fig. 4B). This is best portrayed by the bar graph in Figure 4C, showing L243 MFI over the MFI of the conformation-insensitive XD5 mAb. Surprisingly, those same DR mutants had a dramatically reduced ability to present vSAG7 (Fig. 4E and F) suggesting again overlapping binding regions between L243 and vSAG. As the side-chain of α63 points laterally, the weakened stimulation observed with both hybridomas by the αI63E MHCII mutant cell line suggests that C-vSAG7 binding is somehow affected by this mutation. Indeed, a less obstructive mutation, αI63A, restored vSAG7 stimulation (Supplemental Fig. 2A and 2B).

Interestingly, while DRαA64R allowed a strong Kmls 13.11 stimulation, Kmls 12.6 failed to respond (Fig. 4E and F). This result indicates a TCR recognition effect unrelated to vSAG7 binding and highlights the importance of specific DRα-TCR contacts for efficient T cell stimulation. In line with this, it became difficult to evaluate whether the effect of DRα K67A on vSAG presentation is actually linked to a weakened association between vSAG and DRα or to a TCR recognition defect. Indeed, DRα K67 is characterized by a lack of both L243 reactivity and inefficient presentation of HA peptide to Jurkat cells, making both outcomes plausible (Fig. 2C and D). Although weak, the stimulatory response observed exclusively with the Kmls 13.11 hybridoma suggests that TCR recognition is a factor.

The solvent exposed DRα α-helix is used by SEB to bridge TCRs (62). The fact that vSAG7 presentation implicates DRα-TCR interactions demonstrates that the topology of the ternary complex is different from the one involving SEB. Interestingly, only the DRα mutant A64R cell line was unable to support SEB presentation (Supplemental Fig. 2C). The highly conserved A64 is buried inside

the SEB-DRα interface and the Arg substitute is likely to sterically hinder SEB association, probably reflecting the effect of I63E on vSAG7 presentation. Overall, it is apparent that the mechanism leading to TCR recognition of the vSAG-MHCII complexes differs from SEB and canonical peptide-MHCII recognition.

vSAG7 mediates TCR activation through a conserved T-G-X-Y motif

The specific interactions between the TCR and the MHCII α chain suggest the existence of conserved vSAG-TCR contacts. Given the numerous responsive Vβs for all vSAGs, it is unlikely that the TCR interaction is solely based on the polymorphic vSAG C-terminus as it would severely impede the likelihood of a cognate partnership. Interestingly, an alignment of MMTV SAGs and MMTV SAG-related domain from other viruses (*e.g.* herpesvirus) revealed a conserved T-G-X-Y motif (Fig. 5A), located at residues 226-229 of C-vSAG. Such a motif has been shown to be crucial for γ-aminobutyric acid (GABA) binding to the $GABA_A$ receptor and mutagenesis analysis identified that GABA binding depends on the threonine and the tyrosine (63). Based on this fact, we mutated the tyrosine 229 to a Phe and assessed the ability of vSAG7-YF to stimulate different T cell hybridomas. Figure 5B indicates that the Y229F mutation introduced either in full length or SC vSAG7 abrogated the activity. The TGXY motif could impact vSAG activity in many ways. On one hand, it could perturb C-vSAG binding to MHCIIs or its overall structural integrity. Both these hypotheses are refuted by the fact that the mutation did not affect surface expression of MHCIIs nor vSAG7 (Fig. 5C and D). On the other hand, the tyrosine 229 could be implicated in direct TCR contact. Supporting this mechanism is the presence of a similar motif, LGNY, on a SEB contacting loop that interacts with the HV4 region of the TCRβ. Accordingly, mutation of the Tyr on SEB prevents its presentation (64, 65). Furthermore, Digglemann and coworkers described the region of C-vSAG bearing the TGXY motif as part of the TCR-interacting domain (66). These results suggest that in addition to highly polymorphic regions responsible for Vβ

specificities, vSAG binding also relies on conserved vSAG-specific TCR interactions.

DISCUSSION

The data presented herein define how vSAG7 bridges MHCII to the TCR. C-vSAG binds the MHCII α chain in a conformation-sensitive manner at the interface formed between the α-helix and the β-sheet platform. We demonstrated that, when coerced by vSAG, the TCR recognizes the MHCII in a near canonical manner, which constitutes a unique topology among those previously described for SAGs. Next, our results suggest that maturing N- and C-vSAG7 bind the MHCII β and α chains, respectively, on distinct MHCIIs. Finally, we identified a conserved motif in MMTV vSAGs, responsible for TCR binding independently of the TCR Vβ specificity. Based on our results and those of others, we propose a model in which the N- and C-terminal domains of a single vSAG crosslink two MHCIIs and bridge only specific TCR bearing Vβ elements that can be skewed as to recognize the MHCII α chain instead of the associated-peptide (Fig. 4G).

C-vSAG7 binding to the MHCII α chain is influenced by the associated-peptide

Presentation of vSAG7 requires that MHCIIs be filled with a diverse peptide repertoire (12, 21, 38). Here, we demonstrated that a single peptide supports vSAG7 presentation. However, the MHCII associated-peptide must meet certain criteria in order to be part of a permissive pMHCII. By comparing cell lines expressing either cCLIP-DR1 or lCLIP-DR1, we showed that the $CLIP_{81\text{-}86}$ PFR inhibits vSAG presentation (Fig. 1D). Interestingly, it was previously described that CLIP N-terminal extensions also interfered with SEB binding to MHCII (51). Based on the crystal structures of CLIP-DR3 and CLIP-I-A^b, the $CLIP_{81\text{-}86}$ N-terminal extension is disordered thus failing to discern whether it prevents vSAG binding by steric hindrance, electrostatic repulsion or if this effect is a hallmark of the $CLIP_{81\text{-}86}$ sequence (67, 68). Future studies will address this issue by characterizing the impact of N-terminal extensions on various peptides. Nevertheless, knowing the profound effect of PFRs on canonical and TSST-1 T

cell responses (39, 69, 70), and that DM favors the binding of peptides that tightly fit the groove, our findings point to N-terminal peptide trimming as a major determinant for vSAG presentation (40, 71). These results explain why DM-deficient cells, either murine or human, are unable to present vSAG7 as they are predominantly charged with CLIP peptide bearing a 4-6 amino acids extension (46, 47, 72). It was reported by Hsu *et al.* that a DM-negative B cell line was able to present vSAG7 (23). However, as opposed to T2 cells expressing a single MHCII (DR3) or our DAP cell lines (DR1), the proportion of the various alleles of DR, DQ or DP that are bound to CLIP at steady state or which form of CLIP is bound is unclear in the DM^- model.

It is unclear whether the previously reported need for peptide diversity reflects a direct contribution of the peptide's sequence to part of the vSAG binding site, or an indirect negative effect echoed in the MHCII conformation. The findings presented herein support the latter hypothesis. It is unlikely that vSAG7 interacts with the MHCII bound-peptide's protruding side chains because severe changes in charge or size between those of HA, TT and CLIP did not affect their ability to activate Vβ6 and Vβ8.1 bearing T cells (Fig. 1 and Supplemental Fig. 2D). While we did not conduct a thorough saturation mutagenesis of the peptides, our observation of DRα-TCR contacts portrays a setting in which vSAG7-peptide interactions are improbable (see below).

Our results suggest that C-vSAG7 binds to the lateral interface formed by the solvent-exposed DRα α-helix/β-sheet junction (Fig. 4A), an area highly susceptible to peptide-induced conformational changes (73). That HA-DR1αI63E, but not HA-DR1αI63A reduced L243 mAb reactivity and reduced vSAG7 presentation capabilities point to an MHCII conformation defect (Fig. 4C-D and S3). It was previously reported that mice expressing Eα-bound $I\text{-}A^b$ as the sole pMHCII were unable to mount vSAG7 specific responses, supporting the conclusion that a diverse MHCII peptide repertoire was required (38). In light of

our results, we can speculate as to why this pMHCII failed to present vSAG. The Eα(52-68) peptide bears no N-terminal PFRs and the C-terminal linker between the peptide and the MHCII β chain does not influence vSAG presentation. Thus, as previously presented by the authors, the inability of Eα-I-A^b to successfully present vSAG must be due to its intrinsic conformation (38). Indeed, whereas the 25-9-17 mAb binds a panel of peptide-bound I-A^b, Eα-I-A^b was not recognized (74, 75). One possibility is that vSAG7 binding is affected by the αF24 residue, reported to be pushed outward by the bulky p1-filling Phe of Eα, at the C-vSAG7 binding site (76). While we did not observe an effect of a Y-A substitution at the p1 HA residue (Supplemental Fig. 2E), it would be interesting to determine if a bulkier amino acid (*e.g.* Trp) substitution would reduce vSAG7 presentation accordingly. Altogether, these results indicate that the interface formed on the DRα α-helix/β-sheet junction is paramount for vSAG7 binding and that its presentation is vulnerable to both peptide-mediated conformational changes and N-terminal PFRs.

TCR engagement by vSAG7 is unique among SAGs

Most of the SAG-mediated T cell signaling complexes outline a typical interaction between the TCR Vβ and the SAG, where the Vα sometimes participates in MHCII β chain binding (4, 77, 78). Consequently, Vβ-MHCII α chain contacts are sterically precluded by the bound bacterial SAGs (bSAGs). Given the lack of an MMTV vSAG crystal structure, it is challenging to predict how vSAGs force MHCII-TCR association. Previous analyses of the response of mature peripheral T cells against vSAGs have clearly established that non-Vβ components of the TCR are involved in the pMHCII-vSAG7 complex recognition (79–82). The Vα chain was shown to be an important part of the complex and a skewed repertoire in responding cells has been identified (83, 84). Within a given Vα family, reactivity was seen with only certain Vβ subfamily members (84, 85). Thus, the variations in the CDR regions, especially CDR3, are likely to affect the capacity of these TCRs to bind the MHCIIs and might be at the origin of many of

the reported cases of MHCII allelic/isotype restriction (33, 49, 84, 86).

Based on these facts and our results demonstrating that DRα A64R and K67A mutant cell lines differentially stimulated distinct hybridomas bearing the same Vβ, it is clear that the TCR-MHCII contacts are imperative to vSAG7 signal transduction (Fig. 4E-F). Moreover, these findings highlight direct MHCII α chain-TCRβ contacts and would imply that vSAG7-mediated TCR engagement resembles that of conventional peptides, as hypothesized by the Marrack and Kappler group following their discovery that the TCR βT24Y mutant abrogated both conventional Ag and vSAG presentation (14, 87). Along the same lines, our MHCII α 64 and 67 mutants were also unable to trigger HA-specific activation of Jurkat cells (Fig. 4D). Based on the crystal structure of HA-DR1-HA1.7 TCR, DRα A64 and K67 are bound to the CDR2β D51 (54). However, one must be cautious in unifying these results. Indeed, as we have shown with our many different peptide-MHCII combinations, the peptide's protruding side chain did not affect vSAG response by the tested hybridomas, as would be expected in a traditional pMHCII-TCR setting (Fig. 1). Furthermore, mutations at residue α65 and α68, which are also implicated in TCR binding (54), had no effect on the ability of MHCIIs to present vSAG7 (Fig. 4D and E). Thus, it is fitting to picture a near canonical docking between MHCII and TCR that is coerced by vSAG. Such architecture allows eschewing of traditional CDR1/3 binding with the associated-peptide in favor of MHCII chain binding as proposed by Nguyen *et al.* (88). These Vα-MHCIIβ and Vβ-MHCIIα contacts remain to be verified biochemically (89).

A large body of literature suggests that the β chain junctional region could influence TCR recognition of vSAGs (80, 90–92). Especially relevant was the demonstration by many groups that Vβ6 thymic deletion is incomplete in vSAG7+ mice and that Vβ junctional diversity regulates vSAG reactivity (92, 93). At first glance, the need for a diverse peptide repertoire and the importance of Vβ

junctional diversity may seem paradoxical. As many peptides support vSAG binding, we do not expect skewing in CDR3. However, our results point to the existence of non-permissive peptides regulating vSAG binding and to unconventional interactions between MHCII and TCR. In order words, there may be extra pressure on CDR3s to have more intimate contacts with the MHCII chains than during canonical peptide recognition. Indeed, thymic positive selection does not directly influence the fine specificity of T cells toward MHCII and it has been suggested that TCR/MHCII interactions taking place during vSAG presentation are unconventional and linked to TCR recognition of haplotype-specific MHCII residues (80, 88). This is in line with the recent demonstration by Kilgannon *et al.* that three out of eight Vβ6+ T cells, although all specific for the same pMHCII (K5-IA^{d}), did not respond to vSAG7 (93).

A recent report by Stadinski *et al.* stresses the fact that TCR specificity for pMHC ligands is not driven by germline-encoded pairwise interactions. Notably, they described a single TCR Vβ using alternate strategies to bind pMHC when paired with different Vα (94). The authors argue that since CDR1 and CDR2 loops have the flexibility to bind their ligands in many ways, this could not fit a pairwise co-evolution model. Accordingly, it demonstrated that the CDR3 loops can markedly alter those evolutionarily selected contacts (95). Canonical CDR-pMHCII contacts can differ under different pressures, supporting a model in which vSAG enforces such unconventional docking.

vSAG7 moieties bind distinct MHCIIs

Given that vSAG7 N- and C-terminal moieties bind respectively the MHCII β1 and α1 domains, one must ask how such binding is possible while remaining non-covalently associated. We propose a model where C-vSAG binds the α chain of an adjacent MHCII, while still bound to N-vSAG, the latter attached to the β chain. In other words, unable to reach the α chain of its MHCII partner in *cis*, C-vSAG interacts with another MHCII in *trans*. This model highly resembles the

manner in which SEA crosslinks MHCII molecules via a low affinity binding site to the α chain and the Zn-dependent binding site on the β chain (96, 97). In the context of the SCT, our results showing that HA presentation to Jurkat cells is null in endogenous $MHCII^-$ as opposed to $MHCII^+$ cell lines strongly support such a model (Fig. 3D). Indeed, we speculate that in the absence of surrounding endogenous pMHCIIs, both vSAG7 moieties remain associated with the parent MHCII, blocking the groove and preventing the TCR from recognizing the HA-peptide. Also, as each MHCII is covalently linked to vSAG, it is possible the C-vSAG prevents any approaching vSAG from contacting the α chain in *trans*. In contrast, in Hela CIITA cells, C-vSAG7 will find numerous vSAG-free endogenous MHCII α chains to associate with, freeing the MHCII membrane-distal region for the HA-1.7 TCR binding. Future studies will address the biochemical basis for vSAG binding to two distinct MHCII molecules.

Highly conserved TCR binding motif in vSAGs

Our results indicate a more intricate vSAG7 presentation than previously acknowledged. vSAG stimulatory activity is paired to the TCR interaction of DRα, a structural aspect that will likely modulate its potency in terms of the responding T cell repertoire and the strength of the signal. Additionally, vSAG recognition of specific TCR vβ elements is mediated through its C-terminal 30 or so highly variable amino acids, complicating speculation as to how this family of vSAGs could mediate such a broad immune response without a conserved binding scheme. Interestingly, the chemical baicalin (BA), shown to block GABA binding to its receptor in the nervous system, also blocked T cell stimulation by TSST and SEB, suggesting a conserved mechanism between those two bSAGs, MMTV vSAG and GABA neurotransmitter linked to the TGXY motif (98, 99).

Conclusion

Our observation that conserved DRα residues are implicated in the recognition of the vSAG-peptide-MHCII by the TCR suggests that T cell activation is influenced by the polymorphic CDR3β region, linked to the recognition of the MHCII α chain. To our knowledge, this represents a novel SAG-mediated MHCII-TCR architecture. According to a recent study by Nur-ur Rahman *et al.* suggesting that the TCR CDR2β is the critical determinant for the functional recognition of bSAGs, it is clear that the topology of vSAG differs from those previously described (100). As both the MHCII allele and associated-peptide influence the potential interaction between MHCII and TCR, a given TCR could only recognize a fraction of the vSAG-pMHCII complexes (80). MMTV vSAGs are expressed at very low density on the cell surface and still remain highly potent T cell activators. This expression pattern is of great importance as it mimics the low density of conventional antigenic peptide-MHCII complexes, critical for T cell activation (101, 102).

AKNOWLEDGEMENTS

We thank Julie Chase and Christopher K. Salmon for proofreading and critical input on the manuscript. We also thank Walid Mourad for providing mAbs and Serge Sénéchal for his assistance with cell sorting.

CONFLIT OF INTEREST

The authors declare that they have no conflict of interest.

BIBLIOGRAPHY

1. Fraser, J. D., and T. Proft. 2008. The bacterial superantigen and superantigen-like proteins. *Immunological reviews* 225: 226–43.

2. Acha-Orbea, H., A. N. Shakhov, and D. Finke. 2007. Immune response to MMTV infection. *Frontiers in bioscience : a journal and virtual library* 12: 1594–609.

3. Scherer, M. T., L. Ignatowicz, G. M. Winslow, J. W. Kappler, and P. Marrack. 1993. SUPERANTIGENS: Bacterial and Viral protein that manipulate the Immune System. *Annu.Rev.Cell.Biol.* 9: 101–28.

4. Sundberg, E. J., L. Deng, and R. A. Mariuzza. 2007. TCR recognition of peptide/MHC class II complexes and superantigens. *Semin Immunol* 19: 262–271.

5. Bueno, C., G. Criado, J. McCormick, and J. Madrenas. 2007. T cell signalling induced by bacterial superantigens. *Chem Immunol Allergy* 93: 161–180.

6. Li, H., A. Llera, E. L. Malchiodi, and R. A. Mariuzza. 1999. The structural basis of T cell activation by superantigens. *Annual Reviews of Immunology* 17: 435–466.

7. Korman, A. J., P. Bourgarel, T. Meo, and G. E. Rieckhof. 1992. The mouse mammary tumour virus long terminal repeat encodes a type II transmembrane glycoprotein. *EMBO Journal* 11: 1901–1905.

8. McMahon, C. W., L. Y. Bogatzki, and A. M. Pullen. 1997. Mouse mammary tumor virus superantigens require N-linked glycosylation for effective presentation to T cells. *Virology* 228: 161–170.

9. Winslow, G. M., P. Marrack, and J. W. Kappler. 1994. Processing and MHC binding of the MTV7 superantigen. *Immunity* 1: 23–33.

10. Delcourt, M., J. Thibodeau, F. Denis, and R. P. Sekaly. 1997. Paracrine transfer of mouse mammary tumor virus superantigen. *Journal of Experimental Medicine* 185: 471–480.

11. Winslow, G. M., P. Marrack, and J. W. Kappler. 1994. Processing and major histocompatibility complex binding of the MTV7 superantigen. *Immunity* 1: 23–33.

12. Grigg, M. E., C. W. McMahon, S. Morkowski, A. Y. Rudensky, and A. M. Pullen. 1998. Mtv-1 superantigen trafficks independently of major histocompatibility complex class II directly to the B-cell surface by the exocytic pathway. *J.Virol.* 72: 2577–2588.

13. Acha-Orbea, H., and H. R. MacDonald. 1995. Superantigens of mouse mammary tumor virus. *Annual Reviews of Immunology* 13: 459–486.

14. Pullen, A. M., J. Bill, R. T. Kubo, P. Marrack, and J. W. Kappler. 1991. Analysis of the Interaction Site for the self superantigen Mls-1a on T cell receptor Vbeta. *Journal of Experimental Medicine* 173: 1183–1192.

15. Pullen, A. M., T. Wade, P. Marrack, and J. W. Kappler. 1990. Identification of the region of T cell receptor á chain that interacts with the self-superantigen Mls-1 a . *Cell* 61: 1365–1374.

16. Cazenave, P. a, P. N. Marche, E. Jouvin-Marche, D. Voegtlé, F. Bonhomme, A. Bandeira, a Coutinho, D. Voegtle, D. Voegtl,, and D. Bandeira. 1990. V beta 17 gene polymorphism in wild-derived mouse strains: two amino acid substitutions in the V beta 17 region greatly alter T cell receptor specificity. *Cell* 63: 717–728.

17. Herman, A., J. W. Kappler, P. Marrack, and A. M. Pullen. 1991. SUPERANTIGENS: mechanism of T-cell stimulation and role in immune responses. *Annual Reviews of Immunology* 9: 745–772.

18. MacNeil, D., E. Fraga, and B. Singh. 1992. Inhibition of superantigen recognition by peptides of the variable region of the T cell receptor á chain. *European Journal of Immunology* 22: 937–941.

19. Torres, B. A., N. D. Griggs, and H. M. Johnson. 1993. Bacterial and retroviral superantigens share a common binding region on class II MHC antigens Bacterial and retroviral superantigens share a common binding region on class II MHC antigens. *Nature* 364: 152–154.

20. Pullen, a M., and L. Y. Bogatzki. 1996. Receptors on T cells escaping superantigen-mediated deletion lack special beta-chain junctional region structural characteristics. *Journal of immunology (Baltimore, Md.: 1950)* 156: 1865–72.

21. Azar, G. A., R. P. Sekaly, and J. Thibodeau. 2005. A defective viral superantigen-presenting phenotype in HLA-DR transfectants is corrected by CIITA. *Journal of Immunology* 174: 7548–7557.

22. Mottershead, D. G., P. N. Hsu, R. G. Urban, J. L. Strominger, and B. T. Huber. 1995. Direct binding of the Mtv7 superantigen (Mls-1) to soluble MHC class II molecules. *Immunity.* 2: 149–154.

23. Hsu, P. N., P. Wolf Bryant, N. Sutkowski, B. McLellan, H. L. Ploegh, and B. T. Huber. 2001. Association of mouse mammary tumor virus superantigen with MHC class II during biosynthesis. *Journal of immunology* 166: 3309–14.

24. Faubert, A., A. Samaan, and J. Thibodeau. 2002. Functional analysis of tryptophans alpha 62 and beta 120 on HLA-DM. *J.Biol.Chem.* 277: 2750–2755.

25. Ho, S. N., H. D. Hunt, R. M. Horton, J. K. Pullen, and L. R. Pease. 1989. Site-directed mutagenesis by overlap extension using the polymerase chain reaction. *Gene* 77: 51–59.

26. Kozono, H., J. White, J. Clements, P. Marrack, and J. W. Kappler. 1994. Production of soluble MHC class II proteins with covalently bound single peptides. *Nature* 369: 151–154.

27. Winslow, G. M., M. T. Scherer, J. W. Kappler, and P. Marrack. 1992. Detection and biochemical characterization of the mouse mammary tumor virus 7 superantigen (Mls-1a). *Cell* 71: 719.

28. Fu, X. T., and R. W. Karr. 1994. HLA-DR alpha chain residues located on the outer loops are involved in nonpolymorphic and polymorphic antibody-binding epitopes. *Human Immunogy* 39: 253–260.

29. Radka, S. F., C. E. Machamer, and P. Cresswell. 1984. Analysis of monoclonal antibodies reactive with human class II beta chains by two-

dimensional electrophoresis and western blotting. *Human Immunogy* 10: 177–188.

30. Wraight, C. J., P. Van Endert, P. Moller, J. Lipp, N. R. Ling, I. C. MacLennan, N. Koch, and G. Moldenhauer. 1990. Human major histocompatibility complex class II invariant chain is expressed on the cell surface. *J.Biol.Chem.* 265: 5787–5792.

31. Denzin, L. K., N. F. Robbins, C. Carboy-Newcomb, and P. Cresswell. 1994. Assembly and intracellular transport of HLA-DM and correction of the class II antigen-processing defect in T2 cells. *Immunity.* 1: 595–606.

32. Mahana, W., R. Al-Daccak, C. Leveille, J. P. Valet, J. Hebert, M. Ouellette, and W. Mourad. 1995. A natural mutation of the amino acid residue at position 60 destroys staphylococcal enterotoxin A murine T-cell mitogenicity. *Infection & Immunity* 63: 2826–2832.

33. Herman, A., G. Croteau, R. P. Sekaly, J. Kappler, and P. Marrack. 1990. HLA-DR alleles differ in their ability to present staphylococcal enterotoxins to T cells. *Journal of Experimental Medicine* 172: 709–717.

34. Hewitt, C. R. A., J. R. Lamb, J. Hayball, M. Hill, M. J. Owen, and R. E. O'Hehir. 1992. Major histocompatibility complex independent clonal T cell anergy by direct interaction of Staphylococcus aureus enterotoxin B with the T cell antigen receptor. *Journal of Experimental Medicine* 175: 1493–1499.

35. Graham, F. L., and A. J. van der Eb. 1973. A new technique for the assay of infectivity of human adenovirus 5 DNA. *Virology* 52: 456–467.

36. Lavoie, P. M., J. Thibodeau, I. Cloutier, R. Busch, and R. P. Sekaly. 1997. Selective binding of bacterial toxins to major histocompatibility complex class II-expressing cells is controlled by invariant chain and HLA-DM. *Proceedings of the National Academy of Sciences of the United States of America* 94: 6892–6897.

37. Tourne, S., T. Miyazaki, A. Oxenius, L. Klein, T. Fehr, B. Kyewski, C. Benoist, and D. Mathis. 1997. Selection of a broad repertoire of CD4+ T cells in H-2Ma 0/0 mice. *Immunity.* 7: 187–195.

38. Golovkina, T., Y. Agafonova, D. Kazansky, and a Chervonsky. 2001. Diverse repertoire of the MHC class II-peptide complexes is required for presentation of viral superantigens. *Journal of immunology (Baltimore, Md.: 1950)* 166: 2244–50.

39. Hogan, R. J., J. VanBeek, D. R. Broussard, S. L. Surman, and D. L. Woodland. 2001. Identification of MHC class II-associated peptides that promote the presentation of toxic shock syndrome toxin-1 to T cells. *Journal of Immunology* 166: 6514–6522.

40. Schulze, M.-S. E. D., and K. W. Wucherpfennig. 2012. The mechanism of HLA-DM induced peptide exchange in the MHC class II antigen presentation pathway. *Current opinion in immunology* 24: 105–11.

41. Mellins, E., L. Smith, B. Arp, T. Cotner, E. Celis, and D. Pious. 1990. Defective processing and presentation of exogenous antigens in mutants with normal HLA class II genes. *Nature* 343: 71–74.

42. Denzin, L. K., N. F. Robbins, C. Carboy-Newcomb, and P. Cresswell. 1994. Assembly and intracellular transport of HLA-DM and correction of the class II antigen-processing defect in T2 cells. *Immunity* 1: 595–606.

43. Ignatowicz, L., G. Winslow, J. Bill, J. Kappler, and P. Marrack. 1995. Cell surface expression of class II MHC proteins bound by a single peptide. *Journal of Immunology* 154: 3852–3862.

44. Labrecque, N., H. Mcgrath, M. Subramanyam, B. T. Huber, and R. P. Sékaly. 1993. Human T Cells Respond to Mouse Mammary Tumor Virus-encoded Superantigen: Vbeta Restriction and Conserved Evolutionary Features. *Biotechnology* 177: 1735–1743.

45. Subramanyam, M., B. McLellan, N. Labrecque, R. P. Sekaly, and B. T. Huber. 1993. Presentation of the Mls-1 superantigen by human HLA class II molecules to murine T cells. *Journal of Immunology* 151: 2538–2545.

46. Riberdy, J. M., J. R. Newcomb, M. J. Surman, J. A. Barbosa, and P. Cresswell. 1992. HLA-DR molecules from an antigen-processing mutnat cell line are associated with invariant chain peptides. *Nature* 360: 474–477.

47. Sette, a, S. Ceman, R. T. Kubo, K. Sakaguchi, E. Appella, D. F. Hunt, T. A. Davis, H. Michel, J. Shabanowitz, R. Rudersdorf, H. M. Grey, and R. DeMars. 1992. Invariant chain peptides in most HLA-DR molecules of an antigen-processing mutant. *Science* 258: 1801–1804.

48. Gorga, J. C., P. J. Knudsen, J. A. Foran, J. L. Strominger, and S. J. Burakoff. 1986. Immunochemically purified DR antigens in liposomes stimulate xenogeneic cytolytic T cells in secondary in vitro cultures. *Cell Immunol.* 103: 160–173.

49. Blackman, M. A., F. E. Lund, S. Surman, R. B. Corley, and D. L. Woodland. 1992. Major histocompatibility complex-restricted recognition of retroviral superantigens by V beta 17+ T cells. *The Journal of experimental medicine* 176: 275–80.

50. Sundberg, E., and T. S. Jardetzky. 1999. Structural basis for the HLA-DQ binding by the streptococcal superantigen SSA. *Nature Structural Biology* 6: 123–29.

51. Vogt, A. B., L. J. Stern, C. Amshoff, B. Dobberstein, G. J. Hammerling, and H. Kropshofer. 1995. Interference of distinct invariant chain regions with superantigen contact area and antigenic peptide binding groove of HLA-DR. *Journal of Immunology* 155: 4757–4765.

52. Günther, S., A. Schlundt, J. Sticht, Y. Roske, U. Heinemann, K.-H. Wiesmüller, G. Jung, K. Falk, O. Rötzschke, and C. Freund. 2010. Bidirectional binding of invariant chain peptides to an MHC class II molecule. *Proceedings of the National Academy of Sciences of the United States of America* 107: 22219–24.

53. Thibodeau, J., N. Labrecque, F. Denis, B. T. Huber, and R. P. Sekaly. 1994. Binding sites for bacterial and endogenous retroviral superantigens can be dissociated on major histocompatibility complex class II molecules. *Journal of Experimental Medicine* 179: 1029–1034.

54. Hennecke, J., a Carfi, and D. C. Wiley. 2000. Structure of a covalently stabilized complex of a human alphabeta T-cell receptor, influenza HA peptide and MHC class II molecule, HLA-DR1. *The EMBO journal* 19: 5611–24.

55. Sullivan, D. O., T. O. M. Arrhenius, J. Sidney, M. D. E. L. Guercio, M. Albertson, M. Wall, C. Oseroff, S. Southwood, S. M. Colon, F. C. A. Gaeta, and A. Sette. 1991. On the interaction of promiscuous antigenic peptides with different DR aleles. *Journal of Immunology* 147.

56. De Magistris, M. T., J. Alexander, M. Coggeshall, a Altman, F. C. Gaeta, H. M. Grey, and a Sette. 1992. Antigen analog-major histocompatibility complexes act as antagonists of the T cell receptor. *Cell* 68: 625–34.

57. Thayer, W. P., C. T. Dao, L. Ignatowicz, and P. E. Jensen. 2003. A novel single chain I-A(b) molecule can stimulate and stain antigen-specific T cells. *Mol Immunol* 39: 861–870.

58. Thibodeau, J., M. Dohlsten, I. Cloutier, P. M. Lavoie, P. Bj”rk, F. Michel, C. Leveille, W. Mourad, T. Kalland, and R. P. Sekaly. 1997. Molecular characterization and role in T cell activation of staphylococcal enterotoxin A binding to the HLA-DRà chain. *Journal of Immunology* 158: 3698–3704.

59. Labrecque, N., J. Thibodeau, and R. P. Sekaly. 1993. Interactions between staphylococcal superantigens and MHC class II molecules. *Seminars in Immunology* 5: 23–32.

60. Natarajan, S. K., L. J. Stern, and S. Sadegh-Nasseri. 1999. Sodium dodecyl sulfate stability of HLA-DR1 complexes correlates with burial of hydrophobic residues in pocket 1. *Journal of Immunology* 162: 3463–3470.

61. Stumptner-Cuvelette, P., S. Morchoisne, M. Dugast, S. Le Gall, G. Raposo, O. Schwartz, and P. Benaroch. 2001. HIV-1 Nef impairs MHC class II antigen presentation and surface expression. *Proceedings of the National Academy of Sciences of the United States of America* 98: 12144–9.

62. Jardetzky, T. S., L. J. Stern, J. H. Brown, J. C. Gorga, R. G. Urban, J. L. Strominger, D. C. Wiley, Y. I. Chi, and C. Stauffacher. 1994. Three-dimensional structure of a human class II histocompatibility molecule complexed with superantigen. *Nature* 368: 711–718.

63. Amin, J., and D. S. Weiss. 1993. GABAA receptor needs two homologous domains of the beta-subunit for activation by GABA but not by pentobarbital. *Nature* 366: 565–69.

64. Kappler, J. W., A. Herman, J. Clements, and P. Marrack. 1992. Mutations Defining Functional Regions of the Superantigen Staphylococcal Enterotoxin B. *Journal of Experimental Medicine* 175: 387–396.

65. Li, H., a Llera, D. Tsuchiya, L. Leder, X. Ysern, P. M. Schlievert, K. Karjalainen, and R. a Mariuzza. 1998. Three-dimensional structure of the complex between a T cell receptor beta chain and the superantigen staphylococcal enterotoxin B. *Immunity* 9: 807–16.

66. Wirth, S., A. Vessaz, C. Krummenacher, F. Baribaud, H. Acha-Orbea, and H. Diggelmann. 2002. Regions of mouse mammary tumor virus superantigen involved in interaction with the major histocompatibility complex class II I-A molecule. *J Virol* 76: 11172–11175.

67. Ghosh, P., M. Amaya, E. Mellins, and D. C. Wiley. 1995. The structure of an intermediate in class II MHC maturation: CLIP bound to HLA-DR3. *Nature* 378: 457–462.

68. Zhu, Y., A. Y. Rudensky, A. L. Corper, L. Teyton, and I. a. Wilson. 2003. Crystal Structure Of MHC Class II I-Ab in Complex with a Human CLIP Peptide: Prediction of an I-Ab Peptide-binding Motif. *Journal of Molecular Biology* 326: 1157–1174.

69. Carson, R. T., K. M. Vignali, D. L. Woodland, and D. A. A. Vignali. 1997. T cell receptor recognition of MHC class II-bound peptide flanking residues enhances immunogenicity and results in altered TCR V region usage. *Immunity* 7: 387–399.

70. Wen, R., D. R. Broussard, S. Surman, T. L. Hogg, M. A. Blackman, and D. L. Woodland. 1997. Carboxy-terminal residues of major histocompatibility complex class II-associated peptides control the presentation of the bacterial superantigen toxic shock syndrome toxin-1 to T cells. *European Journal of Immunology* 27: 772–781.

71. Suri, A., S. B. Lovitch, and E. R. Unanue. 2006. The wide diversity and complexity of peptides bound to class II MHC molecules. *Current opinion in immunology* 18: 70–7.

72. Miyazaki, T., P. Wolf, S. Tourne, C. Waltzinger, A. Dierich, N. Barois, H. Ploegh, C. Benoist, and D. Mathis. 1996. Mice lacking H2-M complexes, enigmatic elements of the MHC class II peptide-loading pathway. *Cell* 84: 531–541.

73. Painter, C. a, M. P. Negroni, K. a Kellersberger, Z. Zavala-Ruiz, J. E. Evans, and L. J. Stern. 2011. Conformational lability in the class II MHC 310 helix and adjacent extended strand dictate HLA-DM susceptibility and peptide exchange. *Proceedings of the National Academy of Sciences of the United States of America* 108: 19329–34.

74. Chervonsky, A. V., R. M. Medzhitov, L. K. Denzin, a K. Barlow, A. Y. Rudensky, C. A. Janeway Jr., and C. a Janeway. 1998. Subtle conformational changes induced in major histocompatibility complex class II molecules by binding peptides. *Proc.Natl.Acad.Sci.U.S.A* 95: 10094–10099.

75. Wong, P., and A. Y. Rudensky. 1996. Phenotype and function of CD4 + T cells in mice lacking invariant chain. *Journal of Immunology* 156: 2133–2142.

76. Tobita, T., M. Oda, H. Morii, M. Kuroda, A. Yoshino, T. Azuma, and H. Kozono. 2003. A role for the P1 anchor residue in the thermal stability of MHC class II molecule I-Ab. *Immunology letters* 85: 47–52.

77. Saline, M., K. E. J. Rödström, G. Fischer, V. Y. Orekhov, B. G. Karlsson, and K. Lindkvist-Petersson. 2010. The structure of superantigen complexed with TCR and MHC reveals novel insights into superantigenic T cell activation. *Nature communications* 1: 119.

78. Wang, L., Y. Zhao, Z. Li, Y. Guo, L. L. Jones, D. M. Kranz, W. Mourad, and H. Li. 2007. Crystal structure of a complete ternary complex of TCR, superantigen and peptide-MHC. *Nat Struct Mol Biol* 14: 169–171.

79. Blackman, M. A., H. Gerhard-Burgert, D. L. Woodland, E. Palmer, J. W. Kappler, and P. Marrack. 1990. A role for clonal inactivation in T cell tolerance to Mls-1a. *Nature* 345: 540–542.

80. Woodland, D. L., H. P. Smith, S. Surman, P. Le, R. Wen, and M. A. Blackman. 1993. Major histocompatibility complex-specific recognition of Mls-1 is mediated by multiple elements of the T cell receptor. *Journal of Experimental Medicine* 177: 433–442.

81. Pircher, H., T. W. Mak, R. Lang, W. Balhausen, E. Ruedi, H. Hengartner, R. M. Zinkernagel, and K. Burki. 1989. T cell tolerance to Mlsa encoded antigens in T cell receptor Vbeta 8.1 chain transgenic mice. *EMBO Journal* 8: 719–727.

82. Yui, K., S. Komori, M. Katsumata, R. M. Siegel, and M. I. Greene. 1990. Self-reactive T cells can escape clonal deletion in T-cell receptor V á 8.1 transgenic mice. *Proceedings of the National Academy of Sciences of the United States of America* 87: 7135–7139.

83. Vacchio, M. S., O. Kanagawa, K. Tomonari, and R. J. Hodes. 1992. Influence of T cell receptor Valpha expression on Mlsa superantigen- specific T cell responses. *Journal of Experimental Medicine* 175: 1405–1408.

84. Smith, H. P., P. Le, D. L. Woodland, and M. A. Blackman. 1992. T cell receptor alpha-chain influences reactivity to Mls-1 in Vbeta8.1 transgenic mice. *Journal of Immunology* 149.

85. Aude-Garcia, C., a Attinger, D. Housset, H. R. MacDonald, H. Acha-Orbea, P. N. Marche, and E. Jouvin-Marche. 2000. Pairing of Vbeta6 with certain Valpha2 family members prevents T cell deletion by Mtv-7 superantigen. *Molecular immunology* 37: 1005–12.

86. Kang, J., C. A. Chambers, J. Pawling, and C. Scott. 1994. Conserved amino acid residues in the CDR1 of the TCR b-chain are involved in the recognition of conventional Ag and Mls-1 superantigen. *Journal of Immunology* 152: 5305–17.

87. Marrack, P., G. M. Winslow, Y. Choi, M. Scherer, A. Pullen, J. White, and J. W. Kappler. 1993. The bacterial and mouse mammary tumor virus

superantigens; two different families of proteins with the same functions. *Immunological Reviews* 131: 79–92.

88. Nguyen, P., D. L. Woodland, and M. A. Blackman. 1996. MHC bias of Mls-1 recognition is not influenced by thymic positive selection. *Cellular Immunology* 167: 224–229.

89. Andersen, P. S., P. M. Lavoie, R. P. Sékaly, H. Churchill, D. M. Kranz, P. M. Schlievert, K. Karjalainen, and R. a Mariuzza. 1999. Role of the T cell receptor alpha chain in stabilizing TCR-superantigen-MHC class II complexes. *Immunity* 10: 473–83.

90. Ciurli, C., D. N. Posnett, R. P. Sekaly, and F. Denis. 1998. Highly biased CDR3 usage in restricted sets of beta chain variable regions during viral superantigen 9 response. *Journal of Experimental Medicine* 187: 253–258.

91. Candéias, S., C. Waltzinger, C. Benoist, D. Mathis, S. Cand,as, and S. Candeias. 1991. The V beta 17+ T cell repertoire: skewed J beta usage after thymic selection; dissimilar CDR3s in CD4+ versus CD8+ cells. *Journal of Experimental Medicine* 174: 989–1000.

92. Chies, J. A., G. Marodon, A. M. Joret, A. Regnault, M. P. Lembezat, B. Rocha, and A. A. Freitas. 1995. Persistence of Vá 6 + T cells in Mls-1 a mice. A role for the third complementarity-determining region (CDR3) of the T cell receptor beta chain in superantigen recognition. *Journal of Immunology* 155: 4171–4178.

93. Kilgannon, P., Z. Novak, A. Fotedar, and B. Singh. 2010. Junctional diversity prevents negative selection of an antigen-specific T cell repertoire. *Molecular immunology* 47: 1154–60.

94. Stadinski, B. D., P. Trenh, R. L. Smith, B. Bautista, P. G. Huseby, G. Li, L. J. Stern, and E. S. Huseby. 2011. A role for differential variable gene pairing in creating T cell receptors specific for unique major histocompatibility ligands. *Immunity* 35: 694–704.

95. Deng, L., R. J. Langley, Q. Wang, S. L. Topalian, and R. A. Mariuzza. 2012. Structural insights into the editing of germ-line–encoded interactions between T-

cell receptor and MHC class II by Vα CDR3. *Proc.Natl.Acad.Sci.USA.* 190: 14960–14965.

96. Mehindate, K., J. Thibodeau, M. Dohlsten, T. Kalland, R. P. Sekaly, and W. Mourad. 1995. Cross-linking of major histocompatibility complex class II molecules by staphylococcal enterotoxin A superantigen is a requirement for inflammatory cytokine gene expression. *Journal of Experimental Medicine* 182: 1573–1577.

97. Petersson, K., M. Thunnissen, G. Forsberg, and B. Walse. 2002. Crystal structure of a SEA variant in complex with MHC class II reveals the ability of SEA to crosslink MHC molecules. *Structure* 10: 1619–1626.

98. Krakauer, T., B. Qun, and H. A. Young. 2001. The Flavonoid baicalin inhibits superantigen-induced in inflammatory cytokines and chemokines. *FEBS Letters* 500: 52–55.

99. Wang, F., Z. Xu, L. Ren, S. Y. Tsang, and H. Xue. 2008. GABA A receptor subtype selectivity underlying selective anxiolytic effect of baicalin. *Neuropharmacology* 55: 1231–7.

100. Nur-ur Rahman, A. K. M., D. A. Bonsor, C. A. Herfst, F. Pollard, M. Peirce, A. W. Wyatt, K. J. Kasper, J. Madrenas, E. J. Sundberg, and J. K. McCormick. 2011. The T cell receptor beta-chain second complementarity determining region loop (CDR2beta governs T cell activation and Vbeta specificity by bacterial superantigens. *The Journal of biological chemistry* 286: 4871–81.

101. Woodland, D. L., R. Wen, and M. A. Blackman. 1997. Why do superantigens care about peptides? *Immunology Today* 18: 18–22.

102. Proft, T., and J. Fraser. 1998. Superantigens: Just like peptides only different. *Journal of Experimental Medicine* 187: 819–821.

103. Blackman, M. A., and D. L. Woodland. 1996. Role of the T cell receptor alpha-chain in superantigen recognition. *Immunological Research* 15: 98–113.

104. Crooks, G. E., G. Hon, J. Chandonia, and S. E. Brenner. 2004. WebLogo : A Sequence Logo Generator. 1188–1190.

FOOTNOTES

[1]These authors contributed equally to this work

[2]Present address: Axenis, centre de Biologie Integrative des Maladies Émergentes (BIME), Institut Pasteur, Paris, France

[3]This research was funded by the Canadian Institute of Health Research CIHR; MOP 36355.

[4]Abreviations: SCD, single chain dimer; SCT, single chain trimer; SAG, superantigen; MMTV, mouse mammary tumor virus; vSAG, MMTV superantigen; bSAG, bacterial superantigen MHCII, major histocompatibility class II molecule; PFR, peptide flanking residues; SEA, staphylococcal enterotoxin A; SEB, staphylococcal enterotoxin B; TSST-1, toxic shock syndrome toxin 1;

FIGURE LEGENDS

Figure 1. vSAG7 presentation is dictated by the MHCII associated-peptide. **A**) vSAG presentation by DM+ and DM- B cell lines following vSAG transfer from the vSAG7+ DAP cell line (10). Presentation is monitored by the stimulation of Vβ6 and 8.1 bearing T cell hybridoma Kmls 13.11 and KR3+. BJAB (DR3) is used as a positive B cell control and COX is a DR3+DM+ B cell line. **B**) Sequence alignment of different peptide constructs covalently linked to DRβ used to assess vSAG presentation. Peptides are aligned according to the residue filling the P1 pocket. Asterisks above the sequences mark the protruding side chains at positions P-1, P2 and P8. MHCII cell surface expression of DAP cells transfected with DRα and cCLIP- or lCLIP- (**C**), HA- or HA_b- (**F**), or TT- or TT_b- (**H**) stained with either L243 or XD5 anti-DR mAbs. The MFI values for cell surface expression are shown are shown in the lower right corner of each histogram and are colored according to the legend. Bar graphs below the histograms represent the MFI of the GFP control plasmid co-transfected with vSAG7, to monitor the transfection efficiency. L243/XD5 MFI ratio of the two CLIP variants, $cCLIP_{87\text{-}101}$ and $lCLIP_{81\text{-}101}$ are shown in **E**. Transfected cell lines from **C**, **F** and **H** were used as APC to stimulate Kmls 13.11, Kmls 12.6 hybridomas or Jurkat T cells (**D**, **G, I** and **J**). All data are representative of at least three independent experiments.

Figure 2. The N-terminal domain of vSAG7 overlaps SEA binding site on the MHCII β chain. A) Schematic representations of SCD and SCT are shown. The C-terminus of DR1 β chains were covalently attached to the N-terminus of vSAG7 by flexible GLY-SER linker. Peut-être ajouter que la meme chose est faite avec α In the SCT, a peptide was appended to the N-terminus of the β chain according to Kozono et. al (26). The linkers between DR and either the peptide, vSAG7 or Ii are represented as light grey boxes. **B**) L243 and VS7 cell surface staining of HEK 293T cells transfected with the αSCD or βSCD and the

appropriate complementary DR chain or a *wt* DR and vSAG7 control. L243 and VS7 mAbs recognize a conformational epitope on DRα and the C-terminal end of vSAG7, respectively. **C**) HEK 293T cells were transiently transfected with *wt* DR and vSAG7, DRα and the vSAG7-SCDs or Ii-βSCDs. 48h post-transfection, cells were harvested, split and incubated on ice with L243 or SEA for 3h. After washing, bound SEA was detected by flow cytometry using an anti-SEA mAb. These staining profiles are representative of at least five independent experiments. **D**) The MFI were plotted as a ratio where the error bars represent the standard deviation to the mean of three stainings on independent populations of transfected cells. **E**) Same as **D**, but using DRα K39A mutant, which prevents SEA binding to the α chain. **F**) Same as **D**, but using a truncated version of the vSAG7-SCDΔCt, devoid of the C-terminal domain. All data are representative of at least three independent experiments.

Figure 3. vSAG7 binding to MHCII α and β chains occurs on distinct MHCII molecules. A) Cell surface expression of MHCII on HEK 293T cells transfected with DR or SCD (right panel) and HADR or SCT (left panel) stained with the L243 mAb. **B**) The MFI of the transfectants bearing the HA peptide were plotted as a ratio against the ones without HA. The error bars represent the standard deviation to the mean of three stainings on independent populations of transfected cells. **C**) Compact SDS-resistant and -sensitive form of DR were assessed by immunoblot (IB) analysis of total protein extracts (boiled or heated to 65°C) from the transfectants in **A**. Ii-SCDs were used as control. The IB was revealed with the anti-DRβ mAb XD5. The two compact complexes are marked with I or II (lane 2 and 8) and schematized next to the gel. **D**) Comparison of HA-specific T cell stimulation between endogenous MHCII positive or negative HeLa cells transfected with different MHCII β chains. HeLa MHCII positive cells expressed DR2, contrary to the transfected DR1. **E**) Same as **D** but comparing vSAG7 specific T cell stimulation. All data are representative of at least three independent experiments.

Figure 4. Residues on the MHCII α chain act in tandem with vSAG to engage TCRs. A) Cartoon depiction of the MHCII with a close-up on the peptide-binding groove that highlights DRα α-helix spanning mutants (pink) and the L243 mAbs binding site (red), depicted as sticks. The α, β chains and peptide are green, blue and yellow, respectively. **B**) MHCII cell surface profiles of DAP cell lines transfected with HADRβ and different DRα mutants as stained with L243 and XD5 mAbs. The MFIs are shown in the lower right corner of each histogram and are colored according to the legend. Co-transfected GFP protein was used to monitor the transfection efficiency of vSAG7 and MFI are shown as bar graphs next to histograms. **C**) L243 and XD5 MFI ratios derived from **B**. Cell lines from **B** were transfected with vSAG7 or a mock control before monitoring Jurkat (**D**), Kmls 13.11 (**E**) and Kmls 12.6 (**F**) T cell proliferation. All data are representative of at least three independent experiments. **G**) Model of vSAG7 binding to MHCII and TCR in which the multiple binding regions between vSAG7, both MHCII chains and the TCR are highlighted. The N-vSAG and C-vSAG moieties remain non-covalently associated after processing and lead to the cross-linking of MHCII molecules. Binding of C-vSAG7 to the MHCII α chain is conformation-dependent and abrogated by a peptide N-terminal extension. The TCRβ CDR3 binds the MHCII α chain specifically instead of the peptide whereas vSAG binds the FR3 and HV4 region of the Vβ. The exact nature of Vα binding to the MHCII β remains to be fully characterized (103).

Figure 5. A conserved *TGXY* motif is central to vSAG7's activity. A) Sequence similarity among 18 MMTV vSAG proteins or vSAG-like domains. The height of a particular position is proportional to the frequency of the corresponding residue type between the aligned sequences and to the sequence information in the alignment and its given bits (104). The residue numbering is based on the vSAG7 protein, genebank ID: M90535.1. The letters T, G and Y of the motif are colored a lighter shade of grey. **B**) Functional assay of transiently

transfected HeLa CIITA cells with multiple β chains against the vSAG7-reactive Kmls 13.11 T cell hybridoma. **C**) L243 cell surface expression profiles of DRα transiently co-transfected with either the βSCD or the Y229F mutant. **D**) Ratios between DR and vSAG MFI were plotted from the transfectants in **C** and the error bars represent the standard deviation to the mean of three independent experiments.

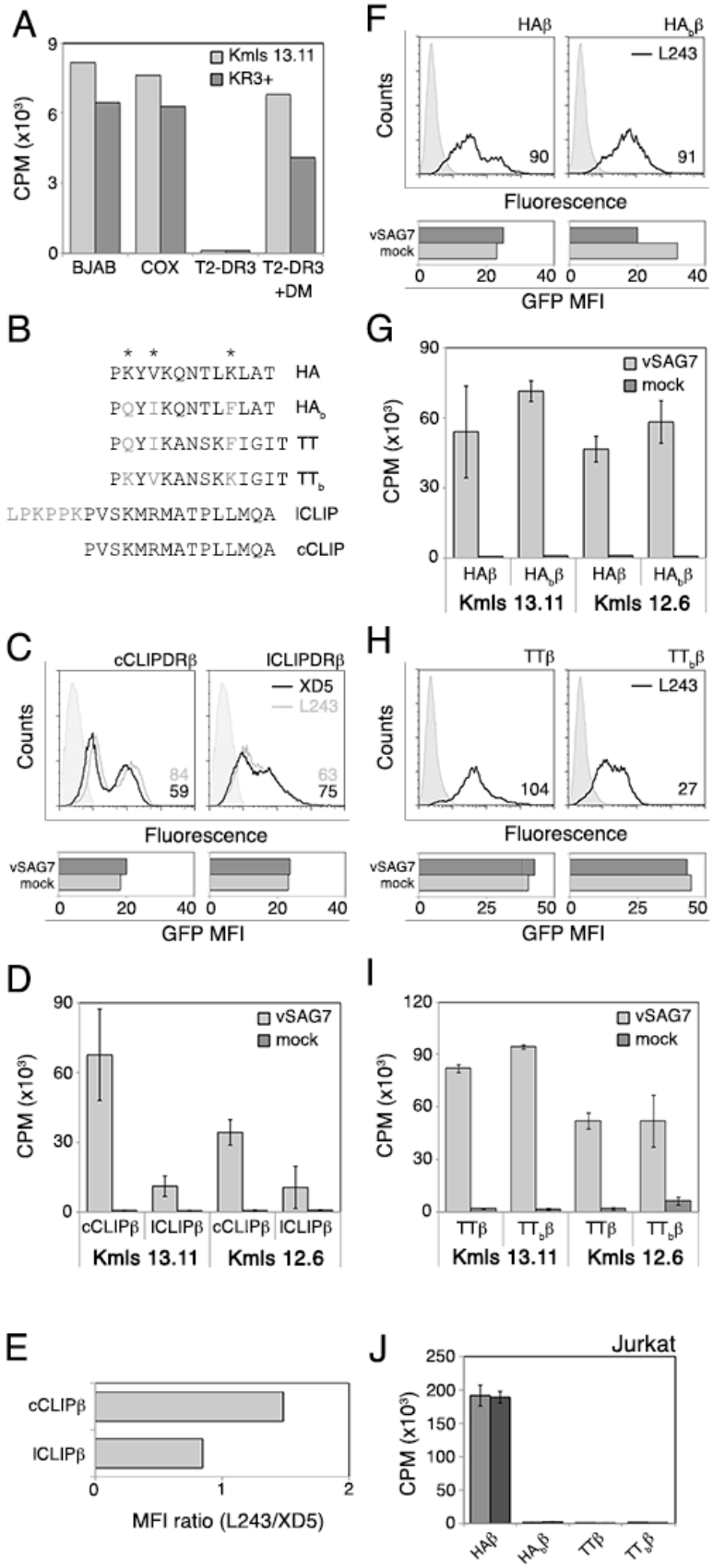
A
CPM (x10³)
Kmls 13.11
KR3+
BJAB
COX
T2-DR3
T2-DR3 +DM
B
PKYVKQNTLKLAT HA
PQYIKQNTLFLAT HAb
PQYIKANSKFIGIT TT
PKYVKANSKKIGIT TTb
LPKPPKPVSKMRMATPLLMQA ICLIP
PVSKMRMATPLLMQA cCLIP
C
cCLIPDRβ
ICLIPDRβ
XD5
L243
Counts
Fluorescence
vSAG7
mock
GFP MFI
D
vSAG7
mock
cCLIPβ
ICLIPβ
Kmls 13.11
Kmls 12.6
E
cCLIPβ
ICLIPβ
MFI ratio (L243/XD5)
F
HAβ
HAbβ
L243
Counts
Fluorescence
GFP MFI
G
vSAG7
mock
CPM (x10³)
HAβ
HAbβ
Kmls 13.11
Kmls 12.6
H
TTβ
TTbβ
L243
Counts
Fluorescence
GFP MFI
I
vSAG7
mock
CPM (x10³)
TTβ
TTbβ
Kmls 13.11
Kmls 12.6
J
Jurkat
CPM (x10³)
HAβ
HAbβ
TTβ
TTbβ

Figure 1

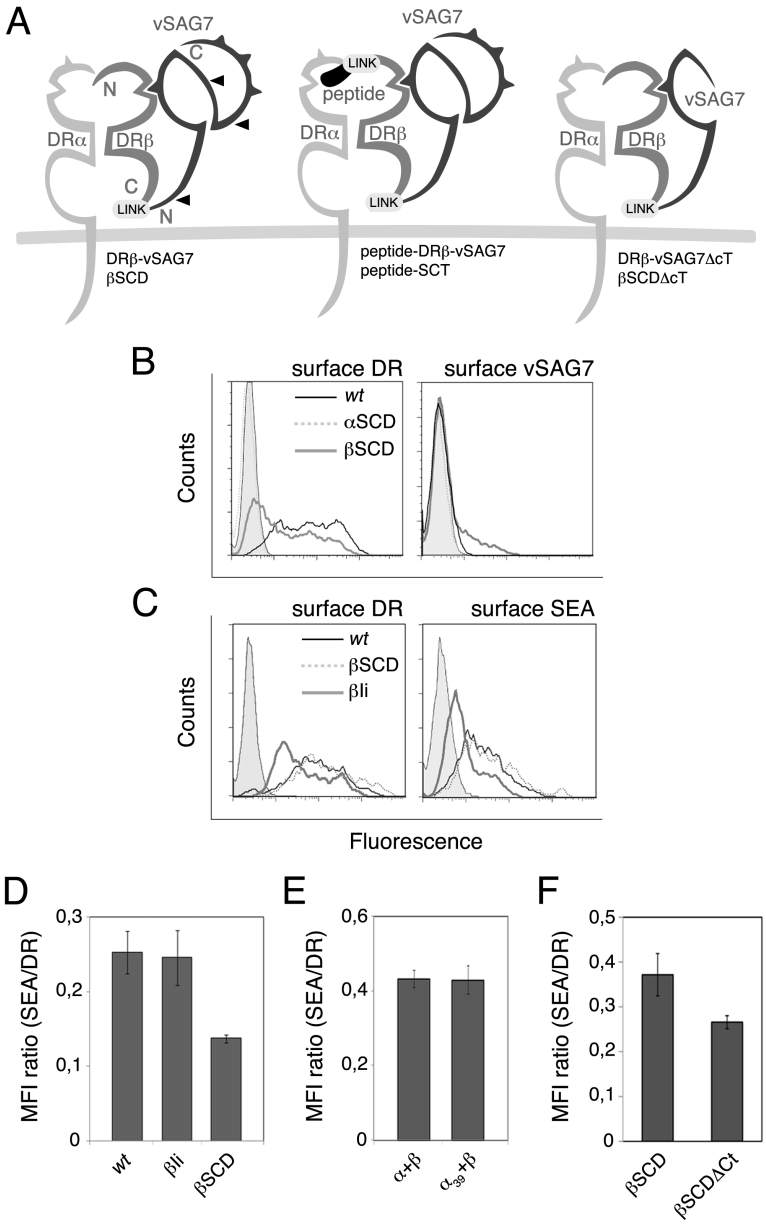
A
vSAG7
C
N
DRα
DRβ
C
LINK
N
DRβ-vSAG7
βSCD
vSAG7
LINK
peptide
DRα
DRβ
LINK
peptide-DRβ-vSAG7
peptide-SCT
vSAG7
DRα
DRβ
LINK
DRβ-vSAG7ΔcT
βSCDΔcT
B
surface DR
surface vSAG7
wt
αSCD
βSCD
Counts
C
surface DR
surface SEA
wt
βSCD
βIi
Counts
Fluorescence
D
MFI ratio (SEA/DR)
0,3
0,2
0,1
0
wt
βIi
βSCD
E
MFI ratio (SEA/DR)
0,6
0,4
0,2
0
α+β
αsc+β
F
MFI ratio (SEA/DR)
0,5
0,4
0,3
0,2
0,1
0
βSCD
βSCDΔCt

Figure 2

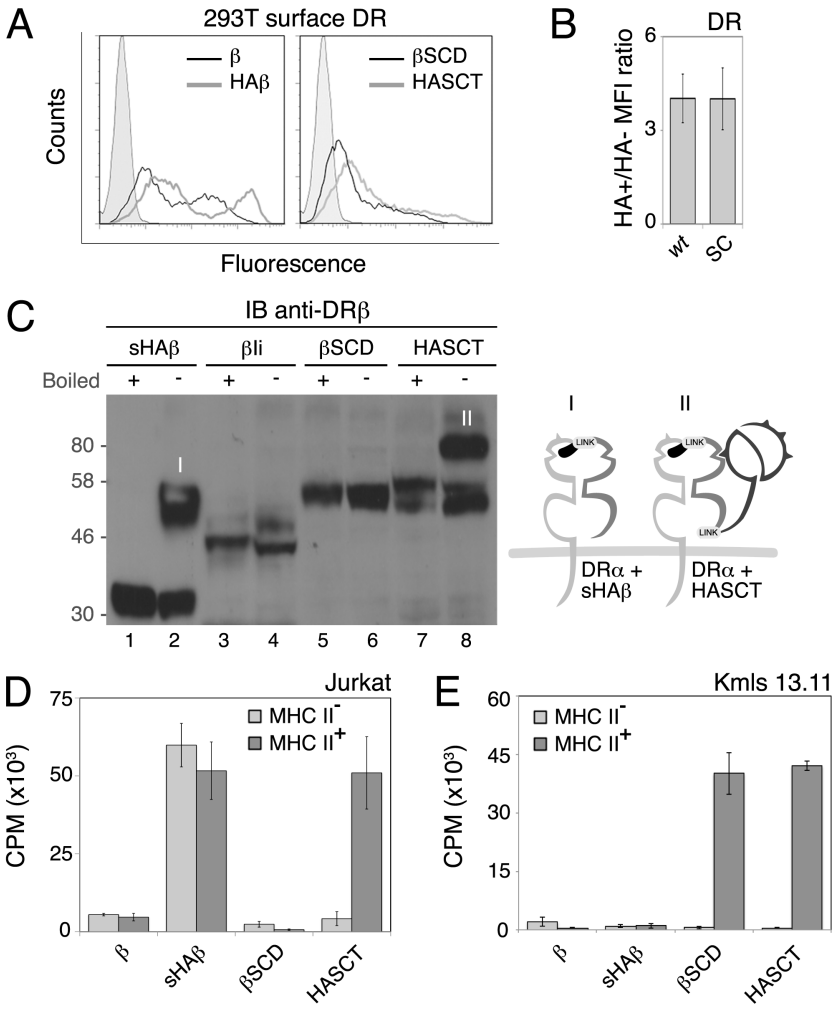
A
293T surface DR
β
HAβ
βSCD
HASCT
Counts
Fluorescence
B
DR
HA+/HA- MFI ratio
6
3
0
wt
SC
C
IB anti-DRβ
sHAβ
βIi
βSCD
HASCT
Boiled
+ - + - + - + -
80
58
46
30
I
II
1 2 3 4 5 6 7 8
I
II
LINK
LINK
LINK
DRα + sHAβ
DRα + HASCT
D
Jurkat
MHC II-
MHC II+
CPM (x10³)
75
50
25
0
β
sHAβ
βSCD
HASCT
E
Kmls 13.11
MHC II-
MHC II+
CPM (x10³)
60
45
30
15
0
β
sHAβ
βSCD
HASCT

Figure 3

Figure 4

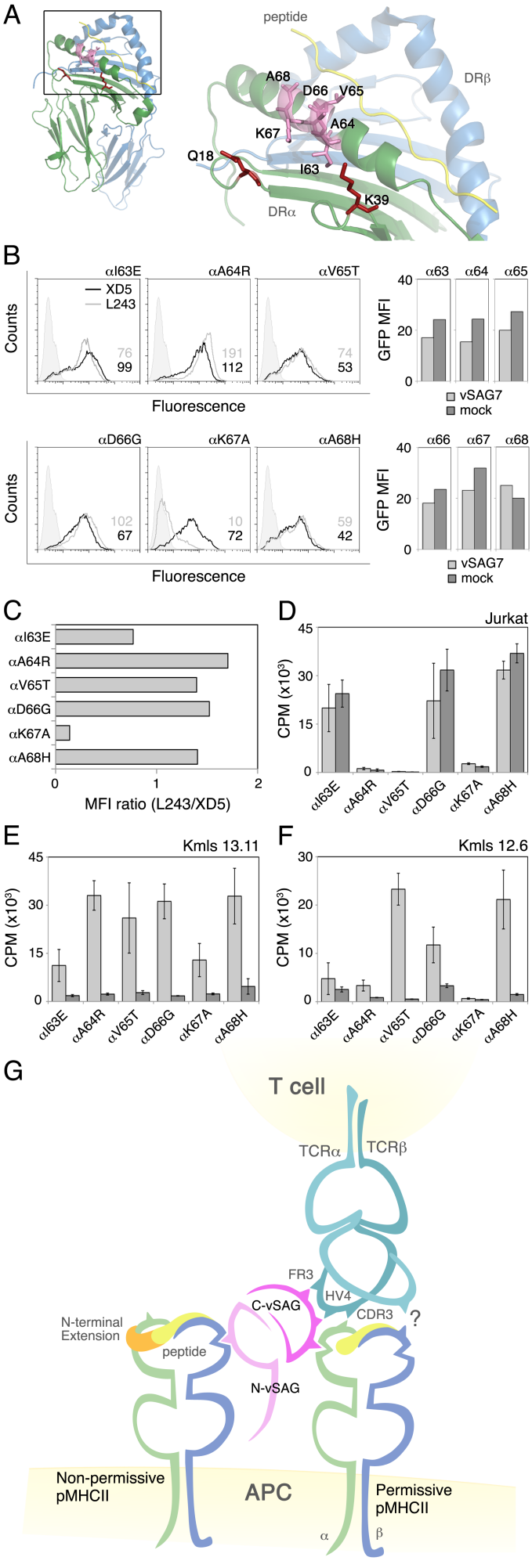
A
peptide
DRβ
A68
D66
V65
A64
K67
Q18
I63
K39
DRα
B
αI63E
αA64R
αV65T
XD5
L243
Counts
76
99
191
112
74
53
Fluorescence
α63
α64
α65
GFP MFI
40
20
0
vSAG7
mock
αD66G
αK67A
αA68H
102
67
10
72
59
42
α66
α67
α68
C
αI63E
αA64R
αV65T
αD66G
αK67A
αA68H
0
1
2
MFI ratio (L243/XD5)
D
Jurkat
CPM (x10³)
45
30
15
0
E
Kmls 13.11
F
Kmls 12.6
G
T cell
TCRα
TCRβ
FR3
HV4
C-vSAG
CDR3
?
N-terminal
Extension
peptide
N-vSAG
Non-permissive
pMHCII
APC
Permissive
pMHCII
α
β

Figure 5

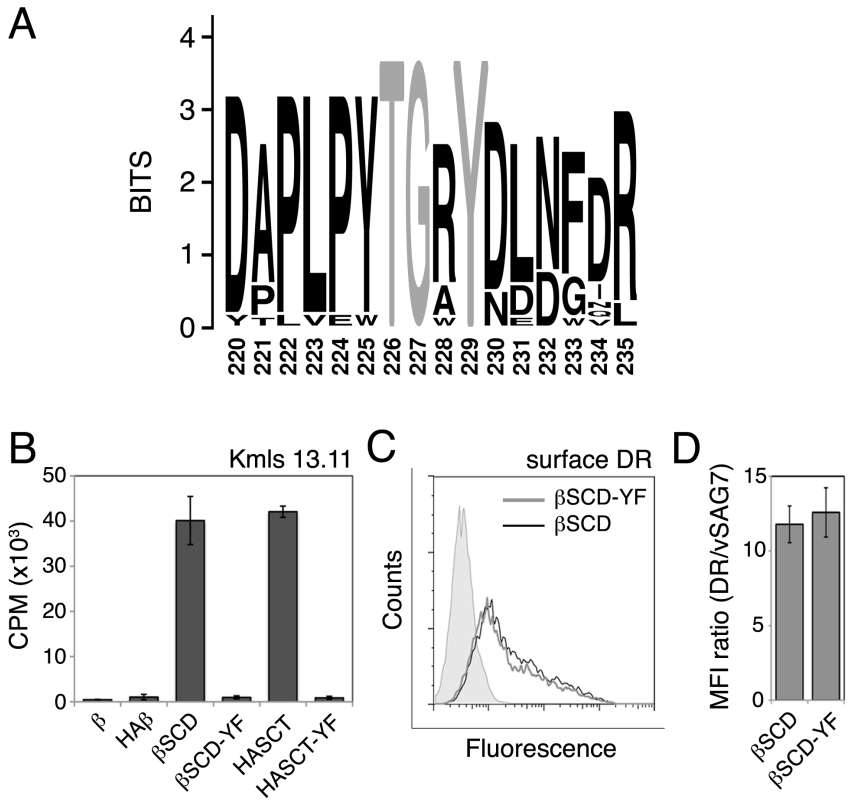
A
BITS
4
3
2
1
0
220 221 222 223 224 225 226 227 228 229 230 231 232 233 234 235
B
Kmls 13.11
CPM (x10³)
50
40
30
20
10
0
β
HAβ
βSCD
βSCD-YF
HASCT
HASCT-YF
C
surface DR
βSCD-YF
βSCD
Counts
Fluorescence
D
MFI ratio (DR/vSAG7)
15
10
5
0
βSCD
βSCD-YF

Chapter 3 : HLA-DM-induced structural change in HLA-DOβ

Experimental design: FD, DAD, JSF and JT

Performed experiments: FD[45%], DAD[30%] and JSF[25%]

Writing: DAD[40%], JSF[30%] and JT[30%]

I could really use a hand

- The salvation of DO by DM

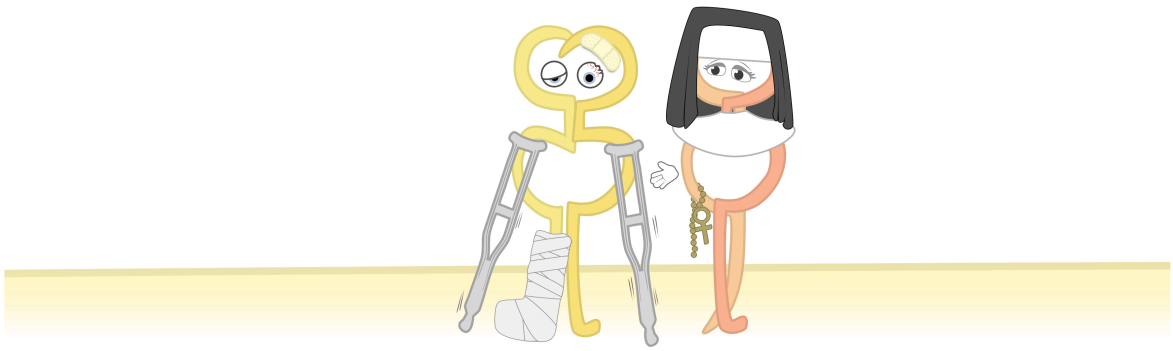

Immunology
The Journal of cells, molecules, systems and technologies

British Society for immunology

IMMUNOLOGY ORIGINAL ARTICLE

Evidence for a human leucocyte antigen-DM-induced structural change in human leucocyte antigen-DOβ

Francis Deshaies,[1,*] Djibril A. Diallo,[1,*] Jean-Simon Fortin,[1,*] Helen M. O'Rourke,[2] Abdul Mohammad Pezeshki,[1] Angélique Bellemare-Pelletier,[1] Nicola Raby,[1] Nathalie Bédard,[1] Alexandre Brunet,[1] Lisa K. Denzin[2] and Jacques Thibodeau[1]

[1]*Laboratoire d'Immunologie Moléculaire, Département de Microbiologie et Immunologie, Université de Montréal, Montréal, QC, Canada, and* [2]*Immunology Program, Weill Graduate School of Medical Sciences, Cornell University, and Sloan-Kettering Institute, Memorial Sloan-Kettering Cancer Center, New York, NY, USA*

doi:10.1111/j.1365-2567.2008.02984.x
Received 27 June 2008; revised 15 September 2008; 29 September 2008; accepted 30 September 2008.
*These authors contributed equally.
Correspondence: J. Thibodeau, Laboratoire d'Immunologie Moléculaire, Département de Microbiologie et Immunologie, Université de Montréal, CP 6128, Succursale Centre-Ville, Montréal, QC H3C 3J7, Canada.

Senior author: Jacques Thibodeau

Summary

Human leucocyte antigen (HLA)-DO is a non-classical major histocompatibility complex class II molecule which modulates the function of HLA-DM and the loading of antigenic peptides on molecules such as HLA-DR. The bulk of HLA-DO associates with HLA-DM and this interaction is critical for HLA-DO egress from the endoplasmic reticulum. HLA-DM assists the early steps of HLA-DO maturation presumably through the stabilization of the interactions between the N-terminal regions of the α and β chains. To evaluate a possible role for HLA-DM in influencing the conformation of HLA-DO, we made use of a monoclonal antibody, Mags.DO5, that was raised against HLA-DO/DM complexes. Using transfected cells expressing mismatched heterodimers between HLA-DR and -DO chains, we found that the epitope for Mags.DO5 is located on the DOβ chain and that Mags.DO5 reactivity was increased upon cotransfection with HLA-DM. Our results suggest that HLA-DM influences the folding of HLA-DO in the endoplasmic reticulum. A mutant HLA-DO showing reduced capacity for endoplasmic reticulum egress was better recognized by Mags.DO5 in the presence of HLA-DM. On the other hand, an HLA-DO mutant capable of endoplasmic reticulum egress on its own was efficiently recognized by Mags.DO5, irrespective of the presence of HLA-DM. Taken together, our results suggest that HLA-DM acts as a private chaperone, directly assisting the folding of HLA-DO to promote egress from the endoplasmic reticulum.

Keywords: antigen presentation; antigen processing; B cells; human; major histocompatibility complex

Introduction

Major histocompatibility complex class II molecules (MHC II) present antigenic peptides to specific $CD4^+$ T lymphocytes.[1] Once synthesized in the endoplasmic reticulum (ER), classical MHC class II αβ heterodimers associate with the invariant chain (Ii). This chaperone stabilizes the MHC II and targets the complex to the proper endosomal/lysosomal compartments.[2–5] In the endocytic pathway, Ii is cleaved by proteases to generate the Class II-associated invariant chain peptide (CLIP) fragment which occupies the peptide-binding groove of the MHC II.[6] Exchange of CLIP for cognate antigenic peptides or polypeptides is catalysed by human leucocyte antigen (HLA) -DM (DM), a class II molecule found within specialized lysosomal structures named MHC class II compartments (MIICs).[7–10]

In contrast to the classical MHC II HLA-DR (DR), -DP and -DQ, DM is a non-classical MHC II molecule mainly because of its monomorphic nature.[11] The inability to present antigenic peptides and the intracellular localization of DM are in line with an indirect role in antigen presentation for this molecule.[8,10,12] Besides its activity on CLIP, DM shapes the final peptide repertoire displayed by a given MHC II isotype.[9,13–15] DM chaperones empty classical class II molecules, allowing binding of suitable peptides capable of filling pocket 1 and of making hydrogen bonds with the DRα backbone.[16–20]

DM and DR interact principally in acidic vesicles and membrane colocalization increases the efficiency of

peptide exchange.[21] The mutual recognition would involve fine structural changes in both molecules. A DM-susceptible, flexible isoform of DR may arise from changes induced by inadequate peptides and from protonation of histidine α33 at low pH.[22,23] For DM, many experiments also suggest that protonation in the endocytic pathway results in minor, reversible structural changes exposing hydrophobic regions of the heterodimer.[24–26] Ullrich *et al.* used 8-anilino-1-naphthalenesulphonic acid (ANS), a fluorescent dye binding to hydrophobic protein patches, to demonstrate subtle pH-induced changes in purified DM and DR molecules.[25] Since the interaction of DM with DR reduces ANS binding to both molecules, it was postulated that the surface of contact is comprised of pH-sensitive regions on both proteins.[7,24,25] In line with this hypothesis and with the critical role of the peptide N-terminal region, Mellins and coworkers recently proposed a model for the DR–DM interaction based on elegant functional mutagenesis data.[27,28]

Another non-classical MHC-related molecule, HLA-DO (DO), was shown to accumulate in MIIC-like compartments.[29] DO was first described as a DM inhibitor since its overexpression in class II transactivator-transfected cells increased the fraction of classical class II molecules bound to the CLIP fragment.[30,31] However, mouse B cells proficient or deficient in H2-DO do not exhibit dramatic variations in the levels of CLIP bound to I-A^b.[32–34] It was proposed that H2-DO promotes the presentation of antigens internalized by membrane immunoglobulins by selectively inhibiting the activity of H2-DM in early endocytic compartments rich in proteins internalized by fluid-phase endocytosis.[33] This hypothesis is consistent with an active inhibitory role of DO *in vitro* at mildly acidic pH (early endosomes) and to a poor inhibitory potential at low pH (MIIC and lysosomal compartments).[33] Also, this model is consistent with results obtained using splenocytes from mice with a targeted mutation in the *H2-DOA* genes and which showed slightly increased efficiency in the presentation of soluble antigens.[33] Accordingly, antigen-presenting cells from H2-DO- or DO-overexpressing transgenic mice showed reduced presentation of exogenous antigens.[32,35] Others suggested that DO stabilizes DM and promotes stable MHC–peptide complexes when physiological conditions are met.[36] Interestingly, the recent demonstrations of DO expression in specific DC subsets argue against a specific role in B cells in the context of the surface immunoglobulin antigen uptake.[37–39] Still, it is now accepted that H2-DO and DO 'modulate' MHC class II antigen processing.[32,34,36,40]

In human B lymphocytes, as opposed to their mouse counterpart, the majority of DO molecules was found associated with DM[30,36,39,41] and this association allows DO to egress the ER.[29,42] The lack of a recognizable di-basic ER retention motif (RXR or KKXX) suggests that the assembled DOαβ heterodimer is improperly folded in the absence of DM and most probably unstable. Misfolding of newly synthesized proteins is known to induce retention and aggregation in the ER.[43] So far, the mode of interaction between DO and DM remains poorly characterized. We have recently shown that DM binds the DOα1 domain, probably by stabilizing the N-terminal regions of DO to allow ER egress.[44] In the present study, using a conformation-dependent DO-specific antibody, we confirm that DM binding impacts on the conformation of DO.

Materials and methods

Plasmids and complementary DNAs

RSV.3DR_{18}/DOβ, pBSDOα.9, RSV.5neo DRα, pBudCE4-A, pBud DOαβ, pBud DM, pBud DRβ and RSV.5gptDN1 have been previously described.[44–46] The DOβ complementary DNA (cDNA) from the 721.45 cell line.[47] was excised with *Bam*HI and the 1·3-kilobase fragment was cloned into the RSV.5neo plasmid to generate RSV.5neo DOβ. Then, RSV.5neo DR_{18}/DOβ (cDOβ) was generated by inserting the *Mlu*I–*Eco*RV fragment of RSV.3 DR_{18}/DOβ into RSV.5neo DOβ. The DR_{18}/DOα chimeric cDNA (cDOα) was made by overlap extension polymerase chain reaction (PCR) as described.[45] using the DRα cDNA cloned in the *Bam*HI site of pBlueScript (Stratagene, La Jolla, CA), and RSV.5gptDN1 (DOα) as templates. The sequences of the oligonucleotides used for PCR are available upon request. The *Sal*I–*Pvu*II fragment encompassing the junction between DR and DO was subcloned into RSV.5gptDN1. The nucleotide sequence was confirmed by DNA sequencing. A 2-kilobase pair *Bam*HI fragment was either cloned into the *Bgl*II site of pBudCE4-A DRβ to generate pBudDR_{18}/DOα $^{+}$DRβ or cloned into SRαpuro to generate SRαpuroDR_{18}/DOα.

The DM variant devoid of its YxxL motif (DMY) was generated by mutating the tyrosine 230 in the DMβ cytoplasmic region. PCR overlap reactions were performed on pBS 1-DMβ.1.[45] and the products were mixed in a final PCR using flanking primers. This PCR product was digested with *Sac*I and *Hin*dIII, cloned into pBS 1-DMβ.1 and sequenced (pBSDMβY230A). A *Sal*I–*Xba*I fragment was subcloned into pBud DMα[46] to generate pBud DMY.

Antibodies

Monoclonal antibodies (mAbs) L243 (DRα-specific), XD5.117 (XD5; DRβ-specific), MAP.DM1 (DM-specific) as well as the rabbit sera against DOα, calnexin and DMβ have been described previously.[45,46,48,49] Anti-actin (immunoglobulin G1; IgG1) is specific for the N-terminal of the molecule (Chemicon International, Temecula, CA). HKC5 is an IgG1 mouse mAb specific for the cytoplasmic tail of DOβ[49] Mags.DO.5 mAb was generated from mice

immunized with purified DO/DM complexes and was described previously.[50] Secondary antibodies were the Alexa Fluor 488-conjugated goat anti-mouse IgG antibody (Molecular Probes, Eugene, OR), peroxidase- and biotin-coupled goat anti-rabbit antibody (Bio/Can Scientific, Mississauga, Canada) and Texas red-coupled streptavidin (Jackson ImmunoResearch, West Grove, PA). All these antibodies were titrated and used at saturating concentrations.

Cell lines and transfections

HeLa DRα $^{+}DR_{18}$/DOβ (DRα/cDOβ), HeLa DO and HeLa DM.5 were previously described.[45,46] Raji and HeLa cells were kindly provided by Dr R.P. Sékaly. HEK293T cells were obtained from Dr Eric Cohen. Cells were cultured in Dulbecco's modified Eagles's minimal essential medium (DMEM), 10% fetal bovine serum. HeLa cells were cotransfected by the calcium phosphate precipitation method.[51] using 2–20 μg of each DNA or transfected with Fugene6 (Roche Diagnostics, Laval, Canada) using 1 μg of each DNA.[45] HeLa DM.5 cells were transfected with Fugene6. HeLa cDO were sorted on magnetic beads (Invitrogen, Toronto, Canada) after staining with Mags.DO5. For transient expression, HEK293T cells were transfected by the calcium phosphate precipitation method using 2 μg of each DNA. Cells were analysed 2 days post-transfection.

Flow cytometry

Cells were harvested using trypsin, washed and stained for surface expression. For intracellular staining, cells were treated with formaldehyde for 20 min, then with 50 mM NH_4Cl for 15 min and permeabilized with phosphate-buffered saline/bovine serum albumin containing 0·05% saponin.[45] Cells were analysed on a FACSCalibur (Becton Dickinson, San José, CA).

Fluorescence microscopy

HeLa cells were plated on coverslips in 24-well plates and cultured for 2 days before intracellular staining as described for flow cytometry analysis. Cells were analysed by fluorescence microscopy on a Zeiss axioplan 2 imaging microscope. Photographs were taken with a Sony DXC-390P digital camera.

Immunoprecipitation, Western blotting and endoglycosidase H treatment

Cells (10^7) were trypsinized, washed in phosphate-buffered saline and lysed into Triton-X100.[45] Post-nuclear supernatants were prepared and analysed directly on immunoblots or used for immunoprecipitations overnight at 4° using primary antibodies bound to protein-G coupled to sepharose 4B (GE Lifesciences, Piscataway, NJ). Samples were analysed on Western blots.[45] For EndoH treatment, lysates containing 2×10^5 cells were directly digested with Endoglycosidase H for 30 min at 37° (New England Biolabs, Pickering, Canada) and resuspended in reducing loading buffer. Samples were boiled and analysed by Western blotting.

Adenovirus production and HeLa cells infection

Production of recombinant adenoviruses (Ad) was as described.[52] AdDO encode both DOα and DOβ. A mutant AdDO was obtained by the same strategy using a DOβ cDNA with substitutions at positions V184H, V186K and E187K (AdDO VVE). The empty adenoviral vector (Ad0) is a replication-deficient recombinant adenovirus derived from serotype 5 with the deletion of E1 and E3 regions.[53]

For adenovirus transduction, HeLa cells were distributed in flat-bottom, 24-well plates at $2{\cdot}5 \times 10^5$ cells/well in 250 μl DMEM without serum. Viruses were added at a multiplicity of infection of 50 and incubated at 37° in the presence of 5% CO_2 for 3 hr. Complete medium was added and cells were cultivated for 2 days.

Results

Mags.DO5 binds the HLA-DOβ chain

In DM-negative cells, transfected DO was shown to be retained in the ER.[29] We postulated that DM assists the folding of the DOαβ heterodimer, allowing its maturation. To gain insights into a possible impact of DM expression on the structure of DO, we made use of the Mags.DO5 mAb obtained following immunization of mice with DO/DM complexes purified from a human B-cell line.[50] Given our recent demonstrations that DM binds to the α chain of DO[44] and that Mags.DO5 recognizes the DO/DM complex,[50] we hypothesized that this mAb binds to the DOβ chain. This was verified using mixed DR/DO pairs expressed in class II-negative HeLa cells.[54] These mixed heterodimers (DRα/cDOβ and cDOα/DRβ) overcome ER retention and were made possible by exchanging the first 18 amino acids of DO for the corresponding sequence of DR (Fig. 1a,b). The cell surface expression of DRα/cDOβ and cDOα/DRβ was controlled using DR-specific antibodies against the α and β chains, respectively (Fig. 1c). Mags.DO5 recognized the DRα/cDOβ mixed pair expressed on HeLa cells but not its cDOα/DRβ counterpart. Although we cannot entirely rule out that the DOα chain somewhat contributes to the efficiency of antibody binding, these results suggested that Mags.DO5 is specific for an epitope located on the DOβ chain. In support of this, although Mags.DO5 does not

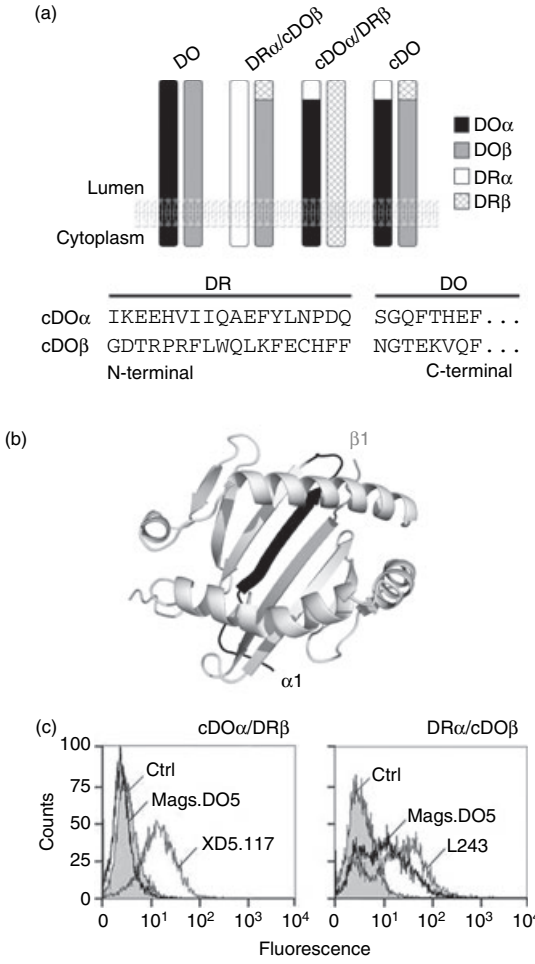

Figure 1. Mags.DO5 epitope is located on the β chain of DO (a) Schematic representation of the various DO constructs used in this study. The predicted amino acid sequence of the N-terminal region of mature cDO chains is shown. (b) The position of the DR α (black) and β (dark grey) regions grafted on cDO chains are highlighted on a top view of human leucocyte antigen-DR. α1 and β1 indicate the position of the N terminus of each domain. (c) Flow cytometry analysis of HeLa cells stably expressing mixed cDOα/DRβ or DRα/cDOβ pairs and stained for cell surface expression using DO-specific Mags.DO5 (bold line), DRβ-specific XD5.117 (thin line; left panel) or DRα-specific L243 (thin line; right panel). Filled histograms represent control staining using HeLa cells incubated only with the Alexa-488-coupled secondary GAM antibody.

bind DR, we observed some competition between this mAb and an anti-serum made against the DRα/cDOβ mixed pair (data not shown).

Mags.DO5 recognizes a conformational epitope

Mags.DO5 does not recognize denatured DOβ (data not shown) suggesting that the mAb recognizes a conformational epitope. This was confirmed by flow cytometry on permeabilized cells. Mags.DO5 did not recognize the DOα chain when expressed independently. However,

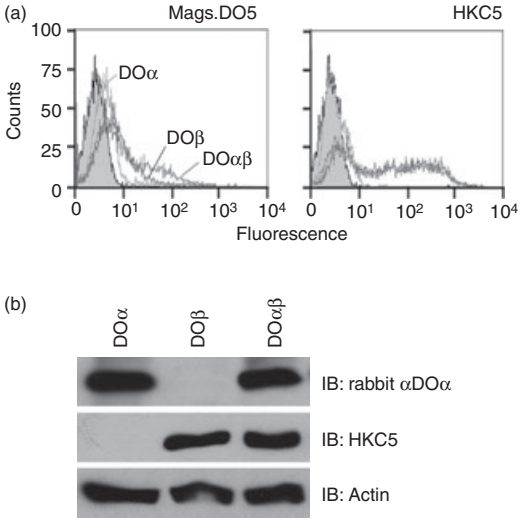

Figure 2. Mags.DO5 monoclonal antibody (mAb) is conformational (a) HEK293T cells were transiently transfected with either DOα alone (light grey), DOβ alone (dark) or DOα $^{+}$DOβ (grey) complementary DNAs and stained with Mags.DO5 and HKC5 after permeabilization. Cells were analysed by flow cytometry. Filled histograms represent control cells stained with the GAM-Alexa-488 secondary antibody. This experiment was done a minimum of 10 times with similar results. (b) Cell lysates were prepared and analysed on immunoblots for the expression of DOα (upper panel), DOβ (middle panel) and actin (lower panel).

slight reactivity to the free DOβ chain was detected and this reactivity increased slightly by the expression of DOα and DOβ together (Fig. 2a). The equivalent binding of HKC5, a mAb specific for a linear epitope on the DOβ cytoplasmic tail,[49] confirms that the observed increased binding of Mags.DO5 in the DOA/DOB transfectant was not caused by an accumulation of β chain in the presence of DOα (Fig. 2). Semi-quantitative Western blotting with HKC5 confirmed that both transfectants express similar levels of DOβ chain (Fig. 2b). Collectively, these results support the notion that Mags.DO5 recognizes a conformational epitope located on DOβ. The conformation change may be subtle as some antibody reactivity is observed on the isolated β chain.

Coexpression of DM with DO enhances Mags.DO5 reactivity

Although Mags.DO5 was generated following immunization of mice with DM/DO complexes, the mAb is specific for DO because it does not recognize DM[50] (data not shown). However, cotransfection of DM and DO together into 293T cells clearly showed that Mags.DO5 reacted more strongly to DO when complexed with DM (Fig. 3a). These differences were not the result of differences in DOβ expression levels because HKC5 staining was identical in the absence and presence of DM (Fig. 3a). The

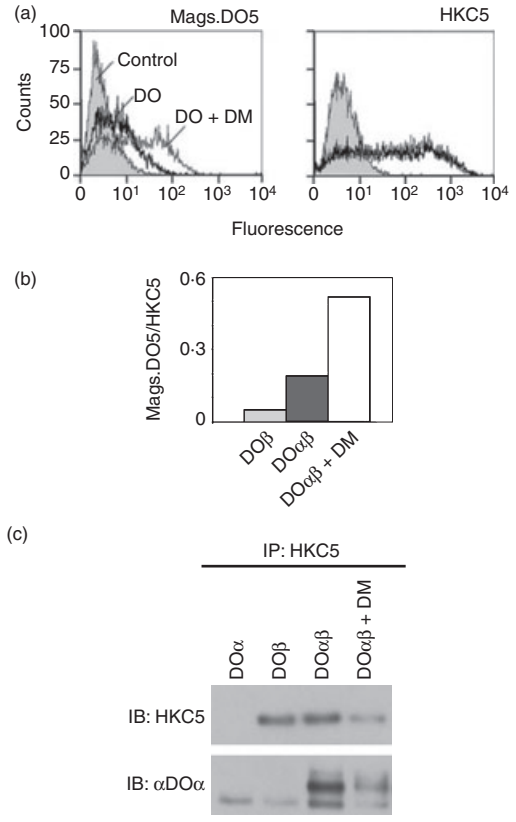

Figure 3. Coexpression of DM increases Mags.DO5 reactivity (a) HEK293T cells were transfected with either DO (thick line) or DO $^{+}$DM (thin line) cDNAs, fixed, permeabilized and stained after 48 hr with Mags.DO5 (left panel) and HKC5 (right panel) monoclonal antibodies (mAbs). (b) HEK293T cells were transiently transfected with either DOβ alone, DOαDOβ or DOαDOβ^{+} DM complementary DNAs (cDNAs) and stained with Mags.DO5 and HKC5 before flow cytometry analysis. The *y*-axis represents the ratio between the mean fluorescence values obtained for the two mAbs. Similar results were obtained in three other independent experiments. (c) HEK293T cells were transiently transfected with either DOα alone, DOβ alone, DOαDOβ or DOαDOβ $^{+}$DM cDNAs. After 48 hr, cells were lysed and immunoprecipitation was performed using the DOβ-specific HKC5 mAb. Samples were analysed on immunoblots by probing with HKC5 or the DOα-specific rabbit antiserum.

positive impact of DM is most apparent when the mean fluorescence values obtained by flow cytometry are expressed as a ratio between Mags.DO5 and HKC5 (Fig. 3b). Importantly, DOβ and DOα were produced from a bi-cistronic vector to minimize transfection-dependent variations in the relative expression of the two chains. Indeed, immunoprecipitation of DOβ revealed that αβ heterodimers were formed, even in the absence of DM (Fig. 3c). The increased Mags.DO5 reactivity in the presence of DM was also observed in transfected HeLa cells (see below).

DO conformation change occurs in the ER

The possibility remained that the effect of DM was indirect and simply the consequence of its ability to target DO to acidic compartments. Indeed, Liljedahl *et al.* demonstrated that DO undergoes a conformation change at low pH.[33] To evaluate if the Mags.DO5 reactivity pattern described above depended on accumulation of DO/DM complexes in acidic vesicles, we transiently expressed DO with wild-type DM or with a DM variant (DMY) devoid of its YxxL lysosomal sorting signal.[44] DMY interacts with DO and the complex accumulates at the plasma membrane (Fig. 4a). Cells expressing DO with DM or DMY were permeabilized and stained with Mags.DO5 (Fig. 4b,c). The results showed that the increase in the reactivity of Mags.DO5 was independent of DO localization to intracellular acidic compartments.

To test if DM interaction with DO in the ER promoted the formation of the Mags.DO5 epitope, we examined mAb reactivity for a DO molecule that bears a triple mutation in the β2 domain (DO VVE) (Fig. 5a). These mutations, originally described in DR, were shown to affect the interaction with DM.[27] When introduced separately into DOβ, these mutations did not affect the binding to DM. However, when introduced together, these three mutations affected the integrity of DO and strongly impaired ER egress (Deshaies and Thibodeau, unpublished data). The mutant β chain was transduced together with DOA into HeLa cells either expressing DM or not.

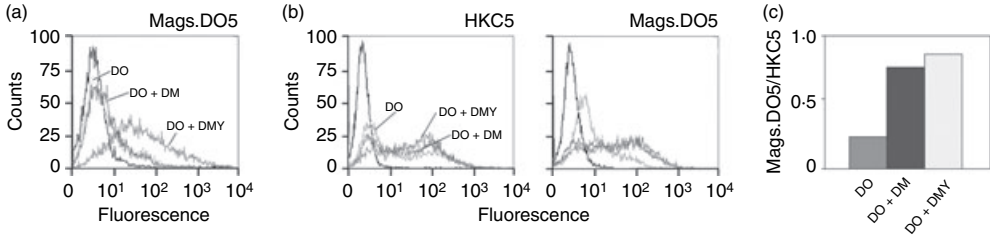

Figure 4. DM-induced conformation change in DO occurs in endoplasmic reticulum (ER) (a) HEK293T cells were transfected with DO alone, DO and DM wild-type (wt) or DO and DMY. After 48 hr, cell surface DO was stained using Mags.DO5. The mean fluorescence values were 119 and 194 for DM and DMY, respectively (not shown). (b) Cells were permeabilized and stained with HKC5 (left panel) or Mags.DO5 (right panel). (c) Mean fluorescence values obtained in (b) were plotted as the Mags.DO5 over HKC5 ratio. This experiment is representative of three independent experiments.

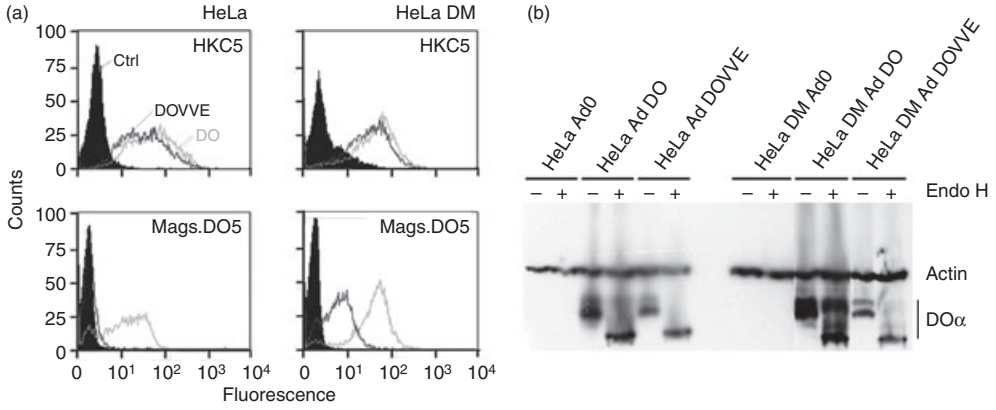

Figure 5. DM affects the conformation of a transport-incompetent DO mutant. (a) HeLa (left panels) and HeLa DM (right panels) cells were transduced with AdDO (thin line) or AdDO VVE (thick line) adenoviral constructs. Cells were fixed, permeabilized and stained with HKC5 (upper panels) or Mags.DO5 (lower panels). (b) Cells were lysed and half of the post-nuclear supernatants was treated with EndoH. Samples were analysed on immunoblots using first the DOα-specific rabbit antiserum and then the control actin-specific probe. Similar results were obtained in an independent experiment.

DO VVE showed a reduced capacity to egress the ER and to acquire complex EndoH-resistant carbohydrates in both the presence and absence of DM (Fig. 5b). Although the ER-retained DO VVE was expressed at levels similar to wild-type DO, this mutant was not efficiently recognized by Mags.DO5 in the absence of DM. Coexpression of DM partially restored Mags.DO5 reactivity, supporting the idea that assembly of DM with DO in the ER generates the epitope recognized by Mags.DO5. Moreover, cells transfected in the presence of brefeldin A exhibited a block in the ER exit of DO/DM complexes but the treatment did not prevent DM from increasing Mags.DO5 reactivity (data not shown).

Relationship between folding of DO and the reactivity of Mags.DO5

We postulated that Mags.DO5 would recognize properly folded DO molecules independent of the presence of DM. To test this hypothesis, we stably expressed a chimeric DO (cDO) in which the first 18 amino acids of both DOα and β chains were substituted for those of the corresponding DR chains (Fig. 1). As opposed to wild-type DO which colocalizes with the ER marker calnexin, the cDO heterodimer was able to egress the ER in DM-negative HeLa cells and to accumulate in Lamp-1^+ vesicles (Fig. 6a and data not shown). In contrast to wild-type DO, the conformation-dependent Mags.DO5 mAb recognized cDO as efficiently as HKC5 in stably transfected HeLa cells (Fig. 6b). Such strong Mags.DO5 staining is reminiscent of the pattern observed for DO in DM^+ cells (Figs 3 and 5).

Since Mags.DO5 reacted strongly with cDO in the absence of DM, we postulated that the Mags.DO5 staining on correctly folded cDO molecules was optimal and could not be improved by coexpressing DM. We first ascertained that the modifications imparted to the DO molecule through the fusion of the first 18 amino acids of DR would still allow a strong interaction with DM. Both DM and DO were transiently transfected in 293T cells and DO was immunoprecipitated from detergent lysates. Western blot analysis showed that DM was efficiently coimmunoprecipitated with cDO in both CHAPS and Triton X-100. This suggests that the cDO/DM interaction is representative of the one observed for DO. This is different from the association of DM/DO with DR, which dissociates from DM upon lysis of Raji cells in Triton X-100 (Fig. 6c). However, as expected, coexpression of DM did not increase the reactivity of Mags.DO5 to cDO (Fig. 6d). Consequently, the Mags.DO5 mAb recognizes properly folded DO molecules.

DM binding discloses the Mags.DO5 epitope on DO

Braunstein and Germain carefully titrated the mAb concentration to determine if avidity or affinity of a class II-specific mAb could explain the differential staining observed between transfectants expressing mismatched MHC heterodimers.[55] The rationale behind such experiments is that at limiting concentrations of the mAb, antigenic molecules of different intrinsic affinities toward the mAb will show divergent staining intensities, even if expressed at similar levels. On the other hand, in these conditions, antigens with the same affinity will show similar binding (read out by flow cytometry as mean fluorescence value) even if expressed differentially. We used a similar approach to determine if the enhanced reactivity of Mags.DO5 for DO in the presence of DM was the result of a difference in affinity or avidity.

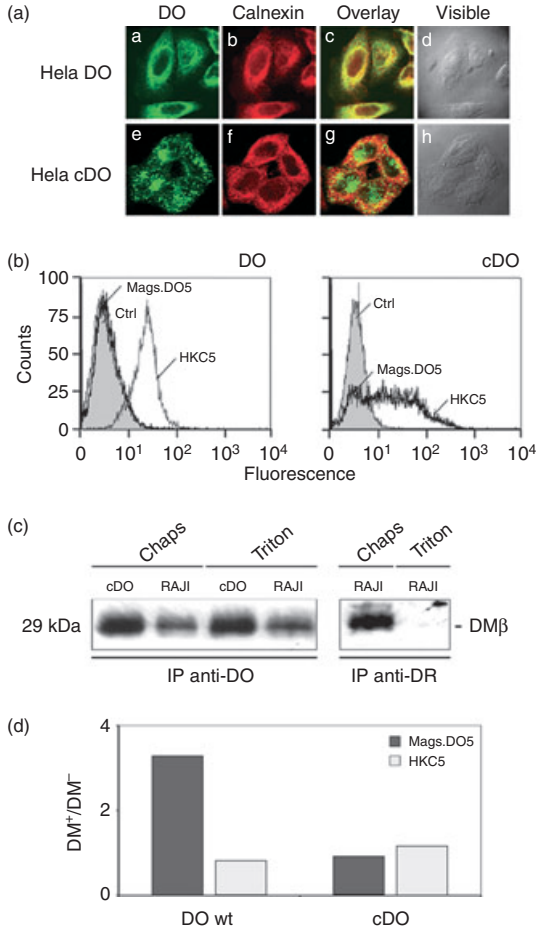

Figure 6. Transport-competent cDO molecules reveal the Mags.DO5 epitope independent of DM (a) Immunofluorescence microscopy analysis of cDO subcellular localization. HeLa DM-negative cells were stably transfected with either wild-type (wt) DO (a–d) or cDO chimera (e–h), permeabilized and incubated with Mag.DO5 and rabbit anti-calnexin followed by Alexa 488-labelled goat anti-mouse antibodies (a,e), biotinylated goat anti-rabbit antibody and Texas-red conjugated streptavidin (b,f). (c) and (g) show the merge of wt DO or cDO images with those obtained for calnexin. (d) and (h) show the cells in visible light. (b) Flow cytometry analysis of HeLa cells stably transfected with DO (left panel) or cDO (right panel). Cells were permeabilized and stained with Mags.DO5 or HKC5. (c) HEK293T cells were transfected with cDO and DM, lysed in Chaps or Triton X-100 (Triton) and DO was immunoprecipitated with the DOα-specific rabbit antiserum. Samples were analysed on immunoblots using the DMβ-specific rabbit antiserum. Control Raji cells were lysed in the same conditions and immunoprecipitation was performed for DO or for DR using XD5. (d) HEK293T cells were transiently transfected with DO or cDO in the absence or presence of DM. After 48 hr, cells were permeabilized and stained with Mags.DO5 and HKC5. Mean fluorescence values obtained for DM^+ and DM^- cells were plotted as a ratio. These ratios are representative of at least two other experiments.

DO with or without DM was transfected into 293T cells and stained with titrated amounts of Mags.DO5 after permeabilization (Fig. 7). At low or saturating concentrations of mAb, the staining was always more efficient on cells coexpressing DM, suggesting that the affinity of the mAb is different for DO or DO/DM complexes. As expected, the control HKC5 showed similar staining patterns independent of DM expression. These results suggest that in the absence of DM, the Mags.DO5 affinity is weak for DO. Upon DM binding, DO most probably goes through a conformation change that fully unveils the epitope.

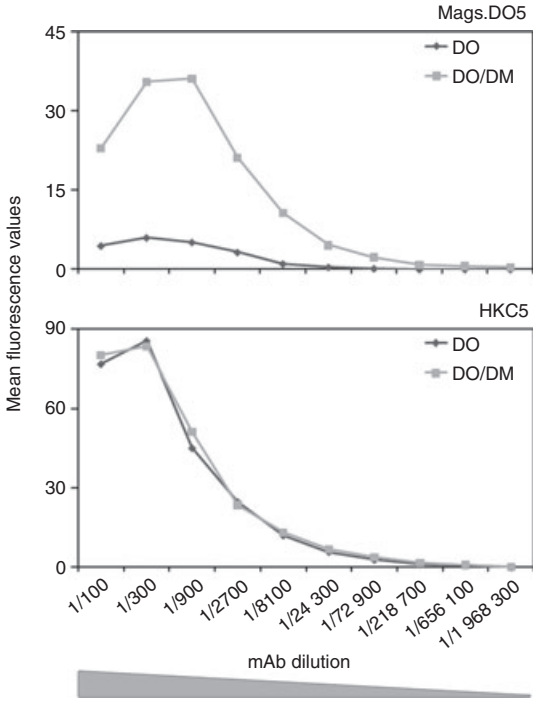

Figure 7. Coexpression of DM reveals the Mags.DO5 epitope on DO molecules. HEK293T cells transiently expressing DO or DO $^+$DM were permeabilized 48 hr post-transfection and stained with serial dilutions of the Mags.DO5 (top panel) or HKC5 (lower panel) monoclonal antibodies. These experiments were repeated three times with similar results.

Discussion

In transfected HeLa cells and in mouse B lymphocytes, under the experimental conditions tested so far, DO or H2-DO molecules did not egress the ER on their own.[29] In the present study, we sought to determine if DM affects the quaternary structure of DO upon formation of the complex in the ER. Interestingly, Liljedahl *et al.* showed by immunoprecipitation that DOα and β chains interact in DM-negative cells.[29] As the primary sequence of the α or β chain do not display known ER retention signals, we postulated that the conformation of DO was not optimal and that the heterodimer was most likely retained by ER chaperones. Consequently, DO does not acquire post-translational modifications in the form of complex Endo H-resistant sugars.[29]

Early after their synthesis in the ER, MHC II α and β chains must associate with Ii to avoid aggregation and premature degradation. Although the exact sequence of events is still a matter of debate, formation of the nonameric complex with Ii prevents aggregation of MHC II.[56] Quality control chaperones like BiP, GRP94, calnexin, calreticulin and ERp72 have been implicated in the ER retention of class II molecules in the absence of Ii.[1] Although binding to these proteins has yet to be demonstrated, we can assume that DO will probably be under the control of similar checkpoints. The association of DO with such public chaperones probably persists until DM intervenes to optimize folding into a more stable, lower energy conformation and to generate a transport-competent multi-unit complex. The fact that the Mags.DO5 staining increases upon coexpression of DM indicated that a conformation change occurs on DO. Although this had been suggested previously from the fact that DM allows DO egress from the ER,[29,42] our results demonstrate for the first time that DM acts on the conformation of DO. We ruled out by flow cytometry that DM simply increases the steady-state amount of DO because the staining with the HKC5 mAb did not increase compared to Mags.DO5. Also, immunoprecipitation experiments revealed similar amounts of DO in DM-positive or -negative cells. The exact nature of the conformation change has not been determined. The membrane distal domains of DO are more hydrophobic than classical MHC II and may need to be shielded by DM, even more so knowing that the groove is empty. Also, the DM may be involved in the oxidation of DO.[37,57] We have tested on DO the reactivity of increasing concentrations of Mags.DO5 and HKC5 in DM^+ and DM^- HEK293T cells (Fig. 7). Although DM clearly impacts on the staining of DO at limiting Mags.DO5 concentrations, such titration experiments may somehow be difficult to interpret in terms of antibody affinity or avidity as we have not tested in parallel a DM^+ control cell line expressing various levels of DO. Still, coupled to our immunoblot and immunoprecipitation data showing equivalent amounts of DOβ in DM^+ and DM^- HEK293T cells (Figs 2b and 3c), these results are in line with an increased affinity of Mags.DO5 for DO/DM complexes as compared to free DO.

Three complementary results allow us to conclude that the conformational change on DO takes place early during maturation and is not merely the consequence of DM-induced transport to the Golgi or the endocytic pathway. First, brefeldin A did not prevent the stronger recognition of DO by Mags.DO5 in the presence of DM (data not shown). Second, point mutations in DO that clearly impair ER egress did not prevent the ability of DM to increase Mags.DO5 binding. Finally, diverting the flow of DO/DM complexes to the plasma membrane instead of the lysosomal compartments by mutating the YxxL motif of DM did not perturb Mags.DO5 recognition. Altogether, the data strongly suggested that the DM-induced conformation change on DO occurs as early as in the ER and they rule out an indirect role of DM in increasing Mags.DO5 reactivity following glycan modification in the Golgi or protonation in acidic vesicles.

Studies on mixed pairs suggested a *cis*-coevolution of α and β chain polymorphisms favouring pairing of molecules from a given haplotype.[58] A role for Ii in facilitating ER egress of mismatched heterodimers has been described.[59] Although DO behaves very much like a mismatched pair, Ii does not seem to affect its sorting.[29] Our results show that DM acts as a chaperone and may give some clues as to the mechanism by which it allows DO to egress the ER. We have recently discovered a point mutation that resulted in some DO egress independent of DM.[44] We proposed that this DOαP11V mutation might improve the folding of the N-terminal regions of DOαβ and reduce the need for DM. This contention is supported by the demonstration that cDO reactivity with Mags.DO5 is maximal and independent of DM. In line with this hypothesis, using the Mags.DO5 conformational mAb, we demonstrated here that DM affects the conformation of DO.

Mags.DO5 was made by immunizing mice with purified DO/DM complexes and we found that the epitope recognized by this mAb is located on the DOβ chain. The possibility that DM contributes to the epitope is unlikely considering that the Mags.DO5 reactivity toward cDO was not increased in the presence of DM (Fig. 6) The fact that amino acid changes in the N-terminal regions of DOα and β improved Mags.DO5 reactivity may indicate that the epitope is located in the membrane-distal β1 domains. Accordingly, DM improved Mags.DO5 binding on the DO VVE mutant, which most likely suffers from a severe conformation defect in its β2 domain. The DM-induced conformation change may be somewhat drastic but still, it could not override the negative impact of the DO VVE mutations on ER egress.

A chaperone role for DM in the ER was suggested by a study showing that in the absence of invariant chain, DM can improve the transport of MHC II.[60] However, the conformation change described here is more reminiscent of the appearance of the 16.23 epitope on DR3 molecules having encountered DM. Verreck *et al.* showed that this effect on the fine structure of the DR3 was independent of CLIP removal or of the peptide editing capabilities of DM.[61] Also, the well-characterized stabilization of peptide-free MHC II molecules points to a chaperone role of DM that is not directly related to its catalytic activity.[17] In this respect, DM would recognize DO just like any other empty MHC II.[62]

Whether DO affects the structure of DM remains to be established. The inhibition of DM by DO is certainly in line with a reciprocal effect of the two molecules on their respective fine structures. This could also explain the

apparent increase in H2-DM half-life in the presence of H2-DO.[35] Comparing the crystal structures of isolated versus associated DO and DM would shed light on the interplay between the two chaperones.

Acknowledgements

We are grateful to M. Serge Sénéchal for helping with flow cytometry analyses. This work was supported by grant MOP 36355 from the Canadian Institutes of Health Research to J.T.

References

1 Cresswell P. Assembly, transport, and function of MHC class-II molecules. *Annu Rev Immunol* 1994; **12**:259–93.
2 Bakke O, Dobberstein B. MHC class II-associated invariant chain contains a sorting signal for endosomal compartments. *Cell* 1990; **63**:707–16.
3 Lotteau V, Teyton L, Peleraux A *et al.* Intracellular transport of class II MHC molecules directed by invariant chain. *Nature* 1990; **348**:600–5.
4 Roche PA, Cresswell P. Invariant chain association with HLA-DR molecules inhibits immunogenic peptide binding. *Nature* 1990; **345**:615–8.
5 Roche PA, Cresswell P. Proteolysis of the class II-associated invariant chain generates a peptide binding site in intracellular HLA-DR molecules. *Proc Natl Acad Sci USA* 1991; **88**:3150–4.
6 Ghosh P, Amaya M, Mellins E, Wiley DC. The structure of an intermediate in class II MHC maturation: CLIP bound to HLA-DR3. *Nature* 1995; **378**:457–62.
7 Sloan VS, Cameron P, Porter G, Gammon M, Amaya M, Mellins E, Zaller DM. Mediation by HLA-DM of dissociation of peptides from HLA-DR. *Nature* 1995; **375**:802–6.
8 Denzin LK, Robbins NF, Carboy-Newcomb C, Cresswell P. Assembly and intracellular transport of HLA-DM and correction of the class II antigen-processing defect in T2 cells. *Immunity* 1994; **1**:595–606.
9 Weber DA, Evavold BD, Jensen PE. Enhanced dissociation of HLA-DR-bound peptides in the presence of HLA-DM. *Science* 1996; **274**:618–20.
10 Mosyak L, Zaller DM, Wiley DC. The structure of HLA-DM, the peptide exchange catalyst that loads antigen onto class II MHC molecules during antigen presentation. *Immunity* 1998; **9**:377–83.
11 Sanderson F, Powis SH, Kelly AP, Trowsdale J. Limited polymorphism in HLA-DM does not involve the peptide binding groove. *Immunogenetics* 1994; **39**:56–8.
12 Fremont DH, Crawford F, Marrack P, Hendrickson WA, Kappler J. Crystal structure of mouse H2-M. *Immunity* 1998; **9**:385–93.
13 Katz JF, Stebbins C, Appella E, Sant AJ. Invariant chain and DM edit self-peptide presentation by major histocompatibility complex (MHC) class II molecules. *J Exp Med* 1996; **184**:1747–53.
14 Kropshofer H, Vogt AB, Moldenhauer G, Hammer J, Blum JS, Hammerling GJ. Editing of the HLA-DR-peptide repertoire by HLA-DM. *EMBO J* 1996; **15**:6144–54.
15 Van Ham SM, Grueneberg U, Malcherek G, Broeker I, Melms A, Trowsdale J. Human histocompatibility leukocyte antigen (HLA)-DM edits peptides presented by HLA-DR according to their ligand binding motifs. *J Exp Med* 1996; **184**:2019–24.
16 Denzin LK, Hammond C, Cresswell P. HLA-DM interactions with intermediates in HLA-DR maturation and a role for HLA-DM in stabilizing empty HLA-DR molecules. *J Exp Med* 1996; **184**:2153–65.
17 Kropshofer H, Arndt SO, Moldenhauer G, Hammerling GJ, Vogt AB. HLA-DM acts as a molecular chaperone and rescues empty HLA-DR molecules at lysosomal pH. *Immunity* 1997; **6**:293–302.
18 Vogt AB, Moldenhauer G, Hammerling GJ, Kropshofer H. HLA-DM stabilizes empty HLA-DR molecules in a chaperone-like fashion. *Immunol Lett* 1997; **57**:209–11.
19 Stratikos E, Wiley DC, Stern LJ. Enhanced catalytic action of HLA-DM on the exchange of peptides lacking backbone hydrogen bonds between their N-terminal region and the MHC class II alpha-chain. *J Immunol* 2004; **172**:1109–17.
20 Natarajan SK, Stern LJ, Sadegh-Nasseri S. Sodium dodecyl sulfate stability of HLA-DR1 complexes correlates with burial of hydrophobic residues in pocket 1. *J Immunol* 1999; **162**:3463–70.
21 Weber DA, Dao CT, Jun J, Wigal JL, Jensen PE. Transmembrane domain-mediated colocalization of HLA-DM and HLA-DR is required for optimal HLA-DM catalytic activity. *J Immunol* 2001; **167**:5167–74.
22 Narayan K, Chou CL, Kim A, Hartman IZ, Dalai S, Khoruzhenko S, Sadegh-Nasseri S. HLA-DM targets the hydrogen bond between the histidine at position beta81 and peptide to dissociate HLA-DR-peptide complexes. *Nat Immunol* 2007; **8**:92–100.
23 Rotzschke O, Lau JM, Hofstatter M, Falk K, Strominger JL. A pH-sensitive histidine residue as control element for ligand release from HLA-DR molecules. *Proc Natl Acad Sci USA* 2002; **99**:16946–50.
24 Busch R, Reich Z, Zaller DM, Sloan V, Mellins ED. Secondary structure composition and pH-dependent conformational changes of soluble recombinant HLA-DM. *J Biol Chem* 1998; **273**:27557–64.
25 Ullrich HJ, Doring K, Grueneberg U, Jaehnig F, Trowsdale J, Van Ham MS. Interaction between HLA-DM and HLA-DR involves regions that undergo conformational changes at lysosomal pH. *Proc Natl Acad Sci USA* 1997; **94**:13163–8.
26 Chou CL, Sadegh-Nasseri S. HLA-DM recognizes the flexible conformation of major histocompatibility complex class II. *J Exp Med* 2000; **192**:1697–706.
27 Doebele CR, Busch R, Scott MH, Pashine A, Mellins DE. Determination of the HLA-DM interaction site on HLA-DR molecules. *Immunity* 2000; **13**:517–27.
28 Pashine A, Busch R, Belmares MP *et al.* Interaction of HLA-DR with an acidic face of HLA-DM disrupts sequence-dependent interactions with peptides. *Immunity* 2003; **19**:183–92.
29 Liljedahl M, Kuwana T, Fung-Leung WP, Jackson M, Peterson PA, Karlsson L. HLA-DO is a lysosomal resident which requires association with HLA-DM for efficient intracellular transport. *EMBO J* 1996; **15**:4817–24.
30 Denzin LK, Sant'Angelo DB, Hammond C, Surman MJ, Cresswell P. Negative regulation by HLA-DO of MHC Class II-restricted antigen processing. *Science* 1997; **278**:106–9.
31 Van Ham SM, Tjin EPM, Lillemeier BF *et al.* HLA-DO is a negative modulator of HLA-DM-mediated MHC class II peptide loading. *Curr Biol* 1997; **7**:950–7.

32 Brocke P, Armandola E, Garbi N, Hammerling GJ. Downmodulation of antigen presentation by H2-O in B cell lines and primary B lymphocytes. *Eur J Immunol* 2003; **33**:411–21.

33 Liljedahl M, Winqvist O, Surh CD *et al.* Altered antigen presentation in mice lacking H2-O. *Immunity* 1998; **8**:233–43.

34 Perraudeau M, Taylor PR, Stauss HJ *et al.* Altered major histocompatibility complex class II peptide loading in H2-O-deficient mice. *Eur J Immunol* 2000; **30**:2871–80.

35 Fallas JL, Tobin HM, Lou O, Guo D, Sant'Angelo DB, Denzin LK. Ectopic expression of HLA-DO in mouse dendritic cells diminishes MHC class II antigen presentation. *J Immunol* 2004; **173**:1549–60.

36 Kropshofer H, Vogt AB, Thery C *et al.* A role for HLA-DO as a co-chaperone of HLA-DM in peptide loading of MHC class II molecules. *EMBO J* 1998; **17**:2971–81.

37 Chen X, Reed-Loisel LM, Karlsson L, Jensen PE. H2-O expression in primary dendritic cells. *J Immunol* 2006; **176**:3548–56.

38 Hornell TM, Burster T, Jahnsen FL *et al.* Human dendritic cell expression of HLA-DO is subset specific and regulated by maturation. *J Immunol* 2006; **176**:3536–47.

39 Fallas JL, Yi W, Draghi NA, O'Rourke HM, Denzin LK. Expression patterns of H2-O in mouse B cells and dendritic cells correlate with cell function. *J Immunol* 2007; **178**:1488–97.

40 van Ham M, van Lith M, Lillemeier B *et al.* Modulation of the major histocompatibility complex class II-associated peptide repertoire by human histocompatibility leukocyte antigen (HLA)-DO. *J Exp Med* 2000; **191**:1127–36.

41 Jensen PE. Antigen processing: HLA-DO – a hitchhiking inhibitor of HLA-DM. *Curr Biol* 1998; **8**:R128–31.

42 Douek DC, Altmann DM. HLA-DO is an intracellular class II molecule with distinctive thymic expression. *Int Immunol* 1997; **9**:355–64.

43 Marquardt T, Helenius A. Misfolding and aggregation of newly synthesized proteins in the endoplasmic reticulum. *J Cell Biol* 1992; **117**:505–13.

44 Deshaies F, Brunet A, Diallo DA, Denzin LK, Samaan A, Thibodeau J. A point mutation in the groove of HLA-DO allows egress from the endoplasmic reticulum independent of HLA-DM. *Proc Natl Acad Sci USA* 2005; **102**:6443–8.

45 Brunet A, Samaan A, Deshaies F, Kindt TJ, Thibodeau J. Functional characterization of a lysosomal sorting motif in the cytoplasmic tail of HLA-DObeta. *J Biol Chem* 2000; **275**:37062–71.

46 Faubert A, Samaan A, Thibodeau J. Functional analysis of tryptophans alpha 62 and beta 120 on HLA-DM. *J Biol Chem* 2002; **277**:2750–5.

47 Tonnelle C, DeMars R, Long EO. DOb: a new β chain gene in HLA-D with a distinct regulation of expression. *EMBO J* 1985; **4**:2839–47.

48 Hammond C, Denzin LK, Pan M, Griffith JM, Geuze HJ, Cresswell P. The tetraspan protein CD82 is a resident of MHC class II compartments where it associates with HLA-DR, -DM, and -DO molecules. *J Immunol* 1998; **161**:3282–91.

49 Khalil H, Deshaies F, Bellemare-Pelletier A, Brunet A, Faubert A, Azar GA, Thibodeau J. Class II transactivator-induced expression of HLA-DOβ in HeLa cells. *Tissue Antigens* 2002; **60**:372–82.

50 Glazier KS, Hake SB, Tobin HM, Chadburn A, Schattner EJ, Denzin LK. Germinal center B cells regulate their capability to present antigen by modulation of HLA-DO. *J Exp Med* 2002; **195**:1063–9.

51 Graham FL, van der Eb AJ. A new technique for the assay of infectivity of human adenovirus 5 DNA. *Virology* 1973; **52**:456–67.

52 Bellemare-Pelletier A, Tremblay J, Beaulieu S *et al.* HLA-DO transduced in human monocyte-derived dendritic cells modulates MHC class II antigen processing. *J Leukoc Biol* 2005; **78**:95–105.

53 Ogorelkova M, Elahi SM, Gagnon D, Massie B. DNA delivery to cells in culture: generation of adenoviral libraries for high-throughput functional screening. *Methods Mol Biol* 2004; **246**:15–27.

54 Samaan A, Thibodeau J, Mahana W, Castellino F, Cazenave PA, Kindt TJ. Cellular distribution of a mixed MHC class II heterodimer between DR*a* and a chimeric DOβ chain. *Int Immunol* 1999; **11**:99–111.

55 Braunstein NS, Germain RN. Allele-specific control of Ia molecule surface expression and conformation: implications for a general model of Ia structure–function relationship. *Proc Natl Acad Sci USA* 1987; **84**:2921–5.

56 Bonnerot C, Marks MS, Cosson P, Robertson EJ, Bikoff EK, Germain RN, Bonifacino JS. Association with BiP and aggregation of class II MHC molecules synthesized in the absence of invariant chain. *EMBO J* 1994; **13**:934–44.

57 van Lith M, Benham AM. The DMalpha and DMbeta chain cooperate in the oxidation and folding of HLA-DM. *J Immunol* 2006; **177**:5430–9.

58 Braunstein NS, Germain RN, Loney K, Berkowitz N. Structurally interdependent and independent regions of allelic polymorphism in class II MHC molecules: implications for Ia function and evolution. *J Immunol* 1990; **145**:1635–45.

59 Layet C, Germain RN. Invariant chain promotes egress of poorly expressed, haplotype-mismatched class II major histocompatibility complex Aαβ dimers from the endoplasmic reticulum/*cis*-Golgi compartment. *Proc Natl Acad Sci USA* 1991; **88**:2364–50.

60 Serradell L, Muntasell A, Catalfamo M, Marti M, Costa M, De Preval C, Jaraquemada D. HLA-DM can partially replace the invariant chain for HLA-DR transport and surface expression in transfected endocrine epithelial cells. *Tissue Antigens* 1999; **53**:447–58.

61 Verreck FA, Fargeas CA, Hammerling GJ. Conformational alterations during biosynthesis of HLA-DR3 molecules controlled by invariant chain and HLA-DM. *Eur J Immunol* 2001; **31**:1029–36.

62 Hansen TH, Lybarger L, Yu L, Mitaksov V, Fremont DH. Recognition of open conformers of classical MHC by chaperones and monoclonal antibodies. *Immunol Rev* 2005; **207**:100–11.

Chapter 4 : Directed evolution

4.1. Yeast Display of DO single chain

In order to get insights about the mechanism underlying DO function, we generated a library of DO mutants (Esteban and Zhao, 2004). A single chain DO (DOsc) was generated (**Error! Reference source not found.**1), mutagenized and expressed in *Saccharomyces cerevisiae*. A library of 2.1×10^6 unique clones was obtained and selected for surface expression, as the DOsc would not escape the ER. I selected yeast that stained positive for both Mags.DO5 mAb and the HA-tag, appended at the C-terminal end of the β chain.

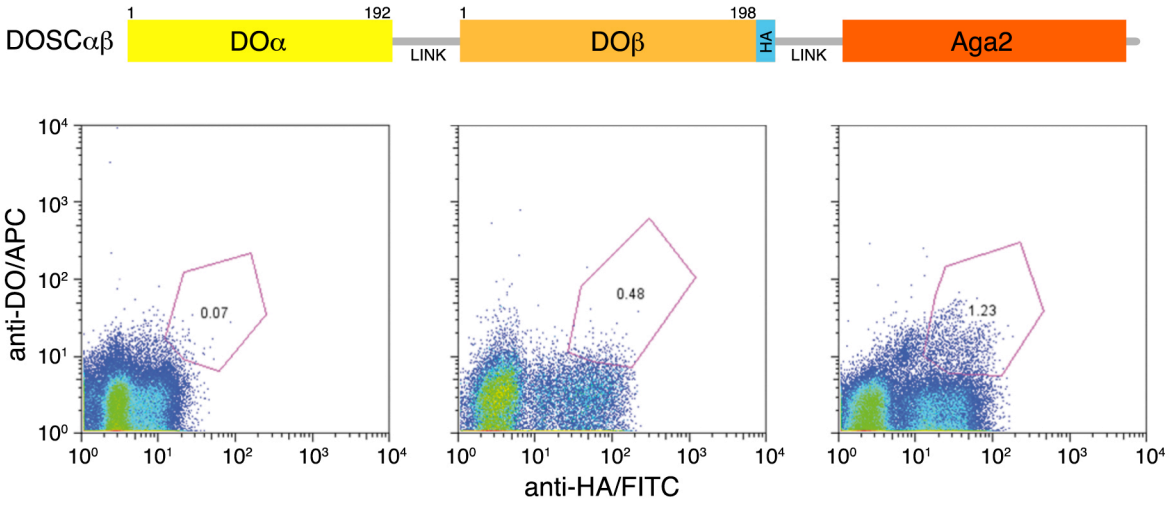

Figure 4.1. Yeast display design and sorting

a) Schema of the DO single chain construct. The α chain is linked to the β chain by a linker of 15 aa (Esteban and Zhao, 2004) and the latter to the Aga2 protein (Boder and Wittrup, 2000) as a single polypeptide. **b**) Histograms showing the fluorescence of cells displaying the DOsc after one, two and three rounds of sorting using both Mags.DO5 and the anti-HA mAbs.

After three rounds of enrichment, selecting only the highest DOsc expressing yeast, I isolated and sequenced 18 individual yeast clones. These mutants are presented in Table 4.1 and included between three to five point mutations and some silent ones. Figure 4.2 and Figure 4.3 locate those mutants on DO model and the DO-DM structure (Figure 4.5).

clone	DOα	DOβ
1	G10aA, A11P	*T21S
2	V87S, T122I, G127D	-
3	P61T, D161E	F122S, V158M, T164N
4	H8L, S82C, H169Y, G171D	-
5	-	T90S, K130T, F132S
6	G17D	-
7	-	P97S, G141V
8	F12L, V167L	V186M
9	-	Q60L, V91E
10	-	R34C, Y83N, A191D, S193T
11	-	P104L
12	-	R39C, S71S, Y83N, A190D, S192T
13	A65G	T120N
14	G49Q	P56R, R70K
15	I112S	S185T
16	L70P, R79L	Q25Q, G141V
17	-	E166E, E187K
18	V34V, L45Q, G58S, V109A, N111N, A172G	L115Q

Table 4.1: Mutation identified from sequenced clones after yeast sorting

**This mutant abrogates DOβ glycosylation site*

Of the 41 unique mutants obtained, five occurred in others DO species. For example, G17D is present on the Gorilla DOα sequence (**Error! Reference source not found.**). On the one hand, given the use of DOsc, in which the linker

connects the α2 domain to the β1 domain, the potential linker site would be on the solvent expose face of the α2 domain, on the C-terminal end of the groove. Hence, it seems reasonable to link DOα isolated mutation to a linked artefactual effect. On the other hand, many of the mutations are localized in two hot spots in the α1 and β1 domain (Table 4.2). Those two regions, located in the first beta-sheet connecting the α and β chain and at the P1 pocket vicinity, are crucial for the heterodimer pairing and stability (Deshaies et al., 2005; Natarajan et al., 1999a; Starwalt et al., 2003).

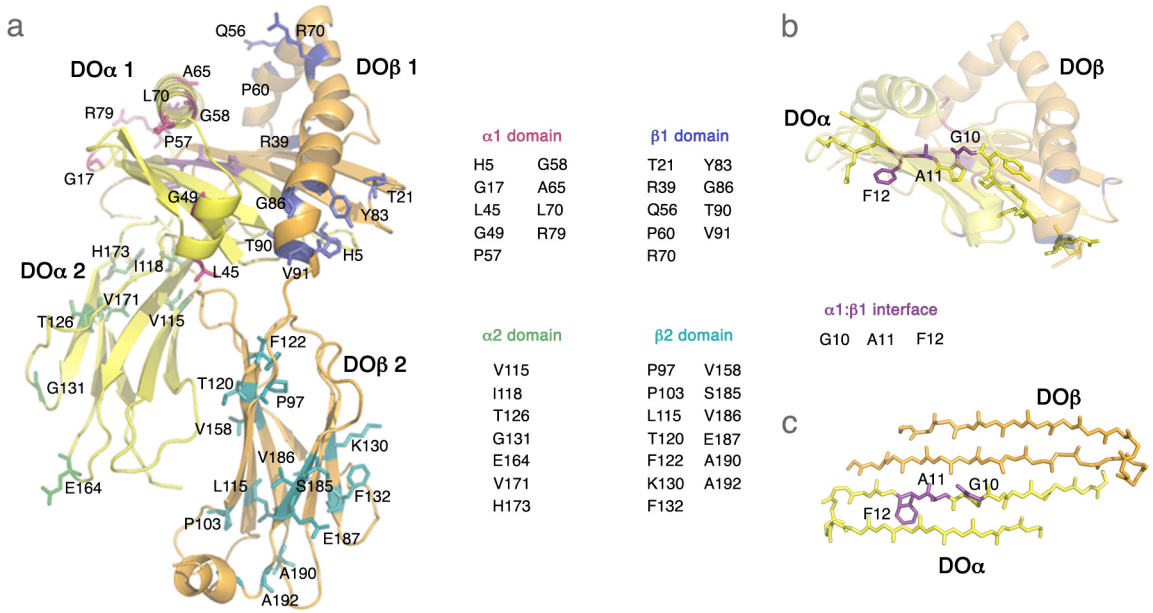

Figure 4.2. DO mutants obtained after directed evolution

Model of DO based on IAk and DQ2 (I-TASSER) showing the 41 single mutants isolated after sorting a 2.1x10^6 mutants library. The three mutants situated on the α1 first β-strand (G10A, A11P and F12D) are shown on the enlargement of the β-sheet platted floor of the α:β1 domain. Noteworthy is the T120N mutation, at the α2:β2 interface, which has been describe has stabilizing on DR1 (Starwalt et al., 2003).

α1:β1	α1 domain	β1 domain	β2 domain

GLY 10 ALA	GLY 18 ASP	HIS 5 LEU	PRO 97 SER
ALA 11 PRO	LEU 45 GLN	TYR 83 ARG	PRO 103 LEU
PHE 12 ASP	GLY 49 GLN	THR 90 SER	PHE 122 SER
	PRO 57 THR	VAL 91 GLU	SER 185 THR
	GLY 58 SER	THR 21 SER	VAL 186 MET
	ALA 65 GLY		GLU 187 LYS

Table 4.2: Selected DO mutants

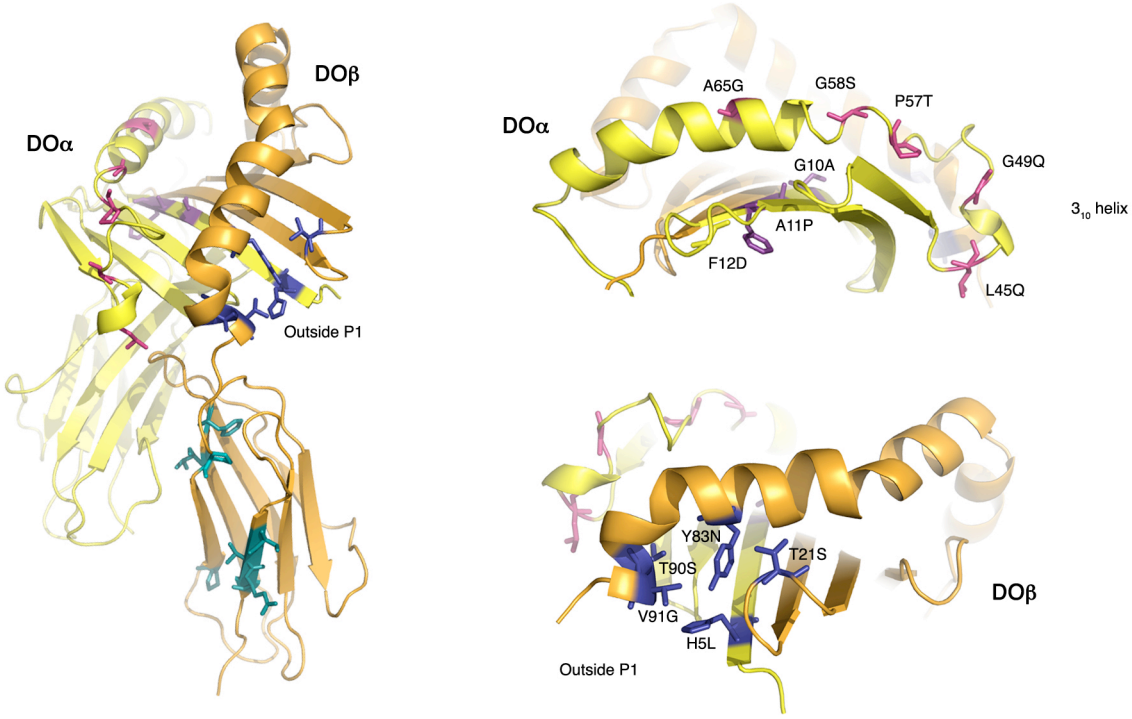

Figure 4.3. Rationalized DO mutants obtained from Yeast Display

Potentially important conformational DO residues. In teal and pink are shown the isolated mutants located at the DO-DM interface I and III (Guce et al., 2012; Pos et al., 2012). In blue are the mutants that also increase Mags.DO5 reactivity.

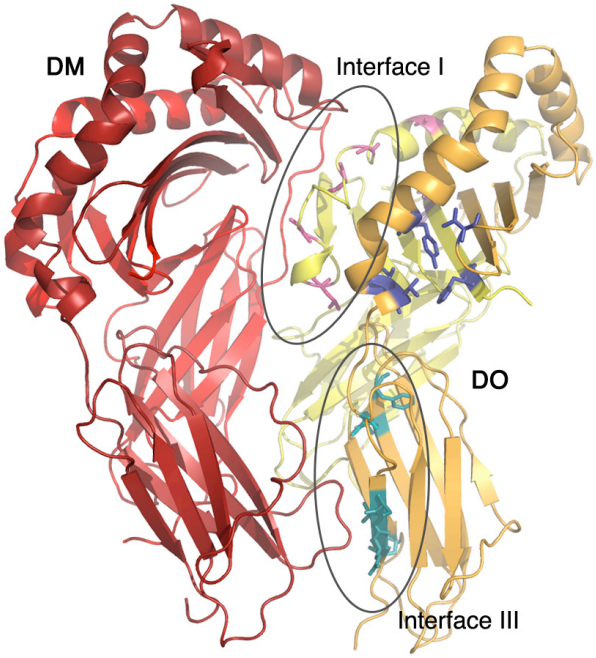

DO-DM	MAGS-DO
Interface I	
GLU 40	LEU 45
TRP 43	GLY 49
SER 53	PRO 57
PRO 57	GLY 58
Interface III	
96-100	PRO 97
183-187	SER 185
	VAL 186
	GLU 187

Figure 4.4. DO residues affecting both DM binding and MAGS-DO5 reactivity

Selected mutants when shown on the DM-DO crystal structure (4I0P). The colors are as shown in Figure 4.4

Furthermore, 25% of the isolated mutants were localized at the DM-DO binding interface ( ) and 12% are at the solvent-exposed β1 domain, which can rationally be the Mags.DO5 epitope. However, it is hard to pinpoint which of the isolated yeast clone mutation was accountable for the increase Mags.DO5 reactivity. So, to further evaluate every variant contribution, these point mutations were applied singularly and tested in cellular setting, examining both Mags.DO5 reactivity ER-exit and DM inhibition.

4.1.1. Effect of DO mutations on the peptide exchange

Normalized to *wt* DO staining and to the total DO expression (HKC5 mAb, which recognizes DOβ cytoplasmic tail), only a handful of mutant had increased Mags.DO5 reactivity (**Error! Reference source not found.**5, orange bars). I also tested the ability of HLA-DO to inhibit HLA-DM and assayed for the amount of CLIP. Interestingly, most of the mutants showed a decrease inhibitory effect, supporting the notion that the intrinsic instability of DO is a required for its function. Finally, these results support the model in which DO competes against classical MHCII molecules by sequestering DM chaperone's function.

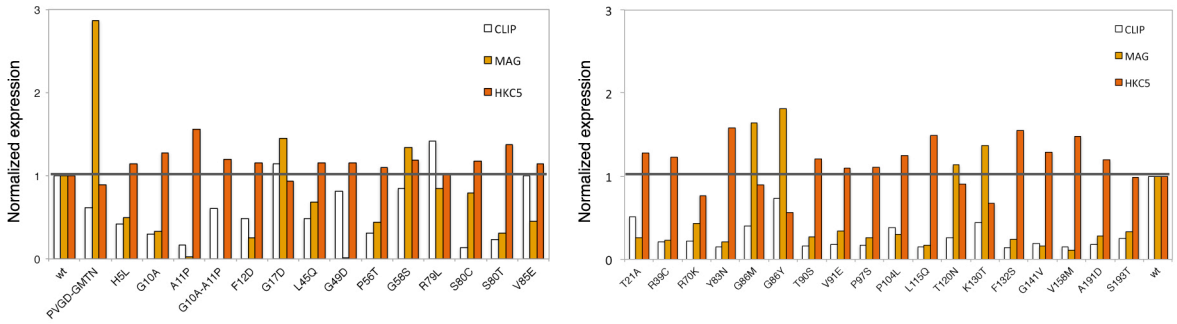

Figure 4.5. Characteristics of DO mutants

Normalized MAGS.DO5, HKC5 and cerCLIP expression after transfection of DO mutants, stemming from directed evolution and yeast display selection, into 293T CIITA cells. The MFIs were normalized for HKC5 expression, allowing comparison between different transfections. Then, the obtained ratio was normalized to the one of wild type DO in order to compare the mutants to the normal DO behavior. Thus, a value of 1 means that a given mutants behaves similarly to the wild type. Higher and lower value means that this mutant is better or worst, respectively. Note that these data are preliminary and that the lack of MAGS-DO5 or CLIP inhibition must be interpreted with caution. The left and right histograms show the α and β mutants, respectively.

What is interesting here is that even when Mags-DO5 reactivity for DO increases, there is not a higher amount of CLIP-MHCII at the plasma membrane. Moreover, none of the mutant selected by yeast display showed improved capability to inhibit DM.

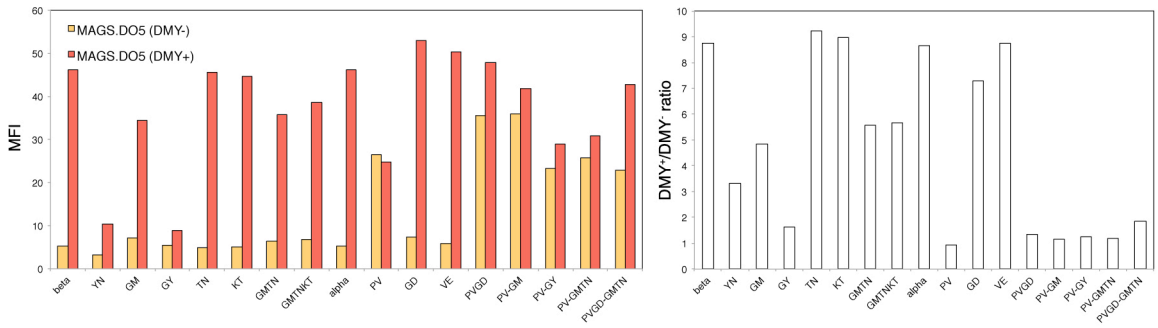

Figure 4.6. DMY effect on DO mutants

Expression of DMY increases Mags.DO5 staining at the plasma membrane. In yellow are the Mags.DO5 MFI without DMY expression and in orange are the Mags.DO5 MFI with DMY. Mutations selected by yeast display do not require DM assistance to disclose Mags.DO5 epitope and those mutants egress similarly to the PV mutant (Deshaies et al., 2005).

Chapter 5 : Iip35 isoform promotes formation of nonamers

Experimental design: MC, JSF and JT

Performed experiments: MC[75%], JSF[25%]

Writing: MC[85%], JSF[5%] and JT[10%]

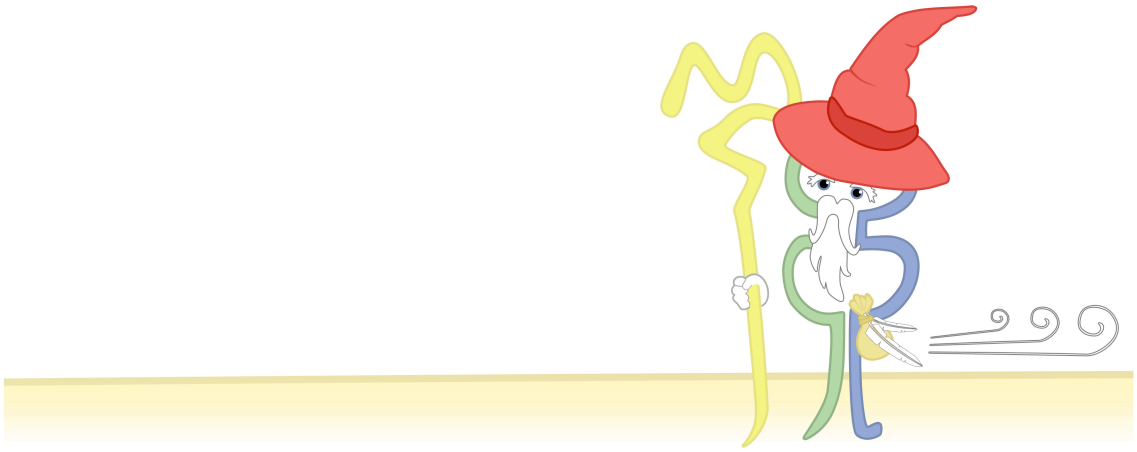

I've always wanted to travel far away

- The invariant chain guiding MHCII out of the ER

The human invariant chain p35 isoform promotes formation of nonameric complexes with MHC class II molecules

Maryse Cloutier, Jean-Simon Fortin and Jacques Thibodeau

Laboratoire d'Immunologie Moléculaire, Département de Microbiologie et Immunologie, Université de Montréal

Correspondance: Jacques Thibodeau

Department of Microbiology and Immunology

Université de Montréal, C.P. 6128 succ. Centre-ville, Montréal, Québec, Canada H3C 3J7

Tel: 514-343-6279; Fax: 514-343-5701

Running head title: Iip35 forms nonamers with MHC II molecules

5.1. Abstract

The invariant chain (Ii) trimerizes in the endoplasmic reticulum (ER) and associates with MHC class II (MHCII) molecules. However, the exact stoichiometry of the complex that egresses the ER remains debated. To shed light on this issue, we used a functional approach based on a single-chain dimer construct in which Ii was covalently linked to MHCII β chain (βSCD). In HEK293T transfected cells, nonamer-like complexes including three SCDs and three MHCII α chains $(\alpha+\beta SCD)_3$ were shown to egress the ER. Disrupting these pseudo-nonamers by co-expressing Iip33 showed that pentameric ($Ii_2(\beta SCD+\alpha)_1$) and/or heptameric ($Ii_1(\beta SCD+\alpha)_2$) complexes can also reach the plasma membrane. By co-expressing various Ii isoforms together with wild-type HLA-DR and/or a variant fused to a cytoplasmic di-lysine (DR_{KKAA}) ER retention motif, we showed that the stoichiometry of Ii/MHCII complexes may vary and that Iip35 promotes formation of nonamers. Finally, we provide evidence for the existence of mixed complexes containing both DR and DQ isotypes. Altogether, our results demonstrate that Iip35 affects the stoichiometry of the MHCII/Ii complexes that gain access to the endosomes.

5.2. ntroduction

The invariant chain (Ii; CD74) is endowed with pleiotropic functions and is best characterized for its role as a chaperone for major histocompatibility complex class II molecules (MHCIIs) (1). In the ER, Ii functions as a scaffold protein, favoring the association of certain α and β MHCII allotypes and preventing the binding of ER peptides. A type II transmembrane glycoprotein, Ii's N-terminal tail contains two cytoplasmic leucine-based endosomal sorting signals (2). Its luminal part is composed of a membrane-proximal disordered region, the class II-associated Ii peptide (CLIP) segment and a C-terminal trimerization domain (3,4). According to the current model proposed by Roche *et al.*, three MHCII $\alpha\beta$ heterodimers associate with a preformed Ii trimer, forming the nonameric structure that then egresses the ER (5). Once in endosomes, Ii is sequentially degraded, leaving CLIP in the peptide-binding groove (6). The exchange of CLIP for a high-affinity peptide is catalyzed by HLA-DM, a non-classical MHCII molecule that resides in the endocytic pathway (7).

Mice express two Ii isoforms (p31 and p41), which result from alternative splicing (8). In humans, the corresponding isoforms are known as p33 and p41. Additionally, about 20% of the translation products originate from usage of an upstream start codon. This generates p35 and p43, two additional isoforms which bear a sixteen-amino acid cytoplasmic extension (9). This N-terminal region contains a strong di-arginine (RxR) ER retention motif (10). The current model underlying ER egress of p35 is based on phosphorylation of its serine 8 (11,12). This allows the binding of 14-3-3 proteins, which compete with β-COP in the ERGIC or cis-Golgi to prevent retrograde transport by COPI-coated vesicles (13). Earlier work from our group has shown that the "masking" of the RxR motif requires

the MHCII β chain cytoplasmic domain (14). The molecular mechanism by which MHCII overcomes the ER retention motif is still unknown.

The existence of nonamers has recently been challenged and it was proposed that due to structural constraints, Ii/MHCII complexes can only form pentamers ($\alpha\beta(Ii)_3$) (15). Given the divergent results obtained so far using biochemical techniques, we chose to shed new light on the stoichiometry of the complex using a functional approach in transfected cells. Our data reveal that although pentamers can egress the ER, the need to mask the RxR motif of p35 favors the formation of higher order structures.

5.3. Material and Methods

5.3.1. Plasmids and mutagenesis

The pbud DRα+DRβ, pbud DM and pLNCX DQ plasmids have been described previously (14,16). DRβ was subcloned into pcDNA 3.1 MSC myc to generate $DR\beta_{myc}$. $DR\beta_{KKAA}$ was generated by PCR. Iip33, p35 and $p35_{LIML}$ were subcloned into pcDNA3 from previously described constructs (14). The pcDNA3 $p33_{LIML}$ mutant and $p35_{LIMLS6,8A}$ mutant were created by PCR overlap mutagenesis (14). To create the pbud αSCD and βSCD single-chain dimers, the luminal domains of the mature DRα (aa 1-191) and DRβ (aa 1-199) were linked by PCR overlap to Iip33's luminal region (aa 57-232) using a $(Gly)_3(Ser)_1(Gly)_3$ linker. $p35_{LIMLTRIM}$ coding for aa 1-143 of $p35_{LIML}$ was generated by introducing a stop codon in pcDNA3 $p35_{LIML}$.

5.3.2. Antibodies and Western blotting

The following mouse mAbs were described previously (14,16): BU45 (C-terminal region of human Ii); Pin1 (cytoplasmic tail of human Ii); L243 (HLA-DR); XD5.117 (DRβ); DA6.147 (DRα cytoplasmic tail); CerCLIP.1 (CLIP); MaP.DM1 (DM); HLA-DQ FITC (Life Science Inc., Memphis, TM); 9e10 (myc-tag) (Biolegend, San Diego, CA). The C-2-10 monoclonal anti-PARP antibody was a kind gift from Dr Guy Poirier (Université Laval, Québec)(17). Secondary Alexa-fluor-coupled antibodies (Invitrogen, Burlington, ON) were used for flow cytometry. For Western blotting, Peroxidase-AffiniPure Goat Anti-Mouse IgG (H+L) (Jackson Immunoresearch, West Grove, PA) and Mouse TrueBlot® Western Blot Kit (eBioscience, San Diego, CA) were used. For immunoprecipitations, cells were lysed at 4°C in 1% Triton-X100. Samples were subjected to SDS-PAGE 10%.

Proteins on immunoblots were detected by chemiluminescence (Roche Applie Science, Laval, Qué.).

5.3.3. Sucrose gradient

Sucrose gradients were prepared by gradually mixing 0.4M with 0.8M sucrose in 10mM Tris-buffered saline 0.5% Triton X-100 pH 7.5 (15). Cell lysates (1 mL) were loaded on top of the gradients and submitted to centrifugation at 100 000g for 50h. Twenty-four fractions were collected from each gradient and analyzed on immunoblots.

5.3.4. Cell lines and flow cytometry

For transient expression, HEK293T cells were transfected using polyethyleneimine (Polyscience, Warrington, PA) and stained after 48h. To determine surface expression, live cells were stained on ice and analyzed by flow cytometry. To determine total expression of MHCII or Ii, cells were fixed in 4% paraformaldehyde, permeabilized, and stained, as described previously (16). In some experiments, cells were first surface stained before being permeabilized and stained with different mAbs. As compared to living cells, staining of fixed and permeabilized cells sometimes results in an apparent lower specific fluorescence intensity due to increased autofluorescence and the strong background caused by some combinations of primary and secondary antibodies.

5.4. Results

5.4.1. Single-chain dimers between Ii and MHCII

To shed light on the composition of MHCII/Ii complexes that gain access to the plasma membrane and endosomes, we designed a strategy by which free Ii monomers are allowed to trimerize with other Ii molecules that are already linked to MHCIIs via a covalent link. This strategy limits the availability of MHCIIs and favors the formation of mixed complexes in which one or more Ii subunits will not be directly associated to a DR molecule. To construct the MHCII/Ii single-chain dimer (SCD), the luminal C-terminus of the HLA-DRβ chain (βSCD) was fused to the N-terminus of Ii (18) (Fig. 1). When expressed with the complementary MHCII α chain in HEK293T cells, βSCD accumulated at the plasma membrane just like full length DR/Ii molecules and was recognized by the conformation-sensitive L243 mAb (Fig. 1A-E). Accordingly, Ii was detected at the plasma membrane using the conformation-sensitive BU45 mAb (Fig. 1E). As BU45 recognizes an epitope located within or next to the trimerization domain and since this mAb does not bind Ii monomers, our results suggest that βSCD and DRα can form pseudo-nonamers ($DR\alpha_3\beta SCD_3$) (19-21). In this experiment, the two di-leucine endosomal sorting signals of the wild type (WT) Ii control were mutated ($Iip33_{LIML}$) to facilitate its detection at the plasma membrane (Fig. 1B). Indeed, because this molecule is less efficiently internalized, it has a longer half-life and accumulates preferentially at the cell surface after passage through the Golgi (22,23). Interestingly, βSCD yielded some MHCII-CLIP complexes at the plasma membrane (Fig. 1B, E). As the CLIP fragment can only be detected in association with MHC II molecules and after cleavage of Ii in late endosomes (24), this result suggested that at least a fraction of the complexes recycled between the endocytic pathway and the plasma membrane. Finally, we found that CLIP was efficiently removed upon co-

expression of HLA-DM (Fig. 1C, F). Altogether, these results demonstrate that the DRα/βSCD complex is structurally very similar to WT MHCII/Ii.

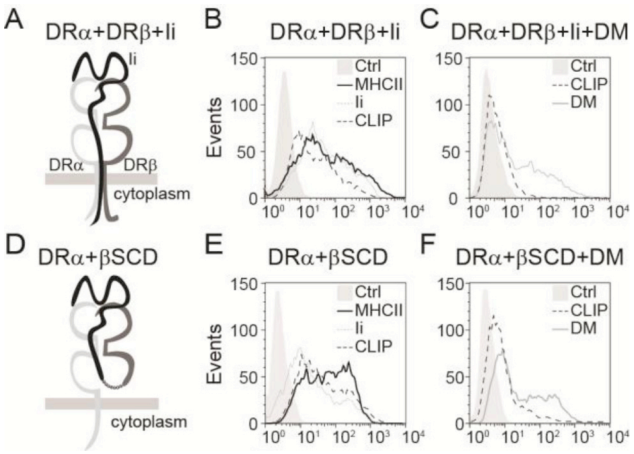

Figure 5.1: Schematic representation and expression of SCD.

(A) Schematic representation of wild-type DRα, DRβ and Ii. **(B)** Wild-type DRα, DRβ and $p33_{LIML}$ were transiently transfected in HEK293T cells. After 48h, cells were stained to detect MHCII, Ii and CLIP using L243, BU45 and Cer-CLIP.1 mAbs, respectively. **(C)** Cells were transfected as above as well as with HLA-DM and stained for surface CLIP and permeabilized to detect HLA-DM. **(D)** Schematic representation of DRα and βSCD. βSCD was designed as to have Ii and HLA-DRβ luminal domains linked by a flexible gly_3/ser/gly_3 sequence. **(E,F)** Transfected cells were analyzed as above. Histograms are representative of at least five independent experiments

5.4.2. The stoichiometry of SCD complexes can vary in the presence of free Ii

To further characterize the Ii/MHCII complex, we investigated the trafficking of βSCD when co-expressed with $Iip33_{LIML}$ and $p35_{LIML}$ (Fig. 2A). First, HEK293T cells were transiently transfected with α+βSCD and surface stained to detect Ii. The same cells were then permeabilized and stained for DR to assess efficacy of transfection and overall expression of the complex. In absence of additional Ii, as shown above, the βSCD and CLIP were detected at the plasma membrane (Fig. 2A, B, left panels). Separate cell aliquots were also stained to measure surface MHCII and total Ii, allowing a molecule's surface expression to be compared to its total protein levels (Fig. 2B, middle and right panels). These normalized (surface/total) mean fluorescence values (MFV), which reflect the efficiency of forward trafficking, tend to be low for ER-retained molecules (14).

Then, we co-expressed βSCD with DRα and $p33_{LIML}$. This combination led to strong Ii, CLIP and DR surface expressions (Fig. 2A, B). However, these results do not indicate if some MHCII/Ii complexes included both SCDs and $p33_{LIML}$ moieties. We reasoned that $p35_{LIML}$, contrary to $p33_{LIML}$, might prevent surface expression of mixed complexes since the SCD lacks a β chain cytoplasmic region capable of shielding the RxR motif. Indeed, co-expression with $p35_{LIML}$ prevented transport of βSCD to the plasma membrane (Fig. 2A, right panel). MHCII staining of permeabilized cells with L243 confirmed the expression of the βSCD and DRα. The absence of CLIP at the plasma membrane is in line with the intracellular retention of this complex (Fig. 2B). Thus, it appears that p35 subunits get efficiently incorporated into SCD-containing complexes, causing a dramatic reduction of cell surface expression.

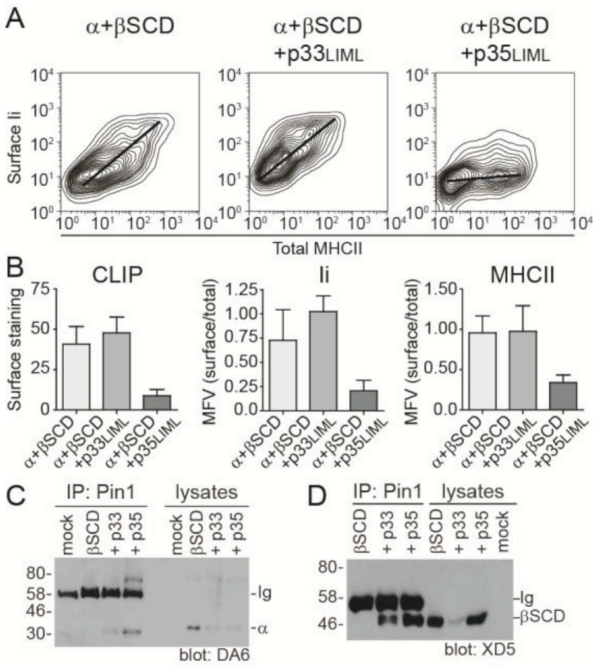

Figure 5.2: Nonameric and pentameric-like complexes can egress the ER

(A) Cells were transfected with DRα and βSCD alone or together with $p33_{LIML}$ or $p35_{LIML}$. Contour plots represent Ii surface expression relative to MHCII total expression. **(B)** The left panel shows the MFVs obtained for CLIP at the cell surface. The right panels show the ratio obtained for surface expression versus total expression. This ratio indicates the proportion of Ii or MHCII expressed at the plasma membrane. **(C)** Cells were transfected with DRα and βSCD alone or together with p33 or p35. Cell lysates (right lanes) and Ii immunoprecipitations (left lanes) were analyzed on immunoblots. The HLA-DRα chain was detected using the DA6.147 mAb specific to the cytoplasmic domain. Heavy chains of the immunoglobulins (Ig) used for immunoprecipitations are indicated. Mock samples are non-transfected HEK293T cells.

(D) Samples were analyzed using the XD5.117 mAb specific to DR's luminal domain. Error bars indicate the SD from five independent experiments.

Our results suggest that the heterotrimerization of full-length $p33_{LIML}$ or $p35_{LIML}$ with the βSCD-included Ii chain generates pseudo-pentamers ($Ii_1(\alpha+\beta SCD)_2$) and/or -heptamers ($Ii_2(\alpha+\beta SCD)_1$). We performed co-immunoprecipitation assays to confirm the association of WT Ii with βSCD using the Pin.1 mAb, which recognizes the cytoplasmic tail of Ii (Fig. 2C). Because Pin.1 is sensitive to mutations in the leucine-based sorting signals, these experiments were performed with WT Ii isoforms. Iip33- and p35-immunoprecipitated samples were analyzed on immunoblots for the presence of DR α and β chains. Results confirmed that both DRα and SCD chains were associated with p33 and p35. While DRα was revealed with the cytoplasmic tail-specific DA6.147 mAb (top panel), the SCD-included DRβ chain was detected at ~50 kDa using the β1 domain-specific XD5 mAb (Fig. 2D). Cell lysates were included as controls. When expressed alone, α+βSCD was not detected as the Ii cytoplasmic portion is deleted. Combined with the fact that p35 prevents expression of the βSCD complex at the cell surface, these results demonstrate that full-length Ii can heterotrimerize with the Ii moiety of SCDs to form pseudo-heptamers and/or pseudo-pentamers. Taken together, these results suggest that the stoichiometry of MHCII-Ii complexes is variable.

5.4.3. Retention of βSCD by Iip35 requires its trimerization domain

To confirm that Iip35 interacts with the Ii moiety of the βSCD, we created a mutant devoid of its trimerization domain ($p35_{LIMLTRIM}$, Fig 3). To do so, the C-terminal region including the three α-helices that mediate Ii trimerization (25,26) was deleted in Iip35 and replaced by a myc/his tag to compensate the loss of the BU45 epitope. As for $p35_{LIML}$, this mutant requires the presence of DR to access

cell surface (Fig 3 A and B) and to unmask the CLIP fragment (data not shown). These results suggest that the overall structure of this Ii variant is not grossly altered. To test if the C-terminal trimerization domain was responsible for the intracellular retention of the βSCD by p35, βSCD was expressed with DRα together with $p35_{LIML}$ or $p35_{LIMLTRIM}$. As observed previously in figure 2, in absence of additional Ii, the Ii and MHCII moieties of the SCD were detected at the plasma membrane (Fig 3C, middle and right panels). Some CLIP was also detected in these conditions (Fig 3C, left panels). Interestingly, while $p35_{LIML}$ caused the intracellular retention of βSCD, the $p35_{LIMLTRIM}$ variant was inactive and CLIP, MHCII and Ii were all detected at the plasma membrane (Fig. 3C). This data strongly suggest that the intracellular retention of SCD by p35 is trimerization-dependent and implies the formation of pseudo-pentamers ($Ii_1(\alpha+\beta SCD)_2$) and/or -heptamers ($Ii_2(\alpha+\beta SCD)_1$). In addition, these results demonstrate that Iip35 did not cause retention simply by displacing the covalently-linked Ii segment of the βSCD.

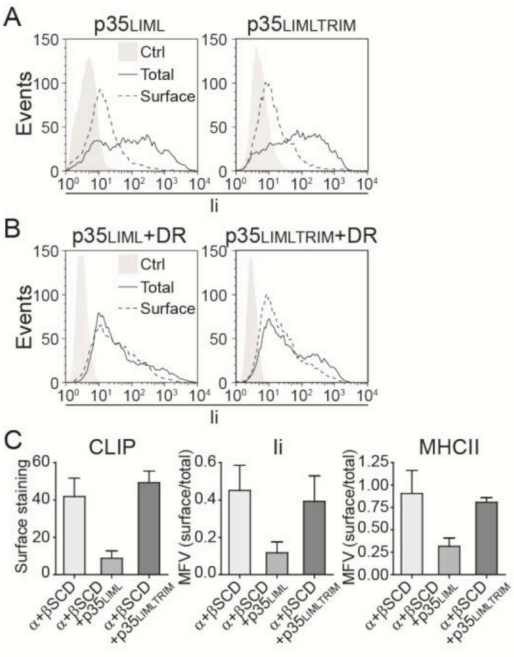

Figure 5.3: C-terminal trimerization domain of full-length Ii allows formation pseudo-heptamers and/or pseudo-pentamers

(A) $p35_{LIML}$ or $p35_{LIMLTRIM}$ were transiently transfected in HEK293T cells. After 48h, cells were stained to detect surface and total Ii using BU45 ($p35_{LIML}$) or anti-myc tag mAb ($p35_{LIMLTRIM}$) **(B)** Wild-type DRα, DRβ and $p35_{LIML}$ or $p35_{LIMLTRIM}$ were transiently transfected. Cells were stained to detect surface and total Ii. **(C)** Cells were transfected with DRα and βSCD alone or together with $p35_{LIML}$ or $p35_{LIMLTRIM}$. The left panel shows the MFVs obtained for CLIP at the cell surface. The right panels show the ratio obtained for surface expression versus total expression of Ii and MHCII.

Error bars indicate the SD from five independent experiments.

5.4.4. p35 forces the formation of high order complexes

The results presented above suggested that βSCD can form pseudo-nonamers and that free Ii can incorporate these complexes to form lower-order structures. In a recent study, Koch *et al*. have suggested that only one MHCII αβ heterodimer can associate with an Ii trimer (15). This conclusion was based, in part, from sedimentation of B cell lysate proteins in sucrose gradients. To gather evidence for the existence of nonamers in the context of non-cavalently linked wild-type molecules, we performed similar experiments using lysates from HEK293T cells expressing HLA-DR and either p33 or p35 (Fig4 A and B). After centrifugation, fractions were collected and analyzed on immunoblots for the presence of DRα. Our results show that p35 and MHCII can generate complexes of an apparent molecular weight superior to those formed around p33. The same applies to the control βSCD and DRα complexes as some were found deep in the gradient (Fig 4C). These data are in line with βSCD forming pseudo-nonamers and suggest that p33 and p35 behave differently, the latter generating larger complexes.

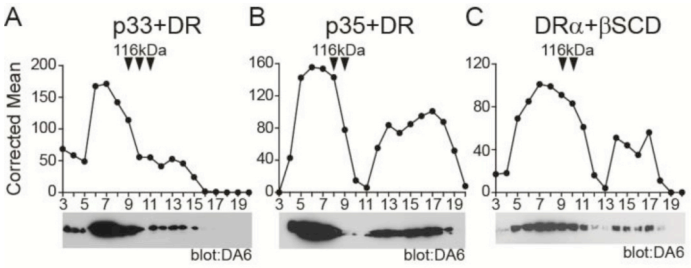

Figure 5.4: DR assembly with p35 and βSCD forms complexes of higher molecular weight than around p33

HEK293T cells were transfected with DR and p33 **(A)** or p35 **(B)** isoforms as well as α+βSCD **(C)**. Cells were analysed by flow cytometry (data not shown) and lysed. Sedimentation on sucrose gradient was performed and 25 resulting fractions were western blotted for DRα using DA6 antibody and parp1 (116kDa). Blots are representative of at least 3 independent experiments

5.4.5. Evidence for the ER egress of Ii/MHCII complexes of variable stoichiometry

The above-described data prompted us to evaluate the assembly and stoichiometry of Ii-MHCII complexes in the context of various Ii isoforms. We generated a DRβ molecule bearing its own ER retention motif in the form of a cytoplasmic Lys-Lys-x-x (KKAA) motif (Fig. 5A). The di-lysine signal acts as a strong retention motif for ER-resident type I transmembrane proteins. Recombinant reporter molecules that bear this sequence also localize in the ER (27). The rationale behind this strategy is that if heptamers and nonamers exist, the DR_{KKAA} variant should trap in the ER a co-expressed WT MHCII. In contrast, if pentamers are the only possible structures, the DR_{KKAA}/Ii complex should be retained in the ER without influencing the trafficking of other MHCIIs.

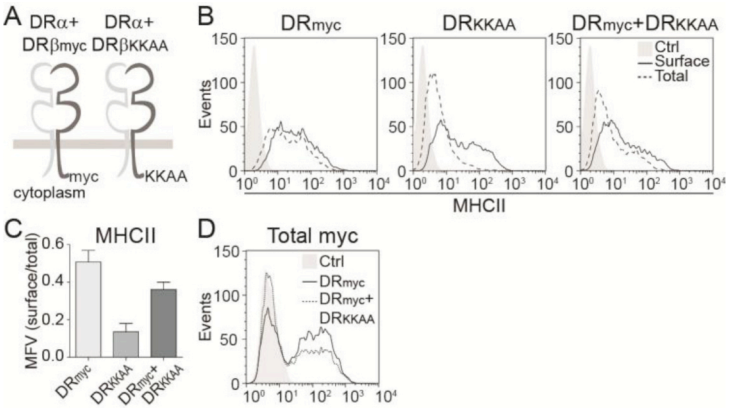

Figure 5.5: Surface expression of DR_{myc} is not affected by ER retained DR_{KKAA}

(A) Schematic representations of DR_{myc} and DR_{KKAA}. **(B)** HEK293T cells were transiently transfected with DRα together with either $DR\beta_{myc}$ (DR_{myc}), $DR\beta_{KKAA}$ (DR_{KKAA}) or with both β chains (right panel). Cells were stained with L243. **(C)** The MFVs obtained in panel B were plotted. **(D)** DR_{myc}, and DR_{myc}+ DR_{KKAA} cells were stained to detect total DR_{myc} expression using 9e10. Error bars indicate the SD from five independent experiments

We first confirmed the lack of surface expression of the transiently co-transfected β_{KKAA} and DRα chains. Cells were stained to detect surface expression of MHCII, while total expression was assessed after permeabilization (Fig. 5B). A

myc-tagged DR molecule (DR_{myc}) was used as control (Fig. 5A). In line with the presence of a functional ER retention motif, the data revealed that DR_{KKAA} was mostly found intracellularly (Fig. 5C). Importantly, when co-expressed with DR_{KKAA}, DR_{myc} was still detected at the plasma membrane (Fig. 5B, C). The relative proportion of MHCII at the surface was somewhat intermediate in these conditions as the DR_{KKAA} was retained in the ER, increasing the pool of "total" molecules. Staining of permeabilized cells with anti-myc mAb revealed that expression of $DR\beta_{myc}$ was similar whether $DR\beta_{KKAA}$ was present or not (Fig. 5D).

We then repeated these experiments using three different forms of Ii. First, we tested a MHCII/Ii SCD based on the DRα chain (αSCD). Upon association with the control β_{myc} chain, αSCD was detected at the cell surface using Ii-, DR- and CLIP-specific mAbs (Fig. 6A-C). However, as predicted, the αSCD was not detected at the plasma membrane when paired with $DR\beta_{KKAA}$. Since SCDs force the formation of nonamer-like structures, we could then ask whether β_{KKAA} would influence the fate of β_{myc}. Interestingly, when both β_{myc} and β_{KKAA} were co-expressed with αSCD, cell surface expression of DR_{myc} decreased dramatically (Fig6. A,B). Yet, β_{myc} was expressed, as confirmed by intracellular staining (Fig. 6D). As DR_{myc}, but not DR_{KKAA}, has the potential to reach the plasma membrane, we also measured the amount of surface MHCII in the context of total β_{myc}. The results confirmed that β_{KKAA} prevented β_{myc} expression at the plasma membrane in presence of αSCD (Fig. 6E).These results suggest that a trimeric αSCD randomly associated with the surrounding available β chains. As probaly one copy of $DR\beta_{KKAA}$ got incorporated into each pseudo-nonamer, all the molecules in the complex (including DR_{myc}) were prevented from reaching the plasma membrane. Accordingly, no CLIP was detected at the cell surface (Fig. 6C).

These data suggest again that nonamers exist, at least for SCDs. However, this nonameric complex could be artefactual due to the absence of potential

structural constraints normally imposed by the TM regions of WT molecules (15). To rule out this possibility, we assessed the impact of the DRβ_{KKAA} in the context of full length DRα and p33 or p35. When the control β_{myc} was the sole source of β chains, DR$_{myc}$, Iip33 and CLIP were all detected at the plasma membrane (Fig. 6A-C, E). In contrast, for β_{KKAA}, MHCII and CLIP were absent at the plasma membrane. Low levels of p33 were detected but these Ii trimers are most likely free of MHCII. Interestingly, when both β chains were co-expressed with p33, Ii and MHCII were detected at the plasma membrane, albeit at low levels (again due to the intracellular accumulation of DR$_{KKAA}$, which traps some Ii and increases the intracellular pool of MHCII). Still, the presence of CLIP at the plasma membrane confirmed that these MHCII molecules trafficked with Ii. Together, these findings suggest that in the presence of p33, β_{myc}-based MHCII heterodimers can most likely egress as pentamers ($Ii_3(\alpha\beta)_1$).

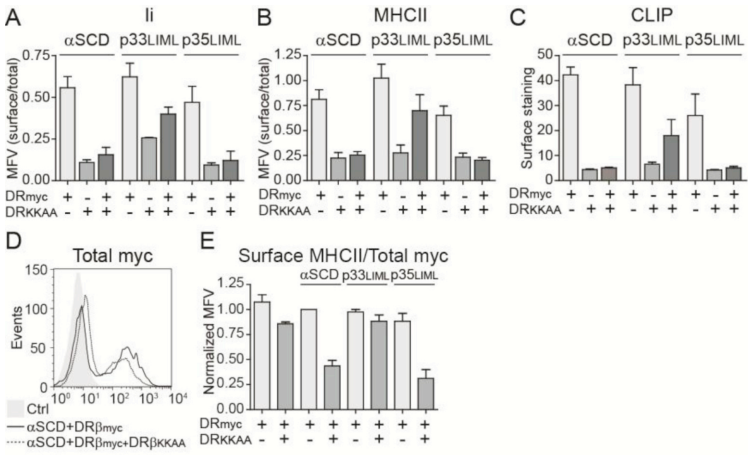

Figure 5.6: DR$_{myc}$ is retained by DR$_{KKAA}$ when p35 expression forces the formation of high order complexes with MHCII

(A, B and C) HEK293T cells were transiently transfected with DRβ_{myc} and/or DRβ_{KKAA} together with αSCD, p33$_{LIML}$ or p35$_{LIML}$. After 48h, cells were analyzed by flow cytometry to evaluate Ii expression **(A)** and MHCII surface to total expression ratio **(B)** using BU45 and L243, respectively. **(C)** Surface CLIP expression was assessed by flow cytometry and the MFVs were plotted. **(D)** Cells expressing αSCD with DRβ_{myc} and/or DRβ_{KKAA} were stained to detect total DRβ_{myc} using anti-myc-tag. **(E)** Cells from **A, B and C** were analyzed for MHCII/myc surface to total expression ratio using L243 and 9e10, respectively. Error bars indicate the SD from at least three independent experiments.

We cannot formally rule out that DR_{myc} was part of nonamers devoid of any DR_{KKAA}. However, it is highly unlikely that nonamers would not randomly include at least one competing DR_{KKAA} subunit. To resolve this issue and to better define the stoichiometry of the complex, we repeated the experiments with Iip35, which cannot egress as a pentamer since all RxR motifs in the complex must be masked. Thus, if pentamers do not exist and some nonamers devoid of DR_{KKAA} are formed, the results should be the same as for p33 and DR_{myc} should be found at the plasma membrane. On the other hand, if nonamers incorporate both DR_{myc} and DR_{KKAA}, no MHCII will be found at the plasma membrane. To discriminate between these possibilities, we next assessed the impact of expressing $DR\beta_{KKAA}$ and β_{myc} in the context of a p35 homotrimer. When expressed together with DR_{myc}, p35 and CLIP were found at the plasma membrane. On the other hand, in presence of $DR_{KKAA,}$ p35 was retained intracellularly. As this isoform cannot egress on its own, Ii was not detected at the cell surface. Interestingly, when β_{myc} and β_{KKAA} were co-expressed, results were different than those described above for p33. No MHCII, Ii or CLIP was found at the cell surface (Fig. 6A-C, E). Based on these findings, we conclude that p35 trimers are retained in the ER until saturated with MHCIIs. However, since β chains are incorporated randomly, it is likely that each and every nonamer contains at least one β_{KKAA} chain, thereby preventing ER egress and causing retention of the associated β_{myc}. Altogether, our results demonstrate that while pentamers can exit the ER, the presence of p35 and the need to mask its RxR motif are conditions that will most likely generate nonameric complexes.

5.4.6. Iip35 generates nonamers composed of mixed MHCII isotypes.

The ability of p35 to generate high-order structures suggests that different isotypes may be part of a given heptamer or nonamer. To test this possibility, we assessed the capacity of the DR_{KKAA} mutant to retain HLA-DQ in the ER (Fig 7A, B). Cells were transfected with either DQ alone, DQ and DR or DQ and $DR\beta_{KKAA}$ in

presence of either $p33_{LIML}$ or $p35_{LIML}$. First, when co-expressed with $p33_{LIML}$ or $p35_{LIML}$, DQ was found at the plasma membrane and some CLIP was generated (Fig. 7A, B). Similar results were obtained upon co-expression of DR, suggesting that the two isotypes behave the same in this assay. Interestingly, when co-expressed with DR_{KKAA}, DQ expression was only reduced in the context of $Iip35_{LIML}$ (Fig. 7A). As shown above for β_{myc}, this suggests that DQ can egress as pentamers with Iip33 independently of the presence of DR_{KKAA}. However, p35 trapped some DQ molecules. Noteworthy, the expression of DQ was not totally abolished as compared to DR_{myc} in the same conditions (Fig. 6B and E). The fact that no CLIP was detected at the cell surface suggested that these cell-surface DQ molecules did not interact with Ii and trafficked on their own (Fig. 7B). To test this possibility, we compared the capacity of DR and DQ to escape ER retention by $p35_{S6,8A}$, an unphosphorylated Ii variant which cannot exit the ER (12,28). Figure 7C and D show that while DQ and DR are well expressed at the plasma membrane and produce CLIP with Iip33, only DQ was detected at the cell surface with $p35_{S6,8A}$. As there was no trace of CLIP, we conclude that some DQ molecules egress the ER without Ii. Altogether, these results showed the existence of mixed nonamers containing different MHCII isotypes.

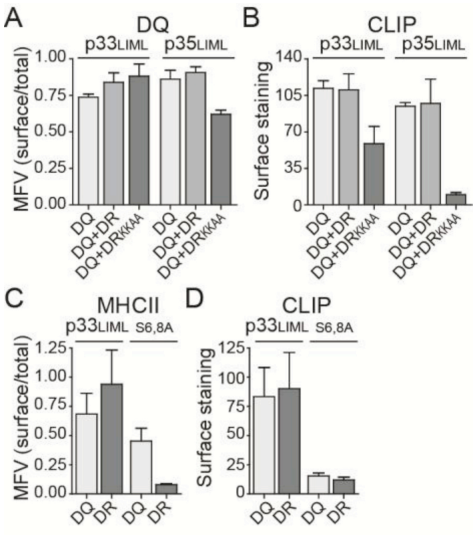

Figure 5.7: Different MHCII isotypes can associate with the same p35 isoform in nonameric complex

(A and B) HEK293T cells were transiently transfected with DQ, DQ and DR or DQ and DR_{KKAA} together with $p33_{LIML}$ or $p35_{LIML}$. **(A)** After 48h, cells were analyzed by flow cytometry to evaluate DQ surface to total expression ratio using anti-DQ specific antibody. **(B)** Surface CLIP expression was assessed by flow cytometry and the MFVs were plotted. **(C and D)** HEK293T cells were transiently transfected with DQ or DR together with $p33_{LIML}$ or $p35_{LIMLS6,8A}$. **(C)** After 48h, cells were analyzed by flow cytometry to evaluate DQ and DR surface to total expression ratio using anti-DQ and L243 antibody respectively. **(D)** Surface CLIP expression was assessed by flow cytometry and the MFVs were plotted. Error bars indicate the SD from at least three independent experiments.

5.5. Discussion

The exact sequence of events leading to ER egress of the Ii/MHCII complex remains to be fully characterized. In B cell lines, p35 is usually underrepresented as compared to p33, allowing formation of some p33 homotrimers (12,21,29). In MHCII-negative T2 cells, Iip35-including trimers do not reach endosomes and have a long half-life. In contrast, homotrimeric p33 complexes acquire complex sugars in the Golgi and have a much shorter half-life (21). MHCII associate sequentially with Ii to form pentamers, heptamers and, ultimately, nonamers (5,29). However, pentamers were recently proposed to be end points and higher order structures dismissed as experimental artefacts (15). Considering the conflicting biochemistry data obtained so far, we chose to shed new light on the formation of the complex using a functional readout based on the capacity of Ii and MHCII to reach the plasma membrane in transfected cells.

We herein have presented strong evidence that functional high-order structures do arise in the ER. We have shown that SCDs, adopting a nonamer-like structure, are expressed at the plasma membrane and that third party MHCII molecules are retained in the ER in the presence of p35 and DRβ_{KKAA}. However, in the context of p33, similar experiments have demonstrated that some pentameric or heptameric complexes can successfully go through quality control mechanisms and exit the ER, destined for the endocytic pathway or the plasma membrane. Those observations were confirmed by biochemical data showing that MHCII-p35 and SCDs form higher molecular weight structures than MHCII-p33.

Our results are in line with a model in which the various nascent isoforms of Ii homo- and heterotrimerize following translocation in the ER. In the case of p33, MHCII α and β chains (either pre-associated or not) fold on Ii homotrimers to generate pentamers. Such a complex is then competent to egress the ER definitively. This undoubtedly happens under certain experimental conditions and in some cell types. The ratio of Ii and MHCII is likely to be a factor affecting the final stoichiometry. As Ii is often in vast excess and half of the Ii pool exists as p33 homotrimers, some MHCII may fold on their exclusive Ii trimer and egress the ER as pentamers (12,30). What physiological conditions could favor the formation of such complexes? Inflammation could benefit from the rapid expression of MHCIIs resulting from an increase in Ii expression. Although Ii gene expression is co-regulated with MHCII, it is also specifically induced by NF-κB (31). As suggested here, the p33/p35 ratio will also modulate the stoichiometry of the complex. Clearly, the relative proportions of these isoforms can somehow be regulated as overexpression of p35 has been reported in chronic lymphocytic leukemia (32). Whether p35 plays a role in tumor escape from the immune system by modulating the association of Ii and MHCII remains to be determined.

Anderson *et al*. have calculated that 48% of all Ii molecules are part of heterotrimers containing at least one p35 isoform (12). The presence of p35 in an Ii heterotrimer forces the sequential addition of MHCIIs until all RxR motifs are phosphorylated and masked by MHCII β chains. Thus, depending on which Ii subunit binds MHCII first, an heterotrimer containing one p35 should have a 33% chance of being released from the ER as a pentamer. As the sequential binding of MHCII on the Ii trimer was shown to be non-cooperative *in vitro* (33), Ii trimers most likely compete with newly formed pentamers for the available MHCII.

Our results suggest that slowing down transport kinetics modulates stoichiometry of Ii/MHCII complexes. Recently, soluble forms of human Ii and MHCII co-produced in cell line were shown to be secreted in complexes of different stoichiometry but all built around the Ii trimer (34). Such constructs devoid of TM regions may exit the ER quickly, preventing the saturation of Ii. Also, we can speculate that the diversity of Ii/MHCII complexes will be dictated by the nature of the isotypes co-expressed in a given cell. Our results clearly demonstrated that heptamers and pentamers can include different isotypes of MHCII. However, we also showed that a pool of folded and trafficked independently of Ii. The allotype used here (HLA-DQA1*0102/DQB1*0602) confers protection against insulin-dependent diabetes mellitus and was shown to form SDS-resistant compact forms in the absence of HLA-DM (35). If this increased stability is related to the Ii-independent ER egress described here remains to be addressed experimentally. Conversely, it would be interesting to study the protective properties of this MHCII molecule in the context of its potentially inefficient incorporation into nonamers. We can speculate that other factors, such as the affinity for CLIP, may regulate the incorporation (or dissociation) of some allotypes in nonamers. As the trafficking of Iip35 is peculiar, it is possible that some MHCII allotypes are more influenced than others by this Ii isoform. Interestingly, variation of p35 expression was suggested to

result in differential Ag presentation and contribute to the development of type 1 diabetes (36).

Taken together, our results demonstrate that the stoichiometry of the MHCII/Ii complex that reaches the endocytic pathway is influenced by the relative expression of the different Ii isoforms and of MHCIIs. Other variables undoubtedly include MHC haplotypes and cell type intrinsic factors. Ii serves as a chaperone for molecules other than MHCII and the expression of p35 may affect other cellular processes as well. In addition, Ii appears to function as a plasma membrane receptor. Given that p35 regulates surface display of Ii trimers (37), it will be interesting to determine the impact of this isoform on the chaperone-independent functions of Ii. Studies addressing the transport and functional characteristics of p35 in health and disease are warranted.

5.6. Acknowledgements

We thank P. Cresswell, L. Denzin, G.G. Poirier, William W. Kwok, and R.P. Sékaly for reagents, cDNAs, antibodies and hybridomas. We also thank Dr Hayssam Khalil for helpful discussions.

5.7. References

1. Cresswell, P. 1996. Invariant chain structure and MHC class II function. Cell 84: 505-507.
2. Pieters, J., O. Bakke, and B. Dobberstein. 1993. The MHC class II-associated invariant chain contains two endosomal targeting signals within its cytoplasmic tail. J. Cell Sci. 106 (Pt 3): 831-846.
3. Singer, P. A., W. Lauer, Z. Dembic, W. E. Mayer, J. Lipp, N. Koch, G. Hammerling, J. Klein, and B. Dobberstein. 1984. Structure of the murine Ia-associated invariant (Ii) chain as deduced from a cDNA clone. EMBO J. 3: 873-877.
4. Cresswell, P. 1992. Chemistry and functional role of the invariant chain. Curr. Opin. Immunol. 4: 87-92.
5. Roche, P. A., M. S. Marks, and P. Cresswell. 1991. Formation of a nine-subunit complex by HLA class II glycoproteins and the invariant chain. Nature 354: 392-394.
6. Riberdy, J. M., J. R. Newcomb, M. J. Surman, J. A. Barbosa, and P. Cresswell. 1992. HLA-DR molecules from an antigen-processing mutant cell line are associated with invariant chain peptides. Nature 360: 474-477.
7. Denzin, L. K., and P. Cresswell. 1995. HLA-DM induces CLIP dissociation from MHC class II ab dimers and facilitates peptide loading. Cell 82: 155-165.
8. Yamamoto, K., N. Koch, M. Steinmetz, and G. J. Hammerling. 1985. One gene encodes two distinct Ia-associated invariant chains. J. Immunol. 134: 3461-3467.
9. Strubin, M., E. O. Long, and B. Mach. 1986. Two forms of the Ia antigen-associated invariant chain result from alternative initiations at two in-phase AUGs. Cell 47: 619-625.
10. Schutze, M.-P., P. A. Peterson, and M. R. Jackson. 1994. An N-terminal double-arginine motif maintains type II membrane proteins in the endoplasmic reticulum. EMBO J. 13: 1696-1705.
11. Kuwana, T., P. A. Peterson, and L. Karlsson. 1998. Exit of major histocompatibility complex class II-invariant chain p35 complexes from the endoplasmic reticulum is modulated by phosphorylation. Proc. Natl. Acad. Sci. U S A. 95: 1056-1061.
12. Anderson, H. A., D. T. Bergstralh, T. Kawamura, A. Blauvelt, and P. A. Roche. 1999. Phosphorylation of the invariant chain by protein kinase C regulates MHC class II trafficking to antigen-processing compartments. J. Immunol. 163: 5435-5443.
13. O'Kelly, I., M. H. Butler, N. Zilberberg, and S. A. Goldstein. 2002. Forward transport. 14-3-3 binding overcomes retention in endoplasmic reticulum by dibasic signals. Cell 111: 577-588.
14. Khalil, H., A. Brunet, I. Saba, R. Terra, R. P. Sekaly, and J. Thibodeau. 2003. The MHC class II beta chain cytoplasmic tail overcomes the invariant chain p35-encoded endoplasmic reticulum retention signal. Int. Immunol. 15: 1249-1263.

15. Koch, N., M. Zacharias, A. Konig, S. Temme, J. Neumann, and S. Springer. 2011. Stoichiometry of HLA class II-invariant chain oligomers. PLoS. ONE. 6: e17257.

16. Faubert, A., A. Samaan, and J. Thibodeau. 2002. Functional analysis of tryptophans alpha 62 and beta 120 on HLA-DM. J. Biol. Chem. 277: 2750-2755.

17. Lamarre, D., B. Talbot, Y. Leduc, S. Muller, and G. Poirier. 1986. Production and characterization of monoclonal antibodies specific for the functional domains of poly(ADP-ribose) polymerase. Biochem. Cell Biol. 64: 368-376.

18. Thayer, W. P., C. T. Dao, L. Ignatowicz, and P. E. Jensen. 2003. A novel single chain I-A(b) molecule can stimulate and stain antigen-specific T cells. Mol. Immunol. 39: 861-870.

19. Newcomb, J. R., and P. Cresswell. 1993. Structural analysis of proteolytic products of MHC class II-invariant chain complexes generated in vivo. J. Immunol. 151: 4153-4163.

20. Park, S. J., S. Sadegh-Nasseri, and D. C. Wiley. 1995. Invariant chain made in Escherichia coli has an exposed N-terminal segment that blocks antigen binding to HLA-DR1 and a trimeric C-terminal segment that binds empty HLA-DR1. Proc. Natl. Acad. Sci. U. S. A 92: 11289-11293.

21. Newcomb, J. R., C. Carboy-Newcomb, and P. Cresswell. 1996. Trimeric interactions of the invariant chain and its association with major histocompatibility complex class II alpha beta dimers. J. Biol. Chem. 271: 24249-24256.

22. Bakke, O., and B. Dobberstein. 1990. MHC class II-associated invariant chain contains a sorting signal for endosomal compartments. Cell 63: 707-716.

23. Lotteau, V., L. Teyton, A. Peleraux, T. Nilsson, L. Karlsson, S. L. Schmid, V. Quaranta, and P. A. Peterson. 1990. Intracellular transport of class II MHC molecules directed by invariant chain. Nature 348: 600-605.

24. Denzin, L. K., N. F. Robbins, C. Carboy-Newcomb, and P. Cresswell. 1994. Assembly and intracellular transport of HLA-DM and correction of the class II antigen-processing defect in T2 cells. Immunity. 1: 595-606.

25. Park, S. J., S. Sadegh-Nasseri, and D. C. Wiley. 1995. Invariant chain made in Escherichia coli has an exposed N- terminal segment that blocks antigen binding to HLA-DR1 and a trimeric C-terminal segment that binds empty HLA-DR1. Proc. Natl. Acad. Sci. USA 92: 11289-11293.

26. Jasanoff, A., G. Wagner, and D. C. Wiley. 1998. Structure of a trimeric domain of the MHC class II-associated chaperonin and targeting protein Ii. EMBO J. 17: 6812-6818.

27. Teasdale, R. D., and M. R. Jackson. 1996. Signal-mediated sorting of membrane proteins between the endoplasmic reticulum and the golgi apparatus. Annu. Rev. Cell Dev. Biol. 12: 27-54.

28. Kuwana, T., P. A. Peterson, and L. Karlsson. 1998. Exit of major histocompatibility complex class II-invariant chain p35 complexes from the endoplasmic reticulum is modulated by phosphorylation. Proc. Natl. Acad. Sci. U. S. A 95: 1056-1061.

29. Lamb, C. A., and P. Cresswell. 1992. Assembly and transport properties of invariant chain trimers and HLA-DR-invariant chain complexes. J. Immunol. 148: 3478-3482.

30. Marks, M. S., J. S. Blum, and P. Cresswell. 1990. Invariant chain trimers are sequestered in the rough endoplasmic reticulum in the absence of association with HLA class II antigens. J. Cell Biol. 111: 839-855.

31. Pessara, U., and N. Koch. 1990. Tumor necrosis factor alpha regulates expression of the major histocompatibility complex class II-associated invariant chain by binding of an NF-kappa B-like factor to a promoter element. Mol. Cell Biol. 10: 4146-4154.

32. Veenstra, H., P. Jacobs, and E. B. Dowdle. 1993. Processing of HLA-class II invariant chain and expression of the p35 form is different in malignant and transformed cells. Blood 82: 2494-2500.

33. Jasanoff, A., S. Song, A. R. Dinner, G. Wagner, and D. C. Wiley. 1999. One of two unstructured domains of Ii becomes ordered in complexes with MHC class II molecules. Immunity. 10: 761-768.

34. Majera, D., K. C. Kristan, J. Neefjes, D. Turk, and M. Mihelic. 2012. Expression, purification and assembly of soluble multimeric MHC class II-invariant chain complexes. FEBS Lett. 586: 1318-1324.

35. Ettinger, R. A., A. W. Liu, G. T. Nepom, and W. W. Kwok. 2000. Beta 57-Asp plays an essential role in the unique SDS stability of HLA-DQA1*0102/DQB1*0602 alpha beta protein dimer, the class II MHC allele associated with protection from insulin-dependent diabetes mellitus. J. Immunol. 165: 3232-3238.

36. Yan, G., L. Shi, A. Penfornis, and D. L. Faustman. 2003. Impaired processing and presentation by MHC class II proteins in human diabetic cells. J. Immunol. 170: 620-627.

37. Warmerdam, P. A., E. O. Long, and P. A. Roche. 1996. Isoforms of the invariant chain regulate transport of MHC class II molecules to antigen processing compartments. J. Cell Biol. 133: 281-291.

Chapter 6 : Discussion & Conclusion

6.1. The relation between DO and DM

DO requires DM for maturation and to exit the ER. In Chapter 3, the interaction between DO and DM was examined with the Mags.DO5 mAb. Using this strategy, we showed that DM stabilizes the interactions between the DO α1 and β1 chains and that DM influences DO folding in the ER. Furthermore, following the work from Deshaies *et al.*, this conformation can also be achieved via a point mutation in the α1:β1 β-strand interface, regardless of DM binding (Deshaies et al., 2005). Thus, the Mags.DO5^{+} conformation correlates with DO egress from the ER.

6.1.1. DO conformation and Mags.DO5 epitope

Like DQα, DOα possesses an insertion (position 10b, or 11) between the residue 10 and 11 (or 12), which forms a bulge that protrudes toward the groove (**Error! Reference source not found.**). However, in contrast to the GLY inserted in DQ, DO has a PRO which disrupts the HB network tying the α and β first β-strands together (Guce et al., 2012). One must wonder why would certain MHCIIs have a conserved insertion/bulge at this position. One hypothesis is that it is to prevent pairing with certain β chains that bear a long side chain at position β78, which would sterically clashes with the bulge.

As discussed in section 3.5, DM most probably stabilizes the poor DOα:β pairing upon binding, as interchanging these two strands for those of DR disclosed the Mags.DO epitope. This epitope is one that is conformation-sensitive and located on DOβ chain. Three regions, defined as DR1 most flexible, are possible candidates for this mAb binding: i) the C-terminal end of the α-helix, ii) the most carboxy-distal β-strand of the Ig domain or iii) the association of the N-terminal end

of the α-helix and the loop between the first and second strands forming the groove platform (Painter et al., 2008).

It seems unlikely that the epitope is located on the Ig β2 domain as this flexible strand gets buried at the DM interface (Guce et al., 2012; Pos et al., 2012). Next, the βG86Y/M point mutant, where the Y/M fills the P1 pocked, highly increases Mags.DO5 reactivity (data not shown and **Error! Reference source not found.**3) in addition to make empty-state DR1 resistant to SDS denaturation (Natarajan et al., 1999b). Although I do not have formal evidence confirming Mags.DO5, it seems safe to argue that it binds the β1 domain, most probably at the N-terminal end of the peptide binding groove.

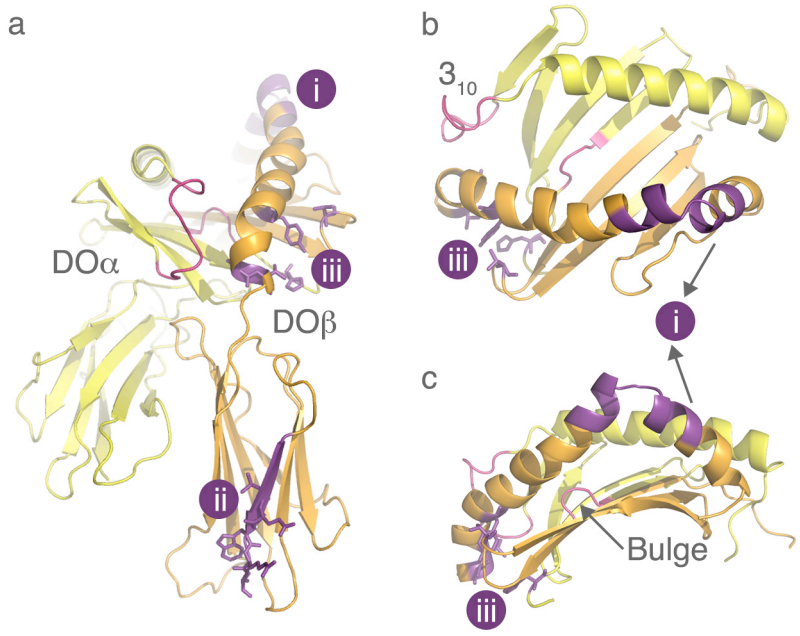

Figure 6.1. DO modelization based on DQ2.

Highlights of the three potential Mags.DO epitopes and the insertion creating the bulge at the α1:β1 interface. i) N-terminal end of the β1 α-helix; ii) last Ig strand of the β2 domain; iii) C-terminal end of the β1 α-helix, at the platform-helix junction.

6.1.2. Concluding remarks

DO necessitates DM for maturation and to exit the ER. Interestingly, a conformation change occurs in DO upon its binding with DM, which can be monitored by the Mags.DO5 mAb. Of the 41 unique mutants screened through directed evolution, 25% were localized at the DM-DO binding interface and 12% are at the solvent-exposed C-terminal β1 domain, a potential Mags.DO5 epitope. Most of the mutants showed a decrease DM-inhibitory effect, supporting the notion that the intrinsic instability of DO is required and that subtle conformation change are partially responsible for this function.

DO is highly conserved between species, so its structure-function must depend on its sequence to exhibit such role. First, although DO has over 80% homology with classical MHCIIs, it cannot bind peptides, probably because of a lack of available HBs to bind the peptide backbone with enough kinetic stability. Interestingly, 8% of the mutants are observed in *wt* DO sequences of other species. This suggested that in human DO, some mutations have cumulative or subtractive "stabilization" effect.

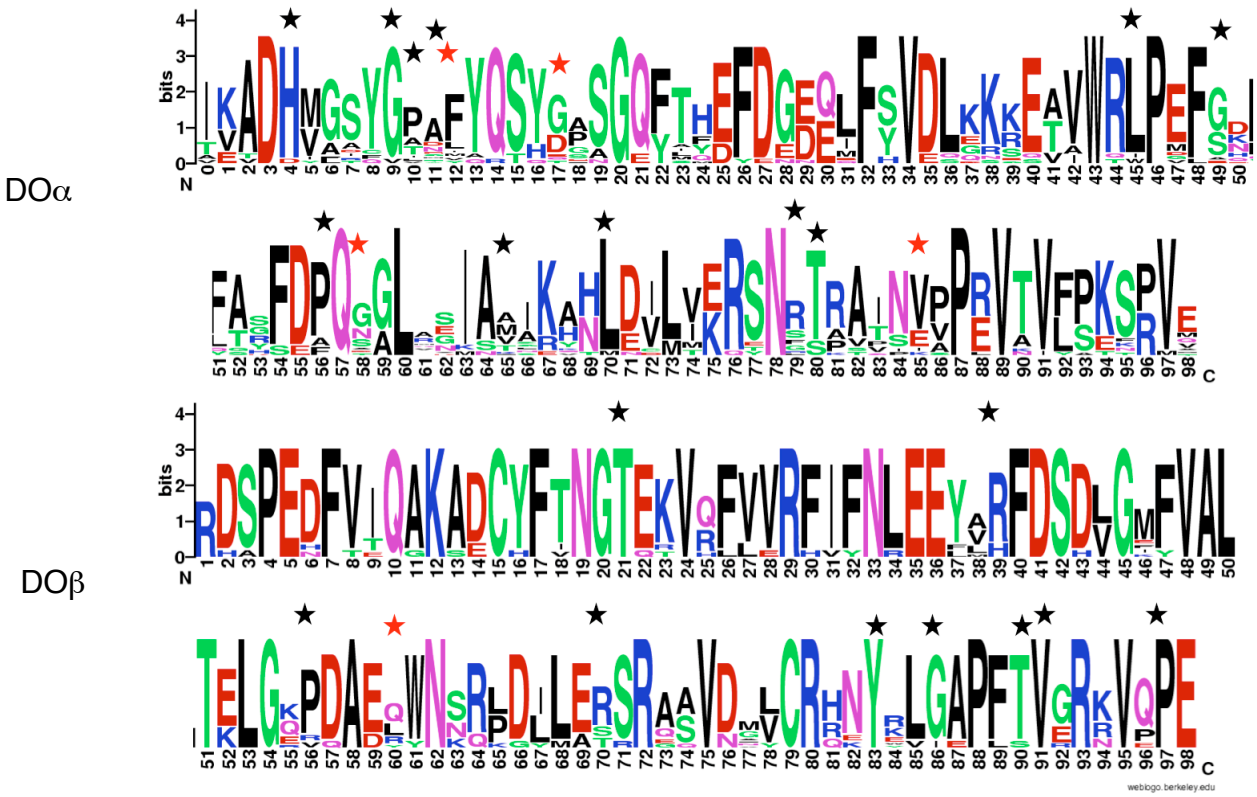

Figure 6.2. DO sequence Logo.

20 DOα and 13 DOβ sequences were aligned and are shown as a logo depiction. The size of the letters represents the residue conservation between species. The red and black stars indicate isolated residues from directed evolution that are or not present in other DO species, respectively.

Second, DO must remain in a permissive DM-binding state, a state that, once lost, renders it unable to bind DM again (The Stern Lab, personal communication). This conformation transition could be the key to clearly understand DO function and its relation with DM. Whether DO-DM dissociation in the MIICs is ligand-dependent or triggered by an unknown event remain to be evaluated. Given the particular DO-DM complexes location compared to the one of unbound-DM in the MHCIIs, one can't exclude that accessory protein are also implicated.

6.2. vSAG7 presentation

The activity of vSAGs has been known since the 70s but still remains poorly defined. vSAGs are produced in vanishingly small quantities rendering structure-function studies quite a challenge, as reflected by conflicting discoveries. Although there is no crystal structure available, I have nonetheless undertaken the characterization of the trimolecular complex between vSAG, MHCII and TCR. My results reconcile many caveats pertaining to the field and provide new insights about vSAGs mechanistic and MHC-TCR docking topology

In Chapter 2, I addressed the question: what is the topology of the TCR signaling complex mediated by vSAGs? My key finding was that TCR concomitantly binds both the MHCII α chain and vSAG. Therefore, the pressure exerted by vSAG alters conventional TCR-MHCII interactions and indicates that the TCR-MHCII docking is almost canonical when coerced by vSAGs. Furthermore, my results demonstrate that vSAG binding to MHCII molecules is conformation-dependent and abrogated by the CLIP amino-terminal residues extending outside the peptide-binding groove. In addition, they also suggest that vSAGs cross-link adjacent MHCIIs and activate T cells via a TGXY motif.

6.2.1. Model

It has long been clear that vSAGs have two binding sites on MHCIIs, one on the α chain and the other on the β chain, both overlapping those of SEA (Delcourt et al., 1997a; Mottershead et al., 1995; Torres et al., 1993). Given that C-vSAG binds to the MHCIIα chain and N-vSAG binds to the MHCIIβ chain, and that both moieties remain non-covalently associated upon maturation, one must carefully consider how these proteins interact together. First, vSAG must bind without hindering nominal Ag

interaction with the distinctive MHCII's open groove, as vSAG presentation depends on the bound-peptide (Woodland et al., 1997). Thus, in order to bind to both MHCII chains, vSAG7 must either: i) skirt around one or the other ends of the peptide groove; ii) go over it; or iii) bind an adjacent MHCII (**Error! Reference source not found.**3).

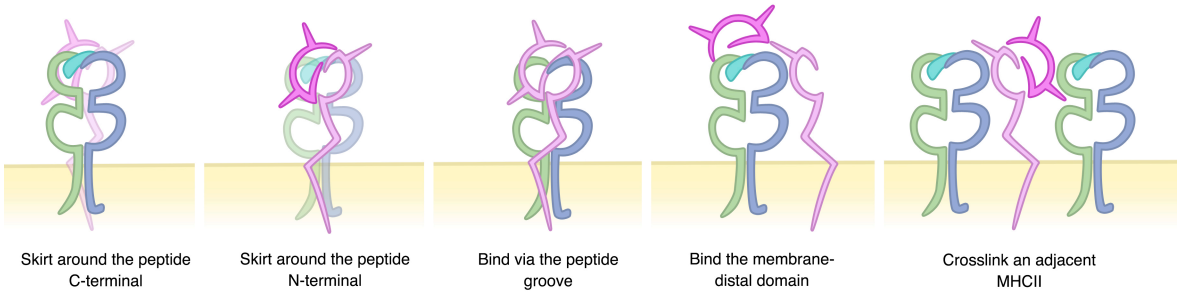

Figure 6.3. Possible ways vSAG can bind MHCIIs

From left to right: vSAG binds the MHCII on the peptide C-terminal end; on the N-terminal ends; through the peptide groove; over the groove, at the membrane distal region; or binds adjacent MHCIIs.

We can easily discern that vSAG7 does not surround MHCIIs at the C-terminal end of the peptidic groove (according to the canonical peptide orientation) because of the linker joining the peptide to the MHCIIβ chain in the tested constructs, which is likely to create sterical clash. Also, the identified binding sites of both vSAG7 moieties are closer to the N-terminal end of the peptidic groove, limiting the likelihood of such binding (Delcourt et al., 1997a; Mottershead et al., 1995). As described in section 2.3.3, vSAGs do not bind the MHCII peptide groove. Next, although it seems equally possible that N-vSAG encircles the N-terminal groove opening, many facts argue otherwise. Indeed, a panel of mutants located at this MHCII interface do not affect vSAG presentation (**Error! Reference source not found.**4) (Thibodeau et al., 1994). Furthermore, peptide extending outside the groove at this end would likely hinder such binding mode. Also, concomitantly expressing the βSCD with the αIi SCD in 293T allows the pairing of both SCDs, suggesting that C-vSAG does not cross over to the MHCII α chain when it is bound to the MHCII β chain (5).

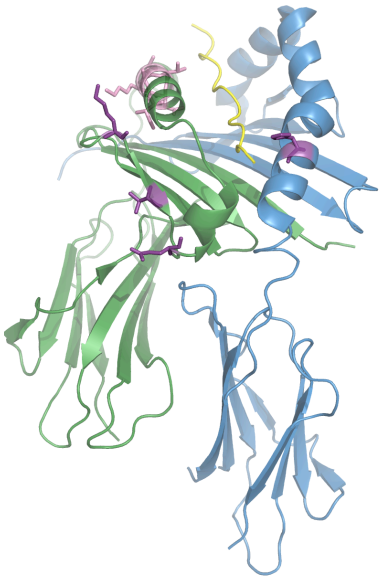

Figure 6.4. MHCII α or β mutants affecting or not vSAG presentation

Cartoon of CLIP-DR3 (16A6) showing in pink the residues implicated in C-vSAG binding and in purple those that do no affect its presentation.

A model in which vSAG binds the membrane-most distal region of MHCIIs, *i.e.* in a TCR-like binding fashion, does not fit our results highlighting the requirement of the TCR conjoint binding to both the MHCII α chain as C-vSAG would prevent both Ag and vSAG stimulation. Lastly, as discussed in section 2.4.3, it is more likely that C-vSAG binds adjacent MHCIIs than the one to which its N-vSAG moiety is bound.

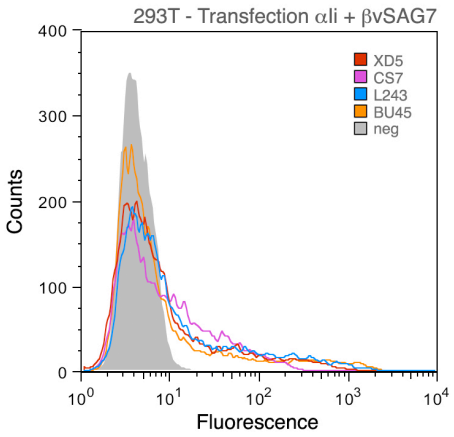

Figure 6.5. Coexpression of αIi and βvSAG7

Histogram showing transfection of the αIi and βvSAG SCDs. BU45 and L243 positive stainings imply that Ii trimerized and that the MHCII α and β chain paired correctly. As both Ii and vSAG are linked to a MHCII chain, existence of such multimeric complexes suggests that Ii and vSAG have distinct binding sites, arguing against vSAG binding to the N-terminal end of the groove.

Based on sequence homology, no other crystallized protein (and bSAGs) show enough similarity to generate a model accurate enough to formally rule out that vSAGs do not have loops or regions able to be "sandwiched" between the TCR-MHCII interface. Given the short half-life of the vSAGs, the protein bulk may include its share of protruding loops and could fit into such a model. Using the PHYRE^2 server, only a

part of C-vSAG gives a confidence value of over 30% and supports the fact that vSAG has a unique fold. In **Error! Reference source not found.**6, the predicted structure of the C-vSAG 195-258 stretch is given, based on the C-terminal domain of FAD-linked reductase fold (Kelley and Sternberg, 2009). Interestingly, even though the confidence of this model is only 34.3% based on a sequence homology of 15%, the β-stranded sheet including the TGXY motif - implicated in TCR contact - would complement the lateral face of the TCR Ig domain well.

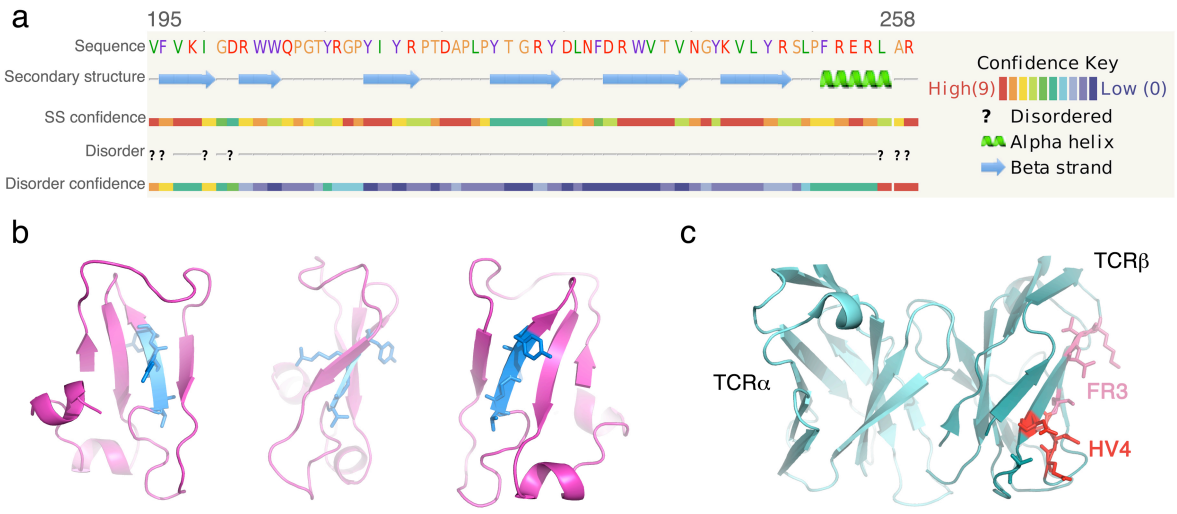

Figure 6.6. Part of C-vSAG predicted structure

a) Predicted secondary structure of C-vSAG (aa 195-258). **b**) Three different views of C-vSAG cartoon structure modelized from the C-terminal domain of the FAD-linked reductase fold. In blue, are shown the sticks of the TGXY motif **c**) Mapping of the TCR region implicated in vSAG binding.

According to the results presented in chapter 2, I proposed a new SAG-mediated T cell activation complex. Stemming from seminal work by Kappler, Pullen and Woodland's groups, my model is fine-tuned to many intricacies described in reports published in the nineties. vSAG7 binds to both MHCII α chain and TCRβ chain, in an arrangement somewhat similar to that observed previously in structures of various complexes of bacterial superantigens, MHCII, and TCR, but with less disruption of the conventional MHCII-TCR interface. We named this

vSAG-mediated MHC-TCR binding "near-canonical" in reference to the expected interaction of MHC and TCR. Most of the well-characterized bSAGs bind in such a way that conventional MHC-TCR interactions are disrupted and replaced by MHCII-SAG and SAG-TCR interactions (**Error! Reference source not found.**7). However, the vSAG-MHCII-TCR architecture is not quite canonical, as many peptides can be tolerated in the center of the interaction. Furthermore, vSAGs exert a pressure on the MHCII-TCR contacts that leads to CDR3β-MHCIIα interactions instead of the traditional CDR3β-peptide interactions.

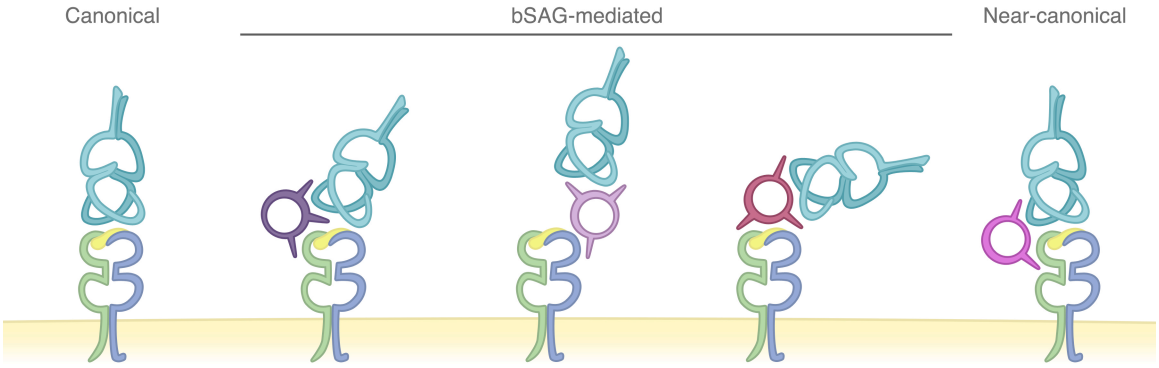

Figure 6.7. Architecture of SAG-mediated T cell signaling complexes

Cartoons of the major docking topologies between MHCII and TCR, whether or not mediated by SAG. From left to right are pictured the canonical, SEB, SEA, MAM and vSAG T cell signaling complexes.

How can the peptide TCR-contacting side chain not influence the vSAG7-mediated response? It is hard to link this effect simply on a near-canonical docking model and thus must also be dictated by the TCR V domain. Indeed, it is possible that different TCR would be sensitive to variation of the protruding side chain while others would be more permissive. My results stem from two Vβ6-bearing hybridomas, which only differ at the Vβ CDR3 and it is unknown if they are paired with the same Vα. Given how TCRα chain paring influence the conformation of the CDRs, the Vα could also allow further pressure (Stadinski et al., 2011). The role of non-germline-encoded structures (Jβ regions and CDR3s) has been disputed in the context of vSAG

recognition as Vβ3+ T cells that escaped thymic selection in vSAG1+ mice showed no bias in the structure of these regions (Pullen and Bogatzki, 1996). However, this may indicate that vSAGs are presented by a vast array of peptides and that these V(D)J combinations were not of high enough affinity to allow thymic deletion. Still, a large body of literature suggests that the β chain junctional region could influence TCR recognition of vSAGs (Candéias et al., 1991b; Cells, 1995; Ciurli et al., 1998; Woodland et al., 1993). Recently, Kilgannon and colleagues proposed a model in which vSAG presentation was highly dependent on the CDR3 (Kilgannon et al., 2010). Interestingly, they reported that highly pMHCII-specific TCR ($V\beta6^{+}$) fail to respond to vSAGs that were cognate to this Vβ. Although this result may sound trivial, it strongly supports the near-canonical docking and represents events in which vSAG cannot eschew such promiscuous TCR-pMHCII interactions. Thus, we can speculate that vSAGs coerce MHCII-TCR binding that may normally be of weak affinity and reorient the topology into a functional T cell signaling complex (**Error! Reference source not found.**8).

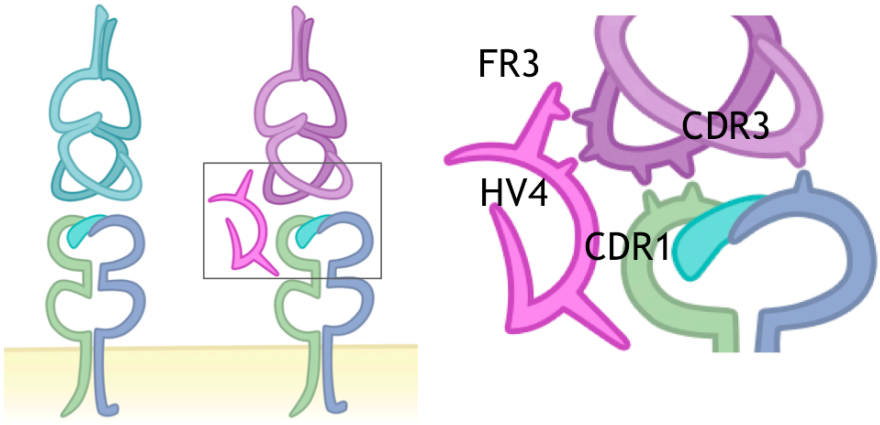

Figure 6.8. Close-up of the vSAG mediated T cell signaling complex

From left to right: Canonical pMHCII-TCR, vSAG-mediated pMHCII-TCR complex and a close-up of the latter. C-vSAG binds the TCR FR3 and HV4 and the MHCIIα chain, the latter also interacting with the TCR CDR1 and CDR3. The MHCIIβ-TCRα contacts remain to be evaluated.

6.2.2. vSAG and the MHCII-associated peptide

In section 2.3.1 and 2.4.1, I described the influence of the MHCII bound-peptide on vSAG presentation and proposed that amino-terminal PFRs are responsible for the inability of these pMHCII complexes to present vSAG. Notwithstanding the $CLIP_{81-87}$ extension, no other distinct PFRs were tested and an idiosyncratic CLIP effect cannot be ruled out. Indeed, as introduced in section 1.3.3. CLIP's mission, the CLIP peptide possesses features that could possibly account for the results observed with vSAG. However, a previous report by Rötzschke and colleagues seems to indicate that any peptide amino-terminal extensions would give similar results. They monitored pMHCII migration patterns on SDS-PAGE or native gels and noticed that MHCIIs loaded with peptides bearing amino-PFR migrated faster than those without extensions (Rötzschke et al., 1999). Interestingly, in SDS-resistant experiments, DR1 loaded with $lCLIP_{81-105}$ but not $cCLIP_{87-105}$, generated fast-migrating heterodimers, similar to what is observed when HA is appended at least 10 amino-terminal PFRs (Rötzschke et al., 1999). They also assayed randomly generated amino-terminal peptide flanking sequences to verify whether this effect was sequence specific. However, every tested sequence, except a $(GSPS)_3$ sequence, still generated the fast migrating pMHCII complexes. Altogether, these results suggest that the effect of lCLIP on vSAG presentation is linked to the presence of amino-terminal PFRs. However, with limited results it remains difficult to pinpoint whether this is due to steric hindrance, in which the extension prevents vSAG binding or a conformation alteration that does not allow vSAG binding to DRα.

6.2.3. vSAG-MHCII cross-linking = activation in *trans*?

The results presented in section 2.4.3 suggest that vSAG7s bind multiple MHCIIs and stimulate TCR in *trans*. *A priori,* this model is rationalized by the inherent ability of the vSAG moieties to bind two opposite faces on MHCIIs. Yet, it is further refined when we compared CIITA+ *versus* CIITA- cell lines which showed that the presence of endogenous pMHCIIs restored HA- and vSAG-specific T cell stimulation after transfection of the SCT (**Error! Reference source not found.**9). In other words, we believe that vSAG (both moieties) are transferred to the endogenous pMHCIIs. By consequence, the HA-DR1 portion of the SCT becomes available to HA-specific T cells and vSAG is presented by the endogenous pMHCIIs. Whether vSAG stimulation can arise from its two moieties remains to be evaluated. However, it was previously shown that vSAG paracrine stimulation is at least 50% less potent, which suggests that N-vSAG may have a role in stabilizing the trimolecular complex (Delcourt et al., 1997a).

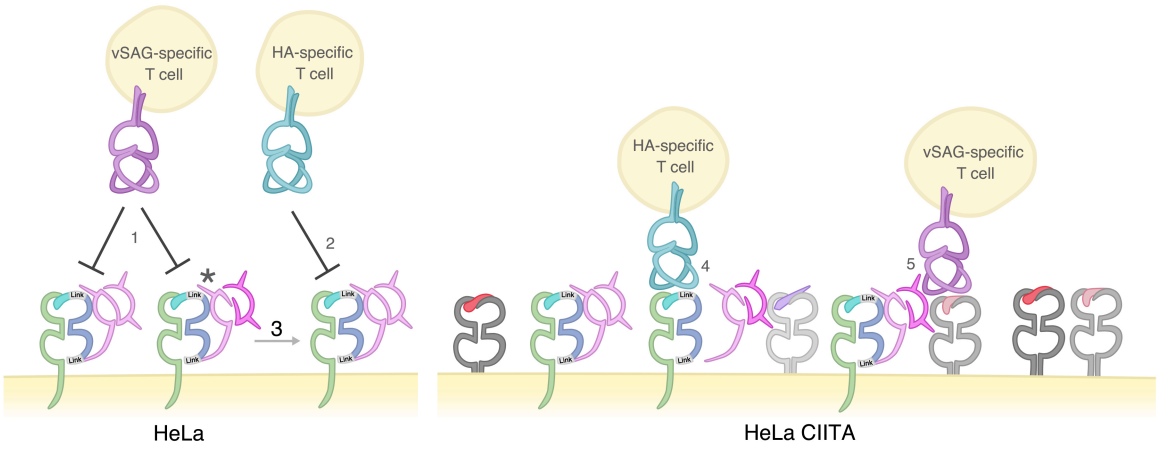

Figure 6.9. Trans activation by vSAGs.

On CIITA- cells, the lack of endogenous pMHCIIs prevents both HAs and vSAG-specific stimulation. 1) vSAG-specific stimulation is prevented because of the limited concentration of pMHCIIs and because the latter is bound to N-vSAG*. 2) HA-specific stimulation is also inhibited by the N-vSAG7* moiety. 3) Even if the vSAG domain of the SCT is transferred to an adjacent pMHCII, which

should restore both HA- and vSAG-specific stimulation, our read-out does not seem to be sensitive enough. In contrast, in CIITA+ cells, the presence of an endogenous population of pMHCIIs allows for vSAG transfer, freeing the SCT of the vSAG moiety, restoring HA stimulation (4). Upon transfer to a permissive endogenous pMHCII, C-vSAG - either bound or not to N-vSAG - can stimulate cognate T cells (5).

6.2.4. Concluding remarks

Altogether, my results reconcile a compendium of studies pertaining to the field but refute the model proposed by the Huber group indicating that vSAGs bind to the MHCII peptide-binding groove (Hsu et al., 2001). In addition to depicting a novel SAG-mediated TCR signaling complex, I answer a question that has remained unresolved for over 20 years, highlighting the plasticity of the TCR complementary determining regions. Given the puzzling nature of vSAGs and my description of a novel SAG-TCR-MHCII fold, I believe that my data brings a much-anticipated finale to decades of research and will serve as a grounding reference for future work, likely seeding new ideas related to MMTV superantigens.

6.3. Single chain constructs

Briefly introduced in section 1.1.8, single chain constructs have been used for almost 20 years to generate pools of MHC bearing the same bound-peptide and shaped our comprehension of pMHC-TCR interaction. Here, I engineered an array of SC constructs to further characterize Ii and vSAG7 relation with MHCIIs. I also generated a single chain DO (DOsc) in which DOα is linked to DOβ. This construct was used to express DO at the surface of yeast cells.

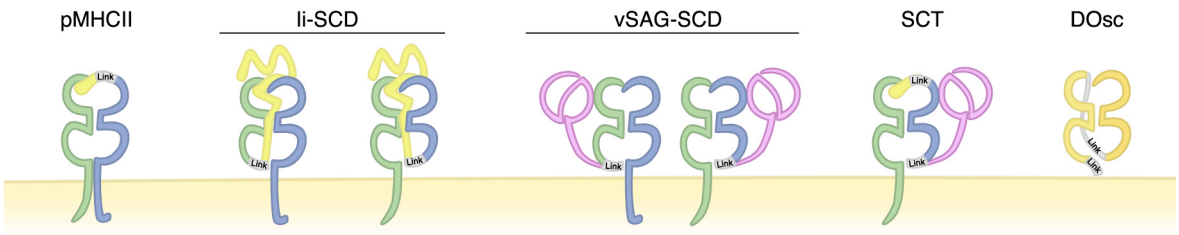

Figure 6.10. Cartoon of the single chain constructs

From left to right: pMHCII: a peptide is appended to the MHCIIβ chain (Kozono et al., 1994); Ii-SCD: the luminal domain of either MHCII chain is attached to Ii by a G_3SG_3 flexible linker; vSAG-SCD: the luminal domain of either MHCII chain is attached to vSAG by a G_3SG_3 flexible linker; SCT: the luminal domain of vSAG is attached to the a pMHCII; DOsc: DO α and β chain are covalently attached by a 15 aa GS flexible linker (Esteban and Zhao, 2004).

6.3.1. vSAG-SCDs

As shown in the Chapter 2 (S2 and Figure 2.2B), the linkage of vSAG to DRα failed to efficiently exit the ER and was rapidly degraded non-specifically. These results, although hypothetical, suggest that vSAG interacts closely with DRβ, which was not allowed enough freedom to reach or pair with the *wt* β chain upon co-expression given the length of the linker (7aa). However, unexpected vSAG-α chain interaction that prevented their pairing with DRβ cannot be excluded.

6.3.2. DOsc

The strategy to link DO luminal domain with a 15 aa linker (**Error! Reference source not found.**1) stems from the study by Esteban & Zhao (Esteban and Zhao, 2004). However, after performing the directed evolution on such constructs, they were tested in 293T for expression and fail to give rise to Mags.DO5 positive DOsc. At this point other constructs were tested, some with longer linker (22 aa) or with the β chain upstream of the α chain (with both linker length). Again, no Mags.DO5 positive DOsc were observed, although the HA-tag stained positively intracellular. Thus, it seems that even in the yeast, DOsc could not exit the cell unless accumulating mutation allowing proper folding into the Mags.DO5 conformation.

6.3.3. Ii-SCDs

Presented in detail in Chapter 4, constructs in which Ii was appended to the luminal domain of either MHCII α or β chain allowed us to describe the variable stoichiometry of the multimeric complexes including up to three MHCIIs and the Ii trimer. This strategy ensures that every Ii isomer is bound to an MHCII and forms nonameric complexes. However, when co-expressed with full-length *wt* Ii, the latter forming mixed-trimers with the Ii SCDs, cannot pair with MHCIIs given the lack of one of the MHCII chain, the other being exclusively expressed as the SCD. These mixed-trimers are well recognized by a battery of mAbs. Also, the SCDs recycle between the plasma membrane and the endosomes and allowed for proper degradation of Ii into the CLIP peptide. Moreover, we found that CLIP was efficiently removed upon co-expression of HLA-DM. Altogether, we demonstrate that Ii-SCDs are structurally very similar to *wt* MHCII/Ii complexes and adopt a *wt*-like traffic.

6.4. Conclusion, Perspectives & Contribution

Improving Ag uptake and peptide loading onto MHCII molecules is one of the challenges limiting the full potential of immunotherapy. One way to achieve this is by investigating MHCIIs chaperoning and processing. The peptide occupancy state leading to the high kinetic stability of MHCIIs is a factor limiting the success of peptide-based vaccines. Interestingly, both Ii and HLA-DM induce MHCII conformational changes and so studying those changes could provide valuable clues as to how to trigger peptide loading, a necessary step in designing peptide-peptide based vaccines. Also, superantigens offer a great tool to monitor those subtle conformation alterations in addition to increase the potency of pMHCIIs.

It was recently proposed that Ii trimers could only bind a single MHCII heterodimer and that this interaction would lock the Ii scaffold, preventing binding of additional MHCIIs (Koch et al., 2011). This report contradicts seminal work in which nonameric complexes were observed (Roche et al., 1991b). As a co-author with Cloutier, M. (Annex I), I recently confirmed that Ii can bind multiple MHCIIs at once, but that different stoichiometry exists. Furthermore, the number of MHCIIs that bind Ii trimer increases with time in the ER, as a result of the Ii p35 isoform ER-retention motif. As of now, it is still unclear how Ii is able to stabilize MHCIIs other than from its association to the peptide-binding groove. Indeed, the field is plagued by the lack of a crystal structure portraying MHCIIs bound to Ii. After many attempts, the Wiley group has demonstrated that upon binding to MHCIIs, the structure of Ii becomes only partially ordered and crystallization assays have failed (Jasanoff et al., 1999b). In light of our results showing that the occupancy state of Ii trimers with different numbers of MHCIIs varies, it is possible that heterogeneity of Ii-MHCII complexes suppressed crystallization.

To counter Ii's disordered state and coerce formation of nonameric complexes, I have engineered an array of single chain dimer (SCD) fusions between the luminal domains of Ii and either MHCII chain, which will likely restrict the flexibility of Ii. Those straightforward constructs are possible because DR and Ii are type I and type II proteins, respectively, allowing fusion of the C-terminus of DR chains to the N-terminus of Ii.

Further structural studies of those SCDs will determine the Ii binding site on MHCIIs and provide insights as to the peptide loading mechanism and how certain MHCII allotypes fail to efficiently pair with Ii. Painters et al. demonstrated that the MHCII α chain region connecting the α1 to the α2 domain undergo a conformation change upon peptide binding (Painter et al., 2011). Analogously, DM interaction with DO induces conformation changes at this region (Personal communication). Besides, a report by Neumann et al. suggests that Ii binds MHCII at the same interface as DM (Neumann and Koch, 2006). Thus, it is conceivable that both Ii and DM alter MHCII conformation similarly. Because both Ii and DM are required for vSAG presentation in HeLa cells, one must wonder if such effect on the MHCII structure is sensed by this family of SAG. The recent DO-DM and DR-DM co-crystal provides grounding information to undertake rational-designed site-directed mutagenesis in order to verify whether Ii or vSAG also bind similar regions and if Ii and DM stabilize empty MHCIIs by targeting the α1-α2 connecting region using a similar mechanism.

Altogether, I aimed to understand the interrelation between Ii, DM, DO and the MHCII heterodimers. My results should provide grounding on the peptide exchange mechanism, proposed to occur synergistically with MHCII conformation transitions and to the impact of the bound-peptide at a structure-function level. To date, only a small segment of Ii, the CLIP region, has been crystallized in association with MHCIIs. Ii fragments extending outside the peptide-binding groove

were disordered on the solved CLIP-MHCII structures. Interestingly, the N-terminal end of the Ii extending outside the peptide-binding groove triggers peptide self-release and is used to enhance the efficacy of peptide-based vaccines (Xu et al., 2012). Of note, two vaccines relying on this characteristic of Ii are currently in phase I clinical trials against breast and prostate cancer. Knowing how this extension is detrimental to both SEB and vSAG presentation one must wonder how it affects MHCIIs. Further studying the structures of the SCDs could provide a model as to how this region of Ii, also referred to as Ii-key, enhances peptide immunotherapy and how vSAGs bind DRα. Finally, one may argue that using crystallography is paradoxical in evaluating protein dynamism. However, amassing a wealth of MHCII structures, especially those in interaction with chaperones, provides different snapshots along the course leading to peptide exchange.

Bibliography

Acha-orbea, H. (1995). Superantigens of mouse mamary tumor virus. Annu.Rev.Immunol. 13, 459-486.

Acha-Orbea, H., and MacDonald, H.R. (1995). Superantigens of mouse mammary tumor virus. Annual Reviews of Immunology *13*, 459–486.

Acha-Orbea, H., and Palmer, E. (1991). Mls-a retrovirus exploits the immune system. Immunology Today *12*, 356–361.

Acha-Orbea, H., Shakhov, A.N., Scarpellino, L., Kolb, E., Muller, V., Vessaz-Shaw, A., Fuchs, R., Blochlinger, K., Rollini, P., Billotte, J., et al. (1991). Clonal deletion of Vβ14-bearing T cells in mice transgenic for mammary tumour virus. Nature *350*, 207–211.

Acha-Orbea, H., Held, W., Waanders, G. a, Shakhov, a N., Scarpellino, L., Lees, R.K., and MacDonald, H.R. (1993a). Exogenous and endogenous mouse mammary tumor virus superantigens. Immunological Reviews *131*, 5–25.

Acha-Orbea, H., Held, W., Waanders, G.A., Shakhov, A.N., Scarpellino, L., Lees, R.K., and MacDonald, H.R. (1993b). Exogenous and endogenous mouse mammary tumor virus superantigens. Immunological Reviews *131*, 5–25.

Acha-Orbea, H., Shakhov, A.N., and Finke, D. (2007). Immune response to MMTV infection. Frontiers in Bioscience : a Journal and Virtual Library *12*, 1594–1609.

Adams, J.J.J., Narayanan, S., Liu, B., Birnbaum, M.E.E., Kruse, A.C.C., Bowerman, N.A. a, Chen, W., Levin, A.M.M., Connolly, J.M.M., Zhu, C., et al. (2011). T cell receptor signaling is limited by docking geometry to peptide-major histocompatibility complex. Immunity *35*, 681–693.

Alfonso, C., and Karlsson, L. (2000). Nonclassical MHC class II molecules. Annual Review of Immunology *18*, 113–142.

Alfonso, C., Liljedahl, M., Winqvist, O., Surh, C.D., Peterson, P.A., Fung-Leung, W.P., and Karlsson, L. (1999). The role of H2-O and HLA-DO in major histocompatibility complex class II-restricted antigen processing and presentation. Immunological Reviews *172*, 255–266.

Alfonso, C., Williams, G.S., Han, J.O., Westberg, J.A., Winqvist, O., and Karlsson, L. (2003a). Analysis of H2-O influence on antigen presentation by B cells. Journal of Immunology *171*, 2331–2337.

Alfonso, C., Williams, G.S., and Karlsson, L. (2003b). H2-O influence on antigen presentation in H2-E-expressing mice. European Journal of Immunology *33*, 2014–2021.

Amin, J., and Weiss, D.S. (1993). GABAA receptor needs two homologous domains of the beta-subunit for activation by GABA but not by pentobarbital. Nature *366*, 565–569.

Anders, A.-K., Call, M.J., Schulze, M.-S.E.D., Fowler, K.D., Schubert, D. a, Seth, N.P., Sundberg, E.J., and Wucherpfennig, K.W. (2011). HLA-DM captures partially empty HLA-DR molecules for catalyzed removal of peptide. Nature Immunology *12*, 54–61.

Andersen, P.S., Lavoie, P.M., Sékaly, R.P., Churchill, H., Kranz, D.M., Schlievert, P.M., Karjalainen, K., and Mariuzza, R. a (1999). Role of the T cell receptor alpha chain in stabilizing TCR-superantigen-MHC class II complexes. Immunity *10*, 473–483.

Apostolopoulos, V., Lazoura, E., and Yu, M. (2008). MHC and MHC-Like Molecules: Structural Perspectives on the Design of Molecular Vaccines. Springer Science. Chapter 19, 252-267

Arad, G., Levy, R., Nasie, I., Hillman, D., Rotfogel, Z., Barash, U., Supper, E., Shpilka, T., Minis, A., and Kaempfer, R. (2011). Binding of superantigen toxins into the CD28 homodimer interface is essential for induction of cytokine genes that mediate lethal shock. PLoS Biology *9*, e1001149.

Arimilli, S., Astafieva, I., Mukku, P. V, Cardoso, C., Deshpande, S., and Nag, B. (1999). Peptide binding inhibits aggregation of soluble MHC class II in solution. IUBMB Life *48*, 483–491.

Arunachalam, B., Lamb, C.A., and Cresswell, P. (1994). Transport properties of free and MHC class II associated oligomers containing different isoforms of human invariant chain. International Immunology *6*, 439–451.

Aude-Garcia, C., Attinger, a, Housset, D., MacDonald, H.R., Acha-Orbea, H., Marche, P.N., and Jouvin-Marche, E. (2000). Pairing of Vbeta6 with certain Valpha2 family members prevents T cell deletion by Mtv-7 superantigen. Molecular Immunology *37*, 1005–1012.

Avery, A.C., Markowitz, J.S., Grusby, M.J., Glimcher, L.H., and Cantor, H. (1994). Activation of T cells by superantigen in class II-negative mice. Journal of Immunology *153*, 4853–4861.

Azar, G.A., and Thibodeau, J. (2002). Human endogenous retrovirus IDDMK(1,2)22 and mouse mammary tumor virus superantigens differ in their ability to stimulate murine T cell hybridomas. Immunol. Lett. *81*, 87–91.

Azar, G.A., Sekaly, R.P., and Thibodeau, J. (2005b). A defective viral superantigen-presenting phenotype in HLA-DR transfectants is corrected by CIITA. Journal of Immunology *174*, 7548–7557.

Bakke, O., and Dobberstein, B. (1990). MHC class II-associated invariant chain contains a sorting signal for endosomal compartments. Cell *63*, 707–716.

Bankovich, A.J., Girvin, A.T., Moesta, A.K., and Garcia, K.C. (2004). Peptide register shifting within the MHC groove: theory becomes reality. Molecular Immunology *40*, 1033–1039.

Basha, G., Omilusik, K., Chavez-Steenbock, A., Reinicke, A.T., Lack, N., Choi, K.B., and Jefferies, W. a (2012). A CD74-dependent MHC class I endolysosomal cross-presentation pathway. Nature Immunology *13*, 237–245.

Batista, F.D., and Harwood, N.E. (2009). The who, how and where of antigen presentation to B cells. Nature Reviews. Immunology *9*, 15–27.

Belmares, M.P., Busch, R., Wucherpfennig, K.W., McConnell, H.M., and Mellins, E.D. (2002). Structural factors contributing to DM susceptibility of MHC class II/peptide complexes. Journal of Immunology *169*, 5109–5117.

Bentley, G.A., Boulot, G., Karjalainen, K., and Mariuzza, R.A. (1995). Crystal structure of the á chain of a T cell antigen receptor. Science *267*, 1984–1987.

Bernhagen, J., Krohn, R., Lue, H., Gregory, J.L., Zernecke, A., Koenen, R.R., Dewor, M., Georgiev, I., Schober, A., Leng, L., et al. (2007). MIF is a noncognate ligand of CXC chemokine receptors in inflammatory and atherogenic cell recruitment. Nat. Med. *13*, 587–596.

Beswick, E.J. (2009). CD74 in antigen presentation, inflammation, and cancers of the gastrointestinal tract. World Journal of Gastroenterology *15*, 2855.

Beswick, E.J., Bland, D.A., Suarez, G., Barrera, C.A., Fan, X., and Reyes, V.E. (2005). Helicobacter pylori Binds to CD74 on Gastric Epithelial Cells and Stimulates Interleukin-8 Production. Infection and immunity. *73*, 2736–2743.

Biasi, G., Panozzo, M., Pertile, P., Mezzalira, S., and Facchinetti, A. (1994). Mechanism underlying superantigen-induced clonal deletion of mature T lymphocytes. International Immunology *6*, 983–989.

Blackman, M.A., Gerhard-Burgert, H., Woodland, D.L., Palmer, E., Kappler, J.W., and Marrack, P. (1990). A role for clonal inactivation in T cell tolerance to Mls-1a. Nature *345*, 540–542.

Blackman, M.A., Lund, F.E., Surman, S., Corley, R.B., and Woodland, D.L. (1992). Major histocompatibility complex-restricted recognition of retroviral superantigens by V beta 17+ T cells. The Journal of Experimental Medicine *176*, 275–280.

Boder, E.T., and Wittrup, K.D. (2000). Yeast surface display for directed evolution of protein expression, affinity, and stability. Methods in Enzymology *328*, 430–444.

Boniface, J.J.A.Y.B., Eich, Z.I.V.R., Yons, D.A.S.L., and Avis, M.A.R.K.M.D. (1999). Thermodynamics of T cell receptor binding to peptide – MHC : Immunology *96*, 11446–11451.

Bridgeman, J.S., Sewell, A.K., Miles, J.J., Price, D. a, and Cole, D.K. (2012). Structural and biophysical determinants of αβ T-cell antigen recognition. Immunology *135*, 9–18.

Brocke, P., Garbi, N., Momburg, F., and Hammerling, G.J. (2002). HLA-DM, HLA-DO and tapasin: functional similarities and differences. Current Opinion in Immunology *14*, 22–29.

Brouillard, J.-N.P., Günther, S., Varma, A.K., Gryski, I., Herfst, C. a, Rahman, a K.M.N., Leung, D.Y.M., Schlievert, P.M., Madrenas, J., Sundberg, E.J., et al. (2007). Crystal structure of the streptococcal superantigen SpeI and functional role of a novel loop domain in T cell activation by group V superantigens. Journal of Molecular Biology *367*, 925–934.

Bueno, C., Lemke, C.D., Criado, G., Baroja, M.L., Ferguson, S.S.G., Rahman, a K.M.N.-U., Tsoukas, C.D., McCormick, J.K., and Madrenas, J. (2006). Bacterial superantigens bypass Lck-dependent T cell receptor signaling by activating a Galpha11-dependent, PLC-beta-mediated pathway. Immunity *25*, 67–78.

Bueno, C., Criado, G., McCormick, J., and Madrenas, J. (2007). T cell signalling induced by bacterial superantigens. Chem Immunol Allergy *93*, 161–180.

Busch, R., Rinderknecht, C.H., Roh, S., Lee, A.W., Harding, J.J., Burster, T., Hornell, T.M., and Mellins, E.D. (2005). Achieving stability through editing and chaperoning: regulation of MHC class II peptide binding and expression. Immunological Reviews *207*, 242–260.

Call, M.J., Xing, X., Cuny, G.D., Seth, N.P., Altmann, D.M., Fugger, L., Krogsgaard, M., Stein, R.L., and Wucherpfennig, K.W. (2009). In vivo enhancement of peptide display by MHC class II molecules with small molecule catalysts of peptide exchange. Journal of Immunology *182*, 6342–6352.

Candéias, S., Waltzinger, C., Benoist, C., Mathis, D., Cand,as, S., and Candeias, S. (1991a). The V beta 17+ T cell repertoire: skewed J beta usage after thymic selection; dissimilar CDR3s in CD4+ versus CD8+ cells. Journal of Experimental Medicine *174*, 989–1000.

Candéias, S., Waltzinger, C., Benoist, C., and Mathis, D. (1991b). The V beta 17+ T cell repertoire: skewed J beta usage after thymic selection; dissimilar CDR3s in CD4+ versus CD8+ cells. The Journal of Experimental Medicine *174*, 989–1000.

Carrasco, Y.R., and Batista, F.D. (2006). B cell recognition of membrane-bound antigen: an exquisite way of sensing ligands. Current Opinion in Immunology *18*, 286–291.

Carson, R.T., Vignali, K.M., Woodland, D.L., and Vignali, D.A.A. (1997). T cell receptor recognition of MHC class II-bound peptide flanking residues enhances immunogenicity and results in altered TCR V region usage. Immunity *7*, 387–399.

Cazenave, P. a, Marche, P.N., Jouvin-Marche, E., Voegtlé, D., Bonhomme, F., Bandeira, A., Coutinho, a, Voegtle, D., Voegtl,, D., and Bandeira, D. (1990). V beta 17 gene polymorphism in wild-derived mouse strains: two amino acid substitutions in the V beta 17 region greatly alter T cell receptor specificity. Cell *63*, 717–728.

Chervonsky, A. V, Medzhitov, R.M., Denzin, L.K., Barlow, a K., Rudensky, A.Y., Janeway Jr., C.A., and Janeway, C. a (1998). Subtle conformational changes induced in major histocompatibility complex class II molecules by binding peptides. Proc.Natl.Acad.Sci.U.S.A *95*, 10094–10099.

Chies, J.A., Marodon, G., Joret, A.M., Regnault, A., Lembezat, M.P., Rocha, B., and Freitas, A.A. (1995). Persistence of Vβ 6 + T cells in Mls-1 a mice. A role for the third complementarity-

determining region (CDR3) of the T cell receptor beta chain in superantigen recognition. Journal of Immunology *155*, 4171–4178.

Choi, Y., Kappler, J.W., and Marrack, P. (1991). A superantigen encoded in the open reading frame of the 3' long terminal repeat of mouse mammary tumour virus. Nature *350*, 203–207.

Chou, C.L., and Sadegh-Nasseri, S. (2000). HLA-DM recognizes the flexible conformation of major histocompatibility complex class II. Journal of Experimental Medicine *192*, 1697–1706.

Chou, C.L., Mirshahidi, S., Su, K.W., Kim, A., Narayan, K., Khoruzhenko, S., Xu, M., and Sadegh-Nasseri, S. (2008). Short peptide sequences mimic HLA-DM functions. Molecular Immunology *45*, 1935–1943.

Ciurli, C., Posnett, D.N., Sekaly, R.P., and Denis, F. (1998). Highly biased CDR3 usage in restricted sets of beta chain variable regions during viral superantigen 9 response. Journal of Experimental Medicine *187*, 253–258.

Cole, D.K., Pumphrey, N.J., Boulter, J.M., Sami, M., Bell, J.I., Gostick, E., Price, D. a, Gao, G.F., Sewell, A.K., and Jakobsen, B.K. (2007). Human TCR-binding affinity is governed by MHC class restriction. Journal of Immunology*178*, 5727–5734.

Colf, L. a, Bankovich, A.J., Hanick, N. a, Bowerman, N. a, Jones, L.L., Kranz, D.M., and Garcia, K.C. (2007). How a single T cell receptor recognizes both self and foreign MHC. Cell *129*, 135–146.

Collins, E.J., and Riddle, D.S. (2008). TCR-MHC docking orientation: natural selection, or thymic selection? Immunologic Research *41*, 267–294.

Cresswell, P., and Blum, J.S. (1988). Intracellular Transport of Class II HLA Antigens. In Processing And Presentation of Antigens, (New York: Academic Press, Inc.), pp. 43–51.

Crooks, G.E., Hon, G., Chandonia, J., and Brenner, S.E. (2004). WebLogo : A Sequence Logo Generator. 1188–1190.

Cuendet, M. a, Zoete, V., and Michielin, O. (2011). How T cell receptors interact with peptide-MHCs: a multiple steered molecular dynamics study. Proteins *79*, 3007–3024.

Dai, S., Huseby, E.S., Rubtsova, K., Scott-Browne, J., Crawford, F., Macdonald, W. a, Marrack, P., and Kappler, J.W. (2008). Crossreactive T Cells spotlight the germline rules for alphabeta T cell-receptor interactions with MHC molecules. Immunity *28*, 324–334.

Danchin, E., Vitiello, V., Vienne, A., Richard, O., Gouret, P., McDermott, M.F., and Pontarotti, P. (2004). The major histocompatibility complex origin. Immunological Reviews *198*, 216–232.

Davis, M.M. (1990). T cell receptor gene diversity and selection. Annual Reviews of Biochemistry *59*, 475–496.

Davis, M.M., and Bjorkman, P.J. (1988). T cell antigen receptor genes and T cell recognition. Nature *334*, 395–402.

Davis, S.J., and Van der Merwe, P. a (1996). The structure and ligand interactions of CD2: implications for T-cell function. Immunology Today *17*, 177–187.

Delamarre, L., Holcombe, H., and Mellman, I. (2003). Presentation of exogenous antigens on major histocompatibility complex (MHC) class I and MHC class II molecules is differentially regulated during dendritic cell maturation. Journal of Experimental Medicine *198*, 111–122.

Delcourt, B.M., Thibodeau, J., and Denis, F. (1997a). Paracrine transefrt of mouse mammary tumor Virus Superantigen. Journal of Experimental Medicine *185*.

Delcourt, M., Thibodeau, J., Denis, F., and Sekaly, R.P. (1997b). Paracrine transfer of mouse mammary tumor virus superantigen. Journal of Experimental Medicine *185*, 471–480.

Deng, L., Langley, R.J., Wang, Q., Topalian, S.L., and Mariuzza, R.A. (2012). Structural insights into the editing of germ-line–encoded interactions between T-cell receptor and MHC class II by Vα CDR3. Proc.Natl.Acad.Sci.USA. *190*, 14960–14965.

Denzin, L.K., and Cresswell, P. (1995). HLA-DM induces CLIP dissociation from MHC class II $\alpha\beta$ dimers and facilitates peptide loading. Cell *82*, 155–165.

Denzin, L.K., Robbins, N.F., Carboy-Newcomb, C., and Cresswell, P. (1994a). Assembly and intracellular transport of HLA-DM and correction of the class II antigen-processing defect in T2 cells. Immunity *1*, 595–606.

Denzin, L.K., Robbins, N.F., Carboy-Newcomb, C., and Cresswell, P. (1994b). Assembly and intracellular transport of HLA-DM and correction of the class II antigen-processing defect in T2 cells. Immunity. *1*, 595–606.

Denzin, L.K., Hammond, C., and Cresswell, P. (1996). HLA-DM interactions with intermediates in HLA-DR maturation and a role for HLA-DM in stabilizing empty HLA-DR molecules. Journal of Experimental Medicine *184*, 2153–2165.

Depoil, D., Fleire, S., Treanor, B.L., Weber, M., Harwood, N.E., Marchbank, K.L., Tybulewicz, V.L.J., and Batista, F.D. (2008). CD19 is essential for B cell activation by promoting B cell receptor-antigen microcluster formation in response to membrane-bound ligand. Nature Immunology *9*, 63–72.

Deshaies, F., Brunet, A., Diallo, D.A., Denzin, L.K., Samaan, A., and Thibodeau, J. (2005). A point mutation in the groove of HLA-DO allows egress from the endoplasmic reticulum independent of HLA-DM. Proc.Natl.Acad.Sci.U.S.A *102*, 6443–6448.

Ding, Y.H., Smith, K.J., Garboczi, D.N., Utz, U., Biddison, W.E., and Wiley, D.C. (1998). Two human T cell receptors bind in a similar diagonal mode to the HLA- A2/Tax peptide complex using different TCR amino acids. Immunity *8*, 403–411.

Doebele, R.C., Busch, R., Scott, H.M., Pashine, A., and Mellins, E.D. (2000). Determination of the HLA-DM interaction site on HLA-DR molecules. Immunity. *13*, 517–527.

Dohlsten, M., Abrahms, N., L., Björk, P., Lando, P.A., Hedlund, G., Forsberg, G., Brodin, T., Gascoigne, N.R.J., Förberg, C., Lind, P., et al. (1994). Monoclonal antibody-superantigen fusion proteins: Tumor-specific agents for T-cell-based tumor therapy. Proceedings of the National Academy of Sciences of the United States of America *91*, 8945–8949.

Dong, G., Wearsch, P. a, Peaper, D.R., Cresswell, P., and Reinisch, K.M. (2009). Insights into MHC class I peptide loading from the structure of the tapasin-ERp57 thiol oxidoreductase heterodimer. Immunity *30*, 21–32.

Esteban, O., and Zhao, H. (2004). Directed evolution of soluble single-chain human class II MHC molecules. Journal of Molecular Biology *340*, 81–95.

Feng, D., Bond, C.J., Ely, L.K., Maynard, J., and Garcia, K.C. (2007). Structural evidence for a germline-encoded T cell receptor-major histocompatibility complex interaction “codon”. Nature Immunology *8*, 975–983.

Festenstein, H. (1973). Immunogenetic and biological aspects of in vitro lymphocyte allotransformation (MLR) in the mouse. Transplant. Rev. *15*, 62–88.

Fields, B.A., Malchiodi, E.L., Li, H.M., Ysern, X., Stauffacher, C. V, Schlievert, P.M., Karjalainen, K., and Mariuzza, R.A. (1996). Crystal structure of a T-cell receptor beta-chain complexed with a superantigen. Nature *384*, 188–192.

Fikri, Y., Pastoret, P.-P., and Nyabenda, J. (2002). Costimulatory molecule requirement for bovine WC1+gammadelta T cells’ proliferative response to bacterial superantigens. Scandinavian Journal of Immunology *55*, 373–381.

Ford, D., and Burger, D. (1983). Precursor frequency of antigen-specific T cells: effects of sensitization in vivo and in vitro. Cell Immunol *79*, 334–344.

Fraser, J.D., and Proft, T. (2008). The bacterial superantigen and superantigen-like proteins. Immunological Reviews *225*, 226–243.

Fremont, D.H., Hendrickson, W. a, Marrack, P., and Kappler, J. (1996). Structures of an MHC class II molecule with covalently bound single peptides. Science *272*, 1001–1004.

Fremont, D.H., Monnaie, D., Nelson, C.A., Hendrickson, W.A., and Unanue, E.R. (1998). Crystal structure of I-Ak in complex with a dominant epitope of lysozyme. Immunity. *8*, 305–317.

Fu, X.T., and Karr, R.W. (1994). HLA-DR alpha chain residues located on the outer loops are involved in nonpolymorphic and polymorphic antibody-binding epitopes. Human Immunogy. *39*, 253–260.

Gagnon, S.J., Borbulevych, O.Y., Davis-Harrison, R.L., Baxter, T.K., Clemens, J.R., Armstrong, K.M., Turner, R. V, Damirjian, M., Biddison, W.E., and Baker, B.M. (2005). Unraveling a hotspot for TCR recognition on HLA-A2: evidence against the existence of peptide-independent TCR binding determinants. Journal of Molecular Biology *353*, 556–573.

Gaboczi, D.N., Ghosh, P., Utz, U., Fan, Q.R., Biddison, W.E., and Wiley, D.C. (1996). Structure of the complex between human T-cell receptor, viral peptide and HLA-A2. Nature *384*, 134–141.

Garcia, K.C. (1998). Structural Basis of Plasticity in T Cell Receptor Recognition of a Self Peptide-MHC Antigen. Science *279*, 1166–1172.

Garcia, K.C. (2012). Reconciling views on T cell receptor germline bias for MHC. Trends in Immunology *33*, 429–436.

Garcia, K.C., and Adams, E.J. (2005). How the T cell receptor sees antigen--a structural view. Cell *122*, 333–336.

Garcia, K.C., Degano, M., Stanfield, R.L., Brunmark, A., Jackson, M.R., Peterson, P.A., Teyton, L., and Wilson, I.A. (1996). An àá T cell receptor structure at 2.5 A and its orientation in the TCR-MHC complex. Science *274*, 209–219.

Garcia, K.C., Adams, J.J., Feng, D., and Ely, L.K. (2009). The molecular basis of TCR germline bias for MHC is surprisingly simple. Nature Immunology *10*, 143–147.

Gascoigne, N.R.J. (2011). T cell receptor structures: three for the price of one. Immunity *35*, 1–3.

Gedde-Dahl, M., Freisewinkel, I., Staschewski, M., Schenck, K., Koch, N., and Bakke, O. (1997). Exon 6 is essential for invariant chain trimerization and induction of large endosomal structures. J.Biol.Chem. *272*, 8281–8287.

Geissmann, F., Manz, M.G., Jung, S., Sieweke, M.H., Merad, M., and Ley, K. (2010). Development of monocytes, macrophages, and dendritic cells. Science*327*, 656–661.

Genot, E., and Cantrell, D. a (2000). Ras regulation and function in lymphocytes. Current Opinion in Immunology *12*, 289–294.

Ghosh, P., Amaya, M., Mellins, E., and Wiley, D.C. (1995). The structure of an intermediate in class II MHC maturation: CLIP bound to HLA-DR3. Nature *378*, 457–462.

Gil, D., Schamel, W.W. a, Montoya, M., Sánchez-Madrid, F., and Alarcón, B. (2002). Recruitment of Nck by CD3 epsilon reveals a ligand-induced conformational change essential for T cell receptor signaling and synapse formation. Cell *109*, 901–912.

Gillogly, M.E., Kallinteris, N.L., Xu, M., Gulfo, J. V, Humphreys, R.E., and Murray, J.L. (2004). Ii-Key/HER-2/ neu MHC class-II antigenic epitope vaccine peptide for breast cancer. Cancer Immunol.Immunother. 53(6), 490-496

Golovkina, T., Agafonova, Y., Kazansky, D., and Chervonsky, a (2001). Diverse repertoire of the MHC class II-peptide complexes is required for presentation of viral superantigens. Journal of Immunology (Baltimore, Md. : 1950) *166*, 2244–2250.

Golovkina, T. V, Chervonsky, A., Dudley, J.P., and Ross, S.R. (1992). Transgenic mouse mammary tumor virus superantigen expression prevents viral infection. Cell *69*, 637–645.

Gorga, J.C., Knudsen, P.J., Foran, J.A., Strominger, J.L., and Burakoff, S.J. (1986). Immunochemically purified DR antigens in liposomes stimulate xenogeneic cytolytic T cells in secondary in vitro cultures. Cell Immunol. *103*, 160–173.

Graham, F.L., and Van der Eb, A.J. (1973). A new technique for the assay of infectivity of human adenovirus 5 DNA. Virology *52*, 456–467.

Gras, S., Chen, Z., Miles, J.J., Liu, Y.C., Bell, M.J., Sullivan, L.C., Kjer-Nielsen, L., Brennan, R.M., Burrows, J.M., Neller, M. a, et al. (2010). Allelic polymorphism in the T cell receptor and its impact on immune responses. The Journal of Experimental Medicine *207*, 1555–1567.

Grigg, M.E., McMahon, C.W., Morkowski, S., Rudensky, a Y., and Pullen, a M. (1998a). Mtv-1 superantigen trafficks independently of major histocompatibility complex class II directly to the B-cell surface by the exocytic pathway. Journal of Virology *72*, 2577–2588.

Grigg, M.E., McMahon, C.W., Morkowski, S., Rudensky, A.Y., and Pullen, A.M. (1998b). Mtv-1 superantigen trafficks independently of major histocompatibility complex class II directly to the B-cell surface by the exocytic pathway. J. Virol. *72*, 2577–2588.

Grubin, C.E., Kovats, S., DeRoos, P., and Rudensky, A.Y. (1997). Deficient positive selection of CD4 T cells in mice displaying altered repertoires of MHC class II-bound self-peptides. Immunity. *7*, 197–208.

Gu, Y., Jensen, P.E., and Chen, X. (2012). Immunodeficiency and Autoimmunity in H2-O-Deficient Mice. Journal of Immunology. 190. 1-12.

Guce, A.I., Mortimer, S.E., Yoon, T., Painter, C. a, Jiang, W., Mellins, E.D., and Stern, L.J. (2013). HLA-DO acts as a substrate mimic to inhibit HLA-DM by a competitive mechanism. Nature Structural & Molecular Biology. 20, 90-98.

Günther, S., Varma, A.K., Moza, B., Kasper, K.J., Wyatt, A.W., Zhu, P., Rahman, a K.M.N., Li, Y., Mariuzza, R. a, McCormick, J.K., et al. (2007). A novel loop domain in superantigens extends their T cell receptor recognition site. Journal of Molecular Biology *371*, 210–221.

Günther, S., Schlundt, A., Sticht, J., Roske, Y., Heinemann, U., Wiesmüller, K.-H., Jung, G., Falk, K., Rötzschke, O., and Freund, C. (2010). Bidirectional binding of invariant chain peptides to an MHC class II molecule. Proceedings of the National Academy of Sciences of the United States of America *107*, 22219–22224.

Hahn, M., Nicholson, M.J., Pyrdol, J., and Wucherpfennig, K.W. (2005). Unconventional topology of self peptide-major histocompatibility complex binding by a human autoimmune T cell receptor. Nature Immunology *6*, 490–496.

Van Ham, S.M., Tjin, E.P.M., Lillemeier, B.F., Gruneberg, U., Van Meijgaarden, K.E., Pastoors, L., Verwoerd, D., Tulp, A., Canas, B., Rahman, D., et al. (1997). HLA-DO is a negative modulator of HLA-DM-mediated MHC class II peptide loading. Curr Biol *7*, 950–957.

Hammond, C., Denzin, L.K., Pan, M., Griffith, J.M., Geuze, H.J., and Cresswell, P. (1998). The tetraspan protein CD82 is a resident of MHC class II compartments where it associates with HLA-DR, -DM, and -DO molecules. Journal of Immunology *161*, 3282–3291.

Han, C., Gong, Z., Hao, L., Yang, J., Hu, J., Dong, B., Fan, T., Tang, W., and Teng, G. (2011). Mechanism of monoclonal antibody-coupled Staphylococcus superantigen-A induced apoptosis in human bladder cancer cells. Cell Biochemistry and Biophysics *61*, 679–684.

Hansen, T.H., and Fremont, D.H. (2005). Recognition of open conformers of classical MHC by chaperones and monoclonal antibodies. *207*, 100–111.

Hennecke, J., Carfi, a, and Wiley, D.C. (2000). Structure of a covalently stabilized complex of a human alphabeta T-cell receptor, influenza HA peptide and MHC class II molecule, HLA-DR1. The EMBO Journal *19*, 5611–5624.

Herman, A., Croteau, G., Sekaly, R.P., Kappler, J., and Marrack, P. (1990). HLA-DR alleles differ in their ability to present staphylococcal enterotoxins to T cells. Journal of Experimental Medicine *172*, 709–717.

Herman, A., Kappler, J.W., Marrack, P., and Pullen, A.M. (1991). SUPERANTIGENS: mechanism of T-cell stimulation and role in immune responses. Annual Reviews of Immunology *9*, 745–772.

Hewitt, C.R.A., Lamb, J.R., Hayball, J., Hill, M., Owen, M.J., and O'Hehir, R.E. (1992). Major histocompatibility complex independent clonal T cell anergy by direct interaction of Staphylococcus aureus enterotoxin B with the T cell antigen receptor. Journal of Experimental Medicine *175*, 1493–1499.

Hogan, R.J., VanBeek, J., Broussard, D.R., Surman, S.L., and Woodland, D.L. (2001). Identification of MHC class II-associated peptides that promote the presentation of toxic shock syndrome toxin-1 to T cells. Journal of Immunology *166*, 6514–6522.

Hsu, P.N., Wolf Bryant, P., Sutkowski, N., McLellan, B., Ploegh, H.L., and Huber, B.T. (2001). Association of mouse mammary tumor virus superantigen with MHC class II during biosynthesis. Journal of Immunology *166*, 3309–3314.

Huang, N.-N., Han, S.-B., Hwang, I.-Y., and Kehrl, J.H. (2005). B cells productively engage soluble antigen-pulsed dendritic cells: visualization of live-cell dynamics of B cell-dendritic cell interactions. Journal of Immunology *175*, 7125–7134.

Humphreys, R.E., Adams, S., Koldzic, G., Nedelescu, B., Von Hofe, E., and Xu, M. (2000). Increasing the potency of MHC class II-presented epitopes by linkage to Ii-Key peptide. Vaccine *18*, 2693–2697.

Husson, J., Chemin, K., Bohineust, A., Hivroz, C., and Henry, N. (2011). Force generation upon T cell receptor engagement. PloS One *6*, e19680.

Ignatowicz, L., Winslow, G., Bill, J., Kappler, J., and Marrack, P. (1995). Cell surface expression of class II MHC proteins bound by a single peptide. Journal of Immunology *154*, 3852–3862.

Indik, S., Günzburg, W.H., Salmons, B., and Rouault, F. (2005). Mouse mammary tumor virus infects human cells. Cancer Research *65*, 6651–6659.

Jabbari, A., and Harty, J.T. (2006). The generation and modulation of antigen-specific memory CD8 T cell responses.

Jardetzky, T.S., Stern, L.J., Brown, J.H., Gorga, J.C., Urban, R.G., Strominger, J.L., Wiley, D.C., Chi, Y.I., and Stauffacher, C. (1994). Three-dimensional structure of a human class II histocompatibility molecule complexed with superantigen. Nature *368*, 711–718.

Jasanoff, A., Song, S., Dinner, A.R., Wagner, G., and Wiley, D.C. (1999a). One of two unstructured domains of Ii becomes ordered in complexes with MHC class II molecules. Immunity. *10*, 761–768.

Jasanoff, A., Song, S., Dinner, A.R., Wagner, G., and Wiley, D.C. (1999b). One of Two Unstructured Domains of Ii Becomes Ordered in Complexes with MHC Class II Molecules. *10*, 761–768.

Jensen, P.E. (2007). Recent advances in antigen processing and presentation. Nature Immunology *8*, 1041–1048.

Jensen, P.E., Weber, D.A., Thayer, W.P., Westerman, L.E., and Dao, C.T. (1999). Peptide exchange in MHC molecules. Immunological Reviews *172*, 229–238.

Jerne, N.K. (1971). The somatic generation of immune recognition. European Journal of Immunology *34*, 1234–1242.

Joffre, O., Nolte, M. a, Spörri, R., and Reis e Sousa, C. (2009). Inflammatory signals in dendritic cell activation and the induction of adaptive immunity. Immunological Reviews *227*, 234–247.

Jones, E.Y., Fugger, L., Strominger, J.L., and Siebold, C. (2006). MHC class II proteins and disease: a structural perspective. Nat.Rev.Immunol. *6*, 271–282.

Joshi, D., and Buehring, G.C. (2012). Are viruses associated with human breast cancer? Scrutinizing the molecular evidence. Breast Cancer Research and Treatment *135*, 1–15.

Kallies, A. (2008). Distinct regulation of effector and memory T-cell differentiation. Immunology and Cell Biology *86*, 325–332.

Kallinteris, N.L., Lu, X., Blackwell, C.E., Von Hofe, E., Humphreys, R.E., and Xu, M. (2006). Ii-Key/MHC class II epitope hybrids: a strategy that enhances MHC class II epitope loading to create more potent peptide vaccines. Expert Opinion on Biological Therapy *6*, 1311–1321.

Kane, M., Case, L.K., Kopaskie, K., Kozlova, A., MacDearmid, C., Chervonsky, A. V, and Golovkina, T. V (2011). Successful transmission of a retrovirus depends on the commensal microbiota. Science (New York, N.Y.) *334*, 245–249.

Kang, J., Chambers, C.A., Pawling, J., and Scott, C. (1994). Conserved amino acid residues in the CDR1 of the TCR b-chain are involved in the recognition of conventional Ag and Mls-1 superantigen. Journal of Immunology *152*, 5305–5317.

Kappler, J.W., Staerz, U., White, J., and Marrack, P.C. (1988). Self-tolerance eliminates T cells specific for Mls-modified products of the major histocompatibility complex. Nature *332*, 35–40.

Kappler, J.W., Herman, A., Clements, J., and Marrack, P. (1992). Mutations Defining Functional Regions of the Superantigen Staphylococcal Enterotoxin B. Journal of Experimental Medicine *175*, 387–396.

Karlsson, L., Surh, C.D., Sprent, J., and Peterson, P.A. (1991). A novel class II MHC molecule with unusual tissue distribution. Nature *351*, 485–488.

Kelley, L. a, and Sternberg, M.J.E. (2009). Protein structure prediction on the Web: a case study using the Phyre server. Nature Protocols *4*, 363–371.

Khalil, H., Brunet, A., Saba, I., Terra, R., Sekaly, R.P., and Thibodeau, J. (2003). The MHC class II beta chain cytoplasmic tail overcomes the invariant chain p35-encoded endoplasmic reticulum retention signal. International Immunology *15*, 1249–1263.

Khalil, H., Brunet, A., and Thibodeau, J. (2005). A three-amino-acid-long HLA-DRbeta cytoplasmic tail is sufficient to overcome ER retention of invariant-chain p35. J.Cell Sci. *118*, 4679–4687.

Kilgannon, P., Novak, Z., Fotedar, A., and Singh, B. (2010). Junctional diversity prevents negative selection of an antigen-specific T cell repertoire. Molecular Immunology *47*, 1154–1160.

Kim, J., Urban, R.G., Strominger, J.L., and Wiley, D.C. (1994). Toxic shock syndrome toxin-1 complexed with a class II major histocompatibility molecule HLA-DR1. Science *266*, 1870–1874.

Kim, S.T., Takeuchi, K., Sun, Z.-Y.J., Touma, M., Castro, C.E., Fahmy, A., Lang, M.J., Wagner, G., and Reinherz, E.L. (2009). The alphabeta T cell receptor is an anisotropic mechanosensor. The Journal of Biological Chemistry *284*, 31028–31037.

Koch, N., Mclellan, a, and Neumann, J. (2007). A revised model for invariant chain-mediated assembly of MHC class II peptide receptors. Trends in Biochemical Sciences *32*, 532–537.

Koch, N., Zacharias, M., Ko, A., Temme, S., Neumann, J., and Springer, S. (2011). Stoichiometry of HLA Class II-Invariant Chain Oligomers. Plos ONE. 6, e17257

Korman, A.J., Bourgarel, P., Meo, T., and Rieckhof, G.E. (1992). The mouse mammary tumour virus long terminal repeat encodes a type II transmembrane glycoprotein. EMBO Journal *11*, 1901–1905.

Kozono, H., White, J., Clements, J., Marrack, P., and Kappler, J.W. (1994). Production of soluble MHC class II proteins with covalently bound single peptides. Nature *369*, 151–154.

Krakauer, T., Qun, B., and Young, H.A. (2001). The Flavonoid baicalin inhibits superantigen-induced in inflammatory cytokines and chemokines. FEBS Letters *500*, 52–55.

Kremer, A.N., Van der Meijden, E.D., Honders, M.W., Goeman, J.J., Wiertz, E.J.H.J., Falkenburg, J.H.F., and Griffioen, M. (2012). Endogenous HLA-class-II epitopes that are immunogenic in vivo show distinct behavior towards HLA-DM and its natural inhibitor HLA-DO. Blood. 120, 3246-3255

Kropshofer, H., Vogt, A.B., Stern, L.J., and Hammerling, G.J. (1995a). Self-release of CLIP in peptide loading of HLA-DR molecules. Science *270*, 1357–1359.

Kropshofer, H., Vogt, A.B., Hammerling, G.J., and Kropshofer, T. (1995b). Structural features of the invariant chain fragment CLIP controlling rapid release from HLA-DR molecules and inhibition of peptide binding. PNAS *92*, 8313–8317.

Kropshofer, H., Vogt, A.B., Moldenhauer, G., Hammer, J., Blum, J.S., and Hammerling, G.J. (1996). Editing of the HLA-DR-peptide repertoire by HLA-DM. EMBO Journal *15*, 6144–6154.

Kropshofer, H., Arndt, S.O., Moldenhauer, G., Hammerling, G.J., and Vogt, A.B. (1997a). HLA-DM acts as a molecular chaperone and rescues empty HLA-DR molecules at lysosomal pH. Immunity *6*, 293–302.

Kropshofer, H., Hammerling, G.J., and Vogt, A.B. (1997b). How HLA-DM edits the MHC class II peptide repertoire: Survival of the fittest? Immunology Today *18*, 77–82.

Kropshofer, H., Vogt, A.B., Thery, C., Armandola, E.A., Li, B.C., Moldenhauer, G., Amigorena, S., and Hammerling, G.J. (1998). A role for HLA-DO as a co-chaperone of HLA-DM in peptide loading of MHC class II molecules. EMBO Journal *17*, 2971–2981.

Kropshofer, H., Hammerling, G.J., and Vogt, A.B. (1999). The impact of the non-classical MHC proteins HLA-DM and HLA-DO on loading of MHC class II molecules. Immunological Reviews *172*, 267–278.

Krummel, M.F., Sullivan, T.J., and Allison, J.P. (1996). Superantigen responses and co-stimulation: CD28 and CTLA-4 have opposing effects on T cell expansion in vitro and in vivo. International Immunology *8*, 519–523.

Krummenacher, C., and Diggelmann, H. (1993). The mouse mammary tumor virus long terminal repeat encodes a 47 kDa glycoprotein with a short half-life in mammalian cells. Mol Immunol *30*, 1151–1157.

Labrecque, N., Mcgrath, H., Subramanyam, M., Huber, B.T., and Sékaly, R.P. (1993a). Human T Cells Respond to Mouse Mammary Tumor Virus-encoded Superantigen: Vbeta Restriction and Conserved Evolutionary Features. Biotechnology *177*, 1735–1743.

Labrecque, N., Thibodeau, J., and Sekaly, R.P. (1993b). Interactions between staphylococcal superantigens and MHC class II molecules. Seminars in Immunology *5*, 23–32.

Van Laethem, F., Sarafova, S.D., Park, J.-H., Tai, X., Pobezinsky, L., Guinter, T.I., Adoro, S., Adams, A., Sharrow, S.O., Feigenbaum, L., et al. (2007). Deletion of CD4 and CD8 coreceptors permits generation of alphabetaT cells that recognize antigens independently of the MHC. Immunity *27*, 735–750.

Lavoie, P.M., Thibodeau, J., Cloutier, I., Busch, R., and Sekaly, R.P. (1997). Selective binding of bacterial toxins to major histocompatibility complex class II-expressing cells is controlled by invariant chain and HLA-DM. PNAS *94*, 6892–6897.

Lazarski, C. a, Chaves, F. a, Jenks, S. a, Wu, S., Richards, K. a, Weaver, J.M., and Sant, A.J. (2005). The kinetic stability of MHC class II:peptide complexes is a key parameter that dictates immunodominance. Immunity *23*, 29–40.

Lee, C., and McConnell, H.M. (1995). A general model of invariant chain association with class II major histocompatibility complex proteins. PNAS *92*, 8269–8273.

Leng, L., Metz, C.N., Fang, Y., Xu, J., Donnelly, S., Baugh, J., Delohery, T., Chen, Y., Mitchell, R.A., and Bucala, R. (2003). MIF signal transduction initiated by binding to CD74. Journal of Experimental Medicine *197*, 1467–1476.

Li, H., Llera, A., and Mariuzza, R.A. (1998a). Structure-function studies of T-cell receptor-superantigen interactions. Immunological Reviews *164*, 177–186.

Li, H., Llera, a, Tsuchiya, D., Leder, L., Ysern, X., Schlievert, P.M., Karjalainen, K., and Mariuzza, R. a (1998b). Three-dimensional structure of the complex between a T cell receptor beta chain and the superantigen staphylococcal enterotoxin B. Immunity *9*, 807–816.

Li, H., Llera, A., Malchiodi, E.L., and Mariuzza, R.A. (1999). The structural basis of T cell activation by superantigens. Annual Reviews of Immunology *17*, 435–466.

Li, Y., Li, H., Dimasi, N., McCormick, J.K., Martin, R., Schuck, P., Schlievert, P.M., and Mariuzza, R.A. (2001). Crystal structure of a superantigen bound to the high-affinity, zinc-dependent site on MHC class II. Immunity. *14*, 93–104.

Li, Y.-C., Chen, B.-M., Wu, P.-C., Cheng, T.-L., Kao, L.-S., Tao, M.-H., Lieber, A., and Roffler, S.R. (2010). Cutting Edge: mechanical forces acting on T cells immobilized via the TCR complex can trigger TCR signaling. Journal of Immunology *184*, 5959–5963.

Liljedahl, M., Kuwana, T., Fung-Leung, W.P., Jackson, M., Peterson, P.A., and Karlsson, L. (1996). HLA-DO is a lysosomal resident which requires association with HLA-DM for efficient intracellular transport. EMBO Journal *15*, 4817–4824.

Liljedahl, M., Winqvist, O., Surh, C.D., Wong, P., Ngo, K., Teyton, L., Peterson, P.A., Brunmark, A., Rudensky, A.Y., Fung-Leung, W.P., et al. (1998). Altered antigen presentation in mice lacking H2-O. Immunity *8*, 233–243.

Lith, M. Van, Ham, M. Van, Griekspoor, A., Tjin, E., Verwoerd, D., Calafat, J., Janssen, H., Reits, E., Pastoors, L., and Neefjes, J. (2001). Regulation of MHC Class II Antigen Presentation by Sorting of Recycling HLA-DM/DO and Class II within the Multivesicular Body. Journal of Immunology. 167, 884-892.

Van Lith, M., van, H.M., and Neefjes, J. (2003). Stable expression of MHC class I heavy chain/HLA-DO complexes at the plasma membrane. European Journal of Immunology *33*, 1145–1151.

Loh, M.S. (2006). Superantigens as Vaccine Delivery Vehicles for the Generation of Cellular Immune Responses. Molecular Medicine and Pathology, University of Auckland. Thesis.

MacDonald, H.R., Glasebrook, A.L., Schneider, R., Lees, R.K., Pircher, H., Pedrazzini, T., Kanagawa, O., Nicolas, J.F., Howe, R.C., Zinkernagel, R.M., et al. (1989). T-cell reactivity and tolerance to Mls a- encoded antigens. Immunological Reviews *107*, 89–108.

MacNeil, D., Fraga, E., and Singh, B. (1992). Inhibition of superantigen recognition by peptides of the variable region of the T cell receptor á chain. European Journal of Immunology *22*, 937–941.

Madden, D.R. (1995). The three-dimensional structure of peptide-MHC complexes. Annual Reviews of Immunology *13*, 587–622.

De Magistris, M.T., Alexander, J., Coggeshall, M., Altman, a, Gaeta, F.C., Grey, H.M., and Sette, a (1992). Antigen analog-major histocompatibility complexes act as antagonists of the T cell receptor. Cell *68*, 625–634.

Mahana, W., Al-Daccak, R., Leveille, C., Valet, J.P., Hebert, J., Ouellette, M., and Mourad, W. (1995). A natural mutation of the amino acid residue at position 60 destroys staphylococcal enterotoxin A murine T-cell mitogenicity. Infection & Immunity *63*, 2826–2832.

Mantovani, B., Rabinovich, M., and Nussenzweig, V. (1972). Phagocytosis of immune complexes by macrophages. Journal of Experimental Medicine *135*. 780-792.

Manz, B.N., Jackson, B.L., Petit, R.S., Dustin, M.L., and Groves, J. (2011). T-cell triggering thresholds are modulated by the number of antigen within individual T-cell receptor clusters. PNAS *108*, 9089–9094.

Marks, M.S., Blum, J.S., and Cresswell, P. (1990). Invariant chain trimers are sequestered in the rough endoplasmic reticulum in the absence of association with HLA class II antigens. Journal of Cell Biology *111*, 839–855.

Marrack, P., and Kappler, J. (1990). The staphylococcal enterotoxins and their relatives. Science *248*, 1066.

Marrack, P., Winslow, G.M., Choi, Y., Scherer, M., Pullen, A., White, J., and Kappler, J.W. (1993). The bacterial and mouse mammary tumor virus superantigens; two different families of proteins with the same functions. Immunological Reviews *131*, 79–92.

Marrack, P., Scott-Browne, J.P., Dai, S., Gapin, L., and Kappler, J.W. (2008a). Evolutionarily conserved amino acids that control TCR-MHC interaction. Annual Review of Immunology *26*, 171–203.

Marrack, P., Rubtsova, K., Scott-Browne, J., and Kappler, J.W. (2008b). T cell receptor specificity for major histocompatibility complex proteins. Current Opinion in Immunology *20*, 203–207.

Matza, D., Wolstein, O., Dikstein, R., and Shachar, I. (2001). Invariant chain induces B cell maturation by activating a TAF(II)105-NF-kappaB-dependent transcription program. J.Biol.Chem. *276*, 27203–27206.

Matza, D., Lantner, F., Bogoch, Y., Flaishon, L., Hershkoviz, R., and Shachar, I. (2002). Invariant chain induces B cell maturation in a process that is independent of its chaperonic activity. Proc.Natl.Acad.Sci.U.S.A *99*, 3018–3023.

Matza, D., Kerem, A., and Shachar, I. (2003). Invariant chain, a chain of command. Trends Immunol. *24*, 264–268.

McKeithan, T.W. (1995). Kinetic proofreading in T-cell receptor signal transduction. PNAS *92*, 5042–5046.

McMahon, C.W., Bogatzki, L.Y., and Pullen, A.M. (1997). Mouse mammary tumor virus superantigens require N-linked glycosylation for effective presentation to T cells. Virology *228*, 161–170.

Mehindate, K., Thibodeau, J., Dohlsten, M., Kalland, T., Sekaly, R.P., and Mourad, W. (1995). Cross-linking of major histocompatibility complex class II molecules by staphylococcal enterotoxin A superantigen is a requirement for inflammatory cytokine gene expression. Journal of Experimental Medicine *182*, 1573–1577.

Mellins, E., Smith, L., Arp, B., Cotner, T., Celis, E., and Pious, D. (1990). Defective processing and presentation of exogenous antigens in mutants with normal HLA class II genes. Nature *343*, 71–74.

Van der Merwe, P.A., and Dushek, O. (2011). Mechanisms for T cell receptor triggering. Nature Reviews. Immunology *11*, 47–55.

Miller, P.J., Pazy, Y., Conti, B., Riddle, D., Appella, E., and Collins, E.J. (2007). Single MHC mutation eliminates enthalpy associated with T cell receptor binding. Journal of Molecular Biology *373*, 315–327.

Minguet, S., and Schamel, W.W. a (2008). Permissive geometry model. Advances in Experimental Medicine and Biology *640*, 113–120.

Mitaksov, V., Truscott, S.M., Lybarger, L., Connolly, J.M., Hansen, T.H., and Fremont, D.H. (2007). Structural engineering of pMHC reagents for T cell vaccines and diagnostics. Chem.Biol. *14*, 909–922.

Miyazaki, T., Wolf, P., Tourne, S., Waltzinger, C., Dierich, A., Barois, N., Ploegh, H., Benoist, C., and Mathis, D. (1996). Mice lacking H2-M complexes, enigmatic elements of the MHC class II peptide-loading pathway. Cell *84*, 531–541.

Mohan, J.F., Petzold, S.J., and Unanue, E.R. (2011). Register shifting of an insulin peptide-MHC complex allows diabetogenic T cells to escape thymic deletion. The Journal of Experimental Medicine *208*, 2375–2383.

Morris, G.P., and Allen, P.M. (2012). How the TCR balances sensitivity and specificity for the recognition of self and pathogens. Nature Immunology *13*, 121–128.

Mosyak, L., Zaller, D.M., and Wiley, D.C. (1998). The structure of HLA-DM, the peptide exchange catalyst that loads antigen onto class II MHC molecules during antigen presentation. Immunity *9*, 377–383.

Mottershead, D.G., Hsu, P.N., Urban, R.G., Strominger, J.L., and Huber, B.T. (1995). Direct binding of the Mtv7 superantigen (Mls-1) to soluble MHC class II molecules. Immunity. *2*, 149–154.

Moza, B., Varma, A.K., Buonpane, R. a, Zhu, P., Herfst, C. a, Nicholson, M.J., Wilbuer, A.-K., Seth, N.P., Wucherpfennig, K.W., McCormick, J.K., et al. (2007). Structural basis of T-cell specificity and activation by the bacterial superantigen TSST-1. The EMBO Journal *26*, 1187–1197.

Mundiñano, J., Berguer, P.M., Cabrera, G., Lorenzo, D., Nepomnaschy, I., and Piazzon, I. (2010). Superantigens Increase the Survival of Mice Bearing T Cell Lymphomas by Inducing Apoptosis of Neoplastic Cells. PLoS ONE *5*, e15694.

Narayan, K., Chou, C.L., Kim, A., Hartman, I.Z., Dalai, S., Khoruzhenko, S., and Sadegh-Nasseri, S. (2007). HLA-DM targets the hydrogen bond between the histidine at position beta81 and peptide to dissociate HLA-DR-peptide complexes. Nat.Immunol. *8*, 92–100.

Natarajan, S.K., Stern, L.J., and Sadegh-Nasseri, S. (1999a). Sodium dodecyl sulfate stability of HLA-DR1 complexes correlates with burial of hydrophobic residues in pocket 1. Journal of Immunology *162*, 3463–3470.

Natarajan, S.K., Stern, L.J., and Sadegh-Nasseri, S. (1999b). Sodium dodecyl sulfate stability of HLA-DR1 complexes correlates with burial of hydrophobic residues in pocket 1. Journal of Immunology *162*, 3463–3470.

Neefjes, J., Jongsma, M.L.M., Paul, P., and Bakke, O. (2011). Towards a systems understanding of MHC class I and MHC class II antigen presentation. Nature Reviews. Immunology *11*, 823–836.

Neumann, J., and Koch, N. (2006). A novel domain on HLA-DRbeta chain regulates the chaperone role of the invariant chain. Journal of Cell Science *119*, 4207–4214.

Nguyen, P., Woodland, D.L., and Blackman, M.A. (1996). MHC bias of Mls-1 recognition is not influenced by thymic positive selection. Cellular Immunology *167*, 224–229.

Nur-ur Rahman, A.K.M., Bonsor, D.A., Herfst, C.A., Pollard, F., Peirce, M., Wyatt, A.W., Kasper, K.J., Madrenas, J., Sundberg, E.J., and McCormick, J.K. (2011). The T cell receptor beta-chain second complementarity determining region loop (CDR2beta governs T cell activation and Vbeta specificity by bacterial superantigens. The Journal of Biological Chemistry *286*, 4871–4881.

O'Rourke, A.M., Mescher, M.F., and Webb, S.R. (1990). Activation of polyphosphoinositide hydrolysis in T cells by H-2 alloantigen but not MLS determinants. Science *249*, 171–174.

O'Shea, J.J., and Paul, W.E. (2010). Mechanisms underlying lineage commitment and plasticity of helper CD4+ T cells. Science *327*, 1098–1102.

Painter, C. a, Cruz, A., López, G.E., Stern, L.J., and Zavala-Ruiz, Z. (2008). Model for the peptide-free conformation of class II MHC proteins. PloS One *3*, e2403.

Painter, C. a, Negroni, M.P., Kellersberger, K. a, Zavala-Ruiz, Z., Evans, J.E., and Stern, L.J. (2011). Conformational lability in the class II MHC 310 helix and adjacent extended strand dictate HLA-DM susceptibility and peptide exchange. PNAS *108*, 19329–19334.

Panter, M.S., Jain, A., Leonhardt, R.M., Ha, T., and Cresswell, P. (2012). Dynamics of major histocompatibility complex class I association with the human peptide-loading complex. The Journal of Biological Chemistry *287*, 31172–31184.

Park, C.G., Jung, M.Y., Choi, Y., and Winslow, G.M. (1995). Proteolytic processing is required for viral superantigen activity. Journal of Experimental Medicine *181*, 1899–1904.

Pashine, A., Busch, R., Belmares, M.P., Munning, J.N., Doebele, R.C., Buckingham, M., Nolan, G.P., and Mellins, E.D. (2003). Interaction of HLA-DR with an acidic face of HLA-DM disrupts sequence-dependent interactions with peptides. Immunity. *19*, 183–192.

Peaper, D.R., and Cresswell, P. (2008). Regulation of MHC class I assembly and peptide binding. Annual Review of Cell and Developmental Biology *24*, 343–368.

Pellicci, D.G., Patel, O., Kjer-Nielsen, L., Pang, S.S., Sullivan, L.C., Kyparissoudis, K., Brooks, A.G., Reid, H.H., Gras, S., Lucet, I.S., et al. (2009). Differential recognition of CD1d-alpha-galactosyl ceramide by the V beta 8.2 and V beta 7 semi-invariant NKT T cell receptors. Immunity *31*, 47–59.

Penninger, J.M., Schilham, M.W., Timms, E., Wallace, V.A., and Mak, T.W. (1995). T cell repertoire and clonal deletion of Mtv superantigen- reactive T cells in mice lacking CD4 and CD8 molecules. European Journal of Immunology *25*, 2115–2118.

Perez, S. a, Von Hofe, E., Kallinteris, N.L., Gritzapis, A.D., Peoples, G.E., Papamichail, M., and Baxevanis, C.N. (2010a). A new era in anticancer peptide vaccines. Cancer *116*, 2071–2080.

Perez, S. a, Kallinteris, N.L., Bisias, S., Tzonis, P.K., Georgakopoulou, K., Varla-Leftherioti, M., Papamichail, M., Thanos, A., Von Hofe, E., and Baxevanis, C.N. (2010b). Results from a phase I clinical study of the novel Ii-Key/HER-2/neu(776-790) hybrid peptide vaccine in patients with prostate cancer. Clinical Cancer Research : an Official Journal of the American Association for Cancer Research *16*, 3495–3506.

Perraudeau, M., Taylor, P.R., Stauss, H.J., Lindstedt, R., Bygrave, A.E., Pappin, D.J., Ellmerich, S., Whitten, A., Rahman, D., Canas, B., et al. (2000). Altered major histocompatibility complex class II peptide loading in H2- O-deficient mice. European Journal of Immunology *30*, 2871–2880.

Petersson, K., Thunnissen, M., Forsberg, G., and Walse, B. (2002). Crystal structure of a SEA variant in complex with MHC class II reveals the ability of SEA to crosslink MHC molecules. Structure *10*, 1619–1626.

Petersson, K., Pettersson, H., Skartved, N.J., Walse, B., and Forsberg, G. (2003). Staphylococcal enterotoxin H induces V alpha-specific expansion of T cells. Journal of Immunology *170*, 4148–4154.

Pezeshki, A.M., Côté, M.-H., Azar, G. a, Routy, J.-P., Boulassel, M.-R., and Thibodeau, J. (2011). Forced expression of HLA-DM at the surface of dendritic cells increases loading of synthetic peptides on MHC class II molecules and modulates T cell responses. Journal of Immunology *187*, 74–81.

Pierre, P., Shachar, I., Matza, D., Gatti, E., Flavell, R.A., and Mellman, I. (2000). Invariant chain controls H2-M proteolysis in mouse splenocytes and dendritic cells. Journal of Experimental Medicine *191*, 1057–1062.

Pircher, H., Mak, T.W., Lang, R., Balhausen, W., Ruedi, E., Hengartner, H., Zinkernagel, R.M., and Burki, K. (1989). T cell tolerance to Mlsa encoded antigens in T cell receptor Vbeta 8.1 chain transgenic mice. EMBO Journal *8*, 719–727.

Platt, C.D., Ma, J.K., Chalouni, C., Ebersold, M., Bou-Reslan, H., Carano, R. a D., Mellman, I., and Delamarre, L. (2010). Mature dendritic cells use endocytic receptors to capture and present antigens. PNAS *107*, 4287–4292.

Pos, W., Sethi, D.K., Call, M.J., Schulze, M.-S.E.D., Anders, A.-K., Pyrdol, J., and Wucherpfennig, K.W. (2012). Crystal Structure of the HLA-DM–HLA-DR1 Complex Defines Mechanisms for Rapid Peptide Selection. Cell *151*, 1557–1568.

Proft, T., and Fraser, J. (1998). Superantigens: Just like peptides only different. Journal of Experimental Medicine *187*, 819–821.

Pullen, a M., and Bogatzki, L.Y. (1996). Receptors on T cells escaping superantigen-mediated deletion lack special beta-chain junctional region structural characteristics. Journal of Immunology *156*, 1865–1872.

Pullen, A.M., Wade, T., Marrack, P., and Kappler, J.W. (1990). Identification of the region of T cell receptor β chain that interacts with the self-superantigen Mls-1 a. Cell *61*, 1365–1374.

Pullen, A.M., Marrack, P., and Kappler, J.W. (1991a). Analysis of the Interaction Site for the Self Superantigen Mls-la on T Cell Receptor Vbeta. Journal of Experimental Medicine. 173, 1183-1192

Pullen, A.M., Bill, J., Kubo, R.T., Marrack, P., and Kappler, J.W. (1991b). Analysis of the Interaction Site for the self superantigen Mls-1a on T cell receptor Vbeta. Journal of Experimental Medicine *173*, 1183–1192.

Purbhoo, M. a, Irvine, D.J., Huppa, J.B., and Davis, M.M. (2004). T cell killing does not require the formation of a stable mature immunological synapse. Nature Immunology *5*, 524–530.

Radka, S.F., Machamer, C.E., and Cresswell, P. (1984). Analysis of monoclonal antibodies reactive with human class II beta chains by two-dimensional electrophoresis and western blotting. Human Immunogy *10*, 177–188.

Riberdy, J.M., Newcomb, J.R., Surman, M.J., Barbosa, J.A., and Cresswell, P. (1992). HLA-DR molecules from an antigen-processing mutnat cell line are associated with invariant chain peptides. Nature *360*, 474–477.

Rinderknecht, C.H., Belmares, M.P., Catanzarite, T.L.W., Bankovich, A.J., Holmes, T.H., Garcia, K.C., Nanda, N.K., Busch, R., Kovats, S., and Mellins, E.D. (2007). Posttranslational regulation of I-Ed by affinity for CLIP. Journal of Immunology *179*, 5907–5915.

Rinderknecht, C.H., Lu, N., Crespo, O., Truong, P., Hou, T., Wang, N., Rajasekaran, N., and Mellins, E.D. (2010). I-Ag7 is subject to post-translational chaperoning by CLIP. International Immunology *22*, 705–716.

Roche, P.A., Marks, M.S., and Cresswell, P. (1991a). Formation of a nine-subunit complex by HLA class II glycoproteins and the invariant chain. Nature *354*, 392–394.

Roche, P.A., Marks, M.S., and Cresswell, P. (1991b). Formation of a nine-subunit complex by HLA class II glycoproteins and the invariant chain. Nature *354*, 392–394.

Rötzschke, O., Falk, K., Mack, J., Lau, J.M., Jung, G., and Strominger, J.L. (1999). Conformational variants of class II MHC/peptide complexes induced by N- and C-terminal extensions of minimal peptide epitopes. PNAS *96*, 7445–7450.

Rubtsova, K., Scott-Browne, J.P., Crawford, F., Dai, S., Marrack, P., and Kappler, J.W. (2009). Many different Vbeta CDR3s can reveal the inherent MHC reactivity of germline-encoded TCR V regions. PNAS *106*, 7951–7956.

Rudensky, A.Y., Preston-Hurlburt, P., Hong, S.C., Barlow, A., Janeway Jr., C.A., and Janeway Jr., C.A. (1991). Sequence analysis of peptides bound to MHC class II molecules. Nature *353*, 622–627.

Rudensky, A.Y., Maric, M., Eastman, S., Shoemaker, L., DeRoos, P.C., and Blum, J.S. (1994). Intracellular assembly and transport of endogenous peptide-MHC class II complexes. Immunity *1*, 585–594.

Rudolph, M.G., Stanfield, R.L., and Wilson, I. a (2006). How TCRs bind MHCs, peptides, and coreceptors. Annual Review of Immunology *24*, 419–466.

Ruffet, E., Blicher, T., Ferre, H., Sylvester-hvid, C., Nielsen, L.L.B., Hobley, T.J., Thomas, O.R.T., and Buus, S. (2003). Purification of correctly oxidized MHC class I heavy-chain molecules under denaturing conditions : A novel strategy exploiting disulfide assisted protein folding. 551–559.

Sadegh-Nasseri, S., and Germain, R.N. (1992). How MHC class II molecules work: peptide-dependant completion of protein folding. Immunology Today *13*, 43–46.

Sadegh-Nasseri, S., Chen, M., Narayan, K., and Bouvier, M. (2008). The convergent roles of tapasin and HLA-DM in antigen presentation. Trends Immunol.

Sadegh-Nasseri, S., Chou, C.-L., Hartman, I.Z., Kim, A., and Narayan, K. (2012). How HLA-DM moldecules work: recognition of MHCII conformational heterogeneity. Front Biosci. *128*, NP.

Saline, M., Rödström, K.E.J., Fischer, G., Orekhov, V.Y., Karlsson, B.G., and Lindkvist-Petersson, K. (2010). The structure of superantigen complexed with TCR and MHC reveals novel insights into superantigenic T cell activation. Nature Communications *1*, 1–9.

Savage, P.A., Boniface, J.J., and Davis, M.M. (1999). A kinetic basis for T cell receptor repertoire selection during an immune response. Immunity *10*, 485–492.

Scherer, M.T., Ignatowicz, L., Winslow, G.M., Kappler, J.W., and Marrack, P. (1993). SUPERANTIGENS: Bacterial and Viral protein that manipulate the Immune System. Annu.Rev.Cell.Biol. *9*, 101–128.

Schlundt, A., Günther, S., Sticht, J., Wieczorek, M., Roske, Y., Heinemann, U., and Freund, C. (2012). Peptide Linkage to the α-Subunit of MHCII Creates a Stably Inverted Antigen Presentation Complex. Journal of Molecular Biology. 423, 294-302.

Schulze, M.-S.E.D., and Wucherpfennig, K.W. (2012). The mechanism of HLA-DM induced peptide exchange in the MHC class II antigen presentation pathway. Current Opinion in Immunology *24*, 105–111.

Schutze, M.P., Peterson, P.A., and Jackson, M.R. (1994). An N-terminal double-arginine motif maintains type II membrane proteins in the endoplasmic reticulum. EMBO Journal *13*, 1696–1705.

Scott-Browne, J.P., Crawford, F., Young, M.H., Kappler, J.W., Marrack, P., and Gapin, L. (2011). Evolutionarily Conserved Features Contribute to αβ T Cell Receptor Specificity. Immunity *35*, 526–535.

Serradell, L., Muntasell, A., Catalfamo, M., Marti, M., Costa, M., De Preval, C., and Jaraquemada, D. (1999). HLA-DM can partially replace the invariant chain for HLA-DR transport and surface expression in transfected endocrine epithelial cells. Tissue Antigens *53*, 447–458.

Sette, a, Ceman, S., Kubo, R.T., Sakaguchi, K., Appella, E., Hunt, D.F., Davis, T.A., Michel, H., Shabanowitz, J., Rudersdorf, R., et al. (1992). Invariant chain peptides in most HLA-DR molecules of an antigen- processing mutant. Science *258*, 1801–1804.

Sette, A., Southwood, S., Miller, J., and Appella, E. (1995). Binding of major histocompatibility complex class II to the invariant chain-derived peptide, CLIP, is regulated by allelic polymorphism in class II. Journal of Experimental Medicine *181*, 677–683.

Sherman, M.A., Weber, D.A., and Jensen, P.E. (1995). DM enhances peptide binding to class II MHC by release of invariant chain-derived peptide. Immunity *3*, 197–205.

Shi, X., Leng, L., Wang, T., Wang, W., Du, X., Li, J., McDonald, C., Chen, Z., Murphy, J.W., Lolis, E., et al. (2006). CD44 is the signaling component of the macrophage migration inhibitory factor-CD74 receptor complex. Immunity. *25*, 595–606.

Sim, B.C., Zerva, L., Greene, M.I., and Gascoigne, N.R.J. (1996). Control of MHC restriction by TCR Valpha CDR1 and CDR2. Science *273*, 963–966.

Sloan, V.S., Cameron, P., Porter, G., Gammon, M., Amaya, M., Mellins, E., and Zaller, D.M. (1995). Mediation by HLA-DM of dissociation of peptides from HLA- DR. Nature *375*, 802–806.

Sloma, I., Zilber, M.T., Vasselon, T., Setterblad, N., Cavallari, M., Mori, L., De, L.G., Charron, D., Mooney, N., and Gelin, C. (2008). Regulation of CD1a surface expression and antigen presentation by invariant chain and lipid rafts. Journal of Immunology *180*, 980–987.

Smith, H.P., Phuong, L., Woodland, D.L., and Blackman, M.A. (1992a). T cell receptor à-chain influences reactivity to Mls-1 in Vá8.1 transgenic mice. Journal of Immunology *149*, 887–896.

Smith, H.P., Le, P., Woodland, D.L., and Blackman, M.A. (1992b). T cell receptor alpha-chain influences reactivity to Mls-1 in Vbeta8.1 transgenic mice. Journal of Immunology *149*.

Smith-Garvin, J.E., Koretzky, G. a, and Jordan, M.S. (2009). T cell activation. Annual Review of Immunology *27*, 591–619.

Stadinski, B.D., Zhang, L., Crawford, F., Marrack, P., and Eisenbarth, G.S. (2010). Diabetogenic T cells recognize insulin bound to IA g7 in an unexpected , weakly binding register. PNAS. 107, 10978-10983

Stadinski, B.D., Trenh, P., Smith, R.L., Bautista, B., Huseby, P.G., Li, G., Stern, L.J., and Huseby, E.S. (2011). A role for differential variable gene pairing in creating T cell receptors specific for unique major histocompatibility ligands. Immunity *35*, 694–704.

Stanners, J., Kabouridis, P.S., McGuire, K.L., and Tsoukas, C.D. (1995). Interaction between G proteins and tyrosine kinases upon T cell receptor.CD3-mediated signaling. The Journal of Biological Chemistry *270*, 30635–30642.

Starwalt, S.E., Masteller, E.L., Bluestone, J. a., and Kranz, D.M. (2003). Directed evolution of a single-chain class II MHC product by yeast display. Protein Engineering Design and Selection *16*, 147–156.

Stern, L.J., and Wiley, D.C. (1992). The human class II MHC protein HLA-DR1 assembles as empty àá heterodimers in the absence of antigenic peptide. Cell *68*, 465–477.

Stow, N.W., Douglas, R., Tantilipikorn, P., and Lacroix, J.S. (2010). Superantigens. Otolaryngologic Clinics of North America *43*, 489–502, vii.

Stratikos, E., Wiley, D.C., and Stern, L.J. (2004). Enhanced catalytic action of HLA-DM on the exchange of peptides lacking backbone hydrogen bonds between their N-terminal region and the MHC class II alpha-chain. Journal of Immunology *172*, 1109–1117.

Stumptner-Cuvelette, P., Morchoisne, S., Dugast, M., Le Gall, S., Raposo, G., Schwartz, O., and Benaroch, P. (2001). HIV-1 Nef impairs MHC class II antigen presentation and surface expression. PNAS *98*, 12144–12149.

Subramanyam, M., McLellan, B., Labrecque, N., Sekaly, R.P., and Huber, B.T. (1993). Presentation of the Mls-1 superantigen by human HLA class II molecules to murine T cells. Journal of Immunology *151*, 2538–2545.

Sugita, M., and Brenner, M.B. (1995). Association of the invariant chain with major histocompatibility complex class I molecules directs trafficking to endocytic compartments. J.Biol.Chem. *270*, 1443–1448.

Sullivan, D.O., Arrhenius, T.O.M., Sidney, J., Guercio, M.D.E.L., Albertson, M., Wall, M., Oseroff, C., Southwood, S., Colon, S.M., Gaeta, F.C.A., et al. (1991). On the interaction of promiscuous antigenic peptides with different DR aleles. Journal of Immunology *147*. 2663-2669.

Sundberg, E., and Jardetzky, T.S. (1999). Structural basis for the HLA-DQ binding by the streptococcal superantigen SSA. Nature Structural Biology *6*, 123–129.

Sundberg, E.J., Li, H., Llera, A.S., McCormick, J.K., Tormo, J., Schlievert, P.M., Karjalainen, K., and Mariuzza, R. a (2002). Structures of two streptococcal superantigens bound to TCR beta chains reveal diversity in the architecture of T cell signaling complexes. Structure *10*, 687–699.

Sundberg, E.J., Deng, L., and Mariuzza, R.A. (2007). TCR recognition of peptide/MHC class II complexes and superantigens. Semin Immunol *19*, 262–271.

Suri, A., Lovitch, S.B., and Unanue, E.R. (2006). The wide diversity and complexity of peptides bound to class II MHC molecules. Current Opinion in Immunology *18*, 70–77.

Sutkowski, N., Conrad, B., Thorley-Lawson, D. a, and Huber, B.T. (2001). Epstein-Barr virus transactivates the human endogenous retrovirus HERV-K18 that encodes a superantigen. Immunity *15*, 579–589.

Thayer, W.P., Dao, C.T., Ignatowicz, L., and Jensen, P.E. (2003a). A novel single chain I-Ab molecule can stimulate and stain antigen-specific T cells. Molecular Immunology *39*, 861–870.

Thayer, W.P., Dao, C.T., Ignatowicz, L., and Jensen, P.E. (2003b). A novel single chain I-A(b) molecule can stimulate and stain antigen-specific T cells. Mol Immunol *39*, 861–870.

Thibodeau, J., and Sékaly, R.P. (1995). Bacterial superantigens: structure, function, and therapeutic potential (Distributor, Springer).

Thibodeau, J., Labrecque, N., Denis, F., Huber, B.T., and Sekaly, R.P. (1994). Binding sites for bacterial and endogenous retroviral superantigens can be dissociated on major histocompatibility complex class II molecules. Journal of Experimental Medicine *179*, 1029–1034.

Thibodeau, J., Dohlsten, M., Cloutier, I., Lavoie, P.M., Björk, P., Michel, F., Leveille, C., Mourad, W., Kalland, T., and Sekaly, R.P. (1997). Molecular characterization and role in T cell activation of staphylococcal enterotoxin A binding to the HLA-DRα chain. Journal of Immunology *158*, 3698–3704.

Tikhonova, A.N., Van Laethem, F., Hanada, K., Lu, J., Pobezinsky, L. a, Hong, C., Guinter, T.I., Jeurling, S.K., Bernhardt, G., Park, J.-H., et al. (2012). αβ T cell receptors that do not undergo major histocompatibility complex-specific thymic selection possess antibody-like recognition specificities. Immunity *36*, 79–91.

Tobita, T., Oda, M., Morii, H., Kuroda, M., Yoshino, A., Azuma, T., and Kozono, H. (2003). A role for the P1 anchor residue in the thermal stability of MHC class II molecule I-Ab. Immunology Letters *85*, 47–52.

Torres, B. a, and Johnson, H.M. (1998). Modulation of disease by superantigens. Current Opinion in Immunology *10*, 465–470.

Torres, B.A., Griggs, N.D., and Johnson, H.M. (1993). Bacterial and retroviral superantigens share a common binding region on class II MHC antigens Bacterial and retroviral superantigens share a common binding region on class II MHC antigens. Nature *364*, 152–154.

Tourne, S., Nakano, N., Viville, S., Benoist, C., and Mathis, D. (1995). The influence of invariant chain on the positive selection of single T cell receptor specificities. European Journal of Immunology *25*, 1851–1856.

Tourne, S., Miyazaki, T., Oxenius, A., Klein, L., Fehr, T., Kyewski, B., Benoist, C., and Mathis, D. (1997). Selection of a broad repertoire of CD4+ T cells in H-2Ma 0/0 mice. Immunity. *7*, 187–195.

Trombetta, E.S., and Mellman, I. (2005). Cell biology of antigen processing in vitro and in vivo. Annual Review of Immunology *23*, 975–1028.

Trowsdale, J. (2011). The MHC, disease and selection. Immunology Letters *137*, 1–8.

Tynan, F.E., Borg, N. a, Miles, J.J., Beddoe, T., El-Hassen, D., Silins, S.L., Van Zuylen, W.J.M., Purcell, A.W., Kjer-Nielsen, L., McCluskey, J., et al. (2005). High resolution structures of highly bulged viral epitopes bound to major histocompatibility complex class I. Implications for T-cell receptor engagement and T-cell immunodominance. The Journal of Biological Chemistry *280*, 23900–23909.

Vacchio, M.S., Kanagawa, O., Tomonari, K., and Hodes, R.J. (1992). Influence of T cell receptor Valpha expression on Mlsa superantigen- specific T cell responses. Journal of Experimental Medicine *175*, 1405–1408.

Valitutti, S., M ller, S., Cella, M., Padovan, E., and Lanzavecchia, A. (1995). Serial triggering of many T-cell receptors by a few peptide- MHC complexes. Nature *375*, 148–151.

Vallabhapurapu, S., and Karin, M. (2009). Regulation and function of NF-kappaB transcription factors in the immune system. Annual Review of Immunology *27*, 693–733.

Vella, a T., Mitchell, T., Groth, B., Linsley, P.S., Green, J.M., Thompson, C.B., Kappler, J.W., and Marrack, P. (1997). CD28 engagement and proinflammatory cytokines contribute to T cell expansion and long-term survival in vivo. Journal of Immunology *158*, 4714–4720.

Viville, S., Neefjes, J.J., Lotteau, V., Dierich, A., Lemeur, M., Ploegh, H., Benoist, C., and Mathis, D. (1993). Mice lacking the MHC class II-associated invariant chain. Cell *72*, 635–648.

Vogt, A.B., and Kropshofer, H. (1999). HLA-DM - an endosomal and lysosomal chaperone for the immune system. Trends in Biochemical Sciences *24*, 150–154.

Vogt, A.B., Stern, L.J., Amshoff, C., Dobberstein, B., Hammerling, G.J., and Kropshofer, H. (1995). Interference of distinct invariant chain regions with superantigen contact area and antigenic peptide binding groove of HLA-DR. Journal of Immunology *155*, 4757–4765.

Vogt, A.B., Kropshofer, H., Moldenhauer, G., and Hammerling, G.J. (1996). Kinetic analysis of peptide loading onto HLA-DR molecules mediated by HLA-DM. Proceedings of the National Academy of Sciences of the United States of America *93*, 9724–9729.

Wahl, C., Miethke, T., Heeg, K., and Wagner, H. (1993). Clonal deletion as direct consequence of an in vivo T cell response to bacterial superantigen. European Journal of Immunology *23*, 1197–1200.

Wang, J., and Reinherz, E.L. (2011). A new angle on TCR activation. Immunity *35*, 658–660.

Wang, F., Xu, Z., Ren, L., Tsang, S.Y., and Xue, H. (2008). GABA A receptor subtype selectivity underlying selective anxiolytic effect of baicalin. Neuropharmacology *55*, 1231–1237.

Wang, L., Zhao, Y., Li, Z., Guo, Y., Jones, L.L., Kranz, D.M., Mourad, W., and Li, H. (2007). Crystal structure of a complete ternary complex of TCR, superantigen and peptide-MHC. Nat Struct Mol Biol *14*, 169–171.

Wang, Y., Jiang, J.-D., Xu, D., Li, Y., Qu, C., Holland, J.F., and Pogo, B.G.-T. (2004). A mouse mammary tumor virus-like long terminal repeat superantigen in human breast cancer. Cancer Research *64*, 4105–4111.

Wearsch, P. a, and Cresswell, P. (2008). The quality control of MHC class I peptide loading. Current Opinion in Cell Biology *20*, 624–631.

Wearsch, P.A., Peaper, D.R., and Cresswell, P. (2011). Essential glycan-dependent interactions optimize MHC class I peptide loading. PNAS, 108, 4950-4955.

Wen, R., Cole, G.A., Surman, S., Blackman, M.A., and Woodland, D.L. (1996). Major histocompatibility complex class II-associated peptides control the presentation of bacterial superantigens to T cells. Journal of Experimental Medicine *183*, 1083–1092.

Wen, R., Broussard, D.R., Surman, S., Hogg, T.L., Blackman, M.A., and Woodland, D.L. (1997a). Carboxy-terminal residues of major histocompatibility complex class II-associated peptides control the presentation of the bacterial superantigen toxic shock syndrome toxin-1 to T cells. European Journal of Immunology *27*, 772–781.

Wen, R., Broussard, D.R., Surman, S., Hogg, T.L., Blackman, M. a, and Woodland, D.L. (1997b). Carboxy-terminal residues of major histocompatibility complex class II-associated peptides control the presentation of the bacterial superantigen toxic shock syndrome toxin-1 to T cells. European Journal of Immunology *27*, 772–781.

White, J., Herman, A., Pullen, A.M., Kubo, R.T., Kappler, J.W., and Marrack, P. (1989). The VBeta-specific superantigen staphylococcal enterotoxin B: stimulation of mature T cells and clonal deletion in neonatal mice. Cell *56*, 27–35.

Wilson, I., and Garcia, K.C. (1997). T-cell receptor structure and TCR complexes. Current Opinion in Structural Biology 26–30.

Wilson, N. a, Wolf, P., Ploegh, H., Ignatowicz, L., Kappler, J., and Marrack, P. (1998). Invariant chain can bind MHC class II at a site other than the peptide binding groove. Journal of Immunology *161*, 4777–4784.

Wilson, R.K., Lai, E., Concannon, P., Barth, R.K., and Hood, L.E. (1988). Structure, organization and polymorphism of murine and human T-cell receptor alpha and beta chain gene families. Immunological Reviews *101*, 149–172.

Winslow, G.M., Scherer, M.T., Kappler, J.W., and Marrack, P. (1992). Detection and biochemical characterization of the mouse mammary tumor virus 7 superantigen (Mls-1a). Cell *71*, 719.

Winslow, G.M., Marrack, P., and Kappler, J.W. (1994a). Processing and major histocompatibility complex binding of the MTV7 superantigen. Immunity *1*, 23–33.

Winslow, G.M., Marrack, P., and Kappler, J.W. (1994b). Processing and MHC binding of the MTV7 superantigen. Immunity *1*, 23–33.

Wirth, S., Vessaz, A., Krummenacher, C., Baribaud, F., Acha-Orbea, H., and Diggelmann, H. (2002). Regions of mouse mammary tumor virus superantigen involved in interaction with the major histocompatibility complex class II I-A molecule. J Virol *76*, 11172–11175.

Wong, P., and Rudensky, A.Y. (1996). Phenotype and function of CD4 + T cells in mice lacking invariant chain. Journal of Immunology *156*, 2133–2142.

Woodland, D.L. (2002). Immunity and retroviral superantigens in humans. Trends in Immunology *23*, 57–58.

Woodland, D.L., Pat Happ, M., Gollob, K.J., and Palmer, E. (1991). An endogenous retrovirus mediating deletion of αβ T cells? Nature *349*, 529–530.

Woodland, D.L., Smith, H.P., Surman, S., Le, P., Wen, R., and Blackman, M.A. (1993). Major histocompatibility complex-specific recognition of Mls-1 is mediated by multiple elements of the T cell receptor. Journal of Experimental Medicine *177*, 433–442.

Woodland, D.L., Wen, R., and Blackman, M.A. (1997). Why do superantigens care about peptides? Immunology Today *18*, 18–22.

Wraight, C.J., Van Endert, P., Moller, P., Lipp, J., Ling, N.R., MacLennan, I.C., Koch, N., and Moldenhauer, G. (1990). Human major histocompatibility complex class II invariant chain is expressed on the cell surface. J.Biol.Chem. *265*, 5787–5792.

Wucherpfennig, K.W., Liao, Y.J., Prendergast, M., Prendergast, J., Hafler, D.A., and Strominger, J.L. (1993). Human fetal liver gamma/delta T cells predominantly use unusual rearrangements of the T cell receptor delta and gamma loci expressed on both CD4+CD8- and CD4-CD8- gamma/delta T cells. Journal of Experimental Medicine *177*, 425–432.

Wucherpfennig, K.W., Call, M.J., Deng, L., and Mariuzza, R. (2009). Structural alterations in peptide-MHC recognition by self-reactive T cell receptors. Current Opinion in Immunology *21*, 590–595.

Wucherpfennig, K.W., Gagnon, E., Call, M.J., Huseby, E.S., and Call, M.E. (2010). Structural biology of the T-cell receptor: insights into receptor assembly, ligand recognition, and initiation of signaling. Cold Spring Harbor Perspectives in Biology *2*, a005140.

Xu, S.X., and McCormick, J.K. (2012). Staphylococcal superantigens in colonization and disease. Frontiers in Cellular and Infection Microbiology *2*, 52.

Xu, M., Kallinteris, N.L., and Von Hofe, E. (2012). CD4+ T-cell activation for immunotherapy of malignancies using Ii-Key/MHC class II epitope hybrid vaccines. Vaccine *30*, 2805–2810.

Yaneva, R., Springer, S., and Zacharias, M. (2009). Flexibility of the MHC class II peptide binding cleft in the bound, partially filled, and empty states: a molecular dynamics simulation study. Biopolymers *91*, 14–27.

Yi, W., Seth, N., and Martillotti, T. (2010). Targeted regulation of self-peptide presentation prevents type I diabetes in mice without disrupting general immunocompetence. The Journal of Clinical Investigation 120, 13241336.

Yin, L., Huseby, E., Scott-Browne, J., Rubtsova, K., Pinilla, C., Crawford, F., Marrack, P., Dai, S., and Kappler, J.W. (2011). A single T cell receptor bound to major histocompatibility complex class I and class II glycoproteins reveals switchable TCR conformers. Immunity *35*, 23–33.

Yin, L., Calvo-Calle, J.M., Dominguez-Amorocho, O., and Stern, L.J. (2012a). HLA-DM Constrains Epitope Selection in the Human CD4 T Cell Response to Vaccinia Virus by Favoring the Presentation of Peptides with Longer HLA-DM-Mediated Half-Lives. Journal of Immunology, 189, 3983-3994

Yin, Y., Wang, X.X., and Mariuzza, R. a (2012b). Crystal structure of a complete ternary complex of T-cell receptor, peptide-MHC, and CD4. PNAS *109*, 5405-5410.

Yoon, T., Macmillan, H., Mortimer, S.E., Jiang, W., Rinderknecht, C.H., Stern, L.J., and Mellins, E.D. (2012). Mapping the HLA-DO/HLA-DM complex by FRET and mutagenesis. PNAS 109, 11276-11281

Yui, K., Komori, S., Katsumata, M., Siegel, R.M., and Greene, M.I. (1990). Self-reactive T cells can escape clonal deletion in T-cell receptor V á 8.1 transgenic mice. PNAS *87*, 7135–7139.

Zhang, W., Wearsch, P.A., Zhu, Y., Leonhardt, R.M., and Cresswell, P. (2011). A role for UDP-glucose glycoprotein glucosyltransferase in expression and quality control of MHC class I molecules. PNAS 108, 4956-4961.

Zhao, Y., Li, Z., Drozd, S.J., Guo, Y., Mourad, W., and Li, H. (2004). Crystal structure of Mycoplasma arthritidis mitogen complexed with HLA-DR1 reveals a novel superantigen fold and a dimerized superantigen-MHC complex. Structure. *12*, 277–288.

Zhu, Y., Rudensky, A.Y., Corper, A.L., Teyton, L., and Wilson, I. a. (2003). Crystal Structure Of MHC Class II I-Ab in Complex with a Human CLIP Peptide: Prediction of an I-Ab Peptide-binding Motif. Journal of Molecular Biology *326*, 1157–1174.

Zwart, W., Griekspoor, A., Kuijl, C., Marsman, M., van, R.J., Janssen, H., Calafat, J., van, H.M., Janssen, L., Van Lith, M., et al. (2005). Spatial separation of HLA-DM/HLA-DR interactions within MIIC and phagosome-induced immune escape. Immunity. *22*, 221–233.